IMPACTO DE LA SEQUÍA AGRÍCOLA EN LA FENOLOGÍA Y LA PRODUCCIÓN DEL CEREAL BAJO CONDICIONES MEDITERRÁNEAS

TESIS DOCTORAL

Programa de Doctorado: Agrobiotecnología

Universidad de Salamanca

PILAR BENITO VERDUGO

Director: Dr. José Martínez Fernández

Codirector: Dr. Ángel González Zamora

Instituto de Investigación en Agrobiotecnología – CIALE

Salamanca, 2025

Dr. José Martínez Fernández, Catedrático de Geografía Física del Departamento de Geografía de la Universidad de Salamanca y **Dr. Ángel González Zamora**, Profesor Permanente Laboral del Departamento de Física Fundamental de la Universidad de Salamanca

CERTIFICAMOS:

Que la presente Memoria titulada "**Impacto de la sequía agrícola en la fenología y la producción del cereal bajo condiciones mediterráneas**", ha sido realizada por **Dª Pilar Benito Verdugo** en el Instituto de Investigación en Agrobiotecnología de la Universidad de Salamanca bajo nuestra dirección, se presenta como un compendio de artículos científicos y cumple las condiciones exigidas para optar el grado de Doctor por la Universidad de Salamanca.

Para que así conste, firmamos el presente certificado en Salamanca a 18 de Julio de 2025.

Firmado:

GONZALEZ ZAMORA, ANGEL (FIRMA)

Firmado digitalmente por GONZALEZ ZAMORA, ANGEL (FIRMA)
Fecha: 2025.07.18 20:34:15 +02'00'

Dr. José Martínez Fernández

Dr. Ángel González Zamora

Dr. Pablo Albertos Arranz, coordinador del Programa de Doctorado en Agrobiotecnología de la Universidad de Salamanca

CERTIFICO:

Que la presente Memoria titulada "**Impacto de la sequía agrícola en la fenología y la producción del cereal bajo condiciones mediterráneas**", ha sido realizada en el programa de Doctorado de Agrobiotecnología de la Universidad de Salamanca por **Dª Pilar Benito Verdugo**, bajo la dirección del Prof. **Dr. José Martínez Fernández** y el Prof. **Dr. Ángel González Zamora**, y cumple las condiciones exigidas para optar el grado de Doctor por la Universidad de Salamanca.

Para que así conste, firmo el presente certificado en Salamanca a 18 de Julio de 2025.

Firmado por ALBERTOS ARRANZ PABLO - ***4231** el día 21/07/2025 con un certificado emitido por AC FNMT Usuarios

Fdo: Dr. P. Albertos Arranz

En virtud del Reglamento de Doctorado de la Universidad de Salamanca, la presente Tesis Doctoral está constituida como un compendio de artículos científicos, siendo la doctoranda Pilar Benito Verdugo la autora principal de todos ellos:

- Benito-Verdugo, P., Martínez-Fernández, J., González-Zamora, Á., Almendra-Martín, L., Gaona, J., & Herrero-Jiménez, C. M. (2023). Impact of agricultural drought on barley and wheat yield: A comparative case study of Spain and Germany. *Agriculture*, *13*(11), 2111. https://doi.org/10.3390/agriculture13112111
  Status: publicado

- Benito-Verdugo, P., González-Zamora, Á., & Martínez-Fernández, J. (2024). Recent Cereal Phenological Variations under Mediterranean Conditions. *Remote Sensing*, *16*(11), 1879. https://doi.org/10.3390/rs16111879
  Status: publicado

- Benito-Verdugo, P., González-Zamora, Á., & Martínez-Fernández, J. (2025). Impact of flash droughts on cereal crops under Mediterranean conditions. *Spanish Journal of Agricultural Research* (in press).
  Status: aceptado

AGRADECIMIENTOS

Quiero agradecer a todas las personas que, de una u otra forma, me han ayudado al desarrollo de esta tesis doctoral.

En primer lugar, quiero expresar mi agradecimiento a mi director de tesis, José Martínez Fernández, y a mi codirector, Ángel González Zamora, por su esfuerzo y dedicación durante estos años. A Pepe, por su implicación constante en mi formación desde el primer momento, por su orientación y por haber acompañado con compromiso y rigor cada etapa de mi trayectoria investigadora. A Ángel, por su constante disposición y ayuda en los buenos y malos momentos, por sus valiosas sugerencias y por acompañarme con cercanía en cada etapa de este proceso. Quisiera también agradecer a Carlos Miguel Herrero Jiménez, quien fue mi codirector de tesis durante los primeros años de esta trayectoria, por su apoyo y orientación, contribuyendo al desarrollo de este trabajo.

Asimismo, quiero agradecer a todas las personas que forman o han formado parte del CIALE, por hacer del día a día un entorno más ameno y acogedor. En especial, a mis compañeros de laboratorio, que me acompañaron y ayudaron durante este tiempo, creando siempre el mejor ambiente de trabajo: Laura, Jaime y Ángel, cuya amistad y apoyo hicieron que cada día fuera más llevadero.

A todos mis amigos y familia, su cariño y compañía han sido fundamentales en este camino. En especial, quiero agradecer a mis padres, María del Carmen y Juan Manuel, y a mis hermanas, Mireia y Mª del Carmen. Mis cimientos, mi mayor apoyo y respaldo; gracias a ellos he podido llegar hasta aquí. Quiero reconocer la infinita paciencia que siempre habéis tenido conmigo y la fuerza que me habéis transmitido cuando más la necesitaba. A mi abuela “Marujilla”, por ser siempre refugio y un lugar seguro. A mis dos pilares, Bruno y Rosa, que sin decir una sola palabra y sin entender una tesis, supieron apoyarme mejor que nadie. A Jesús, porque a pesar del “qué cabezona eres”, siempre ha estado a mi lado en cada paso del camino. A la “Piñita”, siempre que toca y sin falta. Y también a la EM, que apareció en medio de este trayecto, decidió quedarse y enseñarme otra forma de entenderme, cuidarme y seguir adelante.

Por último, quiero agradecer a las instituciones que han financiado mi investigación: al Ministerio de Ciencia, Innovación y Universidades por la ayuda a la Formación de Profesorado Universitario (FPU20/00592), al MCIN/AEI/10.13039/501100011033/ por el proyecto PID2020-114623RB-C33, a la Junta de Castilla y León por los proyectos SA112P20 y CLU-2018-04 y al Fondo Europeo de Desarrollo Regional (FEDER).

RESUMEN

La agricultura es un sector fundamental en el mundo, destacando los cereales como el grupo de cultivos más relevante. En este contexto, los sistemas de secano adquieren especial importancia, ya que representan la mayor parte de las tierras cultivadas. Sin embargo, la alta vulnerabilidad climática de estos sistemas plantea desafíos importantes, especialmente en regiones como la mediterránea, reconocida como una de las zonas más sensibles al cambio climático global. La humedad del suelo (*soil moisture*, SM) es una variable crucial en esta región, ya que constituye el principal factor limitante que influye directamente en procesos hidrológicos, fenológicos y productivos. Además, es determinante en la caracterización de fenómenos extremos como las sequías agrícolas, cuya incidencia afecta de forma inmediata al rendimiento de los cultivos y compromete la seguridad alimentaria. Dentro de estos fenómenos, las sequías repentinas (*flash droughts*, FD) caracterizadas por su rápida intensificación, han generado un creciente interés en los últimos años, ya que representan una amenaza cada vez mayor para los cultivos. A pesar del reconocimiento generalizado de la influencia de la SM en la productividad agrícola y su importancia para la identificación de las sequías, su utilización como indicador en estudios de impacto sobre los cultivos es limitada. Su escasa utilización, junto con la falta de una aplicación específica en áreas vulnerables y en vegetación de interés agronómico, evidencia la necesidad de avanzar hacia investigaciones que aborden de manera integral los efectos del estrés hídrico en la agricultura. Partiendo de esta hipótesis, el objetivo de la presente tesis doctoral fue analizar el impacto de las sequías agrícolas sobre la fenología y la producción del cereal en regiones bajo condiciones mediterráneas. Para lograr este propósito, se plantearon tres objetivos específicos.

En primer lugar, se destaca la necesidad de analizar el impacto de la sequía agrícola sobre el rendimiento de los cultivos. A pesar del marcado efecto negativo que los déficits de SM tienen sobre los cultivos, son escasos los estudios que utilizan la SM como variable para identificar este tipo de sequía, a pesar de ser el indicador que la define. En este contexto, el primer objetivo de esta tesis doctoral es analizar y comparar el impacto de la sequía agrícola sobre el rendimiento del trigo y la cebada en las principales regiones cerealistas de España y Alemania, caracterizadas por contrastadas condiciones climáticas, durante el periodo 2001-2020. Para ello, se utilizó la SM de la zona radicular,

extraída de la base de datos del modelo LISFLOOD, y se emplearon sus anomalías como índice de sequía agrícola. Además, se identificó el mes en el que la SM ejercía una mayor influencia sobre las variables de estado del cultivo, como la productividad primaria bruta (*gross primary productivity*, GPP) y el índice de área foliar (*leaf area index*, LAI), obtenidas del sensor MODIS. Los años de sequía agrícola y su impacto en el rendimiento de los cereales se determinaron mediante tres enfoques basados en el mes crítico, considerando diferentes periodos de análisis. Para identificar dicho mes, se aplicaron dos metodologías diferentes según las condiciones ambientales de cada país. Las variables del cultivo mostraron una dependencia de la SM, especialmente durante los meses de primavera. Asimismo, se observó que las sequías agrícolas provocaron reducciones relevantes en el rendimiento de los cereales, presentando variaciones en su magnitud que reflejan el contraste entre las condiciones ambientales de cada país. Tanto en las regiones tradicionalmente afectadas por las sequías agrícolas, como en aquellas que hasta hace poco no lo estaban, este estudio proporciona información útil para la gestión del agua y la agricultura ante escenarios de cambio climático.

En segundo lugar, se partió de la hipótesis de que la evolución temporal de las principales métricas fenológicas antes y después del comienzo del siglo XXI es incierta. Además, la SM raramente se incorpora en los análisis fenológicos basados en teledetección y la mayoría de los estudios se enfocan en la vegetación natural. Por ello, se definió como segundo objetivo de esta tesis doctoral el análisis de los patrones temporales de la fenología de los cereales de secano, extraídos del conjunto de datos GIMMS NDVI3g en las principales regiones cerealistas bajo clima mediterráneo de España, Portugal, Francia e Italia, durante el periodo 1982-2022. Se analizaron por separado las series temporales anteriores y posteriores al inicio del siglo XXI, extrayendo los parámetros fenológicos mediante el método del umbral dinámico modificado, y se estudiaron sus tendencias. Asimismo, se evaluaron las relaciones entre estos parámetros y la influencia de determinadas variables hidroclimáticas sobre el inicio o siembra (*start of season*, SOS) y el final o cosecha (*end of season*, EOS) del ciclo fenológico. Las tendencias fenológicas entre ambos periodos de estudio mostraron una inversión temporal coincidente con la pausa del calentamiento global, reflejándose asimismo en la dinámica de la influencia de las variables hidroclimáticas sobre SOS y EOS. Esta información resulta fundamental para la gestión y planificación de los cultivos de secano en escenarios de cambio climático.

El último objetivo parte del creciente interés por las FD debido a su dinámica específica, su rápida generación, desarrollo y los daños significativos que ocasionan. No obstante, a pesar de la creciente evidencia de su amenaza para los cultivos, los estudios en ámbitos agrícolas siguen siendo limitados. En este contexto, se planteó como tercer y último objetivo de esta tesis doctoral el análisis de las FD en las principales regiones cerealistas de España, Portugal, Francia e Italia entre 2000 y 2023, evaluando sus efectos sobre la GPP, el rendimiento y la fenología de los cereales. Las FD se identificaron mediante la SM obtenida de la base de datos de reanálisis ERA5-Land. La respuesta de los cereales se analizó mediante dos índices basados en el tiempo de respuesta de la GPP, mientras que el impacto sobre la fenología del cereal se evaluó usando el NDVI (*Normalized Difference Vegetation Index*), utilizando datos de MODIS. Se observó que las FD afectaron significativamente a los cereales bajo condiciones mediterráneas, presentando mayor frecuencia e intensidad durante los meses críticos de desarrollo, y provocaron un estrés máximo en los cultivos en dichos periodos. Este análisis aporta información clave para entender la resiliencia de los cultivos frente a las FD y para desarrollar estrategias que mitiguen sus efectos en escenarios futuros de cambio climático.

ÍNDICE

LISTA DE FIGURAS

LISTA DE TABLAS

LISTA DE ACRÓNIMOS Y ABREVIATURAS

AT	Alentejo
AVHRR	*Advanced Very High Resolution Radiometer*
AWD	*Atmosphere Water Deficit*
AWDN	*Automated Weather Data Network*
BS	*Booting stage*
BY	Bayern
C3S	*Copernicus Climate Change Service*
CCI	*Climate Change Initiative*
CL	Castilla y León
CM	Castilla–La Mancha
CMI	*Crop Moisture Index*
CNES	*Centre National d'Études Spatiales*
DVI	*Difference Vegetation Index*
EDDI	*Evaporative Demand Drought Index*
EDO	*European Drought Observatory*
EFAS	*European Flood Alert System*
EMD	*Empirical Mode Decomposition*
ERA	*ECMWF Re-Analysis*
ESA	*European Space Agency*
ESI	*Evaporative Stress Index*
ETDI	*Evapotranspiration Deficit Index*
EU	*European Union*
EVI	*Enhanced vegetation index*
FAO	*Food and Agriculture Organization*
FAPAR	*Fraction of Absorbed Photosynthetically Active Radiation*
FD	*Flash droughts*
FDI	*Flash droughts intensity*

FDR	*Frequency domain reflectometry*
FDS	*Flash droughts severity*
GCOS	*Global Climate Observing System*
GHG	*Greenhouse gas*
GIMMS	*Global Inventory Modeling and Mapping Studies*
GOLD	*Global Offline Land-surface Dataset*
GPP	*Gross primary productivity*
GPR	*Ground Penetrating Radar*
IPCC	*Intergovernmental Panel on Climate Change*
ISMN	*International Soil Moisture Network*
JRC	*Joint Research Centre*
LAI	*Leaf area index*
LC	*Land Cover*
LOS	*Length of growing season*
LSM	*Land Surface Model*
MEMS	*Micro Electro Mechanical System*
MERRA-Land	*Modern-Era Retrospective Analysis for Research and Applications - Land*
MK	Mann-Kendall
MODIS	*Moderate Resolution Imaging Spectroradiometer*
NASA	*National Aeronautics and Space Administration*
NDVI	*Normalized difference vegetation index*
NDVI3g	*Normalized difference vegetation index third-generation*
NOAA	*National Oceanic and Atmospheric Administration*
NPP	*Net Primary Production*
NS	Niedersachsen
NW	Nordrhein-Westfalen
OC	Occitanie
P	Precipitación acumulada
PCI	*Precipitation Condition Index*

PDFD	*Precipitation deficit flash drought*
PG	Puglia
PDSI	*Palmer Drought Severity Index*
RCI	*Rapid Change Rate Index*
REMEDHUS	Red de Estaciones de Medición de la Humedad del Suelo de la Universidad de Salamanca
RH	*Relative humidity*
RVI	*Ratio Vegetation Index*
SAVI	*Soil-Adjusted Vegetation Index*
SERS	*Standard Evaporative Stress Ratio*
SIF	*Solar-induced chlorophyll fluorescence*
SM	*Soil moisture*
SMADI	*Soil Moisture Agricultural Drought Index*
SMAP	*Soil Moisture Active and Passive*
SMI	*Soil Moisture Index*
SMOS	*Soil Moisture Ocean Salinity*
SMDI	*Soil Moisture Deficit Index*
SOS	*Start of season*
SPI	*Standardized Precipitation Index*
SPOT	*Satellite Pour l'Observation de la Terre*
SWDI	*Soil Water Deficit Index*
TDR	*Time domain reflectometry*
Tmax	Temperatura máxima
Tmin	Temperatura mínima
UN-LCCS	*United Nations Land Cover Classification System*
USGS	*United States Geological Survey*
VIC	*Variable Infiltration Capacity*
VIs	*Vegetation indices*
VPD	*Vapor pressure deficit*
WMO	*World Meteorological Organization*

CAPÍTULO 1

INTRODUCCIÓN, OBJETIVOS Y MÉTODOS

1.1 Motivación

La agricultura es un sector fundamental en el mundo, representando aproximadamente el 40% de la superficie terrestre. Dentro de esta extensión, un tercio corresponde a tierras de cultivo, mientras que el resto son praderas y pastizales permanentes (FAO, 2024a). A lo largo del siglo XXI, la superficie de tierras de cultivo ha aumentado, destacando los cultivos anuales como el trigo, la cebada y el maíz, los cuales han experimentado un incremento de 110 millones de hectáreas entre 2001 y 2022, lo que representa un crecimiento del 11% (FAO, 2024a). Los cereales son el principal grupo de cultivos producidos mundialmente (Figura 1.1), destacando entre ellos el maíz, el arroz, el trigo, la cebada y el sorgo (FAO, 2024b).

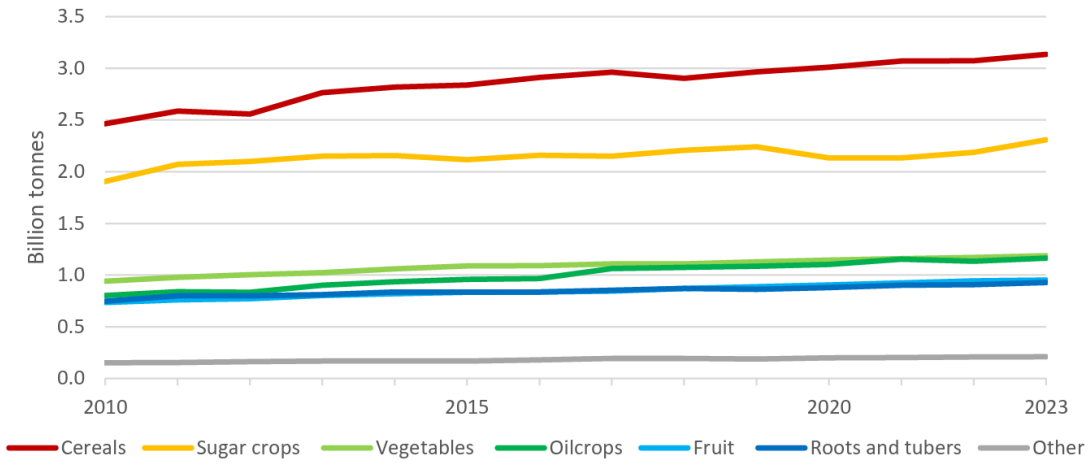

Figura 1.1. Producción mundial de cultivos primarios por grupo de cultivos. Imagen obtenida de FAO (2024b).

El sistema de cultivo de secano es aquel en el que los cultivos dependen exclusivamente de las precipitaciones, sin la aplicación de riego. Este sistema es el más extendido en el mundo, desempeñando un papel crucial en la cadena mundial de producción y suministro de alimentos, ya que cubre aproximadamente el 80% de las tierras cultivadas y genera alrededor del 60% de la producción mundial de cultivos. Su gran extensión lo convierte en un componente clave de la agricultura mundial (FAO, 2024a). La elevada vulnerabilidad climática de los sistemas de cultivo de secano confiere una especial relevancia al impacto del cambio climático, ya que ha contribuido a la

reducción de la seguridad alimentaria, ha afectado a la seguridad hídrica, y ha provocado alteraciones en los patrones de precipitación, así como un aumento en la frecuencia e intensidad de fenómenos climáticos extremos, como las sequías (IPCC, 2023). Aunque se proyectan riesgos de sequía agravados globalmente, los patrones de cambio presentan una notable variabilidad espacial, con incrementos significativos en latitudes medias (Gu et al., 2020). En este contexto destaca la región mediterránea, identificada como uno de los principales puntos críticos del cambio climático mundial (Lionello y Scarascia, 2018). Como consecuencia, las sequías en esta región son más severas y se prevé un aumento sustancial tanto en su frecuencia como en su intensidad (Gu et al., 2020), lo que plantea importantes desafíos hidrológicos, especialmente considerando que se trata de una región con disponibilidad hídrica limitada.

En este escenario de alta dependencia climática, el cambio climático representa una amenaza global creciente para la agricultura y se espera que sus impactos se intensifiquen en el futuro (Borrelli et al., 2020). La región mediterránea ha sido reiteradamente identificada como una de las zonas más sensibles al cambio climático global (Giorgi, 2006), como lo demuestran distintas generaciones de modelos climáticos (Cos et al., 2022; Pulighe et al., 2021; Seker y Gumus, 2022). Se prevé que en esta región la precipitación media disminuirá progresivamente mientras que la temperatura continuará aumentando, acompañado todo ello de un incremento en la evapotranspiración, lo que provocará una disminución anual significativa tanto en la humedad del suelo (SM, *soil moisture*) de la zona radicular como en el almacenamiento de agua subterránea, reforzando así el escenario de creciente escasez hídrica en esta región (Pulighe et al., 2021; Seker y Gumus, 2022). En este contexto, el *Global Climate Observing System* (GCOS) de la *World Meteorological Organization* (WMO) ha identificado 55 variables climáticas esenciales, entre las cuales, desde el año 2010, se encuentra la SM (GCOS, 2022). Estas variables proporcionan la evidencia necesaria para comprender y proyectar la evolución del clima, orientar las medidas de mitigación y adaptación y evaluar riesgos (GCOS, 2022). La SM es especialmente relevante en la región mediterránea, donde constituye un factor limitante que afecta el acoplamiento suelo-atmósfera e influye en procesos clave como la evapotranspiración, el ciclo hidrológico, la productividad agrícola, así como en fenómenos extremos como sequías e inundaciones (Escorihuela y Quintana-Seguí, 2016; Martínez-Fernández et al., 2023). Por ello, su monitorización y análisis son indispensables para la gestión agrícola (Gaona et al.,

2022), la gestión de recursos hídricos (Brocca et al., 2017), la conservación de ecosistemas (González-Zamora et al., 2021; Martínez-Fernández et al., 2019) y la evaluación de riesgos naturales como las sequías (Almendra-Martín et al., 2021a).

El interés por la monitorización de la SM ha crecido de forma notable en las últimas décadas, impulsado por los avances tecnológicos que han permitido su observación a través de sensores remotos. Hasta comienzos del siglo XXI, el estudio de esta variable se basaba principalmente en mediciones *in situ* debido a la falta de herramientas adecuadas para su monitorización a gran escala (Martínez-Fernández et al., 2015). En la actualidad, existen múltiples técnicas que permiten generar series de datos con distintas resoluciones espaciales y temporales. El desarrollo de sensores remotos ha sido clave en esta evolución, permitiendo el paso de mediciones puntuales de la SM a un seguimiento espacial y temporal continuo. En este contexto, destacan las dos primeras misiones espaciales específicamente diseñadas para medir la SM: la misión *Soil Moisture Ocean Salinity* (SMOS) de la Agencia Espacial Europea (ESA, *European Space Agency*) y la misión *Soil Moisture Active and Passive* (SMAP) de la NASA (*National Aeronautics and Space Administration*) (Wigneron et al., 2017). Además de los datos observacionales, los datos de modelos han demostrado ser herramientas complementarias de gran utilidad para monitorizar y estudiar la dinámica de la SM, así como su papel en los intercambios de agua y energía entre el suelo y la atmósfera (Laguardia y Niemeyer, 2008). Modelos como LISFLOOD permiten generar series de SM con una resolución espacial de hasta 5 km × 5 km (Van Der Knijff et al., 2010). Por otro lado, los productos de reanálisis, como, por ejemplo, ERA5-Land, combinan las series satelitales y las de modelización para beneficiarse de las ventajas de ambos (Muñoz-Sabater et al., 2021).

Ante el escenario del cambio climático, una de las aplicaciones más relevantes de las bases de datos de SM es el análisis de fenómenos extremos. Uno de los más interesantes es la sequía, de la que se identifican diferentes tipologías: meteorológica, hidrológica, agrícola y socioeconómica (Mishra y Singh, 2010). Entre ellas, la sequía agrícola tiene un impacto particularmente directo e inmediato, ya que se manifiesta cuando la disponibilidad de SM desciende por debajo del nivel necesario para satisfacer las necesidades fisiológicas de las plantas, afectando negativamente el crecimiento y el rendimiento de los cultivos (Potopova et al., 2016; Quiring y Papakryiakou, 2003). La sequía agrícola representa una de las principales causas de pérdida de productividad en los sistemas de secano en todo el mundo, provocando significativas reducciones en el

rendimiento de los cultivos (Li et al., 2017). Los estudios y evaluaciones de la sequía agrícola son fundamentales, dado que constituye una de las principales preocupaciones a escala global en términos de seguridad alimentaria, estabilidad social y económica (Krishnamurthy et al., 2022). Evaluar la sequía agrícola y sus posibles impactos en la seguridad alimentaria es especialmente crucial en regiones vulnerables y propensas a este fenómeno (Orimoloye, 2022), como la región mediterránea, caracterizada por una escasez hídrica significativa (Essa et al., 2023). A pesar del reconocimiento generalizado de la influencia de la SM en la productividad agrícola y en la caracterización de las sequías, persisten importantes lagunas o carencias al respecto en la literatura científica. Aunque la SM es la variable que define la sequía agrícola, pocas veces se emplea como indicador principal en los análisis de impacto sobre los rendimientos de los cultivos, siendo comúnmente reemplazada por índices meteorológicos, o tratada como una variable derivada (Krueger et al., 2019; Li et al., 2022).

En este contexto, en los últimos años ha aumentado el interés por las sequías repentinas (*flash drought*, FD), ya que representan un subtipo de sequía caracterizado por una rápida intensificación que puede dar inicio a una sequía o agravar una ya existente, afectando de forma severa a la productividad agrícola (Otkin et al., 2022). Aunque estas sequías se originan por múltiples factores, la SM destaca como un indicador eficaz para su identificación y monitorización (Osman et al., 2024). La rápida aparición de las FD dificulta su predicción, lo que reduce considerablemente el tiempo disponible para mitigar sus impactos, agravando las consecuencias negativas en la agricultura y la sociedad (Christian et al., 2024). Sin embargo, gran parte de la investigación sobre FD se ha centrado predominantemente en la vegetación natural (Barbosa, 2023; O y Park, 2023). En los pocos estudios que abordan su impacto en contextos agrícolas, los análisis suelen estar restringidos a escalas locales, limitados a un número reducido de eventos, a menudo enfocados en un caso aislado (Hunt et al., 2021; Otkin et al., 2021) o centrados de forma general en tierras de cultivo sin considerar las repercusiones en cultivos específicos (O y Park, 2024).

En este marco, hay que señalar que el déficit de SM ejerce un impacto significativo cuando ocurre durante las fases principales de crecimiento y reproducción del ciclo de los cultivos (Gaona et al., 2022). Por esta razón, la descripción temporal es crucial, ya que la sensibilidad de los cultivos a condiciones limitantes o de sobreexposición varía en cada etapa fenológica, definiendo períodos críticos específicos

de impacto (Gaona et al., 2022). La dinámica de la vegetación es un importante indicador biológico que refleja las respuestas cíclicas y estacionales de los ecosistemas a los regímenes climáticos e hidrológicos (Zhang et al., 2003). Además, el calentamiento global es un fenómeno innegable que altera los ciclos fenológicos de la vegetación terrestre, por lo que resulta fundamental una caracterización precisa de la fenología y la monitorización de su comportamiento a lo largo del tiempo para comprender las variaciones en los impactos del cambio climático (Zhao et al., 2015). La información fenológica de los cultivos se extrae principalmente mediante registros terrestres *in situ* y datos de teledetección (Zhan et al., 2024). Aunque los seguimientos *in situ* ofrecen datos detallados, sus limitaciones espaciales y temporales dificultan el análisis fenológico a gran escala y largo plazo, mientras que los datos obtenidos por satélite son herramientas eficaces para el seguimiento de la vegetación a escalas espaciales y temporales adecuadas. La fenología derivada de estos datos suele obtenerse a partir de índices de vegetación, como, por ejemplo, el *normalized difference vegetation index* (NDVI) o el *enhanced vegetation index* (EVI) (Liao et al., 2023). Con los avances en las tecnologías de teledetección, que permiten la monitorización de la fenología de la vegetación, se han realizado estudios recientes sobre las tendencias fenológicas y sus respuestas al cambio climático en distintas escalas espaciales y temporales (Hua et al., 2025; Tian et al., 2024a). Sin embargo, la atención se ha dirigido principalmente a los cambios fenológicos de la vegetación natural, siendo mucho menor en el caso de los cultivos agrícolas. En los pocos casos en que se han considerado los cultivos, los estudios suelen limitarse a escalas pequeñas, basados en datos de campo *in situ* (Ren y An, 2021). Además, muchas de esas investigaciones han incorporado variables climáticas como temperatura, precipitación y fotoperiodo en el análisis de los efectos del clima sobre la fenología (Jin et al., 2019a; Yuan et al., 2019a). Sin embargo, la SM ha sido poco considerada en estudios fenológicos basados en datos de teledetección, a pesar de su importancia crítica para los cultivos (Gaona et al., 2023) y su estrecha relación con la sequía agrícola.

En definitiva, la falta de integración de un indicador relevante como la SM y su aplicación específica en áreas vulnerables y vegetación de interés agronómico, pone de manifiesto la necesidad de avanzar hacia investigaciones que aborden de manera integral los efectos del estrés hídrico en la agricultura. Este enfoque no solo es esencial para el desarrollo de estrategias de adaptación y mitigación frente al cambio climático, sino que también resulta fundamental para garantizar la seguridad alimentaria, especialmente en

contextos donde los recursos hídricos son limitados y se proyecta un aumento en la frecuencia e intensidad de fenómenos extremos como las sequías. Motivada por el interés del tema de investigación y por la constatación de lagunas y carencias en la literatura científica, esta tesis doctoral aborda el impacto de la sequía agrícola sobre el rendimiento del trigo y la cebada en regiones con diferentes condiciones climáticas, el estudio de los patrones temporales de la fenología en las últimas décadas, así como la caracterización y efecto de las FD en el rendimiento y la fenología en regiones cerealistas bajo clima mediterráneo.

1.2 Objetivos

Bajo el escenario de cambio climático y el consecuente incremento proyectado en la frecuencia e intensidad de las sequías, el objetivo general de esta tesis es aportar enfoques analíticos y conocimiento sobre el impacto del déficit de SM en la fenología y producción del cereal bajo condiciones mediterráneas. Este análisis se aborda desde diferentes perspectivas, con un enfoque particular en el trigo y la cebada, por ser los cultivos predominantes en las zonas de estudio. Los objetivos específicos son:

- Analizar y comparar el impacto de la sequía agrícola en el rendimiento del trigo y la cebada de secano en las principales regiones cerealistas de España y Alemania durante el periodo 2001-2020, considerando distintas perspectivas de análisis.
- Analizar los patrones temporales de la fenología de los cereales de secano y sus respuestas a diversas variables hidroclimáticas bajo condiciones mediterráneas durante el periodo 1982-2022.
- Identificar y caracterizar las FD en diferentes regiones cerealistas bajo condiciones climáticas mediterráneas, evaluando su impacto en el estado del cultivo, el rendimiento y la fenología de los cereales durante el periodo 2000-2023.

1.3 Producción agrícola bajo condiciones mediterráneas

1.3.1 Características ambientales de la región Mediterránea

La región mediterránea (Figura 1.2) constituye una extensa franja territorial que rodea el mar Mediterráneo y se extiende por el sur de Europa, el norte de África y el suroeste de Asia (Blondel, 2010). Esta región, comprendida entre las latitudes 29°N y 47,5°N, y las longitudes 10°O y 39°E (Aurelle et al., 2022), se caracteriza por un clima mediterráneo, con veranos cálidos y secos e inviernos suaves y húmedos (Lionello et al., 2006). Las precipitaciones se distribuyen de manera irregular a lo largo del año, presentando una marcada estacionalidad, con una estación estival seca (Tramblay et al., 2020), especialmente pronunciada en el sur de la región, donde las precipitaciones son muy escasas o prácticamente inexistentes (Giorgi y Lionello, 2008). La temperatura y la precipitación media anuales en los países mediterráneos de Europa varían considerablemente, alcanzando los 5 °C y 2027 mm en el norte de Italia, mientras que en el sureste de España se registran valores de 18 °C y 228 mm, respectivamente (Ferreira et al., 2022; Llorens y Domingo, 2007). La alta variabilidad temporal del clima mediterráneo, tanto a escala estacional como interanual, se debe a su situación de transición entre las latitudes medias y subtropicales, así como a su asociación con diversos patrones de circulación atmosférica de gran escala (Tramblay et al., 2020).

Las condiciones climáticas de la región mediterránea inciden de forma determinante sobre los ecosistemas, efecto que se ve reforzado por su topografía contrastada, que incluye grandes cordilleras, profundos valles y extensas mesetas interiores, entre otros elementos. Esta compleja geomorfología genera una gran variedad de hábitats que van desde matorrales esclerófilos y estepas semiáridas hasta humedales costeros y bosques ribereños, lo que explica la notable biodiversidad característica del bioma mediterráneo (Blondel, 2010). Por último, la región alberga una amplia diversidad de tipos de suelo, resultado de los diferentes materiales parentales, la topografía, las condiciones climáticas y la influencia de factores biológicos como la vegetación y la fauna, junto con la influencia de actividades humanas (Ferreira et al., 2022). Pese a esta riqueza edáfica, esta región enfrenta importantes desafíos, ya que ha sido identificada

como particularmente vulnerable a la degradación del suelo y a la desertificación, especialmente en zonas de alto estrés, como las áreas áridas y semiáridas debido a su mayor susceptibilidad (López-Bermúdez, 1993; López-Bermúdez et al., 1998).

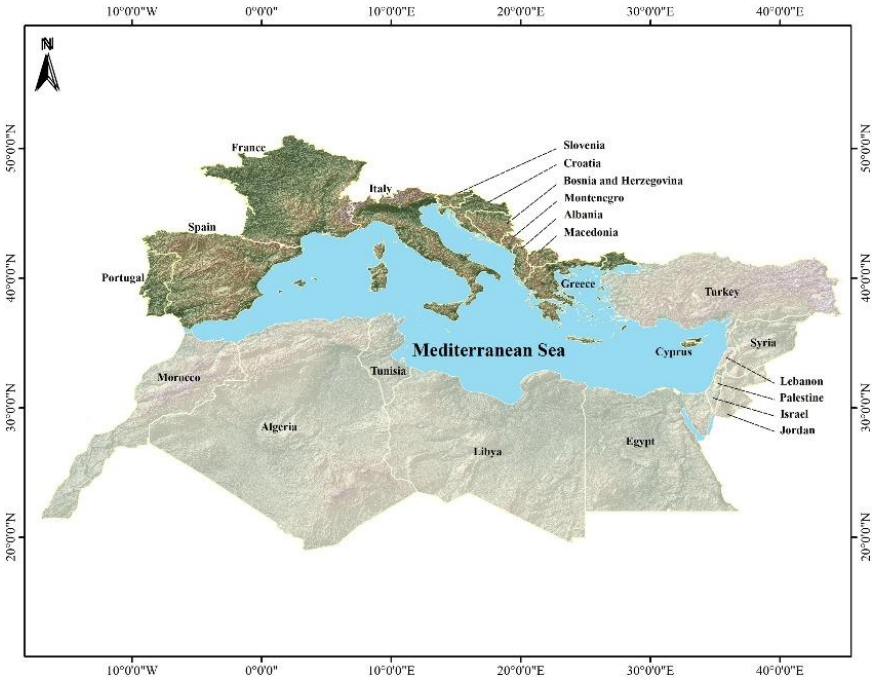

Figura 1.2. Mapa de los países de la región mediterránea. Imagen obtenida de Ferreira et al. (2022).

1.3.2 El cultivo del cereal

Los cereales son plantas herbáceas monocotiledóneas de ciclo vegetativo anual, pertenecientes a la familia de las poáceas (*Poaceae*), comúnmente conocidas como gramíneas. Constituyen la fuente de alimentos más importante en el mundo (Tufail et al., 2023), siendo el trigo (*Triticum* spp.), el maíz (*Zea mays*), el arroz (*Oryza sativa*), la cebada (*Hordeum vulgare*) y el sorgo (*Sorghum* spp.) los principales cultivos, tanto por superficie cultivada como por volumen de producción (Ahmad et al., 2024). Los cereales representan casi el 75% de la superficie total cultivada del mundo y el 60% de la producción mundial de alimentos (Feng et al., 2024). Constituyen además la principal fuente alimentaria de energía, carbohidratos y proteínas vegetales (Poutanen et al., 2022). En la actualidad, aproximadamente el 41% de la producción mundial de cereales se destina al consumo humano, el 35% a la alimentación animal y el resto a otros usos,

principalmente industriales, como la producción de biocombustibles (Poutanen et al., 2022). En la región mediterránea, la agricultura representa aproximadamente el 30% de la superficie total, aunque solo el 8% de las tierras agrícolas está dotada con sistemas de riego (Alrteimei et al., 2022). Como consecuencia, la agricultura de secano constituye el sistema predominante en la región, donde los cereales representan el principal grupo de cultivos (Savin et al., 2022). En este contexto de recursos limitados, la productividad de los cultivos depende fundamentalmente de la disponibilidad y eficiencia en el uso de los factores limitantes, destacando el agua como uno de los más críticos en la región mediterránea (Cossani et al., 2012). Los cultivos de trigo y cebada son los principales cereales cultivados en secano de la región mediterránea, desempeñando un papel estratégico en la economía y en la seguridad alimentaria de toda la zona (Albrizio et al., 2010; Savin et al., 2022).

A pesar de que la producción de cereales ha mostrado una tendencia creciente en las últimas décadas, los sistemas de cultivo se enfrentan a desafíos cada vez más severos derivados del cambio climático, especialmente en regiones semiáridas (Abi Saab et al., 2019). La creciente variabilidad de los regímenes hídricos compromete la estabilidad del rendimiento, lo que incrementa el riesgo de inseguridad alimentaria a escala global (Bracho-Mujica et al., 2019; Sadok et al., 2019). Ante este escenario, se hace imprescindible que la agricultura en la región mediterránea desarrolle una mayor resiliencia al cambio climático y aumente su eficiencia en el uso del agua, a fin de garantizar la sostenibilidad de la producción y la seguridad alimentaria (UnNisa et al., 2022).

1.3.3 Fenología de los cereales

La fenología es el estudio de las etapas recurrentes en el ciclo de vida de plantas y animales (Schwartz, 2003). En el ámbito agrícola, la fenología se refiere al estudio de las diferentes etapas de desarrollo que experimentan los cultivos a lo largo de su ciclo de vida. Estas etapas, conocidas como fases fenológicas, siguen un orden cronológico definido y están estrechamente influenciadas por factores ambientales (Zhao et al., 2015). Los cereales pueden clasificarse en dos grandes grupos según su ciclo de cultivo, aunque algunas especies presentan variedades adaptadas a ambos ciclos. Por un lado, los cereales

de invierno, como el trigo, la cebada, la avena y el centeno, se siembran en otoño y se cosechan en verano; por otro, los de primavera o verano, como el maíz y el sorgo, se siembran a finales de la primavera y se recolectan a finales del verano o principios del otoño. (Sherratt, 1980). En la región mediterránea predominan los cereales de invierno, especialmente el trigo y la cebada, cuyo ciclo fenológico se extiende desde la siembra en otoño hasta la cosecha en verano (Sherratt, 1980). Comprender el ciclo fenológico de los cultivos es esencial para una gestión agrícola eficiente, ya que permite tomar decisiones precisas en momentos clave del desarrollo.

La escala de Zadoks (Zadoks et al., 1974) es la más utilizada para describir y clasificar las fases fenológicas de los cereales, ya que proporciona un sistema estandarizado y detallado que facilita la monitorización y manejo de estos cultivos (Thomas, 2014). Esta escala fue desarrollada a partir de la escala de Feekes (Feekes, 1941), con el objetivo de proporcionar una descripción más precisa y universal de las etapas de crecimiento, aplicable a todas las especies de cereales y adecuada para diversos entornos agrícolas (Zadoks et al., 1974). Además, fue diseñada para facilitar su uso en el registro y procesamiento informatizado de datos, superando las limitaciones de las escalas anteriores (Zadoks et al., 1974). La escala de Zadoks, está estructurada en un sistema de dos dígitos en el que el primer dígito, de 0 a 9, corresponde con el estadio de desarrollo principal del desarrollo de la planta, mientras que el segundo dígito, de 0 a 9, proporciona una subdivisión de esa fase, correspondiendo el valor 5 al punto intermedio de ese estado. Los estadios principales de los cereales según la escala de Zadoks (Figura 1.3) se dividen en los siguientes (Tottman, 1987; Zadoks et al., 1974):

0 – Germinación: conjunto de procesos que ocurren en la semilla desde que el embrión comienza a crecer hasta que se ha formado una pequeña planta capaz de vivir de forma independiente, es decir, que ya no depende del alimento almacenado en la semilla.

1 – Producción de hojas en el tallo principal: en esta fase se inicia el crecimiento vegetativo mediante la emisión de hojas en el tallo principal. La planta comienza a desarrollar sus primeros órganos fotosintéticos, lo que permite un mayor crecimiento y acumulación de nutrientes para el desarrollo posterior.

2 – Macollado: se produce la formación de brotes laterales o macollos que emergen desde los nudos de la base de la planta. Los macollos son tallos secundarios que contribuyen a la producción de nuevos brotes, siendo esenciales para la ramificación de

la planta y tienen un impacto directo en la cantidad de espigas que se formarán posteriormente, lo que afecta a la densidad y el rendimiento de la cosecha.

3 – Encañado: es el proceso en el que los nudos del tallo se estiran y se separan, aumentando la altura de la planta. El primer nudo aéreo, visible como el nudo más bajo del tallo, marca la aparición de la hoja bandera, una de las hojas más importantes para la fotosíntesis. Este alargamiento es crucial para la formación de una estructura que permita la futura emergencia de la espiga.

4 – Vaina engrosada: en esta fase, la espiga joven se está desarrollando dentro de las vainas de las hojas y se hace más notoria. La vaina de la hoja bandera se engrosa para proteger la espiga en formación, aunque aún no es visible externamente.

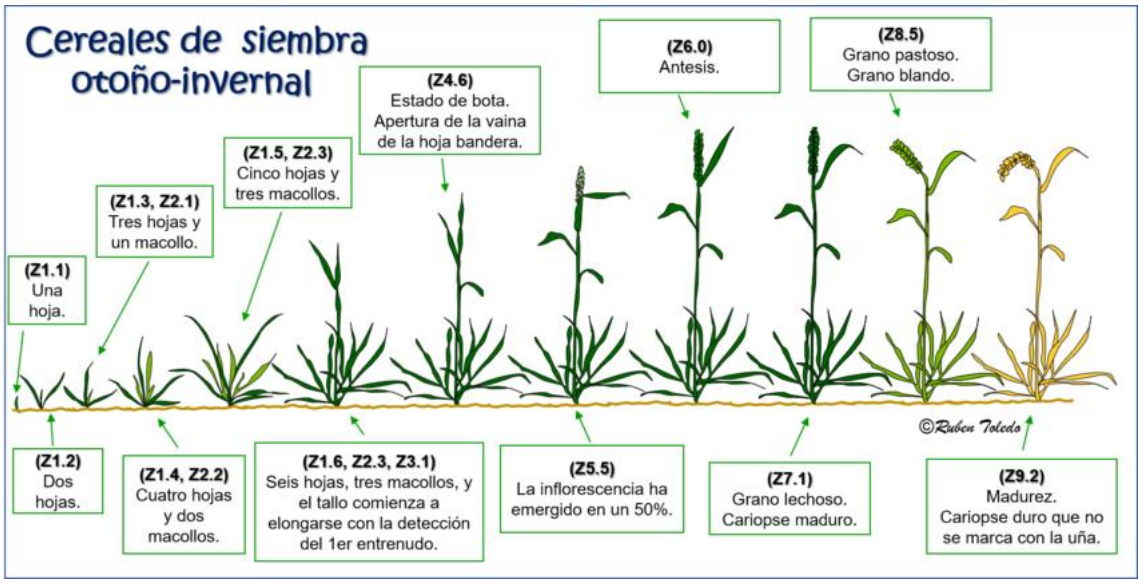

Figura 1.3. Principales fases de desarrollo de los cereales de invierno según la escala de Zadoks. Imagen obtenida de Toledo (2023).

5 – Espigado: la espiga comienza a emerger del tallo, marcando la transición de la etapa vegetativa a la reproductiva. La espiga, que es la estructura que contiene las flores, empieza a ser visible fuera de las vainas y se inicia el proceso de diferenciación floral dentro de la espiga.

6 – Antesis o floración: corresponde a la apertura de las flores y la polinización. En los cereales, la floración ocurre cuando las espiguillas se abren y están listas para ser

polinizadas. Este es un estadio crítico en el que se produce la fecundación de los óvulos de la flor, dando inicio a la formación de granos. El éxito de la polinización es determinante para el número final de granos por espiga.

7 – Estado lechoso del grano: el grano se encuentra en un estado inicial de desarrollo, con alta cantidad de agua y una consistencia blanda. El contenido de almidón y otros componentes en el grano están en proceso de acumulación. Fisiológicamente, la planta transloca nutrientes desde las hojas hacia los granos, lo que favorece su crecimiento.

8 – Estado pastoso del grano: en esta fase, el grano comienza a endurecerse y adquiere una consistencia más densa o pastosa. La acumulación de almidón en el grano se incrementa, aunque el contenido de agua sigue siendo relativamente alto. El grano continúa su desarrollo hacia la madurez perdiendo agua paulatinamente, mientras que la planta reduce su actividad metabólica.

9 – Madurez: este estadio marca la finalización del desarrollo del grano y la madurez fisiológica de la planta. El contenido de agua en los granos se reduce significativamente, indicando que están listos para la cosecha. La planta entra en senescencia, lo que implica que las hojas y tallos se secan progresivamente. El ciclo de vida de la planta llega a su fin y los granos son completamente formados para ser recolectados.

1.3.4 Indicadores ecofisiológicos de la producción agrícola

Los indicadores ecofisiológicos son parámetros cuantitativos que describen cómo responden las plantas a las condiciones del entorno (Lüttge y Scarano, 2004). Estos indicadores son fundamentales para comprender el comportamiento de los cultivos a lo largo de su ciclo de vida y cómo responden a diversos factores ambientales, manejos agronómicos y condiciones climáticas (Moriondo et al., 2021). En este contexto, los índices de vegetación son herramientas empleadas para estimar el vigor y la salud de la vegetación, a partir de combinaciones matemáticas de valores de reflectancia obtenidos en diferentes bandas espectrales y longitudes de onda (Chowdhury et al., 2024). Estos índices se utilizan ampliamente en campos como la agricultura y la ecología para analizar

el estado fisiológico y la productividad de las plantas, estudiar la dinámica de la vegetación y evaluar diversas características de los cultivos, como la biomasa (Chowdhury et al., 2024; Viljanen et al., 2018).

Los índices de vegetación se extraen principalmente a partir de observaciones directas en el terreno y de datos de teledetección (Chowdhury et al., 2024). Los métodos *in situ*, como los radiómetros, colorímetros y espectrómetros portátiles, permiten obtener datos con alta resolución espacial y precisión, pero requieren mediciones de campo meticulosas, lo que compromete la existencia de series temporales prolongadas (Candiago et al., 2015; Chowdhury et al., 2024). Este enfoque presenta limitaciones en cuanto a las escalas espaciales y temporales, lo que dificulta el análisis a gran escala y la realización de estudios a largo plazo. Sin embargo, las observaciones por satélite proporcionan información ecofisiológica de grandes extensiones y de series temporales largas (Marshall et al., 2018), constituyendo una herramienta eficaz para investigar los cambios en la productividad de la vegetación, la estructura del dosel y su respuesta a factores bióticos y abióticos (Tian et al., 2024b).

Los índices de vegetación más utilizados son el *Ratio Vegetation Index* (RVI), *Difference Vegetation Index* (DVI), NDVI, EVI, *Leaf Area Index* (LAI) y *Soil-Adjusted Vegetation Index* (SAVI) (Xue y Su, 2017). Estos índices proporcionan información detallada sobre parámetros ecofisiológicos clave de la vegetación, reflejando su condición y dinámica de crecimiento. Además, existen otros indicadores ecofisiológicos que se centran en la productividad de la vegetación, como el *Gross Primary Production* (GPP), *Net Primary Production* (NPP) y *Fraction of Absorbed Photosynthetically Active Radiation* (FAPAR), que reflejan la capacidad fotosintética y la eficiencia de los ecosistemas (Xue y Su, 2017). Entre los principales satélites y sensores utilizados para el estudio de estos índices se encuentran el *Moderate Resolution Imaging Spectroradiometer* (MODIS), a bordo de los satélites Terra y Aqua de la NASA; el *Advanced Very High Resolution Radiometer* (AVHRR), operado por satélites de la *National Oceanic and Atmospheric Administration* (NOAA); el *Satellite Pour l'Observation de la Terre* (SPOT), desarrollado por el *Centre National d'Études Spatiales* (CNES) de Francia; Landsat, una misión conjunta de la NASA y el *United States Geological Survey* (USGS) y Sentinel, del programa Copernicus de la ESA, entre otros (Qin et al., 2021). Diversos estudios recientes han utilizado estos indicadores

ecofisiológicos, con el fin de evaluar la capacidad de respuesta y resiliencia de los cultivos ante condiciones adversas como la sequía (Deng et al., 2024; Fuentes et al., 2025; Li et al., 2025).

1.3.5 Condicionantes ambientales de los cultivos de cereal en ambientes mediterráneos

En la región Mediterránea, como en otras regiones del Planeta, prevalece un clima mediterráneo típico con precipitaciones irregulares, concentradas en las estaciones equinocciales, y veranos calurosos y secos. Bajo estas condiciones, la producción de cultivos de secano se ve influenciada principalmente tanto por la cantidad como por la distribución de las precipitaciones (Oweis et al., 2000). En este contexto climático, la producción de cereales está fuertemente condicionada por la disponibilidad de agua y las altas temperaturas, lo que expone a los cultivos a distintos grados de estrés hídrico, a menudo acompañado de estrés térmico, limitando así su desarrollo y productividad (Rezzouk et al., 2022; Savin et al., 2015).

Entre los factores climáticos que condicionan el rendimiento de los cereales en ambientes mediterráneos, la disponibilidad de agua representa la principal limitación ambiental, especialmente en regiones donde predomina la agricultura de secano (Araus et al., 2003; Gaona et al., 2022). Asimismo, el bajo nivel freático y la irregularidad del almacenamiento de agua en los embalses para riego, también pueden afectar el rendimiento de los cultivos, así como la supervivencia de todos los agroecosistemas durante la estación seca de verano (Tramblay et al., 2020). En este contexto, el déficit hídrico durante el periodo de crecimiento provoca pérdidas de rendimiento en el cereal debido a la reducción en el número de granos de los cultivos (Albrizio et al., 2010). Además, cuando ocurre el estrés hídrico desde la antesis hasta la madurez del cereal, acelera la senescencia foliar y la tasa de llenado del grano, reduciendo así el tiempo disponible para la translocación de reservas de carbohidratos hacia el grano y, en consecuencia, el peso final del grano (Albrizio et al., 2010; Oweis et al., 2000).

Las altas temperaturas durante el llenado del grano, una fase especialmente sensible, pueden reducir tanto el peso como la calidad del grano (Gulino et al., 2023; Passarella et al., 2002). Se ha demostrado que incluso breves episodios de calor intenso

en este periodo disminuyen el tamaño del grano, con un impacto negativo que depende tanto del momento en que ocurre el estrés térmico como de su intensidad (Passarella et al., 2005). Además, estas condiciones están asociadas con alteraciones en la composición de las proteínas del gluten, afectando negativamente las propiedades tecnológicas del grano (Poggi et al., 2022). El aumento de temperaturas entre la elongación del tallo y la antesis actúa como un factor limitante importante, ya que acelera el ciclo del cultivo y reduce su potencial de rendimiento, efecto que se agrava significativamente cuando coincide con una baja disponibilidad hídrica (Albrizio et al., 2010).

El agua y la energía se reconocen como los factores climáticos limitantes más influyentes para el crecimiento de la vegetación (Karnieli et al., 2019). Desde una perspectiva global, y excluyendo las zonas tropicales, Karnieli et al. (2019) demostraron que el crecimiento de la vegetación en latitudes altas o en zonas de gran altitud está limitado principalmente por la energía, mientras que, en latitudes bajas, como la región mediterránea, el principal factor limitante es la disponibilidad de agua. La escasa disponibilidad hídrica se considera el principal factor ambiental que limita el crecimiento y la productividad vegetal en regiones como la mediterránea (Galmés et al., 2007; Gaona et al., 2023; González-Zamora et al., 2021). En este contexto, como respuesta temprana al déficit hídrico, las plantas cierran sus estomas para reducir la pérdida de agua, lo que a su vez limita la fotosíntesis y ralentiza el crecimiento (Flexas et al., 2014). Los principales condicionantes ambientales que afectan a los cereales en ambientes mediterráneos exigen una atención especial, así como una descripción temporal precisa, ya que la sensibilidad de los cultivos a condiciones limitantes en cada fase fenológica, determina períodos críticos de impacto sobre la productividad.

1.4 La sequía

1.4.1 Definición y tipos de sequía

La sequía es uno de los riesgos naturales de más impacto, ya que implica mecanismos complejos y un poder destructivo significativo, limitando la producción agrícola, obstaculizando el desarrollo económico y, en consecuencia, representando una grave amenaza para la seguridad alimentaria mundial (Zhang et al., 2025). Los eventos de sequía pueden manifestarse en una amplia variedad de zonas, no solo en regiones comúnmente percibidas como secas, sino también en áreas que habitualmente se caracterizan por un excedente de agua (Fioravanti et al., 2025). Sus impactos varían notablemente según la región y el momento en que ocurren, lo que complica aún más su gestión y mitigación (Hao y Singh, 2015). Tradicionalmente la sequía se clasifica en cuatro categorías según su naturaleza (Figura 1.4): sequía meteorológica, hidrológica, agrícola y socioeconómica (Yin et al., 2022). Además de estas, Crausbay et al. (2017) propusieron la categoría de sequía ecológica, que considera de manera integrada los aspectos ambientales, climáticos, hidrológicos, socioeconómicos y culturales del fenómeno. Por otro lado, Svoboda et al. (2002) introdujeron el concepto de *flash drought* (FD) o sequía repentina, con el objetivo de resaltar la intensificación anormalmente rápida de ciertos eventos, en contraste con las sequías típicas que evolucionan de forma gradual.

La sequía meteorológica se define como la deficiencia de precipitaciones durante un período prolongado (Wang et al., 2025a). La sequía agrícola está vinculada a la insuficiencia de SM para satisfacer las necesidades de crecimiento de las plantas o la producción de cultivos (Liu et al., 2016). El déficit de precipitaciones durante un período prolongado provoca caudales anormalmente bajos en los ríos, aguas subterráneas o niveles de embalses, lo que impide satisfacer las demandas del suministro de agua, originando la sequía hidrológica (Van Loon, 2015). Los diferentes tipos de sequías están conectados e interactúan de manera compleja (Figura 1.4), de modo que un tipo de sequía conduce gradualmente a otro a lo largo del tiempo. Este proceso de transmisión de señales de pérdida de agua entre los distintos tipos de sequías se conoce como propagación de sequías (Wei et al., 2024). De esta forma, la sequía meteorológica da origen a otros tipos de sequía, ya que el déficit de precipitaciones, combinado con el aumento de la demanda de evaporación atmosférica, puede provocar una disminución prolongada y pronunciada

de la SM (sequía agrícola) e impactar gravemente los sistemas hidrológicos (sequía hidrológica) (Wang et al., 2025a). Por último, la sequía socioeconómica está relacionada con desequilibrios entre la oferta y la demanda de determinados bienes económicos, e incorpora aspectos de los tres tipos de sequía basados en factores físicos: meteorológica, agrícola e hidrológica (Hao y Singh, 2015). Aunque la escasez de precipitaciones es la causa común de todos los tipos de sequía, sus efectos suelen manifestarse primero en el sector agrícola, debido a su mayor exposición y su alta vulnerabilidad económica (Ndayiragije y Li, 2022). Esta situación se agrava en regiones con limitaciones hídricas como la región mediterránea, donde predomina la agricultura de secano, lo que las hace especialmente vulnerables a este fenómeno (Almendra-Martín et al., 2021a; Martínez-Fernández et al., 2015).

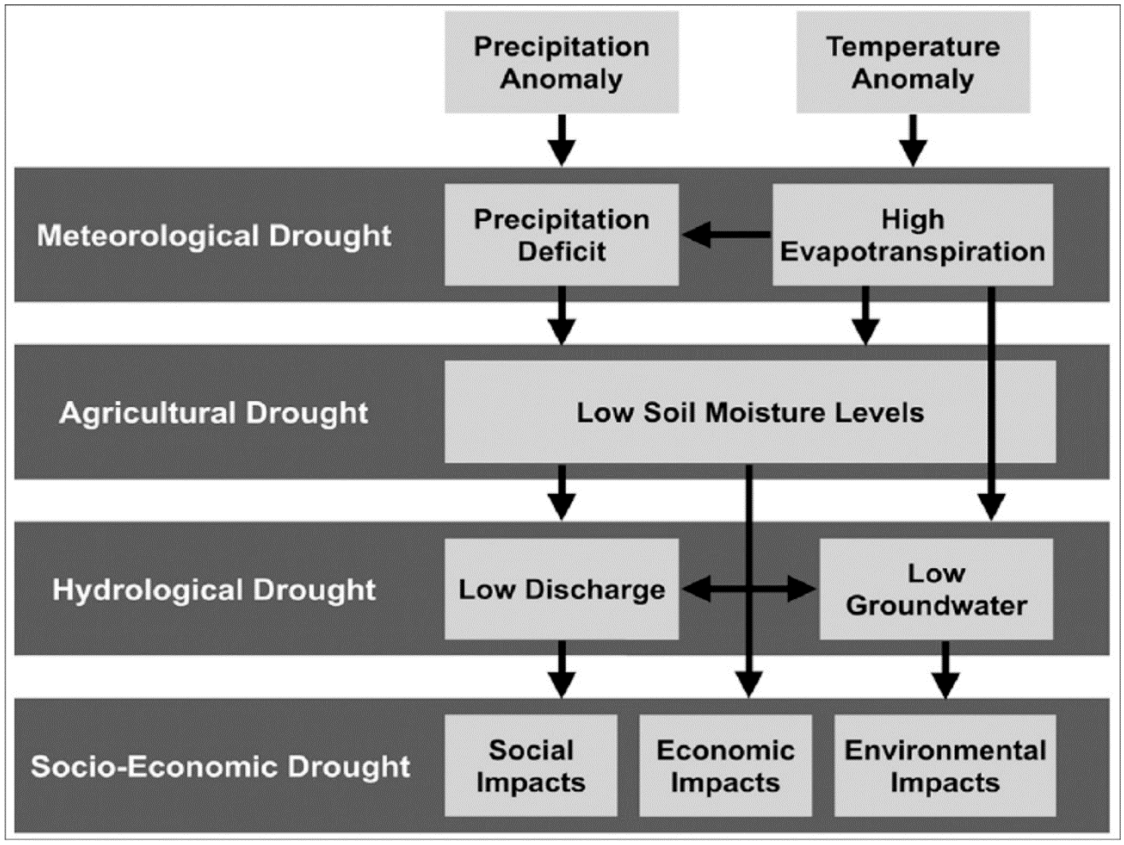

Figura 1.4. Tipos de sequía y sus relaciones causales. Imagen obtenida de Mullapudi et al. (2023).

1.4.2 Sequía agrícola

La sequía agrícola comienza cuando la disponibilidad de SM para las plantas disminuye a tal nivel que afecta negativamente el rendimiento de los cultivos y, por lo tanto, la producción agrícola (Panu y Sharma, 2002; Zhang et al., 2021a). Este concepto hace referencia principalmente al déficit hídrico en los cultivos ocasionado por la reducción del suministro de agua en el suelo. En este sentido, la pérdida de SM, producto de la disminución de las precipitaciones, es la primera señal de este fenómeno (Liu et al., 2016). A medida que continúan los procesos de evaporación y transpiración, el agua disponible en el suelo se vuelve insuficiente para satisfacer las necesidades fisiológicas de las plantas, inhibiendo su crecimiento y, en consecuencia, reduciendo el rendimiento de los cultivos o, en casos graves, provocando su muerte total (Liu et al., 2016). Debido a que esta reducción de la SM afecta directamente al desarrollo de los cultivos y su rendimiento, repercute negativamente en la seguridad alimentaria mundial y en el desarrollo sostenible (Zhang et al., 2024a).

La sequía agrícola puede tener graves consecuencias económicas y sociales, especialmente en regiones con recursos hídricos limitados o con desequilibrios entre la demanda de agua y la capacidad natural de suministro (Sepulcre-Canto et al., 2012). Diversos estudios han evidenciado su impacto, como en el caso de la sequía agrícola de 2005 en España, que provocó una pérdida del 40% de la producción de cereales, con pérdidas estimadas en cultivos de secano y pastos que alcanzaron los 2.500 millones de euros (Sepulcre-Canto et al., 2012). Un estudio realizado por Potopova et al. (2016) sobre cultivos de secano en el sureste de Europa, demostró que la sequía agrícola durante la etapa reproductiva de los cultivos puede reducir significativamente el rendimiento potencial del grano, explicando hasta un 62 % de la variabilidad observada en los bajos rendimientos anuales. Mohammed et al. (2022) observaron que los cultivos de secano son particularmente susceptibles a los eventos de sequía agrícola, especialmente durante el periodo de crecimiento, destacando que 2003 fue el año más drástico para la producción de trigo en Hungría, con las mayores reducciones de rendimiento del periodo 2000-2020, lo que subraya el impacto directo de los episodios de sequía en la producción de cultivos en ese país.

1.4.3 Sequía repentina

El término de "sequía repentina" (*flash drought*, FD) fue introducido por primera vez en 2002 para describir condiciones de sequía que se intensificaban rápidamente (Peters et al., 2002; Svoboda et al., 2002). En los últimos años ha crecido el interés investigador hacia los eventos de sequía a corto plazo debido a sus efectos inmediatos, impredecibles y perjudiciales, especialmente en la productividad agrícola (Christian et al., 2021). Estos eventos se caracterizan por un inicio abrupto, rápida intensificación y una corta duración, provocado por altas temperaturas y precipitaciones por debajo de lo normal, que generan una drástica disminución de la SM y, en consecuencia, puede devastar al sector agrícola, ocasionando pérdidas significativas y daños económicos considerables debido a la reducción de los rendimientos (Tyagi et al., 2022). Este escenario es más probable durante la temporada de crecimiento del cultivo, cuando la demanda evaporativa alcanza sus niveles más altos desde un punto de vista climático, lo que intensifica los efectos de las FD tanto en la agricultura como en los ecosistemas naturales, provocando un estrés evaporativo excesivo que contribuye a eventos extremos como el aumento del riesgo de incendios forestales, el agotamiento de los recursos hídricos, la disminución de la calidad del aire y la reducción de la seguridad alimentaria (Otkin et al., 2018a). El desarrollo característico de una FD puede explicarse como la convergencia de tres factores clave (Figura 1.5): una rápida intensificación del evento (componente "*flash*"), déficits significativos de SM (componente "*drought*") y los impactos derivados tanto de la intensidad como de la duración de dichos déficits (Christian et al., 2024).

Ante el rápido desarrollo de las FD, la implementación de estrategias de mitigación resulta complejo, ya que estos eventos suelen desarrollarse sin previo aviso, son muy rápidos en producirse y conducen a impactos de amplio alcance en todo el territorio (Noguera et al., 2020). Un claro ejemplo de este fenómeno se presentó en el oeste de Rusia en el año 2010 (Christian et al., 2020). Este evento ocurrió durante la fase crítica de crecimiento para los cultivos de trigo, provocando una disminución de hasta el 70% en los rendimientos de las principales regiones productoras (Hunt et al., 2021). En este contexto, España es una de las regiones más afectadas por la sequía en Europa (Almendra-Martín et al., 2022a) y experimenta impactos severos tanto en los cultivos como en los recursos hídricos (Noguera et al., 2023). Noguera et al. (2020) encontraron

que las FD son bastante frecuentes en el país, representando casi el 40% de todos los eventos de sequía, con una mayor incidencia en las estaciones de verano y primavera. Asimismo, la FD de 2012 en Estados Unidos, se consideró uno de los desastres naturales más costosos de la historia del país, con pérdidas agrícolas significativas, debido a que las FD más severas ocurrieron durante las etapas críticas del desarrollo de los cultivos (Otkin et al., 2016). Sin embargo, a pesar de la amenaza que suponen las FD para los cultivos, los estudios sobre estos fenómenos en contextos agrícolas siguen siendo muy limitados (Barbosa, 2023).

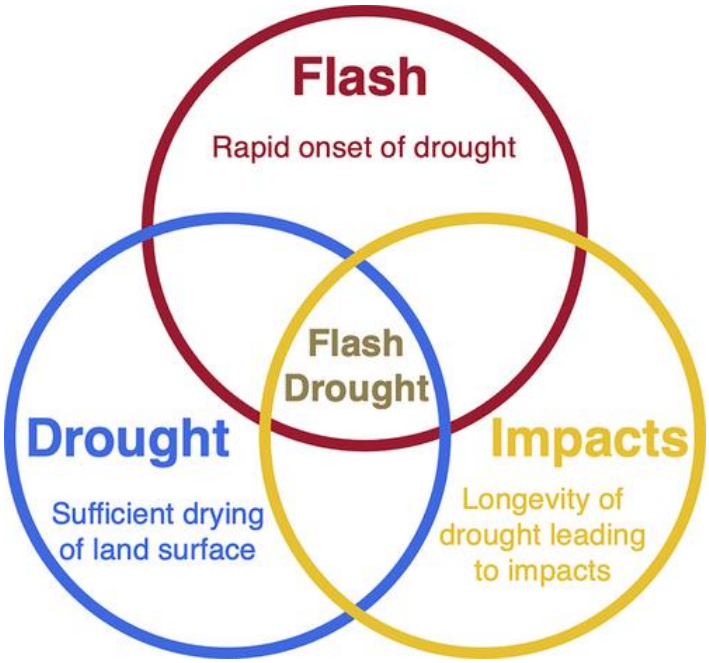

Figura 1.5. Representación esquemática de los factores fundamentales que definen una sequía repentina. Imagen obtenida de Christian et al. (2024).

1.4.4 Humedad del suelo

El agua constituye uno de los recursos naturales más relevantes para los organismos. Su presencia en la Tierra está sujeta a un proceso dinámico conocido como ciclo hidrológico, el cual describe el tránsito constante del agua entre sus diferentes fuentes de almacenamiento. A pesar de que el agua cubre cerca del 75 % de la superficie terrestre, únicamente el 2,5 % corresponde a agua dulce (Oki y Kanae, 2006). De esta proporción, la mayor parte se encuentra almacenada en glaciares o en aguas subterráneas, por lo que solo una fracción muy reducida está fácilmente disponible. Menos del 1% del

agua dulce se encuentra almacenada en sistemas de aguas superficiales, lo que limita aún más las fuentes accesibles (Davamani et al., 2024). Aunque representa solo una pequeña fracción del total de agua del planeta, el agua almacenada en el suelo, denominada humedad del suelo (*soil moisture*, SM) desempeña un papel fundamental en el ciclo hidrológico. La SM se define como el agua presente en la parte no saturada del perfil del suelo, es decir, entre la superficie y el nivel freático (Beldring et al., 1999). Ésta puede expresarse en distintas unidades, siendo la más común y también la más utilizada la humedad volumétrica del suelo, que se refiere a la fracción de volumen de agua en una determinada profundidad (m^3 de agua por m^3 de suelo), o, alternativamente, como la profundidad de una columna de agua contenida en esa misma capa (mm de agua) (Dorigo et al., 2011). Este componente regula el intercambio de agua y energía entre la superficie terrestre y la atmósfera, controla procesos clave como la infiltración, la escorrentía y la evapotranspiración, y actúa como un reservorio temporal de la precipitación (Arora, 2002). Además, el conocimiento de la dinámica de la SM es crucial para el control de eventos extremos como las sequías, especialmente en zonas de secano, donde el agua infiltrada en el suelo a partir de las precipitaciones constituye la única fuente de humedad disponible para los cultivos (Martínez-Fernández y Ceballos, 2003; Martínez-Fernández et al., 2015).

La SM es una variable crítica en numerosos procesos físicos relacionados con la agricultura, la hidrología y la dinámica atmosférica, especialmente en contextos como el mediterráneo, donde constituye un factor limitante. La agricultura de secano en áreas mediterráneas se enfrenta a importantes restricciones debido a la limitada disponibilidad de agua para los cultivos (Jiménez-de-Santiago et al., 2019). En estos entornos, la SM en la zona radicular actúa como un control fundamental en los balances de agua superficial y energía (Detto et al., 2006). Se ha demostrado que el déficit de SM puede alterar significativamente el funcionamiento de la vegetación, siendo la disponibilidad hídrica para las plantas el principal mecanismo responsable de este impacto, con efectos directos sobre la productividad agrícola (Farooq et al., 2009; Huang et al., 2016; Zscheischler et al., 2014). En este sentido, diversos estudios han demostrado que la SM tiene un papel determinante en la productividad vegetal. Por ejemplo, Gaona et al. (2022) analizaron el impacto de la SM de la zona radicular en comparación con otras nueve variables climáticas sobre el rendimiento del trigo y la cebada en las principales regiones cerealistas de España, concluyendo que la SM ejerce una influencia superior, tanto en magnitud

como en duración, respecto a los demás factores, y resulta clave en la variabilidad de los rendimientos de estos cultivos en condiciones de escasez hídrica. De manera similar, González-Zamora et al. (2021) estudiaron la influencia de la SM en la variabilidad del crecimiento de la especie de pino más característica del Mediterráneo frente a diversas variables climáticas, y concluyeron que la SM es el factor determinante en el crecimiento de dicha especie. Esta situación cobra mayor relevancia según el estudio de Almendra-Martín et al. (2022a), en el que investigaron la tendencia de la SM en Europa en las últimas tres décadas y encontraron una tendencia general hacia condiciones más secas junto con un aumento en la frecuencia, la duración y la intensidad de las sequías agrícolas. Estos hallazgos destacan la creciente importancia de monitorizar y comprender la dinámica de la SM y su impacto en los cultivos, especialmente en regiones como las mediterráneas, donde los cultivos de secano son particularmente vulnerables a estos cambios. Este conocimiento es clave para mitigar los impactos negativos en la agricultura, los ecosistemas y los recursos hídricos, y para desarrollar estrategias de adaptación eficaces que aseguren la productividad agrícola y la seguridad alimentaria.

1.4.5 Cambio climático

El cambio climático se refiere a la alteración a largo plazo de los componentes climáticos globales o regionales (Dao et al., 2024). Según el *Intergovernmental Panel on Climate Change* (IPCC) la temperatura global en superficie fue 1,1 ºC más alta en el periodo 2011-2020 que en 1850-1900 (IPCC, 2023). Este aumento de las temperaturas puede influir significativamente en los procesos hidrológicos, ya que incrementa la evaporación del agua superficial y la transpiración de las plantas (Davamani et al., 2024). Esto representa un problema particular para las zonas donde el agua es un factor limitante, ya que el calentamiento asociado al cambio climático acelera la desecación del terreno y aumenta la evapotranspiración, lo que puede tener consecuencias negativas para la productividad agrícola (Dao et al., 2024). En este contexto, la región mediterránea se ha identificado como uno de los puntos críticos del cambio climático global (Giorgi, 2006), y se prevé que el calentamiento en esta área avance a un ritmo superior al promedio mundial (Lionello y Scarascia, 2018). Como resultado, ha sido señalada como una zona de alto riesgo tanto por observaciones actuales como por proyecciones futuras (Lazoglou et al., 2024). Durante el resto del siglo XXI se proyecta un notable aumento de la

temperatura, acompañado de una disminución significativa de las precipitaciones en la región mediterránea (Cos et al., 2022). Además, se espera un fuerte incremento de la evapotranspiración potencial debido al aumento térmico y a la reducción del déficit de presión de vapor de agua en superficie, lo que dará lugar a un acusado incremento de la aridez (Carvalho et al., 2022). El cambio climático representa una amenaza para la seguridad alimentaria, especialmente en las regiones áridas y semiáridas del mundo (Mohammed et al., 2022).

Como resultado del cambio climático, tanto las tendencias observadas como las proyectadas indican un aumento en la frecuencia y severidad de las sequías a escala global, con especial incidencia en regiones que ya sufren un estrés hídrico significativo, como es el caso de la región mediterránea (Cook et al., 2018; Damberg y AghaKouchak, 2014). Los cambios en la frecuencia, intensidad y duración de las sequías tendrían impactos significativos en la gestión del agua, los recursos naturales, la agricultura, los ecosistemas acuáticos y los sectores socioeconómicos, siendo la región mediterránea la más afectada independientemente del tipo de sequía considerado (Lu et al., 2019; Tramblay et al., 2020). Como consecuencia, las pérdidas netas de rendimiento asociadas a la intensificación de las sequías podrían traducirse en una reducción significativa de la productividad agrícola y del valor económico del sector (Naumann et al., 2021).

Las proyecciones climáticas indican un aumento del riesgo de disminución de la SM en el centro, oeste y sur de Europa bajo todos los escenarios considerados (Grillakis, 2019). En este contexto, la sequía agrícola, entendida como el fenómeno en el que la insuficiencia de SM afecta negativamente al desarrollo y rendimiento de los cultivos, ha suscitado una notable atención en todo el mundo, debido a su impacto directo sobre la seguridad alimentaria y el desarrollo socioeconómico sostenible (Pan et al., 2023). Esta preocupación se intensifica ante las proyecciones hacia condiciones más secas para las próximas décadas, lo que plantea nuevas amenazas para la producción agrícola y la disponibilidad de recursos hídricos, especialmente en la región mediterránea (Wang et al., 2022). En este escenario, resulta prioritario mejorar la monitorización y la alerta temprana de la sequía agrícola, así como avanzar en el conocimiento de sus patrones y mecanismos de ocurrencia (Xue et al., 2024). De forma paralela, esta rápida disminución de la SM puede afectar también al desarrollo de las FD (Otkin et al., 2018a). Bajo un escenario de cambio climático global, se prevé un aumento tanto en la frecuencia como en la intensidad de las FD, lo que representa una amenaza creciente para los ecosistemas y, en particular,

para las tierras de cultivo (Lovino et al., 2024). En la región mediterránea se ha observado una intensificación de estos eventos, afectando de forma especial a las zonas agrícolas de secano (Li et al., 2024; O y Park, 2023).

1.5 Métodos para la identificación de la sequía agrícola y su impacto en los cereales.

1.5.1 La humedad del suelo en el estudio de las sequías

1.5.1.1 Técnicas y métodos para la monitorización de la humedad del suelo

La SM es una variable clave que desempeña un papel fundamental en los procesos de retroalimentación entre la superficie terrestre y la atmósfera, siendo esencial en numerosas aplicaciones hidrológicas, meteorológicas y agrícolas (Eswar et al., 2018). Existen diversos métodos para medir o estimar el contenido de agua del suelo, ya sea de forma directa o indirecta. La SM puede obtenerse mediante mediciones de campo (*in situ*), técnicas de teledetección y modelos de simulación del balance hídrico del suelo. Las observaciones *in situ* de la SM consisten en mediciones realizadas directamente en el terreno. Dentro de éstas, el método gravimétrico es el único considerado directo, ya que determina la SM a partir del peso de muestras extraídas a distintas profundidades, las cuales se secan y se pesan antes y después del proceso (Lekshmi et al., 2014). Aunque esta técnica proporciona datos precisos y homogéneos, su aplicación implica mucho tiempo y es destructiva, lo que limita su aplicabilidad a gran escala o en campañas de monitorización continua o prolongadas. En la práctica, esto ha favorecido el uso generalizado de métodos indirectos que, no obstante, requieren calibración previa mediante el método gravimétrico para garantizar la fiabilidad de los resultados (Dorigo et al., 2011).

Los métodos indirectos de medición de la SM se fundamentan en la relación entre esta y ciertas propiedades físicas del suelo como, por ejemplo, la constante dieléctrica, lo que permite obtener estimaciones no invasivas (González-Zamora, 2017). Entre estos métodos se encuentran las sondas de neutrones, cuyas mediciones se basan en la interacción entre los neutrones emitidos por una fuente radiactiva y los átomos de

hidrógeno presentes en el agua del suelo. Esta interacción permite estimar con precisión el contenido de SM, siempre que se lleve a cabo una calibración adecuada con muestras gravimétricas (Zreda et al., 2008). Otro ejemplo son los sensores electromagnéticos, basados en la medición de la constante dieléctrica del suelo, permitiendo una monitorización continua del contenido de agua con mínima perturbación del medio. Estas técnicas, no destructivas ni radiactivas, pueden automatizarse, lo que posibilita obtener mediciones frecuentes en tiempo real a lo largo del día (Lekshmi et al., 2014). Entre ellas, destacan las basadas en principios de reflectometría en el dominio del tiempo (TDR, *time domain reflectometry*) o en el dominio de la frecuencia (FDR, *frequency domain reflectometry*) (Dobriyal et al., 2012). En todos los casos, es necesaria una calibración previa con muestras gravimétricas para asegurar la fiabilidad de los resultados. Existen otras técnicas indirectas para la estimación de la SM, como el método de atenuación de rayos gamma, *Ground Penetrating Radar* (GPR), *Micro Electro Mechanical System* (MEMS), así como técnicas ópticas, entre otras (Lekshmi et al., 2014).

En todo el mundo existen numerosas redes de estaciones *in situ* que monitorizan la SM, cuyas características varían considerablemente según la ubicación geográfica, los sensores empleados y su cobertura espacial (Al-Yaari et al., 2019). Desde hace más de quince años, la *International Soil Moisture Network* (ISMN) se encarga de recopilar y consolidar conjuntos de datos de SM *in situ*, configurando una base de datos global que integra la mayoría de las series temporales generadas por las distintas redes existentes (Dorigo et al., 2011). Aunque su distribución es global, la mayoría de estas redes se concentra en regiones de latitudes medias (Dorigo et al., 2011).

La teledetección es una técnica indirecta que permite estimar la SM a partir de la radiación electromagnética emitida o reflejada por la superficie terrestre (Rahman y Zhang, 2019). A través de sensores a bordo de plataformas aéreas o satélites, se obtienen imágenes que permiten monitorizar variables del suelo de forma global y continua (Mohanty et al., 2017). La SM puede estimarse en diferentes regiones del espectro, desde el visible hasta las microondas (Njoku y Entekhabi, 1996). La región de las microondas en el espectro electromagnético comprende las longitudes de onda entre 1 m y 1 mm (frecuencias 300 MHz–300 GHz) (Norgard y Best, 2017) y son especialmente adecuadas para estimar la SM. Además, al no verse afectadas por la atmósfera ni depender de la iluminación solar, permiten estimaciones continuas de la SM en distintas condiciones climáticas y ecosistemas (Das y Paul, 2015). Se han utilizado habitualmente diversas

frecuencias bajas (bandas X, C y L) para detectar el contenido de humedad de la superficie del suelo desnudo o con vegetación (Mohanty et al., 2017). Sin embargo, la banda L se ha considerado la más adecuada para la estimación de la SM (Laymon et al., 2001). La estimación de la SM en el rango de microondas se fundamenta en la medida de la constante dieléctrica a partir de la emisividad o retrodispersión de la superficie (Das y Paul, 2015). En este sentido, existen dos enfoques: sensores pasivos, que captan la radiación natural emitida por el suelo, y sensores activos, que miden la radiación reflejada tras emitir una señal conocida (Mladenova et al., 2014). Para la monitorización global de la SM, han sido puestos en órbita varios radiómetros y radares de banda L a bordo de satélites (Mohanty et al., 2017). La primera misión satelital diseñada específicamente para estimar la SM fue SMOS (*Soil Moisture and Ocean Salinity*) de la ESA, la cual se lanzó el 2 de noviembre de 2009 y sigue operativa actualmente (Kerr et al., 2016). Esta misión incorporó el primer radiómetro de microondas en banda L enviado al espacio. Posteriormente, la NASA puso en órbita las misiones SAC-D/Aquarius (2011) y SMAP (2015), que incorporaron radiómetros en banda L junto con sensores activos, para aprovechar las ventajas de ambas técnicas (Bruscantini et al., 2014; Chan et al., 2018).

En este contexto, surgió el proyecto *Climate Change Initiative* (CCI) de la ESA, el cual se creó para satisfacer las necesidades de monitorización de las principales variables ambientales, entre ellas la SM, en apoyo a la investigación climática (Dorigo et al., 2015). Aunque un solo sensor podría cubrir algunos de los requisitos básicos, las misiones satelitales individuales suelen tener una duración limitada, lo que impide construir registros climáticos prolongados. Por esta razón, el proyecto integra datos de múltiples sensores de microondas, tanto activos como pasivos (Figura 1.6), para generar una base de datos de SM global, consistente y a largo plazo (Dorigo et al., 2015). No obstante, presenta ciertas limitaciones inherentes, como la presencia de lagunas en los datos. Estas pueden deberse a factores como los tiempos de revisita de los satélites, presencia de hielo, nieve o vegetación muy densa, entre otros. En este contexto, Almendra-Martín et al. (2021b) compararon diferentes métodos para abordar esta limitación y conseguir el relleno de lagunas, considerando tanto enfoques temporales como espaciales, así como distintos conjuntos de variables de entrada. Concluyeron que el método *support vector machine* puede ser adecuado para completar las lagunas en la base de datos de SM del CCI. Los productos de SM de CCI han sido ampliamente validados (An et al., 2016; González-Zamora et al., 2019; McNally et al., 2016) y usados

para diversas aplicaciones (Martínez-Fernández et al., 2019; Nicolai-Shaw et al., 2017; Zhang et al., 2019).

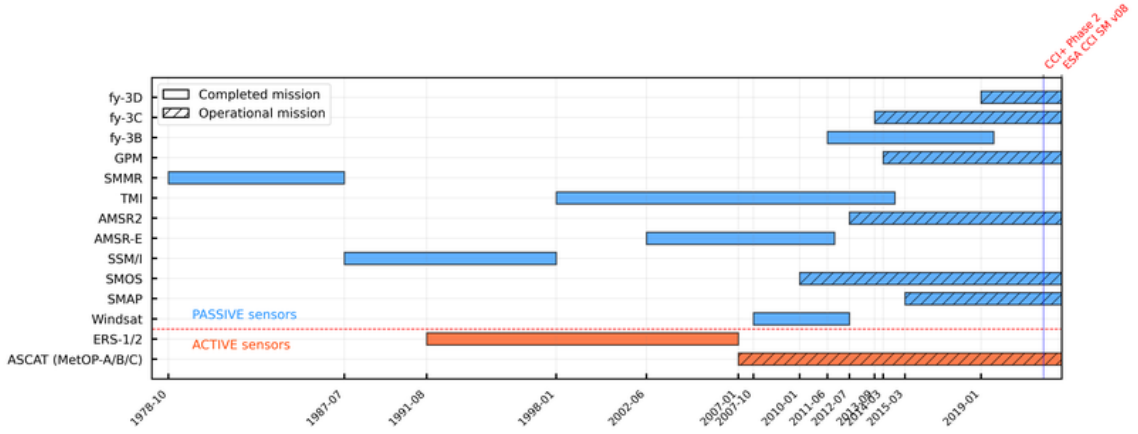

Figura 1.6. Cronología de los sensores de teledetección de microondas pasivos y activos utilizados en la generación del producto ESA CCI SM v08.1. Imagen obtenida de https://climate.esa.int/es/proyectos/soil-moisture/about/

La modelización es una técnica común para estimar series de datos en diversos campos (Lawless, 2011). La SM se ha estimado a través de una multitud de modelos con diferentes características y diferente grado de complejidad, requerimiento de datos o cobertura espacial, entre otras (Brocca et al., 2017). Los modelos hidrológicos y de superficie terrestre (*Land Surface Model*, LSM) son los más usados, ya que ambos simulan el balance hídrico y energético del suelo mediante ecuaciones similares, permitiendo estimar la SM a diferentes escalas temporales y espaciales (Famiglietti y Wood, 1994). Los modelos hidrológicos evolucionaron desde enfoques centrados en estimar la escorrentía o el caudal (modelos de lluvia-escorrentía) que apenas consideraban la SM, hasta incluir su dinámica (Engman, 1990). Existen diversos enfoques de modelización para simular la dinámica temporal de la SM, que se diferencian según su estructura, complejidad y requerimiento de datos. Según el método empleado para representar los procesos, estos modelos pueden clasificarse en tres grandes grupos: modelos de base física, modelos estadísticos y modelos conceptuales (Brocca et al., 2014). Los modelos de tipo conceptual son los más utilizados, lo que permite simular la SM con suficiente precisión sin requerir conjuntos de datos detallados para su calibración y parametrización, empleando diferentes formulaciones para representar los tres

componentes principales del balance hídrico del suelo, es decir, la infiltración, la percolación y la evapotranspiración (Brocca et al., 2014).

Paralelamente, los LSM se desarrollaron para representar los intercambios acoplados de agua, energía y carbono entre la tierra y la atmósfera, incorporando procesos complejos como la dinámica del agua en capas profundas, lo que mejora la representación de la SM y amplía las aplicaciones hidrológicas (Rosero et al., 2009). En conjunto, aunque la modelización es una herramienta valiosa para numerosas aplicaciones, su uso requiere precaución, ya que las estimaciones están condicionadas por la resolución y cobertura espaciotemporal del modelo, la calidad de los datos de entrada y la adecuación del propio modelo. Por ello, resulta imprescindible contar con una correcta validación mediante redes de estaciones *in situ* para garantizar su fiabilidad. Un ejemplo destacado es el modelo hidrológico LISFLOOD, desarrollado por el *Joint Research Centre* (JRC), que utiliza sistemas de información geográfica para simular procesos hidrológicos en grandes cuencas fluviales europeas, y ofrece series de SM con una resolución espacial de hasta 5 km x 5 km (De Roo et al., 2000).

Las series de SM modelizada presentan diversas incertidumbres asociadas a los modelos. Por ello, cada vez es más frecuente el uso de sistemas de asimilación de datos que integran observaciones *in situ* y satélite, lo que ha permitido importantes avances en la generación de lo que se conoce como series de datos de reanálisis (Valmassoi et al., 2023). Esta técnica contribuye a mitigar errores intrínsecos de los modelos y mejorar la representación de los procesos hidrológicos y de la superficie terrestre en las zonas donde existen observaciones (Li et al., 2020). Sin embargo, las bases de datos de estas observaciones también presentan sus propias fuentes de error, lo que puede introducir incoherencias temporales y espaciales al ser integradas en los modelos (Muñoz-Sabater et al., 2021). La eficacia de esta técnica depende de la disponibilidad de dichas observaciones, lo que refuerza la necesidad de contar con redes *in situ* y datos satelitales para una correcta validación de las series de datos (Compo et al., 2011). Ejemplos de bases de datos de reanálisis de SM son la *Global Offline Land-surface Dataset* (GOLD) (Dirmeyer y Tan, 2001), la *Modern-Era Retrospective Analysis for Research and Applications - Land* (MERRA-Land) (Reichle et al., 2011) o las ECMWF Re-Analysis (ERA), como ERA-Interim/Land (Balsamo et al., 2015) y su versión mejorada ERA5-Land (Muñoz-Sabater et al., 2021).

1.5.1.2 Humedad del suelo como indicador de sequía

La SM es un componente clave en el transporte de agua dentro del sistema terrestre, por lo que constituye un indicador fundamental para la monitorización de la sequía agrícola (Pan et al., 2023). No obstante, los datos obtenidos por las diferentes metodologías de medición y estimación de la SM vistos anteriormente, no siempre reflejan de forma explícita la presencia o severidad de una sequía, debido a la complejidad inherente de este fenómeno, cuyo desarrollo, duración y extensión espacial son difíciles de observar directamente (Mishra et al., 2017). Por lo tanto, es habitual transformar los valores observados en indicadores derivados, como anomalías de SM (Shukla et al., 2014), índices de sequía (Martínez-Fernández et al., 2015) o percentiles calculados a partir de distribuciones de probabilidad ajustadas a datos de SM a largo plazo (Eswar et al., 2018). Estas métricas, sin necesidad de conformar índices complejos, permiten evaluar la desviación de la SM actual respecto a las condiciones consideradas normales en un lugar determinado, así como estimar la disponibilidad hídrica en relación con la capacidad del suelo o las necesidades hídricas de la vegetación.

En cuanto al uso de índices, la sequía agrícola fue abordada inicialmente desde una perspectiva principalmente climatológica utilizando índices basados en datos meteorológicos como el *Standardized Precipitation Index* (SPI; McKee et al., 1993), *Precipitation Condition Index* (PCI; Zhang y Jia, 2013), *Atmosphere Water Deficit* (AWD; Purcell et al., 2003), entre otros. Uno de los primeros indicadores de sequía agrícola desarrollados fue el *Crop Moisture Index* (CMI; Palmer, 1968), basado en el *Palmer Drought Severity Index* (PDSI; Palmer, 1965), un índice meteorológico ampliamente utilizado. La SM se considera un factor crítico para el crecimiento de los cultivos y, en consecuencia, una variable fundamental para caracterizar la sequía agrícola (Cao et al., 2022). Inicialmente, la SM se estimaba a partir de balances hídricos o mediante modelización hidrológica a partir de datos meteorológicos. Por ejemplo, Sheffield et al. (2004) desarrollaron un índice de sequía a partir de la SM denominado *Variable Infiltration Capacity (*VIC), Narasimhan y Srinivasan, (2005) propusieron el *Soil Moisture Deficit Index* (SMDI) y el *Evapotranspiration Deficit Index* (ETDI) para analizar la sequía agrícola basándose en la SM modelada con SWAT. Con el avance en la disponibilidad de datos, la SM comenzó a utilizarse directamente para la generación de índices de sequía agrícola. Sridhar et al. (2008) introdujeron el *Soil Moisture Index* (SMI) a partir de observaciones de la *Automated Weather Data Network* (AWDN), destacando

su utilidad en la monitorización de sequías. Más recientemente, Martínez-Fernández et al. (2015, 2016) propusieron el *Soil Water Deficit Index* (SWDI), utilizando series de SM obtenidas de SMOS en el área de la Red de Estaciones de Medición de la Humedad del Suelo (REMEDHUS) y lo compararon con el mismo índice calculado a partir de observaciones *in situ*, obteniendo una buena concordancia y evidenciando el gran potencial de la SM satelital para la monitorización de la sequía agrícola. Si bien el uso de datos *in situ* ha demostrado ser eficaz, el notable avance de la teledetección en las últimas décadas ha proporcionado una alternativa atractiva para la monitorización de sequías agrícolas gracias a su amplia cobertura espacial. Los productos de SM derivados de teledetección han sido aplicados activamente en el desarrollo de diversos índices de sequía agrícola. Por ejemplo, los datos de SMOS se integraron en el SWDI propuesto por Martínez-Fernández et al. (2016). Asimismo, Sánchez et al. (2016) desarrollaron el *Soil Moisture Agricultural Drought Index* (SMADI), combinando datos de SMOS con observaciones del sensor MODIS. En general, se sugiere que la aplicación directa de métricas derivadas de la SM, como anomalías o percentiles, así como el uso de índices basados únicamente en esta variable, constituyen enfoques particularmente eficaces para la monitorización de la sequía agrícola (Cao et al., 2022).

Las FD son un subconjunto de todos los tipos de sequía que se caracterizan por una intensificación inusualmente rápida, ya sea para iniciar una sequía o para exacerbar una sequía existente (Otkin et al., 2018b). Este tipo de eventos puede desarrollarse en el transcurso de pocas semanas, lo que limita significativamente el tiempo disponible para implementar medidas de mitigación y respuesta. Los índices de sequía tradicionales, en muchos casos, no logran captar adecuadamente la rapidez del desarrollo ni los impactos inmediatos asociados, lo que genera importantes lagunas en su monitorización y predicción (Osman et al., 2024). Desde que se introdujo el término de FD por primera vez en 2002 (Peters et al., 2002; Svoboda et al., 2002), el interés por la investigación de este fenómeno ha crecido de forma notable, especialmente durante la última década, motivado por la ocurrencia de eventos de alto impacto, como la FD ocurrida en 2012 en el centro de Estados Unidos (Lisonbee et al., 2022). La mayoría de los estudios coinciden en señalar un déficit de precipitación, una elevada evapotranspiración y/o demanda evaporativa para el desarrollo de una FD (Christian et al., 2024). La combinación de una reducción en el suministro de agua y un incremento en la demanda provoca un rápido descenso en los niveles de SM y de agua subterránea. Por lo tanto, la SM es un indicador

crítico para la monitorización de las FD, ya que integra los efectos del déficit de precipitación y de la evapotranspiración, regula la absorción de agua por las raíces de las plantas y puede influir en la persistencia e intensidad del fenómeno mediante retroalimentaciones suelo-atmósfera (Seneviratne et al., 2010). La monitorización de las FD y el desarrollo de indicadores para su detección se han abordado principalmente desde este marco conceptual, prestando atención a variables como la precipitación (Noguera et al., 2020), la evaporación o demanda evaporativa (Christian et al., 2019a), la SM (O y Park, 2023) y las condiciones de la vegetación (Otkin et al., 2016). Existen diversos índices para la identificación de FD, como el *Evaporative Demand Drought Index* (EDDI) (Hobbins et al., 2016; McEvoy et al., 2016), *Evaporative Stress Index* (ESI, Anderson et al., 2016), *Standard Evaporative Stress Ratio* (SESR, Basara et al., 2019) y la combinación de ESI y el *Rapid Change Rate Index* (RCI, Otkin et al., 2014). Además, las FD suelen identificarse mediante dos enfoques principales: el análisis de tasas de intensificación anómalamente rápidas y la identificación implícita de características de desarrollo a corto plazo (Liu et al., 2020a). Este segundo enfoque clasifica las FD en dos tipos: *precipitation deficit flash drought* (PDFD) y *heat wave flash drought* (HDFD). Aunque ambos se manifiestan por déficits de SM, no la consideran. El otro enfoque se basa en identificar cambios abruptos en variables relevantes (Hunt et al., 2009; Otkin et al., 2018b). Sin embargo, dado que el enfoque para identificar eventos de PDFD y HWFD no incorpora explícitamente la evolución temporal de la SM, no puede garantizar que los eventos presenten una intensificación rápida ni captar eficazmente el inicio de las FD (Liu et al., 2020a). Las FD deben identificarse no solo por su intensidad, sino también por el corto periodo de tiempo en el que se desarrollan, con el fin de diferenciarlas de sequías tradicionales de larga duración (O y Park, 2023). Diversos estudios han propuesto que el cambio de la SM a lo largo del tiempo es un indicador fundamental para su detección, dada su estrecha relación con las condiciones de la vegetación (Hunt et al., 2009; Otkin et al., 2018a). En esta línea, Osman et al. (2024) analizaron las principales variables climáticas empleadas en la definición de FD, incluyendo la precipitación, SM de la zona radicular, temperatura, así como la evapotranspiración real y potencial, y encontraron que la SM de la zona radicular era el indicador más eficaz para identificar las FD. Esta situación reviste especial preocupación en regiones como la mediterránea, caracterizada por condiciones de disponibilidad hídrica limitada, donde predomina el cultivo de cereales de secano (Savin et al., 2022). Sin embargo, a pesar de la amenaza y

las graves consecuencias que suponen las FD para los cultivos, los pocos estudios sobre las FD en regiones agrícolas, se encuentran restringidos a áreas geográficas muy concretas o eventos aislados (Hunt et al., 2021; Otkin et al., 2021), o se enfocan de manera general en las tierras de cultivo sin considerar los impactos en cultivos específicos (O y Park, 2024). Esto pone de manifiesto una brecha importante en el conocimiento sobre los efectos particulares de las FD en la productividad agrícola. Por esta razón, Shah et al. (2022) enfatizaron la necesidad de evaluar de manera integral los efectos de las FD sobre el crecimiento de los cultivos y las pérdidas en productividad, resaltando la urgencia de llevar a cabo investigaciones que aborden los impactos de estos eventos en la agricultura y permitan el desarrollo de estrategias de adaptación efectivas.

1.5.2 Caracterización ecofisiológica y fenológica mediante teledetección

La ecofisiología vegetal representa el estudio de las interacciones entre las plantas y el medio ambiente, proporcionando información sobre la capacidad de las plantas para persistir en un entorno determinado, incluidos aquellos que están cambiando (Valliere et al., 2022). En este contexto, la fenología vegetal, entendida como la secuencia anualmente recurrente de etapas de desarrollo de la vegetación, adquiere especial relevancia, ya que desempeña un papel esencial en la regulación de la variabilidad interanual de los ciclos del carbono y del agua en los ecosistemas terrestres (Zhou et al., 2022). Las métricas fenológicas del ciclo vegetativo de los cultivos, como el inicio o siembra (*start of season*, SOS) y el final o cosecha (*end of season*, EOS), se han consolidado como indicadores ampliamente utilizados para evaluar las respuestas de la vegetación a las condiciones ambientales (Xu et al., 2020). Estas métricas permiten analizar tanto el comportamiento estacional de las plantas como su sensibilidad a factores de estrés, lo cual resulta fundamental para explicar la dinámica interanual del carbono terrestre (Zhou et al., 2022). Comprender cómo varía la fenología vegetal frente a cambios climáticos es, por tanto, esencial para anticipar los efectos del cambio global sobre los ecosistemas terrestres (Wang et al., 2020).

La obtención de información fenológica de los cultivos se ha basado tradicionalmente tanto en observaciones de campo como en datos de teledetección (Gong et al., 2024). Si bien los registros *in situ* ofrecen datos precisos y detallados sobre el

desarrollo de las plantas, su aplicación se ve limitada por la escala espacial y temporal que abarcan, lo que dificulta el seguimiento de dinámicas fenológicas a gran escala o durante largos periodos de tiempo. Aunque numerosos estudios han empleado estos datos para analizar tendencias fenológicas, reconocen sus limitaciones en cuanto a cobertura geográfica y continuidad en el tiempo, especialmente en entornos complejos (Meng et al., 2021; Walther et al., 2002). Asimismo, ante la intensificación del cambio climático global, que está generando alteraciones significativas en los ecosistemas terrestres, se hace cada vez más urgente comprender y monitorizar los cambios fenológicos de la vegetación a escalas espaciales y temporales más amplias (Piao et al., 2019).

Frente a estas limitaciones, los datos obtenidos mediante teledetección se han consolidado como una herramienta eficaz para la monitorización de la fenología de la vegetación en grandes extensiones territoriales y con una frecuencia temporal adecuada (Xu et al., 2020). El seguimiento fenológico mediante sensores satelitales comenzó en la década de 1970, cuando la tecnología de teledetección se encontraba aún en sus primeras etapas. Los investigadores empleaban principalmente datos del programa Landsat, desarrollado conjuntamente por la NASA y el USGS (Gong et al., 2024). Aunque Landsat cuenta con una extensa serie temporal, su ciclo de revisita de 16 días limita su capacidad para capturar cambios fenológicos con más detalle. Posteriormente, la incorporación de sensores como MODIS y AVHRR marcó una nueva etapa en la observación remota de la fenología vegetal, al ofrecer una cobertura espacial más adecuada para estudios a gran escala (Gong et al., 2024).

Las series temporales de índices de vegetación derivados de imágenes de satélites constituyen la principal fuente de datos para inferir parámetros fenológicos de la vegetación (Jin y Eklundh, 2014). Entre los índices comúnmente empleados destacan el NDVI (*Normalized Difference Vegetation Index*) y el EVI (*Enhanced Vegetation Index*). El NDVI, propuesto por Rouse et al. (1974), es el índice más utilizado en la estimación fenológica a partir de teledetección, debido a su simplicidad de cálculo y amplia aplicabilidad. Este índice mitiga en gran medida los efectos de factores como la topografía, las condiciones de iluminación, la cobertura nubosa y la interferencia atmosférica, proporcionando información representativa sobre el estado de la vegetación y su cobertura (Huete et al., 2002). No obstante, el NDVI presenta limitaciones en zonas con alta biomasa, ya que tiende a saturarse, lo que reduce su sensibilidad en áreas con vegetación densa (Rocha y Shaver, 2009). En estos contextos, el EVI se presenta como

una alternativa más adecuada en coberturas vegetales de moderada a alta densidad, permitiendo una monitorización más precisa de la fenología de la vegetación (Son et al., 2014). Además otros indicadores derivados de teledetección, como el LAI (*Leaf Area Index*) y la GPP (*Gross Primary Production*), desempeñan un papel clave en la evaluación de la respuesta de la vegetación frente a los condicionantes ambientales (Fang et al., 2023; Li y Qu, 2018). El LAI es un indicador fundamental para representar la estructura y evolución de la cobertura vegetal, y ha sido reconocido como una variable indispensable en la investigación del cambio climático global (Wang et al., 2025b). Por su parte, la GPP cuantifica la cantidad de dióxido de carbono fijado por la vegetación por unidad de superficie y tiempo, y constituye un indicador esencial del crecimiento vegetal y de la actividad fotosintética (Sun et al., 2019).

El proceso de monitorización de la fenología de la vegetación mediante teledetección (Figura 1.7) se inicia con la adquisición de imágenes a través de plataformas como satélites o drones. Estas imágenes son sometidas a un preprocesamiento orientado a corregir interferencias atmosféricas y otros contaminantes. Posteriormente, se calculan diversos índices de vegetación que, tras ser suavizados mediante técnicas adecuadas, permiten una extracción precisa y fiable de los parámetros fenológicos (Gong et al., 2024). Existen diversos enfoques para la extracción de parámetros fenológicos a partir de series temporales de índices de vegetación obtenidas mediante teledetección. Entre los métodos más utilizados se encuentran aquellos basados en umbrales (fijos o dinámicos), que identifican el momento en que la curva del índice de vegetación supera ciertos valores predefinidos (White et al., 2014). Mientras que los métodos de umbral fijo comparan la evolución estacional con un valor constante, los enfoques más adaptativos, como el umbral dinámico modificado, ajustan la detección fenológica a la dinámica temporal de cada serie, lo que mejora su precisión (Huang et al., 2019). Además, se han empleado otros muchos métodos como el método de media móvil (Duchemin et al., 1999), el método de ajuste de funciones (Beck et al., 2006), el método de regresión lineal segmentada (Magney et al., 2016) y el método de pendiente máxima (Sakamoto et al., 2005).

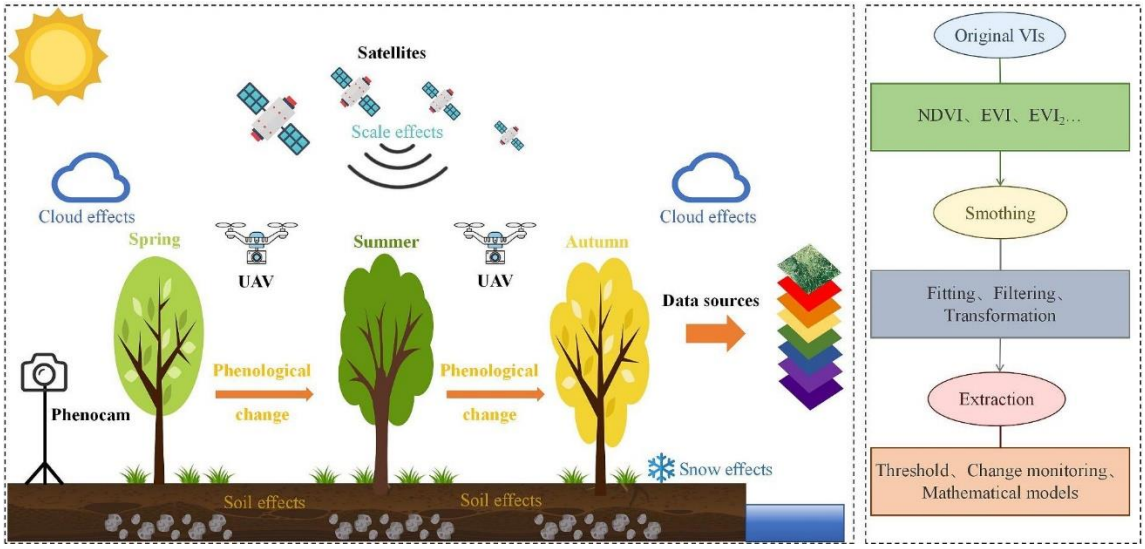

Figura 1.7. Representación esquemática de la monitorización mediante teledetección de la fenología de la vegetación. Imagen obtenida de Gong et al. (2024).

1.5.3 Evaluación de tendencias de la sequía agrícola y su impacto en el cereal.

El calentamiento global ha provocado que en las últimas décadas se incremente el interés por analizar las tendencias en series temporales climáticas e hidrológicas. Este tipo de estudios se ha consolidado como una herramienta fundamental para comprender la evolución de las variables hidrológicas, tanto a partir de registros históricos como de escenarios proyectados por modelos climáticos (Almazroui y Şen, 2020). En este contexto, el análisis de tendencias permite identificar cambios temporales significativos en fenómenos hidroclimáticos, parámetros fenológicos e índices agroclimáticos, proporcionando una base científica para mejorar las proyecciones futuras y orientar la toma de decisiones en materia de mitigación y adaptación (Almazroui y Şen, 2020). Su aplicación es especialmente relevante en regiones donde el agua es un factor limitante, donde el riesgo de escasez hídrica es elevado y la planificación eficiente de los recursos depende en gran medida del conocimiento de las dinámicas fenológicas, climáticas e hidrológicas (Achite et al., 2021).

Los métodos estadísticos empleados en el análisis de tendencias suelen agruparse en dos grandes categorías: paramétricos y no paramétricos (Bianchi et al., 1999). Esta clasificación responde tanto a criterios estadísticos como a las características propias de las series temporales, las cuales a menudo presentan comportamientos no lineales, no

estacionarios y con presencia de datos atípicos. Los métodos paramétricos parten del supuesto de que los datos siguen una distribución específica (normalidad), así como de la estacionariedad y la independencia de las series temporales, condiciones que rara vez se cumplen en las series hidrológicas (Jamali y Eslamian, 2023). En esta categoría se incluyen técnicas clásicas como la regresión lineal de mínimos cuadrados (Watson, 1967), la prueba *t* de Student (Kim, 2015) y la regresión cuantílica (Koenker, 2005). Si bien son herramientas sencillas y computacionalmente eficientes, su aplicación puede ser limitada cuando los supuestos estadísticos no se cumplen, lo cual es frecuente en datos hidrológicos (Jamali y Eslamian, 2023). Además, estos métodos son sensibles a la presencia de valores atípicos y pueden inducir errores en la interpretación de las tendencias si no se manejan adecuadamente (Hirsch et al., 1991). Por esta razón, el uso de métodos paramétricos es menos frecuente en comparación con los no paramétricos (Lakhankar et al., 2009).

Los métodos no paramétricos no requieren que los datos cumplan condiciones de normalidad o linealidad, y presentan mayor tolerancia a la presencia de valores atípicos (Jamali y Eslamian, 2023). Entre los más utilizados se encuentran aquellos que operan en el dominio temporal, como la prueba de Mann-Kendall (MK) o el coeficiente de correlación de Spearman, ampliamente utilizados en la detección de tendencias en series hidroclimáticas, incluida la SM (Almendra-Martín, 2022). La prueba de MK (Kendall, 1948; Mann, 1945), es una de las herramientas no paramétricas más utilizadas para evaluar la presencia de tendencias en series temporales (Hamed, 2008). Dado que muchas variables hidrometeorológicas presentan distribuciones asimétricas, el uso de este tipo de prueba resulta especialmente apropiado (Yue y Pilon, 2004). Se trata de un método estadístico simple y no paramétrico que permite analizar series temporales incluso en presencia de datos con lagunas. No obstante, presenta limitaciones frente a la autocorrelación de las series, una característica común en muchas variables hidro-climáticas (Hamed y Rao, 1998).

Además, existen enfoques más avanzados que incorporan análisis en el dominio de frecuencias, como la transformada de Fourier o el test de medias móviles. Estos métodos requieren asumir condiciones de estacionariedad y linealidad en las series temporales, lo cual puede ser restrictivo en el caso de las variables hidrológicas, ya que éstas suelen presentar comportamientos no lineales y no estacionarios (Coulibaly y Baldwin, 2005). Finalmente, ha cobrado relevancia el uso de los métodos híbridos que

combinan información de los dominios temporal y de frecuencias, como el test basado en *wavelet* o el *Empirical Mode Decomposition* (EMD) (Almendra-Martín, 2022; Nazari et al., 2025). Estos enfoques son ampliamente utilizados en hidrología para analizar señales no estacionarias y no lineales, permitiendo su descomposición de manera eficaz (Joseph et al., 2024).

La mayoría de los estudios que analizan tendencias en sequías agrícolas se basan en métodos no paramétricos, especialmente en la prueba de MK (Golian et al., 2015; Pan et al., 2023; Potopova et al., 2016). Además, esta prueba ha sido ampliamente aplicada en el análisis fenológico, especialmente para detectar tendencias en los ciclos de las plantas, utilizando datos de teledetección y observaciones *in situ* (Bandoc et al., 2022; Estefania-Salazar y Iglesias, 2025; Sisheber et al., 2023). Esta elección metodológica adquiere particular importancia ante el aumento de la frecuencia e intensidad de eventos hidrológicos extremos, como las sequías, cuyo riesgo se prevé que siga incrementándose como consecuencia del cambio climático (Bjarke et al., 2024). En este contexto, el análisis de tendencias resulta esencial para evaluar de forma precisa los impactos de estos fenómenos sobre la dinámica hidrológica y fenológica (Jamali y Eslamian, 2023; Jiao et al., 2020).

Además del análisis de tendencias, para analizar el impacto en el cultivo del cereal, se emplean comúnmente técnicas estadísticas de correlación que permiten cuantificar la relación entre variables climáticas, parámetros fenológicos, índices agroclimáticos o parámetros agronómicos, entre otros (Garcia y Garcia et al., 2008; Peña-Gallardo et al., 2019; Reidsma et al., 2009). Entre estas técnicas, el coeficiente de correlación de Pearson es uno de los métodos paramétricos más utilizados para evaluar relaciones lineales bajo el supuesto de normalidad en los datos (Sung et al., 2021). Además, este coeficiente se ha empleado ampliamente para analizar la relación entre variables climáticas, parámetros fenológicos y productividad vegetal, con el objetivo de identificar los factores que impulsan las respuestas de la vegetación frente al cambio climático (Li et al., 2021; Yang et al., 2024; Zhao et al., 2024). Ante el incumplimiento de los supuestos de normalidad, el coeficiente de correlación de Spearman se utiliza como alternativa. El coeficiente de Pearson refleja la magnitud de la relación lineal entre dos variables, mientras que el coeficiente de Spearman mide la relación monótona entre ellas, sin asumir linealidad ni normalidad. Ambos coeficientes de correlación devuelven un valor más cercano a 1 (o −1) cuando los dos conjuntos de datos diferentes tienen una

fuerte relación positiva (o negativa). Estas herramientas permiten identificar cómo se relacionan variables climáticas, parámetros fenológicos, índices agroclimáticos o parámetros agronómicos, entre otros, facilitando así la detección de factores de riesgo asociados a la sequía y otras condiciones climáticas adversas.

CAPÍTULO 2

IMPACT OF AGRICULTURAL DROUGHT ON BARLEY AND WHEAT YIELD: A COMPARATIVE CASE STUDY OF SPAIN AND GERMANY

Benito-Verdugo, P., Martínez-Fernández, J., González-Zamora, Á., Almendra-Martín, L., Gaona, J., Herrero-Jiménez, C.M. (2023). Impact of agricultural drought on barley and wheat yield: A comparative case study of Spain and Germany. *Agriculture*, *13*(11), 2111. https://doi.org/10.3390/agriculture13112111

Resumen

Ante el creciente interés por los impactos de la sequía en los cultivos, este trabajo analiza el impacto de la sequía agrícola sobre el trigo y la cebada durante el periodo 2001–2020. El estudio se llevó a cabo en las regiones españolas de Castilla y León y Castilla–La Mancha, con superficies aproximadas de 94.000 km² y 79.000 km² respectivamente, y en las regiones alemanas de Nordrhein-Westfalen, Niedersachsen y Bayern, con superficies aproximadas de 34.000 km², 48.000 km² y 71.000 km², respectivamente. Estas regiones representan las principales zonas cerealistas de España y Alemania. La humedad del suelo (SM) en la zona radicular se obtuvo a partir de la base de datos del modelo LISFLOOD, empleándose las anomalías de SM como índice de sequía agrícola. Las variables del estado del cultivo, como la productividad primaria bruta (*gross primary productivity*, GPP) y el índice de área foliar (*leaf area index*, LAI), se obtuvieron del sensor MODIS (*Moderate Resolution Imaging Spectroradiometer*), identificando el mes en el que la SM ejerce la mayor influencia sobre ellas. Los datos de los rendimientos de los cultivos en España y Alemania se obtuvieron del Ministerio de Agricultura, Pesca y Alimentación de España y de la Oficina Federal de Estadística de Alemania, respectivamente. Los años de sequía agrícola y su impacto sobre el rendimiento de los cereales se determinaron a escala regional, aplicando tres enfoques diferentes en torno al mes crítico, considerando distintos periodos de tiempo: el mes crítico, el mes crítico junto con el anterior o el posterior, y el mes crítico junto con el anterior y el posterior. Para determinar el mes crítico se aplicaron dos análisis diferentes, en función de las diferentes condiciones medioambientales de cada país. En España se realizó un análisis de correlación mensual entre las anomalías de la SM y el rendimiento de los cereales y, en Alemania se empleó un análisis de tendencias mensuales de las anomalías de la SM. Los resultados mostraron una dependencia de las variables del cultivo respecto a la SM durante los meses de primavera en ambos países, y también en los meses de verano en Alemania. Se observaron diferencias ligadas a las condiciones ambientales. En España, se registró una considerable reducción del rendimiento de los cereales que superó el 30%. De igual forma, en Alemania se observó un indicio preocupante, con una tendencia creciente a la aparición de sequías agrícolas y una reducción del rendimiento de los cereales cercana al 5%. Ante las previsiones futuras sobre el impacto negativo del cambio climático en la producción mundial de alimentos, este estudio aporta información útil para

la gestión hídrica y agrícola en un contexto de cambio climático. Tanto en las regiones ya amenazadas como en aquellas que hasta hace poco no estaban afectadas, resulta fundamental estudiar medidas de adaptación que permitan mitigar el impacto de la sequía agrícola sobre los cultivos, mejorando así la productividad hídrica y la seguridad alimentaria futura.

Palabras clave: humedad del suelo; rendimiento; trigo; cebada; sequía agrícola; cereal de secano; España; Alemania.

Abstract

Given the growing interest in drought impacts on crops, this work studied the impact of agricultural drought on wheat and barley during the period 2001–2020. The study was carried out in the Spanish regions of Castilla y León and Castilla–La Mancha, with approximate areas of 94,000 km2 and 79,000 km2, respectively, and in the German regions of Nordrhein-Westfalen, Niedersachsen and Bayern, with approximate areas of 34,000 km2, 48,000 km2 and 71,000 km2, respectively. These are the main cereal-growing regions of Spain and Germany. Soil moisture (SM) in the root zone was extracted from the LISFLOOD model database, and SM anomalies were used as the agricultural drought index. Gross primary productivity (GPP) and leaf area index (LAI) variables were obtained from the Moderate Resolution Imaging Spectroradiometer (MODIS), and the month in which SM is most influential on these crop state variables was identified. Crop yields in Spain and Germany were obtained from the Spanish Ministry of Agriculture, Fisheries and Food and the German Federal Statistical Office, respectively. Agricultural drought years and their impact on cereal yields were determined on a regional scale using three approaches based on the critical month with different time periods. These approaches were the use of the critical month and the two (before or after) and the three months (before and after) around the critical month. Two different analyses were used to identify the critical month, depending on the different environmental conditions in each country. These two approaches consisted of a monthly correlation analysis between SM anomalies and cereal yield in Spain and a monthly trend analysis of SM anomalies in Germany. The results showed a dependence of crop variables on SM in spring months in both countries and in summer months in Germany. Differences were found depending on the environmental conditions. A considerable reduction in cereal yields was obtained in Spain which exceeded 30%. Similarly, a worrying sign was observed in Germany, with a positive agricultural drought trend and a yield reduction of almost 5% in cereal crops. In view of future forecasts of the negative impact of climate change on global food production, this study provides valuable information for water and agricultural management under climate change scenarios. Both in regions that are already threatened and in those that until recently were not affected, it is necessary to study adaptation measures to avoid aggravating the impact of agricultural drought on crops, which could improve water productivity and future food security.

Keywords: soil moisture; yield; wheat; barley; agricultural drought; rainfed cereal; Spain; Germany.

2.1. Introduction

Global warming has led to rising temperatures, causing environmental changes that have accelerated the water cycle, thus increasing extreme hydrological events and, therefore, reducing water availability and increasing water resource vulnerability (Chagas et al., 2022; Kundzewicz, 2008). Over much of the globe, as a result of climate change, drought has become one of the worst disasters (Spinoni et al., 2018), and its frequency and intensity are expected to increase (Dube et al., 2022; Martínez-Fernández et al., 2015), particularly in water-limited regions (Vicente-Serrano et al., 2020). Droughts adversely affect crops, but the consequences vary according to plants, soils and regions (Labedzki and Bak, 2014). Thus, drought is considered one of the major natural hazards with significant impacts on the environment, society, agriculture and the economy (Alkhalidi et al., 2023).

Drought is classified into four categories based on its nature: meteorological, hydrological, agricultural and socioeconomic drought (Yin et al., 2022). Agricultural drought is a period in which the soil moisture (SM) supply is less than the minimum needs of plants, so them yields of crops and, therefore, their production are negatively affected (Palmer, 1965; Quiring and Papakryiakou, 2003). Studies and assessments of agricultural drought are crucial, as it is considered the most serious concern in many countries from food security, social stability and economic perspectives (Feng et al., 2019; He et al., 2013).

Agriculture is the main land use type in Europe, which is an activity that requires a significant amount of water, an increasingly scarce resource (Bednar-Friedl et al., 2022; Iglesias and Garrote, 2015). In fact, SM drought risk is projected to increase in central western Europe and southern Europe under all climate scenarios, and the Mediterranean region is expected to be the most affected region, regardless of the type of drought (Bednar-Friedl et al., 2022; Grillakis, 2019; Tramblay et al., 2020). This hazard is especially important, as the European Union (EU) is one of the largest cereal producers in the world, with wheat (*Triticum*) and barley (*Hordeum vulgare*) cereals standing out in terms of planted area (EC, 2023). As a consequence, net yield losses will reduce the economic output of agriculture in the EU (Naumann et al., 2021).

This scenario is emphasized in rainfed agriculture owing to its increased vulnerability to climate anomalies (Rao and Gopinath, 2016). Under rainfed conditions, important crops such as wheat and barley often suffer from droughts that cause significant yield losses (Hossain et al., 2012). Looking ahead to the next decades, it is believed that production levels will stagnate for a variety of reasons, but mainly due to climate change and adverse weather events (EC, 2023). Thus, in the face of a changing climate, it is crucial to analyze and understand the impact of climatic extremes on past and present crop yields to ensure and optimize yields. Thus, several studies (Hernandez-Barrera et al., 2017; Páscoa et al., 2017; Peña-Gallardo et al., 2019) have analyzed the drought vulnerability of crops in Spain and the impact on crop yields and consider the need for further analysis to help unravel the climatic mechanisms influencing yield responses to climate in Spain. In addition, with the same approach, several studies have been conducted in Germany (Eyshi Rezaei et al., 2015; Kloos et al., 2021) suggesting the specifical analysis of individual drought years with respect to relevant variables and the performance of a monthly correlation analysis between drought indices and crop yields to determine possible seasonal focal points.

It is increasingly difficult to ignore SM as a key variable of the natural system (Seneviratne et al., 2010). SM availability is a nexus of the water and the energy and carbon cycles, as well as a primary process in the climate system (Falloon et al., 2011; Jung et al., 2010). SM drought has been shown to alter vegetation processes (Huang et al., 2016), and in many of them, plant water availability is responsible for this effect (Zscheischler et al., 2014). In fact, in agriculture, SM is an essential variable because its scarcity is an obstacle to proper plant productivity (Farooq et al., 2009), reducing crop yields (Rossato et al., 2017).

However, despite the importance and interest in agricultural impacts caused by soil moisture deficits, few studies have quantified the impact in terms of crop yields in each zone (Yao et al., 2022). Many drought indices have been developed (Zargar et al., 2011), but meteorological drought indices are usually used to assess the impact of drought on agricultural production (Li et al., 2022; Nath et al., 2017). When agricultural drought indicators are used, SM is usually not used as the primary variable but as a derived variable (Krueger et al., 2019), despite SM being the variable by which agricultural drought is defined. This is so, even though SM has been shown to be the critical variable

in the productivity of strategic crops under certain environmental conditions (Gaona et al., 2023).

This study aims to analyze the impact of agricultural drought on wheat and barley crop yields in rainfed systems from different perspectives and under different environmental scenarios. The analysis was performed in the main cereal-growing regions of Spain and Germany, two of the most important countries for the production of these crops in Europe, during the 2001–2020 period. For this purpose, the monthly SM anomalies in the root zone, obtained from the LISFLOOD model database (Sepulcre-Canto et al., 2012), were considered as the agricultural drought index. The study allows for a comparison of the effect of agricultural drought on wheat and barley crops in two areas with different climatic (water-limited vs. energy-limited) conditions over the last two decades. This work can help inform management decisions to face future scenarios, both in water-limited and in energy-limited regions, for these two key cereals.

2.2. Materials and Methods

2.2.1. Study area

Spain and Germany were selected as study areas (Figure 2.1) for different reasons. The first reason is because several studies have observed significant drought trends in southern and central Europe (Almendra-Martín et al., 2022a; Hänsel et al., 2019). Second, due to the importance of cereal grain production in Spain and Germany, they were among the top 5 producing countries in Europe in 2022 (EUROSTAT, 2023a). Finally, the last reason is due to the different characteristics hindering crop productivity which allow for a comparison of impacts under a wide range of conditions, from the limited water of Spain to the mainly limited energy of Germany (Nemani et al., 2003; Schumacher et al., 2020).

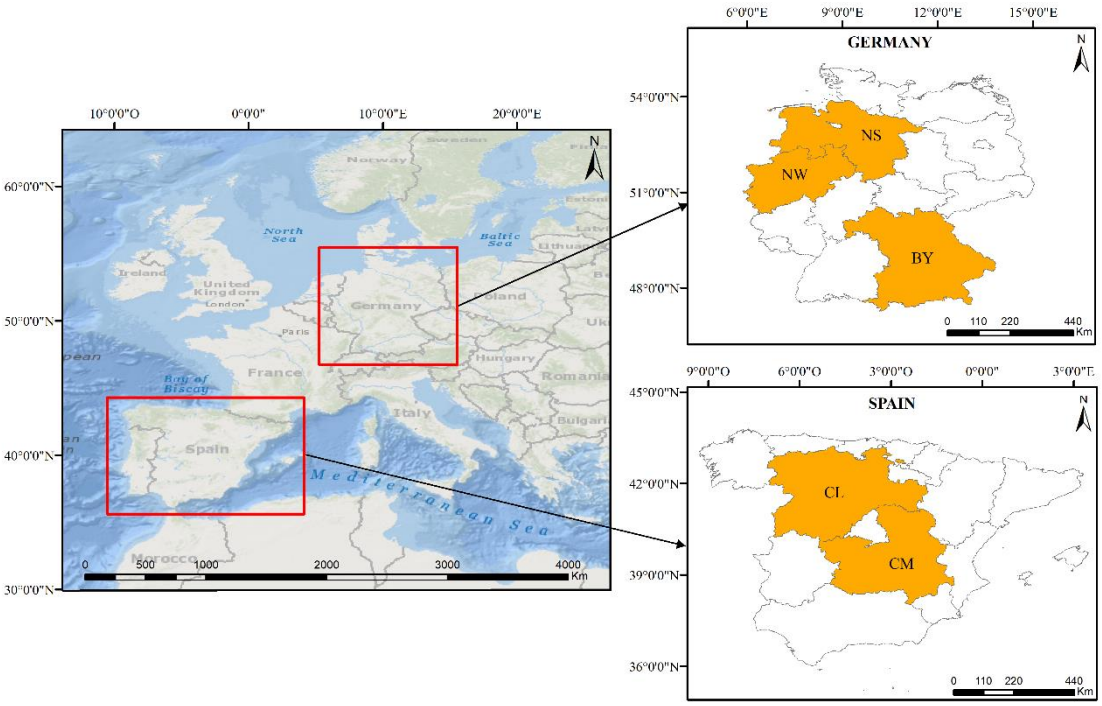

Figure 2.1. Study areas. Regions of Germany (right, top) and Spain (right, bottom) selected for study (shaded orange): Nordrhein-Westfalen (NW), Niedersachsen (NS), Bayern (BY), Castilla y León (CL) and Castilla–La Mancha (CM).

In Spain, the regions of Castilla y León (CL) and Castilla–La Mancha (CM) were selected as the areas to be studied (Figure 2.1) since they are the main cereal-producing regions, accounting for approximately 60% of cereal production (MAPA, 2025a). The CL and CM regions consist of 9 and 5 provinces, respectively, and are characterized by a semiarid Mediterranean climate, with cold winters and hot summers, average temperatures ranging between 10 ˚C and 15 ˚C and total annual rainfall ranging between 350 mm and 600 mm (Csb climate according to Köppen–Geiger classification) (Beck et al., 2018). The same approach was used in Germany, where the regions of Bayern (BY), Niedersachsen (NS) and Nordrhein- Westfalen (NW) were selected (Figure 2.1) as the regions with the highest cereal production, accounting for almost 41% of total production (EUROSTAT, 2023b). BY, NS and NW are composed of 7, 4 and 5 districts, respectively, characterized by a temperate continental climate, with cold winters and mild summers, average temperatures around 9 ˚C and total annual rainfall around 900 mm (Cfb and Dfb according to Köppen–Geiger classification) (Beck et al., 2018).

2.2.2. Irrigation and Cereal Cover Mask

To study the areas of rainfed wheat and barley crops, two databases were used to create a mask that filters out all the areas other than the target areas. To exclude irrigated areas, the Digital Global Map of Irrigation Areas of the Food and Agriculture Organization (FAO) was used, which represents the global area equipped with irrigation at a spatial resolution of 5 arc minutes or 0.083 decimal degrees (Siebert et al., 2013). Additionally, to discard areas with different land cover types, the Climate Change Initiative (CCI) Land Cover (LC) map from the European Space Agency (ESA) was used. It describes Earth's land surface in 37 original LC classes based on the United Nations Land Cover Classification System (UN-LCCS) (Di Gregorio, 2005), with a spatial resolution of 300 m (Defourny et al., 2012).

In this study, ArcGIS v10.8 software (ESRI®, Redlands, CA, USA) was used to create the mask of irrigated areas, together with land cover maps. First, the irrigation and the land cover maps were resampled in the grids of the soil moisture and the GPP-LAI databases. Then, one mask for each database (soil moisture and GPP-LAI) was calculated by hiding all the pixels with more than 10% irrigated area and those with a land cover other than rainfed cropland, assuming that barley and wheat are the main cereals in those areas.

2.2.3. Soil Moisture Database

The hydrological rainfall-runoff model LISFLOOD developed by the floods group of the Natural Hazards Project of the Joint Research Centre (JRC) of the European Commission (Burek et al., 2013; De Roo, 1999) was used as the SM database. It is utilized by the European Flood Alert System (EFAS) and the European Drought Observatory (EDO) for flood and drought monitoring, respectively (Cammalleri et al., 2017; Thielen et al., 2009). The database has been validated (Laguardia and Niemeyer, 2008) and satisfactorily used in many studies (González-Zamora et al., 2022; Sarmiento et al., 2023). The model provided SM data with a spatial scale of 5 × 5 km and a daily temporal resolution, with data from 1991 to the present (De Roo et al., 2000).

Moreover, it provides SM in three different depth layers in each pixel, but in this work, only the first two layers (0–100 cm) were selected. The SM value of the two layers

was averaged to first obtain a daily series of root zone SM, and then a monthly series of root zone SM throughout the study period was obtained from 2001 to 2020.

2.2.4. Wheat and Barley Crop Data

Yield data for wheat and barley crops were obtained on an annual scale, for every province of the study area, from 2001 to 2020. Provincial and regional yield data for the Spanish regions CL and CM were obtained from the Statistical Yearbook of the Ministry of Agriculture (MAPA, 2025a), which provides provincial and regional grain yields (kg/ha) of wheat and barley in rainfed systems for the period 1904–2020. The crop yield data for the NW, NS and BY regions of Germany were obtained from the German Federal Statistical Office (DESTATIS, 2023), which provides winter wheat and barley grain yields for administrative districts and federal states from 1999 to 2022.

It was assumed that there was no need to eliminate the trend in the crop yield series because the increase in yields due to technological improvements mainly occurred in the 20th century (Gouveia and Trigo, 2008; Páscoa et al., 2017), prior to the study period.

The gross primary production (GPP) and leaf area index (LAI) were also used, as they are two important indicators of vegetation growth and biomass and, therefore, have become essential for studying vegetation and climate change interactions (Anav et al., 2015; Fang et al., 2019). The GPP describes the amount of carbon dioxide fixed by plants through photosynthesis, a key component of the terrestrial carbon cycle (Beer et al., 2010). The LAI quantifies leaf area in an ecosystem and is therefore a fundamental variable in processes such as respiration, rainfall interception and photosynthesis (Fang et al., 2019). Thus, both variables were obtained from the Moderate Resolution Imaging Spectroradiometer (MODIS). The product MCD15A2H was used to obtain the annual LAI, and the products MOD17A2H and MYD17A2H were used to obtain the annual GPP. The MCD15A2H product version 6 derived from the MODIS Terra/Aqua combined product has a temporal resolution of eight days and a spatial resolution of 500 m (Myneni et al., 2023). The MOD17A2H and MYD17A2H version 6 products are derived from the MODIS sensors onboard NASA's Terra and Aqua satellites, respectively, with a temporal resolution of eight days and a spatial resolution of 500 m (Running et al., 2015a; 2015b).

In this study, only the months of the phenological cycle of wheat and barley characteristic of each region for each year were considered. For this purpose, the sowing and harvesting months for wheat and barley crops in the regions of Spain were extracted from the sowing, harvesting and marketing calendar (MAPA, 2025b), which provides data at the provincial and regional scales. For the choice of dates, those corresponding to semihard and soft wheat (*Triticum aestivum*) and malting barley (two races, *Hordeum distichum*) were considered since they are predominant in CL and CM (MAPA, 2025a). In addition, the calendar provides for each month of the year a percentage of sowing and harvesting occurrence. Thus, the months with the highest percentage of sowing and harvesting were selected to establish the beginning and end of the phenological cycle. Due to the high degree of similarity between the provincial and regional phenological cycles in each study region, the regional phenological cycle of each crop was considered for both scales. Thus, the phenological cycle of barley in CL and CM is from November to July, and the phenological cycle of wheat is from October to July in CL and from November to July in CM.

In the federal states of Germany, the sowing and harvesting months of wheat and barley crops were extracted from the phenological database of Germany's national weather service (DWD, 2023). It provides the dates of the sowing, emergence, earing, grain filling, milky ripening and harvesting phases, but in this work, only the dates of the sowing and harvesting phases were considered. For the choice of dates, an average of the available dates in the study period was made, and the resulting month was selected. In addition, as in the Spanish regions, the regional phenological cycle of each crop was considered for each region under study and its provinces. Thus, in BY, NS and NW, the phenological cycle of barley is from September to July, and that of wheat is from October to August.

2.2.5. Agricultural Drought Index: Soil Moisture Anomalies

SM anomalies have been successfully used in many works (Almendra-Martín et al., 2022b; Champagne et al., 2015; Scaini et al., 2015) and have been proven to be a good indicator of agricultural drought (Almendra-Martín et al., 2021a; Shukla et al., 2014). In the present study, monthly SM anomalies at the provincial scale in the root zone were used to analyze the impact of agricultural drought on cereal yields. For this purpose,

first, a provincial-scale spatial average of SM in the selected cereal areas was obtained. Then, provincial-scale SM anomalies were calculated as follows:

$$SM\ anomalies = SM_t - \overline{SM}/\delta_{SM} \quad (2.1)$$

where SM_t is the monthly SM series for year t, $\overline{SM}$ is the monthly average using the entire study period and δ_{SM} is the standard deviation of SM in the study period at the provincial scale (Almendra-Martín et al., 2022b; Champagne et al., 2015; Scaini et al., 2015).

2.2.6. Analysis of Biophysical Indicators: GPP and LAI

The GPP and LAI data series were used to identify the state of cereals as a whole since it was not possible to characterize wheat and barley crops separately. The phenological cycle considered was that in which the months of the wheat and barley phenological stages coincided. Although differentiation at the crop scale was not feasible, the study focuses mainly on wheat and barley cereal crops, which are the main rainfed crops in the study regions.

For the study of the month in which the two biophysical parameters of cereals are most affected by agricultural drought, a Pearson correlation analysis was performed between the cereal GPP and LAI and the agricultural drought index using MATLAB v.R2023b software (MathWorks®, Natick, MA, USA). The analysis was performed at the provincial scale from 2001 to 2020, thus obtaining a monthly correlation coefficient (R) value during the phenological cycle of the cereal. In each province, the month with the highest absolute R value was considered the critical month. To obtain the critical month for each region, the most frequent critical month at the provincial scale was selected.

2.2.7. Identification of Agricultural Drought Years

The countries studied in the present work have different environmental conditions. Specifically, Spain is a territory with mainly water-limited conditions, whereas Germany mainly has energy-limited conditions. Several studies (Dudney et al.,

2023; Rehana and Monish, 2020) have analyzed drought by differentiating zones according to the predominant limiting variable, thus dividing the territory between water-limited and energy-limited zones. Therefore, due to the different environmental conditions and limiting factors, a different procedure was followed in each country for the identification of agricultural drought years.

2.2.7.1. Spain

In Spain, the critical month for crop yield was determined by performing a Pearson correlation analysis between wheat and barley yields and the agricultural drought index from 2001 to 2020, thus obtaining a monthly R value during the phenological cycle of wheat and barley. The analysis was performed at the provincial level, and subsequently, the most frequent critical month in each region was extracted, considering the month with the highest correlation as critical.

Once the critical month for CL and CM was obtained, it was used to identify the drought years. One of the most commonly used methods for drought detection is based on the definition of a threshold level below which drought is said to have occurred (Dracup et al., 1980). This approach was applied in the present work, using a percentile as a threshold. A percentile is defined as the value that divides a linearly ordered dataset, so that it indicates the value below which a percentage of the dataset is equal to or less than that value (Moreno et al., 2022). A common value adopted in the literature to detect agricultural drought is the 20th percentile (Andreadis et al., 2005; Liu et al., 2020b; Sheffield et al., 2009). Accordingly, the 20th percentile was used as the threshold level, below which the onset of agricultural drought was defined.

In addition, three approaches were studied for wheat and barley with different time periods as the criteria to identify drought years. The critical month (M) and two (2M, the critical month plus the next or the previous month) or three (3M, the critical month plus the previous and next months) months around the critical month were used. Thus, for the identification of drought years for wheat and barley crops in each Spanish region and for each year of the study period, the threshold level was applied to the three approaches.

2.2.7.2. Germany

Germany is a temperate country in which agriculture is mainly energy-limited. However, environmental and climate conditions are changing, and positive drought trends have recently been observed in many regions of central Europe (Almendra-Martín et al., 2022a; Schumacher et al., 2023). Consequently, for the selection of the critical month for the yield variable and, therefore, the detection of drought years, a provincial and monthly scale analysis of agricultural drought index trends was performed. The Mann–Kendall (MK) statistical test is a nonparametric test used to identify trends in time-series data (Kendall, 1948; Mann, 1945). It is widely used to detect whether there are statistically significant increasing or decreasing trends in hydrometeorological time series (Tan et al., 2015; Tian and Quiring, 2019). The ability of this test to detect trends in hydrology studies has been demonstrated (Burn and Elnur, 2002), and it has been applied in several agricultural drought studies (Almendra-Martín et al., 2021a; Golian et al., 2015; Potopová et al., 2016). Many studies have reported that correlations in the time series may affect the results of the MK test (Bayazit and Önöz, 2007; Von Storch, 1999); nevertheless, in this study, the anomalies of the SM series were studied, which, according to (Albergel et al., 2013), is a technique for avoiding these inconveniences. In this study, the MK test was used to detect whether there were statistically significant increasing or decreasing trends in the agricultural drought index during 2001–2020 to identify the critical month (month in which statistical significance predominates) of administrative districts. Under the null hypothesis of no trend Ho, the MK test statistic (*S*) was calculated as follows (Kendall, 1948; Mann, 1945):

$$S = \sum_{i=1}^{n-1} \sum_{j=i+1}^{n} sgn(x_j - x_i) \tag{2.2}$$

Where

$$sgn(x) = \begin{cases} 1 & if\ x > 0 \\ 0 & if\ x = 0 \\ -1 & if\ x < 0 \end{cases} \tag{2.3}$$

For an upward trend, the *S* statistic is increased by +1, while it is decreased by −1 for a downward trend. The *S* statistics remain unchanged for a zero difference. The statistical parameter *Z* allows us to determine whether a trend is significant:

$$Z = \begin{cases} \dfrac{S-1}{\sqrt{var(S)}} & if\ S > 0 \\ 0 & if\ S = 0 \\ \dfrac{S+1}{\sqrt{var(S)}} & if\ S > 0 \end{cases} \quad (2.4)$$

Throughout this study, a *p* value of 0.05 (confidence level of 95%) was used as the criterion for the statistical significance of a trend. Thus, for an absolute value of *Z* greater than 1.96, a significant trend was considered. The month with the most districts with statistically significant trends was considered the critical month for all German regions.

Once the critical month for the yield variable in the German regions was obtained, the years with agricultural drought were identified using the same procedure explained above for the Spanish regions. Thus, for the three approaches studied (M, 2M and 3M), the 20th percentile was used as the threshold level, below which years with agricultural drought were defined.

2.2.8. Yield Reduction Calculation

Once the years with agricultural drought were identified, the percentage reduction in wheat and barley yields was calculated for those years in each region and for the three criteria. A normal year for crop yield is considered when the drought index is between the 40th and 60th percentiles (Salazar et al., 2012), and the average yield in normal years is estimated and used as a reference. In years classified as agricultural drought years, the annual yield reduction rate is calculated as follows:

$$\mathrm{Yield_{ref}} = \frac{\mathrm{Yield_{n1}} + \mathrm{Yield_{n2}} + \cdots + \mathrm{Yield_{nx}}}{\mathrm{x}} \quad (2.5)$$

$$YR_m = \frac{Yield_{ref} - Yield_{dm}}{Yield_{ref}} \times 100\% \quad (2.6)$$

where $Yield_{ref}$ represents the benchmark yield of the selected region, *x* represents the number of normal years in the study period, and $Yield_{nx}$ (x = 1,2,..., 4) represents the yield of year x. YR_m is the yield reduction rate of the selected region in the m^{th} year (m = 1,2,..., 20), and $Yield_{dm}$ (m = 1,2,..., 20) represents the yield in year m identified as dry (Yao et al., 2022).

2.3. Results and Discussion

2.3.1. Biophysical Variables versus Agricultural Drought

The average R values for the relationships of the agricultural drought index with GPP and the LAI for the predominant month are given in Table 2.1. The results of the correlation analysis between GPP and the agricultural drought index (Table 2.1) show that the months of the reproductive stage (April, May and June) of cereals are predominant in the provinces of all the regions considered. Moreover, the average R value (resulting from averaging the R values of the critical month of the provinces belonging to the region studied) shows a clear difference between the Spanish and German regions, presenting a direct relationship between SM anomalies and GPP in the Spanish regions (0.50 in CL and 0.29 in CM) and an inverse relationship in the German regions (−0.57, −0.44 and −0.48 in BY, NS and NW, respectively). These results are consistent with those of Fu et al. (2022), which show that in times of drought, in areas where soil water content is high, an increase in plant GPP is promoted, as occurred in this study in the regions of Germany. Thus, moderate drying of wet soil causes an increase in the carboxylation capacity of plants (Fu et al., 2022). Several studies have reported improved vegetation conditions during drought in wet regions (O and Park, 2023; Orth and Destouni, 2018). In contrast, in areas where the water content is below a threshold, GPP decreases under drought conditions, as is the case in regions of Spain. Vegetation in arid regions reacts quickly to SM deficiency, which would imply greater drought stress in vegetation, as this is a limiting factor of vegetation functioning in water-limited environments (Vicente-Serrano et al., 2013).

Table 2.1. Predominant month and mean R of the predominant month for each study region (Castilla y León, CL; Castilla–La Mancha, CM; Bayern, BY; Niedersachsen, NS and Nordrhein-Westfalen, NW) resulting from the correlation analysis between biophysical parameters and the agricultural drought index.

Region	Predominant Month		Average R	
	GPP	LAI	GPP	LAI
CL	May	May	0.50	0.69
CM	April	April	0.29	0.69
BY	May	July	−0.57	0.16
NS	June	July	−0.44	0.57
NW	May	July	−0.48	0.49

Regarding the relationship between the LAI and agricultural drought index (Table 2.1), it is observed that in Spanish regions, the predominant months correspond to the reproductive stage of the plant, as in the results obtained with GPP. In the German regions, July is the predominant month, and the mean R values (0.16, 0.57 and 0.49 in BY, NS and NW, respectively) are lower than those in the Spanish regions (0.69 in both regions, CL and CM). Both cereal variables, GPP and the LAI, show different behavior in the regions of the two countries, in accordance with the fact that one has water-limited and the other energy-limited conditions. In BY, NS and NW, there is an inverse relationship between SM anomalies and GPP and a direct relationship with the LAI. Conversely, in CM and CL, there is a direct relationship in both cases. The results are consistent with those obtained by Hu et al. (2022), who demonstrated decoupling between the LAI and GPP as aridity decreases. Hence, areas in water-limited environments, such as CM and CL, showed a stronger link between GPP and the LAI. In contrast, in the BY, NS and NW regions, under energy-limited conditions, a decreased LAI in drought years could facilitate carbon uptake by smaller leaves and consequently enhance GPP (Hu et al., 2022).

2.3.2. Critical Month Identification

In Spain, the critical month for cereal crops in CL and CM (Figure 2.2) is predominantly May, except for wheat in CM, where it is April. In both regions and for both crops, the critical month is in the spring phenological stages, i.e., during the reproductive and maturation phases of the crop. The R values are within the range of 0.60 to 0.80, which shows that SM is a fundamental variable for the development of cereals. These results are also consistent with those of Gaona et al. (2022), which observed that

in the main cereal-growing areas of Spain, the critical periods of impact on the wheat and barley yields of SM were concentrated in the spring phases. Several studies (Abeledo et al., 2008; Cossani et al., 2007) have shown that grain yields are strongly affected by water stress during anthesis in May. In addition, Capa-Morocho et al. (2016) observed that the dry conditions in those months in Spain led to a marked decrease in yields.

Analyzing the agricultural drought trends for each month of the year in all districts of the study regions in Germany (Figure 2.3), a generalized negative trend is observed in all months and areas. This result is consistent with that reported in the study by Almendra-Martín et al. (2022a), in which the authors observed a trend toward drier conditions in central Europe over the last three decades. The month with the maximum number of districts with a significant trend was April, followed by May. Thus, April was selected as a critical month in the regions of Germany to identify drought years. Several studies (Hlavinka et al., 2009; Panek and Gozdowski, 2020) prove that for winter cereals that dominate agricultural production in central Europe, the development stage in early spring is crucial for determining grain yield, as the cereals are very susceptible to drought in that period. Thus, Eitzinger et al. (2003) studied the effect of water stress on winter wheat production in central Europe and found that during the month of April, the crop is very sensitive to water stress, causing low yields.

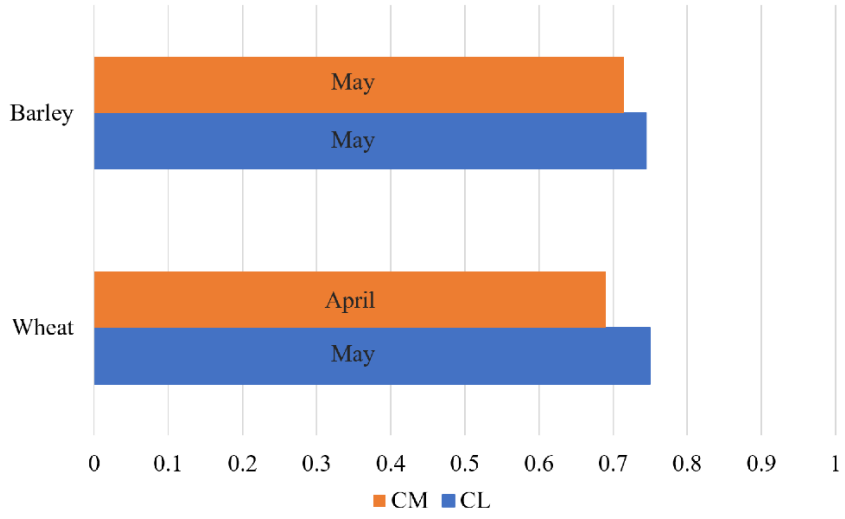

Figure 2.2. Most frequent critical month and its average R, obtained from monthly and provincial correlations between SM anomalies and the annual yields of barley and wheat during the growing season in the Castilla y León (CL, blue) and Castilla–La Mancha (CM, orange) regions.

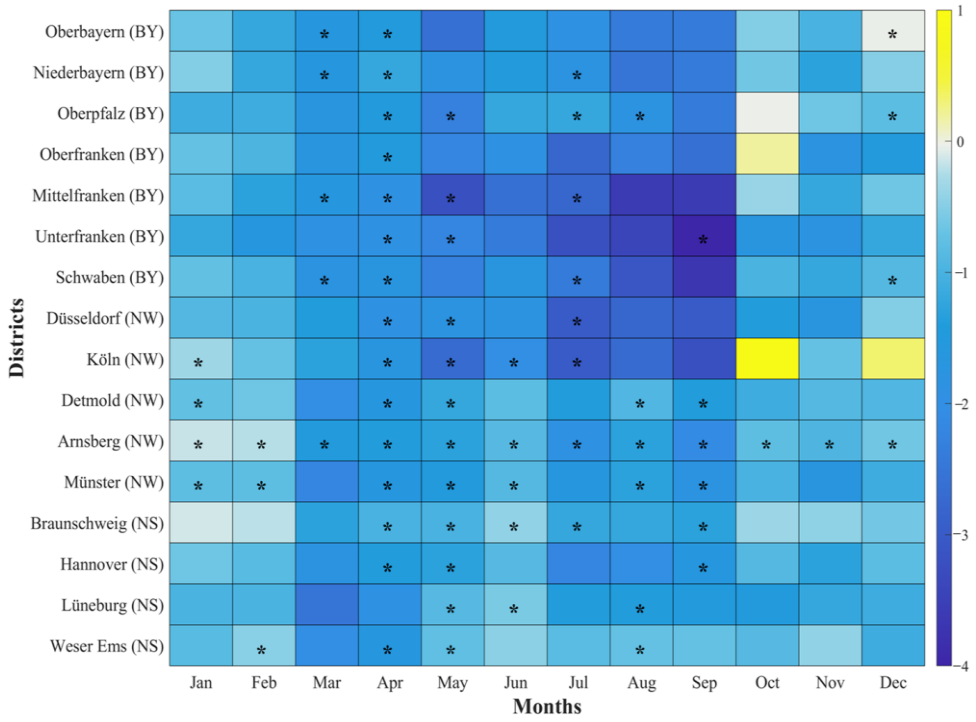

Figure 2.3. Monthly results of SM anomaly trends (Z) and months with statistical significance $p < 0.05$ (*) in the Bayern (BY), Nordrhein-Westfalen (NW) and Niedersachsen (NS) districts. The yellow and blue blocks indicate positive and negative trends, respectively.

2.3.3. Agricultural Drought Year Detection

For the identification of drought years, the 20th percentile of the agricultural drought index was calculated, using it as the threshold below which years were considered dry years (Figure 2.4). As a general result, in all regions except CM, dry years were coincident in wheat and barley crops since the critical month used for drought year selection was the same for both crops. Of the three approaches applied (M, 2M and 3M) for wheat and bar-ley, in the case of 2M, April and May were detected in all regions. Furthermore, for the three temporal approaches, very similar patterns were observed for each crop and region. Hence, the three criteria used mostly adequately identify the predominant dry years in CM and CL, as well as in BY, NS and NW. In the case of German regions, the years with agricultural drought were grouped in the last decade of study, in accordance with the soil moisture trend observed in this study and others (Jaagus et al., 2022). Therefore, it could be said that the three criteria used are equally valid for the identification of agricultural drought years.

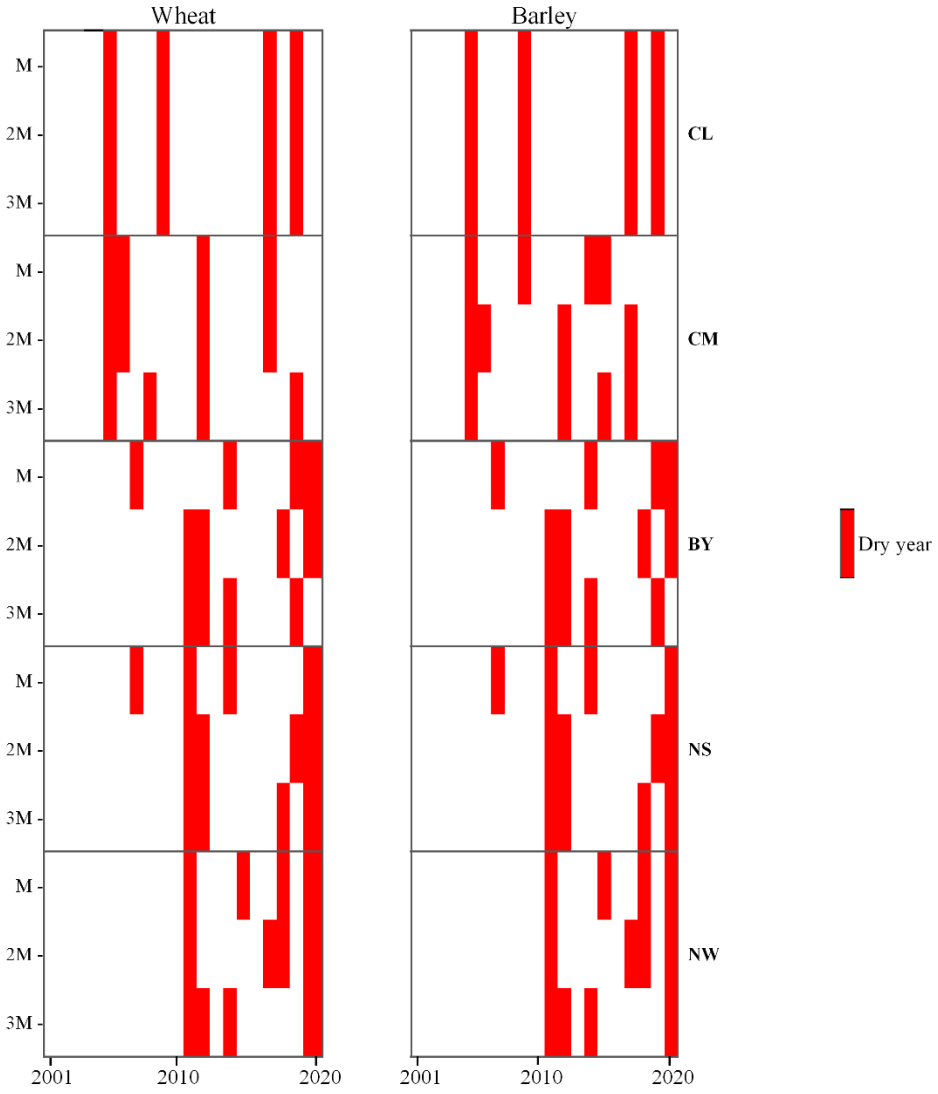

Figure 2.4. Dry years detected (red bars) in each region (Castilla y León, CL; Castilla-La Mancha, CM; Bayern, BY; Niedersachsen, NS and Nordrhein-Westfalen, NW) for wheat (left) and barley (right) and for the three criteria (M, 2M and 3M) from 2001 to 2020.

In the CL region, the dry years identified (2005, 2009, 2017 and 2019) coincide for the three approaches used. In the CM region, there is variation in dry years in the three periods as well as between the two crops. Thus, the years 2005, 2012 and 2017 coincide mostly for both crops and time periods in CM. The years 2006 and 2015 were especially dry for wheat and barley crops, respectively. The drought episodes identified in CL and CM have also been detected and studied by other authors, but mostly from a meteorological drought perspective. The study by García-Herrera et al. (2007) describes that 2005 was characterized by extremely dry conditions on the Iberian Peninsula, which had a significant impact on cereal production, decreasing it by 60% on average. The 2015

event first appeared in early spring (May and earlier) in southern France and on the Iberian Peninsula (Ionita et al., 2017; Laaha et al., 2017). Several studies have identified 2012 as a year with drought (Lorenzo et al., 2022; Páscoa et al., 2021). García-Herrera et al. (2019) analyzed the drought that affected Europe from July 2016 to June 2017. They found that during that period, most of Western Europe suffered a major drought event resulting in severely affected crops, especially cereals in Spain. Khoury and Coomes (2020) indicate that Spain suffered major droughts in 2005, 2012 and 2017. Moreover, the consequences of drought events for vegetation, such as those observed in 2015, 2018 or 2019 in most parts of Europe, are productivity losses (Obladen et al., 2021).

In the German regions, a cluster of dry years was observed in the second decade of study. Almost 90% of the dry years identified in the German regions occurred from 2010 onward, with a clear incidence in 2011, 2012 and 2020, showing a clear climatic trend, which led to an increase in frequency droughts. These results are consistent with those obtained by Erfurt et al. (2020), who reported that droughts identified in southwestern Germany from 1801 to 2018 based on meteorological indices were distributed over the study period, but in the last decade, drought episodes showed greater severity (Erfurt et al., 2019) also classified the period from 2003 onward as one with the highest incidence of severe drought events in southwestern Germany. Markonis et al. (2021) argued that the most abrupt change in increasing warm season droughts in Europe has been observed in central Europe in the last 15 years, with dry events identified in agreement with those of the present study.

Agriculture is facing changing climatic conditions, and severe droughts are expected to increase in the coming years (Dai, 2013; Spinoni et al., 2018). The results obtained show an increase in droughts in the most recent decade of study in the German regions. Despite the apparent lower dependence on irrigation in temperate regions, the impacts of drought on agriculture in these areas are considered a major abiotic stress (Rey et al., 2017). One of the actions aimed at reducing drought risks is increasing the water supply (Iglesias et al., 2009, 2012). Irrigation can greatly mitigate adverse impacts resulting from water stress by maintaining higher SM requirements (Vogel et al., 2019). This fact becomes even more evident and corroborates the evolution of the agricultural drought years identified in this study when analyzing the evolution of the irrigated area in German regions. According to data obtained from the German Federal Statistical Office (DESTATIS, 2023), from 2010 to 2020, the irrigated area increased by 86%, 27% and

86% in BY, NS and NW, respectively. Therefore, there are worrying signs of increasing water stress in areas where this variable was not previously a limiting factor.

2.3.4. Impact of Agricultural Droughts on Grain Yield

According to the identification of dry years in each region and for wheat and barley crops, the yield reduction for these years was calculated by averaging the 4 years identified in each region for each of the three approaches used (Tables 2.2 and 2.3).

Table 2.2. Average percentage of yield reduction in drought years in Castilla y León (CL) and Castilla–La Mancha (CM) for wheat and barley and for the three criteria (M, 2M and 3M).

Month Period	CL		CM	
	Wheat	Barley	Wheat	Barley
M	32.8	28.8	28.5	33.7
2M	34.9	32.2	31.5	33.9
3M	34.9	32.2	8.4	34.8

Table 2.3. Average percentage of yield reduction in drought years in Bayern (BY), Nordrhein-Westfalen (NW) and Niedersachsen (NS) for wheat and barley and for the three criteria (M, 2M and 3M).

Month Period	BY		NS		NW	
	Wheat	Barley	Wheat	Barley	Wheat	Barley
M	−11.57	−11.38	1.31	3.69	2.85	−0.33
2M	−0.09	4.78	2.90	−0.79	1.88	4.41
3M	0.82	−2.49	11.80	16.18	−4.62	1.35

In drought years, the Spanish regions of CL and CM (Table 2.2) suffered a significant decrease in crop yields, which was evident in all cases. The average yield reduction in both crops was greater than 30%, which demonstrates the importance of soil water in the root zone for wheat and barley yields (Gaona et al., 2023). These results are in agreement with the evidence obtained by the authors of Janáček (1994), confirming that in semiarid agricultural areas, the most important limiting factor for crop productivity is water stress caused by reduced soil water availability and, therefore, agricultural drought. Comparing the two regions, a greater reduction is observed for wheat in CL and for barley in CM. However, the difference in crop reduction in both regions is small, usually less than 5%.

There is an interesting debate as to whether wheat or barley is better adapted to drought. Some authors (Albrizio et al., 2010; López-Castañeda and Richards, 1994) found better adaptation of barley to drought conditions, displaying a better yield potential than wheat in the Mediterranean basin. In contrast, several studies (Cossani et al., 2009; Slafer and Savin, 2023) did not find consistent differences between the yields of the two crops. In general, in the present work, in both regions and crops, a similar yield reduction of between 29% and 35% predominates. These reductions are larger than those obtained in the projection of Olesen et al. (2007) for winter wheat in Spain, with a predicted average yield decrease of 21% by the end of the 21st century.

These results highlight the susceptibility of rainfed crops to the increasing intensity of soil drought and warn of the severe impacts on crop yields that are already occurring. It is well known that the Mediterranean area is among the most vulnerable regions to climate change, and this is likely to worsen in the future (Gu et al., 2020). Indeed, climate models project a decrease in SM and an increase in the duration and intensity of droughts in the Mediterranean region (Spinoni et al., 2018; Tramblay et al., 2020). Therefore, this observed reduction in crop yields could be exacerbated in the future, and in the face of growing global food needs, this finding is of great concern and may aggravate the global food crisis (Brisson et al., 2010; Spiertz and Ewert, 2009).

In the case of Germany, there is notable variability in cereal yield variations in all three regions (Table 2.3). In BY, an increase in yield was observed, reaching 11% when the critical month approach was applied for both crops. In contrast, the NS and NW regions showed mostly yield reductions. In NS, the average yield reduction was 5% for wheat and 10% for barley, reaching 11% and 16%, respectively, with the 3M approach. The NW region showed smaller values than NS, with an average yield reduction of 2% for wheat and 3% for barley.

Yield increases in years of agricultural drought identified in BY can be explained by drought periods also being characterized by increased energy availability (Orth and Destouni, 2018). In this way, the main limiting variable for crops in this area increases, favoring the conditions for crop development and, therefore, yield. Furthermore, in the same context, this result can also be explained by consequences resulting from climate change, which have already been seen to influence crop yields in Europe, affecting them differently according to region and a variety of other factors (EEA, 2023a). Thus, due to

global warming, energy factors such as the average annual temperature in Europe in the period 2006–2015 increased by approximately 1.52 ˚C (EEA, 2023b) and were found to cause crop yields to increase, except in southern Europe (Ewert et al., 2005). This is consistent with the slight increase in crop yield obtained in dry years in BY, where the yield increase implied by an increase in energy variables probably outweighs the yield reduction caused by agricultural drought. However, some regions with little or small positive impacts of climate change could reverse this circumstance, leading to more severe drought situations (Forzieri et al., 2014; Van Lanen et al., 2017). This idea is further reinforced as climate change is projected to worsen in the near future (Malhi et al., 2021).

In northern Germany, there are other factors that could explain the results obtained for NS and NW. In those regions, the soils are mostly sandy (Drastig et al., 2016) and therefore have a low water-holding capacity. The sand fraction has an inverse relationship with important soil water properties such as water-holding capacity (Martínez-Fernández et al., 2021). This circumstance increases the susceptibility to soil drought in the regions of NS and NW, located in northwestern Germany, where decreases in wheat and barley yields have been reported. Therefore, this finding warns of the deleterious consequences already occurring for the yield of the two main exported cereals from Europe (Schils et al., 2018) in areas where SM was not previously a limiting factor for crop development. Drastig et al. (2011) found several years ago that those agricultural regions of northern Germany could lose productivity if they are subjected to more frequent and long-lasting droughts without irrigation.

Evidence of all this was observed in 2011, a year of particularly intense agricultural drought in the German regions (Figure 2.4), causing an average yield reduction of more than 9% in cereals (Table 2.4). This result is consistent with that of Oikonomou et al. (2020), which classified the 2011 drought in the EU as having the largest spatial extent on record. In the same context, Erfurt et al. (2020) studied droughts using meteorological indices for southwestern Germany and classified 2011 as one of the most extreme years with precipitation shortages accompanied by high temperatures. Thus, 2011 was identified as a dry year in Germany due to a precipitation deficit in early April, ending the month with a soil moisture deficit and leading to vegetation stress in mid-May and consequent reductions in crop yields, especially for cereals (Sepulcre-Canto et al., 2012). Consistent with the aforementioned research, the present study finds that in

2011, identified as an agricultural drought year in Germany, both cereals showed a marked reduction in yield for all regions and approaches (Table 2.4). Barley showed an average yield reduction of 13%, which was much larger than that of wheat, with an average reduction of 5% (Table 2.4). Therefore, this shows that in areas where, until now, soil water content was not a limiting factor, a soil moisture deficit in April is promoting a reduction in cereal yields, with barley being more vulnerable than wheat.

Table 2.4. Average percentage of yield reduction in the drought year 2011 in Bayern (BY), Nordrhein-Westfalen (NW) and Niedersachsen (NS) for wheat and barley and for the three criteria used (M, 2M and 3M). ND means not a drought year.

Month Period	BY		NS		NW	
	Wheat	Barley	Wheat	Barley	Wheat	Barley
M	ND	ND	4.67	12.02	6.16	11.87
2M	3.26	12.30	5.60	10.36	2.70	12.78
3M	5.75	12.10	10.63	21.57	0.96	11.59

Several studies have shown that in recent decades, there has been a general trend of change toward drier conditions, mainly in central and eastern Europe (Almendra-Martín et al., 2022a; Capa-Morocho et al., 2016). Some studies projected a progressive increase in climate threats in Europe, mainly driven by a trend toward more likely and severe extreme soil drought events in central Europe under future warming scenarios (Grillakis, 2019; Hänsel et al., 2019).

The detrimental effect observed for wheat and barley yields in Spain due to the decrease in SM may be an indication of what may happen to areas where soil water content was not previously a crop constraint. In Germany, an area where SM was not historically a limiting factor, an observed and significant reduction trend in SM reported in recent years is starting to cause reductions in crop yields that, according to future projections, could increase. In fact, this likely hypothesis is reinforced by a recent study by Denissen et al. (2022) conducted for the period 1980–2100, in which a widespread shift in the ecosystem from energy- to water-limited conditions was found, which the authors attributed to global warming. This finding warns against a possible increase in the frequency of agricultural drought events and consequent yield loss in cereals, such as that already detected in this study for Germany in the last decade.

2.4. Conclusions

The impact of agricultural drought on wheat and barley crops in the main cereal-growing regions of Spain and Germany during the 2001–2020 period was analyzed. In general, the results of all the analyses carried out in this study show the importance of SM in cereals, especially in the months of the reproductive and ripening phases of the crops. Moreover, with respect to the three approaches studied, the results obtained showed similar patterns. Therefore, it can be stated that the three criteria were useful for the identification of drought years and for the calculation of yield loss.

The analysis of the GPP and LAI variables revealed similar behaviors in water-limited environments and the inverse in energy-limited environments, showing the influence of soil water content on the development of these variables. The use of SM anomalies evidenced their suitability for the identification of years with agricultural drought, in agreement with previous findings. Furthermore, a cluster of drought years was observed in the second decade of study in Germany, which is a clear indicator of warning in terms of SM deficit in areas where this variable is not the main constraint.

As expected, in water-constrained areas, a considerable reduction in crop yields has been observed, exceeding 30% yield reduction, because of agricultural drought. Unexpectedly, in regions located in energy-constrained areas, where water is not the main limiting factor, a singular yield reduction of around 5% has been observed for both crops. Thus, the results suggest that, in the face of increased droughts, the worsening of cereal yield losses is likely, which will increase notably in southern regions, as is happening in Spain. Similarly, Germany, where the SM was not considered a constraint until now, is starting to show increasing water stress that may lead to unprecedented reductions in cereal yields.

This finding has important implications for agriculture, as it was proven that in recent years, in areas where water was not the main limiting factor, it is now having detrimental effects on crop yields. Although the yield decrease detected in the German regions shows moderate values, it is an indicator of change in environmental conditions and will have negative consequences on agricultural production. Indeed, in view of climate change impacts, the results obtained warn against a new uncertain scenario for crop yields. This likely transformation suggests that in areas where SM has not yet been

a limiting factor, the situation can reverse and lead to a significant decrease in cereal yields. This possible scenario could be similar to that currently being observed in Spanish regions, where yields have declined by more than 30% in drought years over the last two decades due to soil water deficits. The results of this study are of interest for adaptation and/or mitigation strategies to cope with these detrimental impacts on crop yields due to agricultural drought.

CAPÍTULO 3

RECENT CEREAL PHENOLOGICAL VARIATIONS UNDER MEDITERRANEAN CONDITIONS

Benito-Verdugo, P., González-Zamora, Á., Martínez-Fernández, J. (2024). Recent Cereal Phenological Variations under Mediterranean Conditions. *Remote Sensing.*, *16*(11), 1879. https://doi.org/10.3390/rs16111879

Resumen

Este estudio analiza los patrones temporales de la fenología de los cereales de secano a partir del conjunto de datos GIMMS NDVI3g en las principales regiones cerealistas bajo clima mediterráneo de España, Portugal, Francia e Italia, durante el periodo 1982–2022. Se analizaron por separado las series anteriores y posteriores del inicio del siglo XXI. Los parámetros fenológicos se obtuvieron mediante el método del umbral dinámico modificado y se analizaron sus tendencias. También se realizaron análisis de correlación para estudiar las relaciones entre estos parámetros y evaluar la influencia de variables hidroclimáticas sobre el inicio (SOS) y el final (EOS) del ciclo fenológico. Los resultados mostraron un cambio de tendencia de los patrones fenológicos entre ambos periodos de estudio, coincidiendo con la pausa del calentamiento global. En el primer periodo (1982–2002), el SOS y el EOS se adelantaron (−7,5 y −3,1 días, respectivamente), y la duración del ciclo fenológico (LOS) aumentó. Sin embargo, durante la segunda etapa (2003–2022), el SOS y el EOS se retrasaron (7,5 y 1,7 días, respectivamente) y la LOS disminuyó. Se observaron dinámicas similares en cuanto a la influencia de las variables hidroclimáticas sobre el SOS y el EOS, con mayor impacto en el primer periodo y menor en el segundo. Este estudio presenta aportaciones relevantes sobre la dinámica fenológica de los cereales de secano que puede ser útil para su gestión y planificación frente a escenarios de cambio climático.

Palabras clave: fenología del cereal; cereal de secano; clima mediterráneo; pausa del calentamiento global; NDVI; humedad del suelo.

Abstract

This study analyzes the temporal patterns of rainfed cereal phenology extracted from the GIMMS NDVI3g dataset in the main cereal-growing regions under a Mediterranean climate in Spain, Portugal, France and Italy during the period 1982–2022. The series before and after the beginning of the 21st century were analyzed separately. Phenological parameters were extracted using the modified dynamic threshold method, and their trends were analyzed. Correlation analyses were performed to study the relationships among these parameters and to analyze the influence of hydroclimatic variables on the start (SOS) and end (EOS) of the growing season. Results showed a temporal reversal in phenological trends between both study periods, coinciding with the global warming hiatus. In the first period (1982–2002), SOS and EOS advanced (−7.5 and −3.1 days, respectively), and the length of growing season (LOS) increased. However, during the second stage (2003– 2022), SOS and EOS were delayed (7.5 and 1.7 days, respectively), and LOS decreased. Similar dynamics were observed for the influence of the hydroclimatic variables on SOS and EOS, stronger in the first period and weaker in the second. This study provides valuable information on the phenological dynamics of rainfed cereals that may be useful for their management and planning in climate change scenarios.

Keywords: cereal phenology; rainfed cereal; Mediterranean climate; global warming hiatus; NDVI; soil moisture

3.1. Introduction

Vegetation phenology dynamics are considered important biological indicators that reflect the cyclical and seasonal responses of ecosystems to climate and hydrological regimes (Zhang et al., 2003). In this context, global warming is an undeniable phenomenon with a significant impact on terrestrial vegetation, altering its phenological cycles (Zhao et al., 2015). Thus, an accurate characterization of phenology and monitoring of its behavior at different times are fundamental to understanding the variations in climate change impacts. This is of particular interest in water-limited areas, such as the Mediterranean, as it is one of the most vulnerable regions to climate change, and this vulnerability is likely to worsen in the future (Gu et al., 2020). The soil moisture (SM) drought risk is projected to increase around the world, resulting in increased frequency and intensity of agricultural droughts under all climate scenarios, with the Mediterranean region being the most affected (Benito-Verdugo et al., 2023; Tramblay et al., 2020). The Mediterranean region is characterized by water-limited conditions, where rainfed cereal cultivation predominates (Jacobsen et al., 2012). This increases the interest in the study of the phenological behavior of cereals under the Mediterranean climate, which could be an essential tool for better agronomic management under a global climate change scenario (Jiao et al., 2020).

Crop phenological information is mainly extracted from in situ ground records and remote sensing data (Zhan et al., 2024). In situ monitoring of vegetation is mainly based on field observation methods and provides detailed and accurate information on plant development. However, this approach is limited by its spatial and temporal scales, making it impossible to detect phenological dynamics at larger spatial scales and to conduct long-term studies. Several studies used information from in situ observations for the analysis of phenological trends but recognized that the geographic extent is limited, as are long-term observations in complex environments (Meng et al., 2021; Walther et al., 2002).

However, satellite data are effective tools for monitoring land surfaces at large spatial and suitable temporal scales, which allow tracking of the phenological dynamics of vegetation over large areas (Liao et al., 2023). The phenology obtained from satellite data is usually determined from vegetation indices (VIs), such as the normalized

difference vegetation index (NDVI) or the enhanced vegetation index (EVI) (Gerard et al., 2020; Kibret et al., 2020; Liao et al., 2023). Many studies have investigated the vegetation phenology using satellite sensors, including mainly the Advanced Very High Resolution Radiometer (AVHRR) (Tian et al., 2024a; You et al., 2013), the Moderate Resolution Imaging Spectroradiometer (MODIS) (Gerard et al., 2020) and the Satélite Pour l'Observation de la Terre (SPOT) (Meroni et al., 2014). In particular, the NDVI derived from the AVHRR sensor is the most widely used tool for studying the long-term phenological dynamics of vegetation at global, continental and regional scales. It is the longest NDVI time series to date and has been shown to have a good capability for long-term vegetation monitoring (Fu et al., 2018).

With the impressive advancements in remote sensing technologies, which make it possible to effectively monitor vegetation phenology, recent research on phenological trends and their responses to climate change has been performed at different scales. Various climatic factors, such as temperature, precipitation, photoperiod, etc., can influence the seasonal development of plants and the calendar of phenological phases (Gordo and Sanz, 2010; Menzel et al., 2020). Many studies have incorporated these variables into analyses of climatic impacts on phenology (Jin et al., 2019a; Yuan et al., 2019a). However, the use of other important factors, such as the soil water content, in phenological analyses using remote sensing data is uncommon, despite its crucial importance for crops and the impacts that agricultural drought is causing (Benito-Verdugo et al., 2023).

The main vegetation parameters that are extracted to monitor phenological dynamics are the start of the growing season (SOS), the end of the growing season (EOS) and the length of the growing season (LOS); the latter is calculated from the previous two parameters. Many studies have shown that prior to the 2000s, there was a general trend of advanced SOS in many regions, and different time periods and study methods were used (Piao et al., 2006; Stöckli and Vidale, 2004). However, since the start of the 2000s, several studies have suggested that the trend may have slowed (Cong et al., 2013; Jeong et al., 2011) or even reversed (Fu et al., 2014; Touhami et al., 2022; Zhang et al., 2023). In contrast, the overall trend of the EOS was more heterogeneous and less marked than that of the SOS, with a majority of advances (Jeong et al., 2011; Zhu et al., 2012) but also some delays (Touhami et al., 2022). The discrepancy in the trends of the main phenological metrics before and after the beginning of the 21st century has been attributed

to the global warming hiatus (Piao et al., 2019). However, it is still not clear how these trends evolved beyond that period and whether they have persisted in recent years, specifically in agricultural areas. Accordingly, Piao et al. (2019) recommended continuous monitoring and analysis using satellite observations to verify whether and how the trends in phenological parameters will continue in the coming decades. Several studies (Guo and Hu, 2022; Measho et al., 2023; Ren and An, 2021) have noted that, despite the interest in detecting the phenological dynamics of cultivated plants at a regional scale, most researchers did not consider it due to the perception that it was influenced by anthropogenic activities. Thus, instead of focusing on cultivated plants, attention has been mostly focused towards phenological changes in natural vegetation. Moreover, in the few cases where cultivated plants have been considered, they were small-scale studies based on in situ field data (Ren and An, 2021). Therefore, assessments of plant phenology covering both the periods before and after the global warming hiatus are needed, especially for cultivated plants. This would provide a more complete understanding of the temporal phenological dynamics of vegetation and would allow verification of the trends of most current phenological parameters.

This study aimed to analyze the patterns of the temporal phenological parameters of rainfed cereals based on the NDVI AVHRR data and their responses to hydroclimatic variables under Mediterranean conditions. The analysis was performed in the main cereal-growing regions with a Mediterranean climate in Spain, Portugal, France and Italy during the period from 1982 to 2022. This study provides a deep understanding of the phenological dynamics of crops as important as cereals, particularly in water-limited regions. In these environments, accurate management and yield forecasting are crucial to ensure food security and agricultural sustainability under a climate change scenario. This work can significantly contribute to inform management decisions with the aim to address future situations in water-limited regions for these key crops.

3.2. Materials and Methods

3.2.1. Study area

In the Mediterranean region, the most common crops are rainfed cereals, with wheat and barley being the main crops (Mefleh, 2021; Savin et al., 2022). The area is characterized by water-limited conditions, with dry, hot summers and mild, humid winters. The main cereal-growing regions under a Mediterranean climate in Spain (e.g., Castilla y León and Castilla-La Mancha, CL and CM, respectively); Portugal (e.g., Alentejo, AT); France (e.g., Occitanie, OC); and Italy (e.g., Puglia, PG), as highlighted in previous works (DRAAF, 2024; García-León et al., 2020; MAPA, 2025a; Stoate et al., 2000), were selected as the study areas (Figure 3.1).

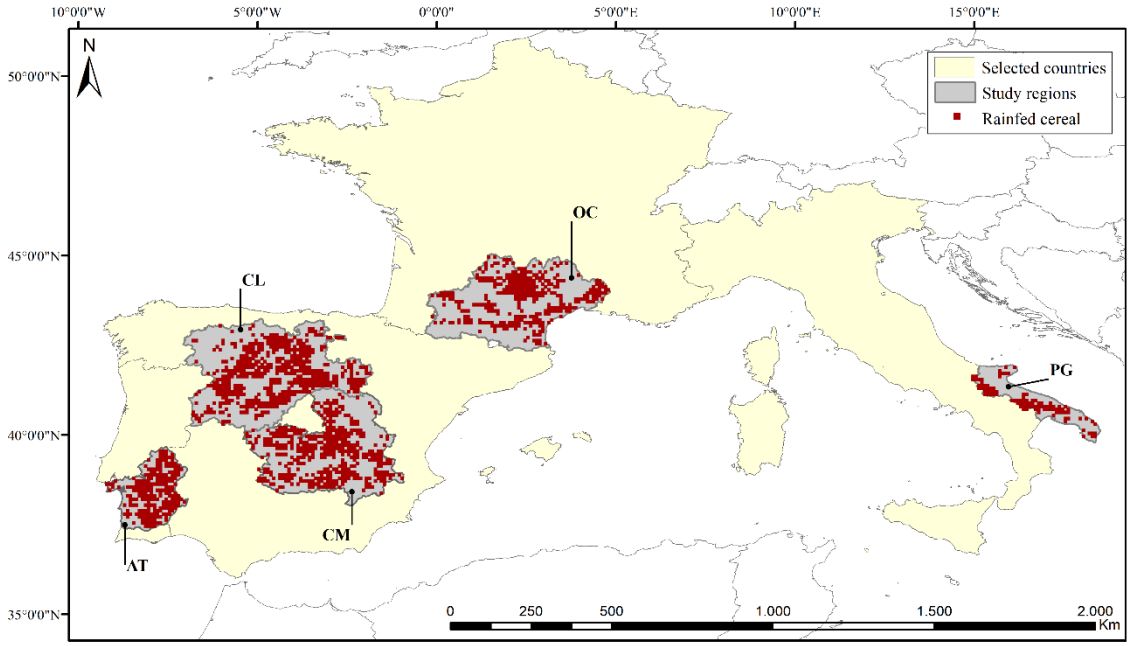

Figure 3.1. Location map of the cereal zones in the study regions: Castilla y León (CL) and Castilla La-Mancha (CM) in Spain; Alentejo (AT) in Portugal; Occitanie (OC) in France; and Puglia (PG) in Italy.

3.2.2. Data Source

3.2.2.1. Detection of Cereal Zones

To study rainfed cereal areas in the selected study areas (Figure 3.1), two databases were used to create a mask that filtered out all the areas other than the target areas. The Climate Change Initiative (CCI) Land Cover (LC) map obtained from the European Space Agency (ESA) was used to discard areas with different land cover types than cereal crops. It describes Earth's land surface in 37 original LC classes based on the United Nations Land Cover Classification System (UN-LCCS) (Di Gregorio, 2005), with a spatial resolution of 300 m (Defourny et al., 2012). Additionally, the Digital Global Map of Irrigation Areas of the Food and Agriculture Organization (FAO) was used to exclude irrigated areas. It represents the global area that is equipped with irrigation at a spatial resolution of 5 arc minutes (Siebert et al., 2013). In this study, pixels with more than a 10% irrigated area and with land cover types different from those of rainfed and mosaic cropland were hidden. This mask was applied to all databases to select those pixels that only represented areas of rainfed cereal crops, assuming that cereals are the predominant crop in each region.

3.2.2.2. Remote Sensing Data and Processing

The normalized difference vegetation index third-generation V1.2 (NDVI3g) dataset for Global Inventory Modeling and Mapping Studies (GIMMS) was used as the remote sensing source data. It is based on corrected and calibrated measurements from the Advanced Very High Resolution Radiometer (AVHRR) that were obtained from different sensors onboard the National Oceanic and Atmospheric Association (NOAA) polar-orbiting meteorological satellites (Pinzon et al., 2023). The dataset provided two NDVI values per month over 14–16 day compositing periods, with a spatial resolution of 0.0833 degrees and global coverage from 1982 to 2022.

The cubic spline interpolation method was used to obtain the daily NDVI time series, since it is one of the most common methods used for time interpolation (Talebi et al., 2023; Wolberg and Alfy, 1999). Cubic spline interpolation of the data with piecewise cubic polynomials allows the NDVI curve to pass through two endpoints with their respective derivatives (Talebi et al., 2023). Additionally, for noise reduction, the

NDVI time series was smoothed by calculating the moving average with a 30-day window.

3.2.2.3. Hydroclimatic Data

Climatic and SM data were used to analyze the relationships among phenological patterns and environmental conditions. The climate variables were obtained from the EOBS database, which is a gridded daily Earth observation dataset over Europe belonging to the Copernicus Climate Change Service (C3S) European climate and assessment dataset (Bandhauer et al., 2022). The E-OBS database used, version 28.0, provides data with a spatial resolution of 0.1° × 0.1° and daily temporal resolution, with data available from January 1950 to December 2023. Climatic data were resampled into NDVI3g GIMMS grids using a majority filter. Among the set of climate variables that is provided by this database, four variables were selected for this study: accumulated precipitation (P), maximum temperature (Tmax), minimum temperature (Tmin) and relative humidity (RH). However, the latter was only used to calculate the vapor pressure deficit (VPD), which was defined for its agronomic relevance in vegetation development. The VPD (kPa) is the difference between the saturated vapor pressure (e_s) and the actual vapor pressure (e_a) and was calculated according to Equations (3.1)–(3.4) (Allen et al., 1998; Yoder et al., 2005), where eo is the saturated vapor pressure at the air temperature (kPa), and T_i is T_{max} or T_{min} (°C).

$$\mathrm{VPD} = e_s - e_a \tag{3.1}$$

$$\mathrm{e_s} = \frac{\mathrm{e^o(T_{max}) + e^o(T_{min})}}{2} \tag{3.2}$$

$$\mathrm{e^o(T_i)} = 0.6108 \exp\left(\frac{17.27\ \mathrm{T_i}}{\mathrm{T_i} + 237.3}\right) \tag{3.3}$$

$$\mathrm{e_a} = \frac{RH}{100}\left(\frac{\mathrm{e^o(T_{max}) + e^o(T_{min})}}{2}\right) \tag{3.4}$$

As in the previous section, the moving averages were calculated using a 30-day window for P, Tmax, Tmin and VPD. Finally, to obtain the variables by season, the averages of each of the variables and for each pixel in each season of the year were

calculated. Thus, autumn was considered to occur from September to November, winter from December to February, spring from March to May and summer from June to August.

The ERA5-Land reanalysis database was used as the SM database. It is provided by the European Centre for Medium-Range Weather Forecasts (ECMWF) in the framework of the C3S (Muñoz-Sabater et al., 2021). This reanalysis database has been widely validated and used (Almendra-Martín et al., 2022b; Gaona et al., 2022; González-Zamora et al., 2023). The series provides SM data from 1981 to the present, with an hourly temporal resolution and a regular grid of 0.1°. The SM data were resampled into NDVI3g GIMMS grids using a majority filter. In addition, it provides the SM in three different depth layers in each pixel (0–100 cm). In this study, the SM values of the three layers at different depths were averaged at 12 am and 12 pm to determine the daily SM in the root zone (0–100 cm). As in the previous subsection, the moving averages SM were calculated with a 30-day window and then averaged for each season of the year.

3.2.3. Data Analyses

Figure 3.2 shows the general technical flow chart of this study. The three main components are: (1) data collection and preprocessing of phenological parameters, (2) data collection and preprocessing of hydroclimatic data, and (3) analysis of phenological parameters and hydroclimatic data.

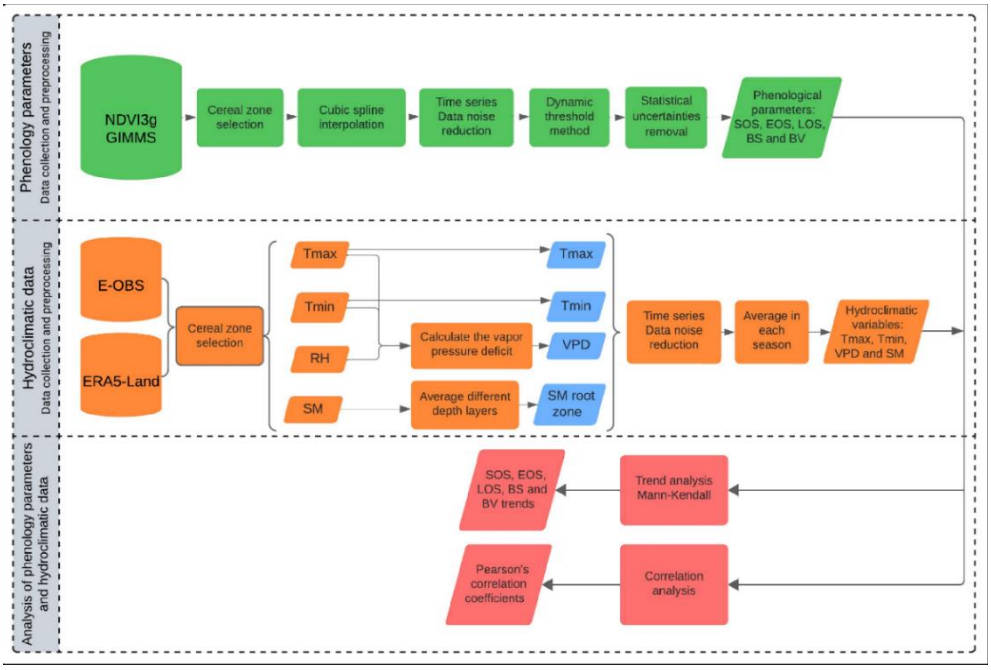

Figure 3.2. The technical flow chart of this study.

3.2.3.1. Phenology Parameter Extraction

The identification of the phenological parameters of cereals was performed using the modified dynamic threshold method (Huang et al., 2019), which is an improved method of the original dynamic threshold method (Jonsson and Eklundh, 2002; White et al., 1997). The time series of crop vegetation indices tend to be asymmetric; therefore, this method solves this problem by using two different amplitudes for the recovery of the SOS and EOS of crops (Huang et al., 2019). A diagrammatic sketch of the modified dynamic threshold method is shown in Figure 3.3.

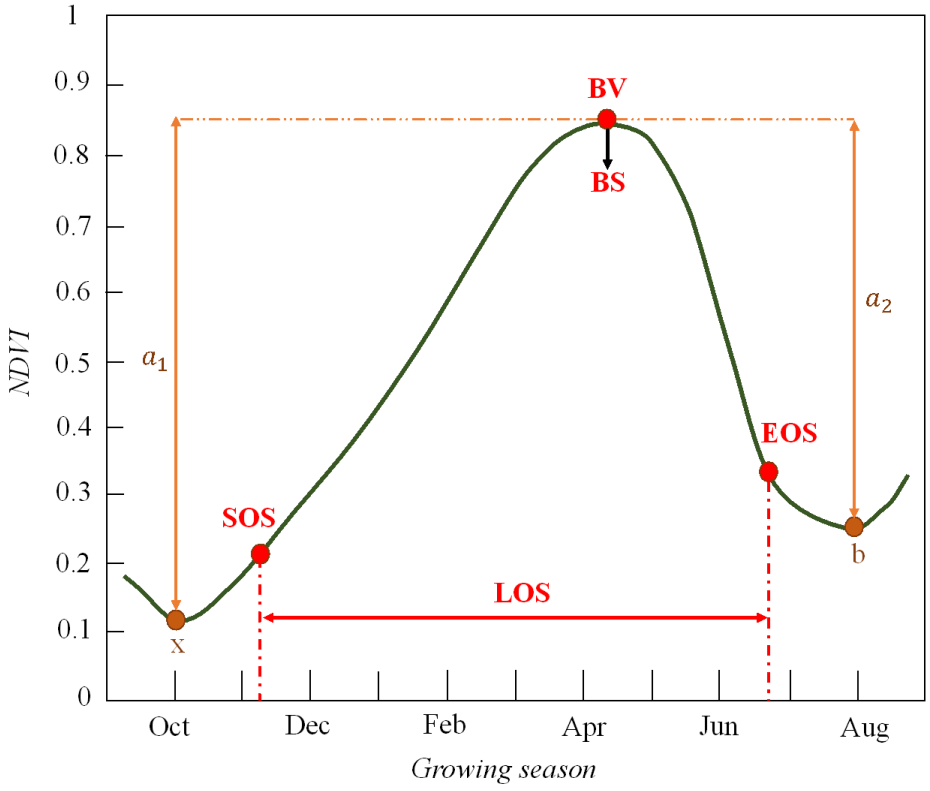

Figure 3.3. Application of the modified dynamic threshold method on the NDVI series throughout the agricultural year to extract the phenological parameters: start (SOS), end (EOS), length (LOS) of the growing season, booting stage (BS), and the NDVI value in the BS (BV). BV is the maximum NDVI value within the growing season, "x" is the minimum NDVI value on the left side of BV and "b" is the minimum value on the right side of BV. The black arrow indicates the retrieval of the BS date from BV. "a1" denotes the difference between BV and x, while "a2" denotes the difference between BV and b; these are the amplitudes used to retrieve SOS and EOS, respectively.

The agricultural year was defined as the period from the season in which the SOS occurred to the season in which the EOS occurred. In all study regions and for cereal crops, the SOS occurs in autumn, and the EOS occurs in summer of the following year (Manfron et al., 2017; MAPA, 2025b; Meyer et al., 2020; Morais et al., 2018; Ventrella et al., 2016; Yang et al., 2020); therefore, the agricultural year was considered to extend from 1 September to 31 August of the following year. The SOS and EOS dates were retrieved at the pixel scale, and the amplitude thresholds were defined to be 20% according to the methodology used in several studies (Ersi et al., 2023; Jin et al., 2019a; Kern et al., 2020; You et al., 2013). The calculations of SOS and EOS thresholds are summarized in Equation (3.5).

$$\begin{cases} NDVI_{SOS} \geq x + 20\% * a_1 \\ NDVI_{EOS} \leq b + 20\% * a_2 \end{cases} \quad (3.5)$$

Derived from these two parameters, the LOS was calculated as the time between the SOS and EOS. In addition, the booting stage (BS) was identified as the date when the NDVI value during the crop year reached its maximum, indicating the peak of green biomass development (Benedetti and Rossini, 1993; Pan et al., 2015), and the NDVI value in the BS (BV) was also determined. Finally, following the methodology of Jeong et al. (2011), 10-year moving averages were calculated to remove statistical uncertainties caused by the first and last values and individual outliers in the time series for each pixel and for all identified phenological parameters.

3.2.3.2. Trend Analysis

The Mann–Kendall (MK) statistical test was used in the present study for the trend analyses. It is a nonparametric test used to identify trends in time-series data (Kendall, 1948; Mann, 1945). The ability of this test to detect trends has been demonstrated in many studies on the dynamics of vegetation phenology based on satellite observations (Jiao et al., 2020; Karkauskaite et al., 2017; Yuan et al., 2019a). In this study, the MK test was used to detect whether there were statistically significant increasing or decreasing trends in phenological parameters at the pixel scale. Under the null hypothesis of no trend H0, the MK test statistic (*S*) was calculated as follows:

$$S = \sum_{i=1}^{n-1} \sum_{j=i+1}^{n} sgn(x_j - x_i) \tag{3.6}$$

where

$$sgn(x) = \begin{cases} 1 & if\ x > 0 \\ 0 & if\ x = 0 \\ -1 & if\ x < 0 \end{cases} \tag{3.7}$$

For an upward trend, the *S* statistic is increased by +1, while it is decreased by −1 for a downward trend. The *S* statistics remain unchanged for a zero difference. The statistical parameter *Z* allows us to determine whether a trend is significant:

$$Z = \begin{cases} \dfrac{S-1}{\sqrt{var(S)}} & if\ S > 0 \\ 0 & if\ S = 0 \\ \dfrac{S+1}{\sqrt{var(S)}} & if\ S < 0 \end{cases} \tag{3.8}$$

Throughout this study, a p value of 0.05 (95% confidence level) was used as the criterion for determining the statistical significance of a trend. Thus, for an absolute value of *Z* greater than 1.96, a significant trend is considered.

3.2.3.3. Correlation Analysis

Pearson's correlation coefficients (R) were calculated at the pixel scale to analyze the relationships among the main phenological parameters (e.g., the SOS, EOS and LOS). The significance of the correlations was identified with p values at the 95% confidence level.

In addition, for the analysis of the influence of the hydroclimatic variables on the SOS and EOS parameters, the mean SOS and EOS dates were previously calculated for all the pixels of the study regions as well as for each season of the hydroclimatic variables. Subsequently, R values were calculated between each hydroclimatic variable and the main phenological parameters, SOS and EOS, with the statistical significance level set to $p < 0.05$. This analysis was conducted during the season in which the SOS and EOS

occurred, as well as during the previous season. Therefore, for the SOS, the autumn season and summer season of the previous agricultural year were considered, while for the EOS, the summer and spring of the current agricultural year were considered.

3.3. Results

3.3.1. Phenological Dynamics over Decades

The initial analysis of the extracted parameters involved comparing the dates of the phenological parameters, SOS, EOS, and BS, with the LOS and BV values between the first and last decades of the study (Figure 3.4).

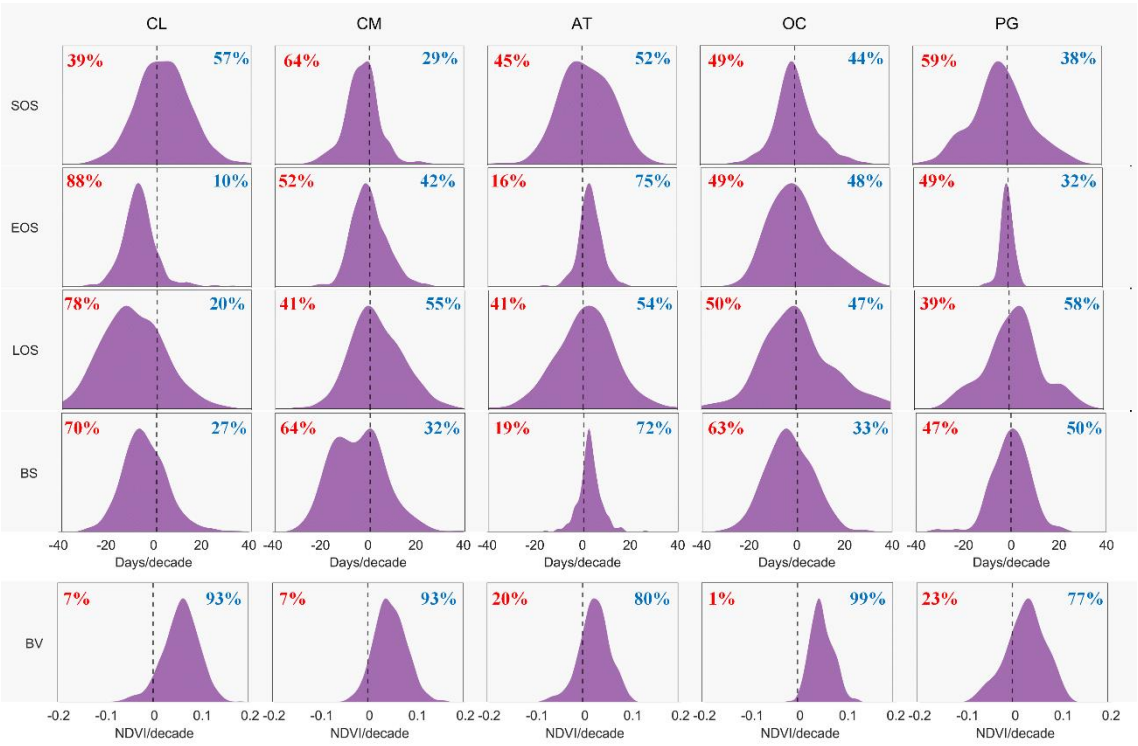

Figure 3.4. Histograms of the distributions of the start (SOS), end (EOS), length (LOS) of the growing season, booting stage (BS), and the NDVI value in the BS (BV) differences between the last (2013– 2022) and first (1982–1992) decades of the study period at the pixel scale in Castilla y León (CL), Castilla La Mancha (CM), Alentejo (AT), Occitanie (OC) and Puglia (PG). Values equal to 0 are excluded from the percentages (advance, red; delay, blue).

Advanced dates predominated for the SOS, EOS, and BS, while the LOS increased. CM stood out, with an advanced SOS in 64% of the pixels. Regarding the EOS and LOS, the CL showed very pronounced advance and shortening, with 88% and 78%, respectively, of negative pixels. For BS, the AT showed a delay in the dates in 72% of the pixels. Conversely, for the BV, all regions showed an increase, with an average increase of 88% of the pixels.

Several authors reported changes in the phenological parameters from the 2000s onward (Cong et al., 2013; Fu et al., 2014) and associated these with the global warming hiatus (Zhu et al., 2012). In the study areas, this slowdown in global warming was also observed between the end of the 20th century and the beginning of the 21st century, as shown in Figure 3.5.

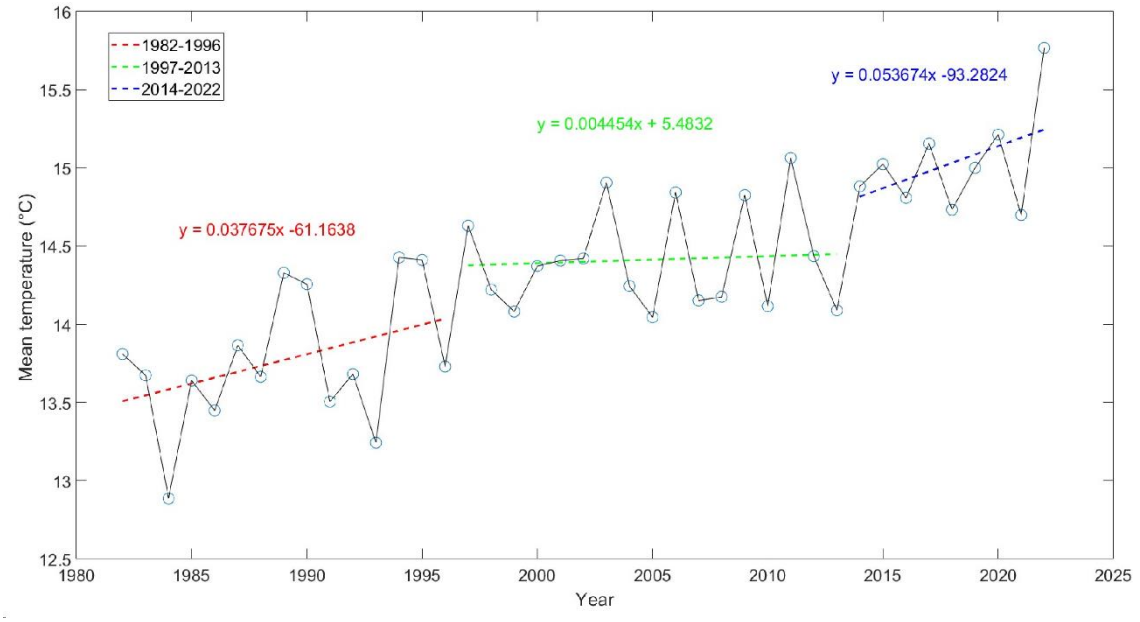

Figure 3.5. Average monthly mean temperature (°C) of the study regions from 1982 to 2022 and the regression lines and their equations for the period associated with the global warming hiatus (green) and the periods before (red) and after (blue).

With the aim of studying the behavioral patterns before and after this climatic inflection, the study period was divided into two parts: the first period covered the first two decades (1982–2002), and the second period covered the last two decades (2003–2022). This approach, which involves dividing the period into two parts, namely, before and after the slowdown in global warming, has been used in other studies (Jeong et al.,

2011; Zhao et al., 2015), although with a shorter observation period and for all types of vegetation cover.

Figures 3.6–3.8 show that the decadal differences in both periods had inverse behaviors, considering the predominant pattern of each phenological parameter, except for BV, which increased in both periods. Thus, in the decadal differences of the first period, advances in the SOS and EOS and an increase in the LOS were predominantly observed (Figures 3.6 and 3.7). The SOS advanced in all regions except for CL, with PG standing out for its advancement in 81% of the pixels, while for the EOS, CL showed an advancement in 75% of the pixels. The length of the phenological cycle of the PG increased in 79% of the pixels. In contrast, the differences in the decades of the second period showed delays in the SOS and EOS and decreases in the LOS (Figures 3.6 and 3.7). The SOS experienced delays in all regions, with the percentages of positive pixels ranging between 52% and 67%, while the LOS decreased in all regions, with the percentages of negative pixels ranging between 56% and 64%. The EOS predominantly experienced delays, with the PG region standing out with a delay for 68% of its pixels.

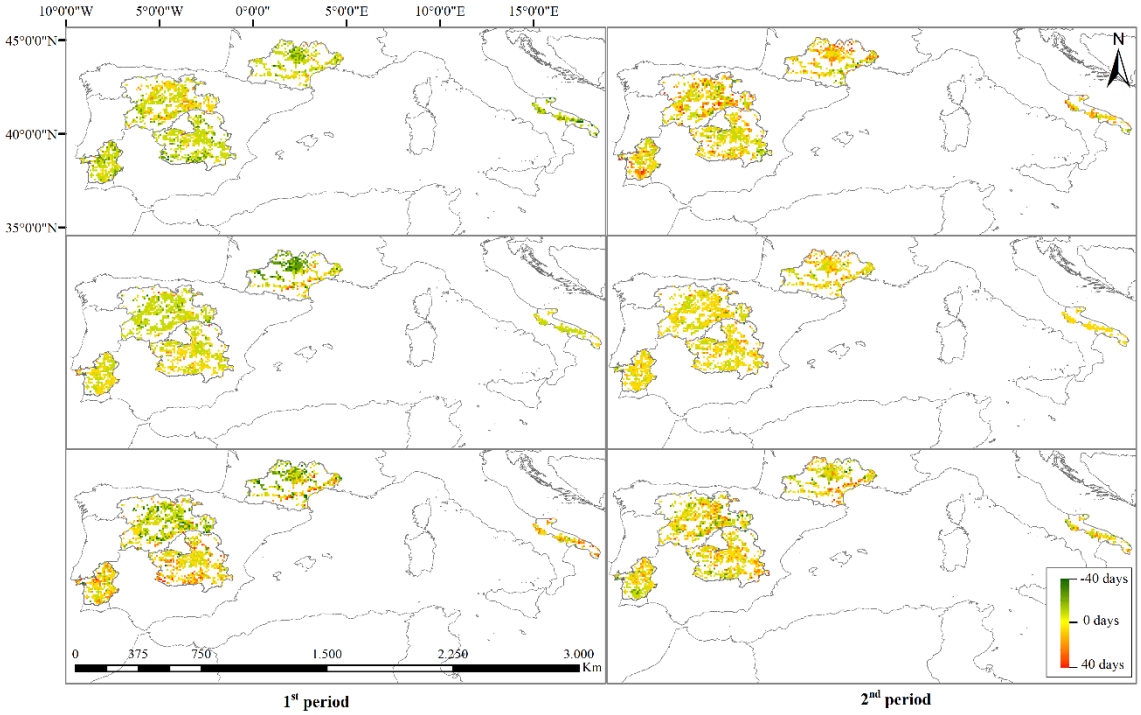

Figure 3.6. Spatial distribution of the differences in the start (SOS), end (EOS) and length (LOS) of the growing season, between the two decades (1993–2002 minus 1982–1992) of the first period and of the second period (2013–2022 minus 2003–2012), represented at the pixel scale in Castilla y León (CL), Castilla-La Mancha (CM), Alentejo (AT), Occitanie (OC) and Puglia (PG).

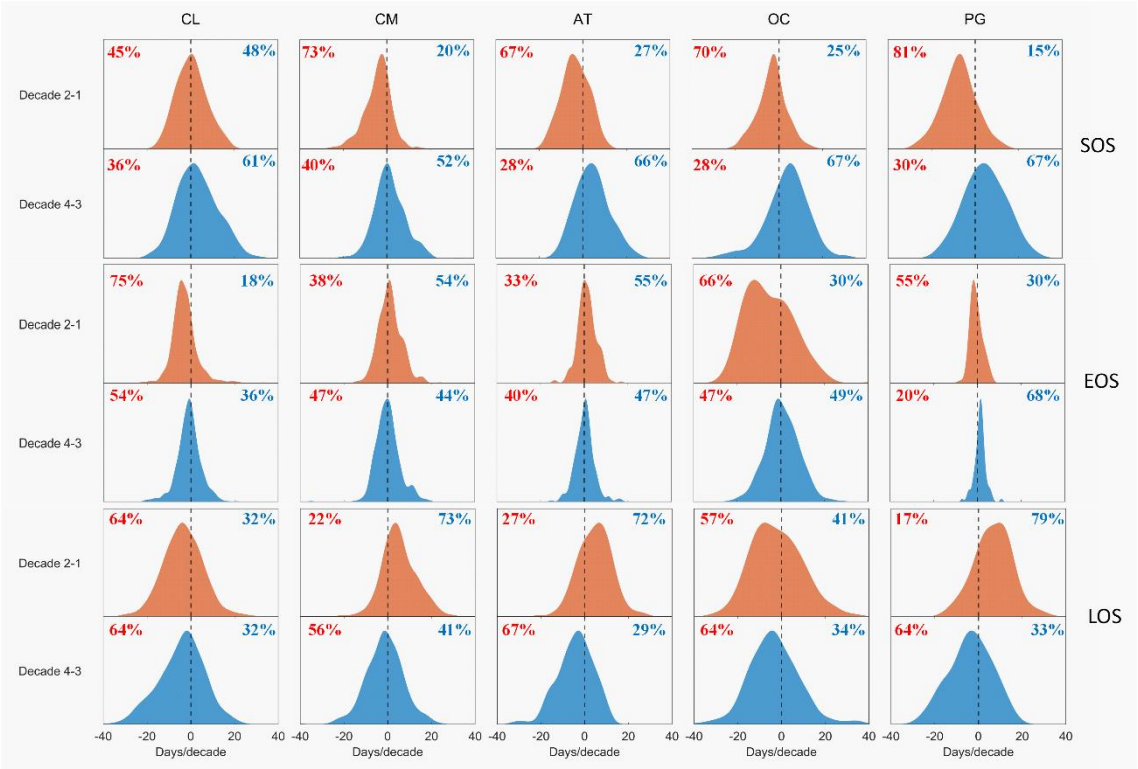

Figure 3.7. Histograms of the distributions of the differences in the start (SOS), end (EOS) and length (LOS) of the growing season between the second (1993–2002) and first (1982–1992) decade (Decade 2–1, brown) and between the fourth (2013–2022) and third (2003–2012) decade (Decade 4–3, blue), represented at the pixel scale in in Castilla y León (CL), Castilla-La Mancha (CM), Alentejo (AT), Occitanie (OC) and Puglia (PG). Values equal to 0 are excluded from the percentages (advance, red; delay, blue).

BS followed the same pattern that was observed for the SOS and EOS in each period (Figure 3.8). During the first period, not only did the SOS and EOS advance, but they also caused a change in the phenological cycle, thus advancing the BS. In all regions, the BS advanced with an average of 76% of the pixels, except in the PG, where delayed pixels predominated, with a negligible difference of 48% compared to 45% for advanced pixels.

However, in the second period, the BS was mostly delayed, with CL occurring in 57% of the delayed pixels. In contrast, the BV showed a consistent pattern in the same direction in both periods, with average percentages of increasing pixels of 70% and 86% in the first and second periods, respectively.

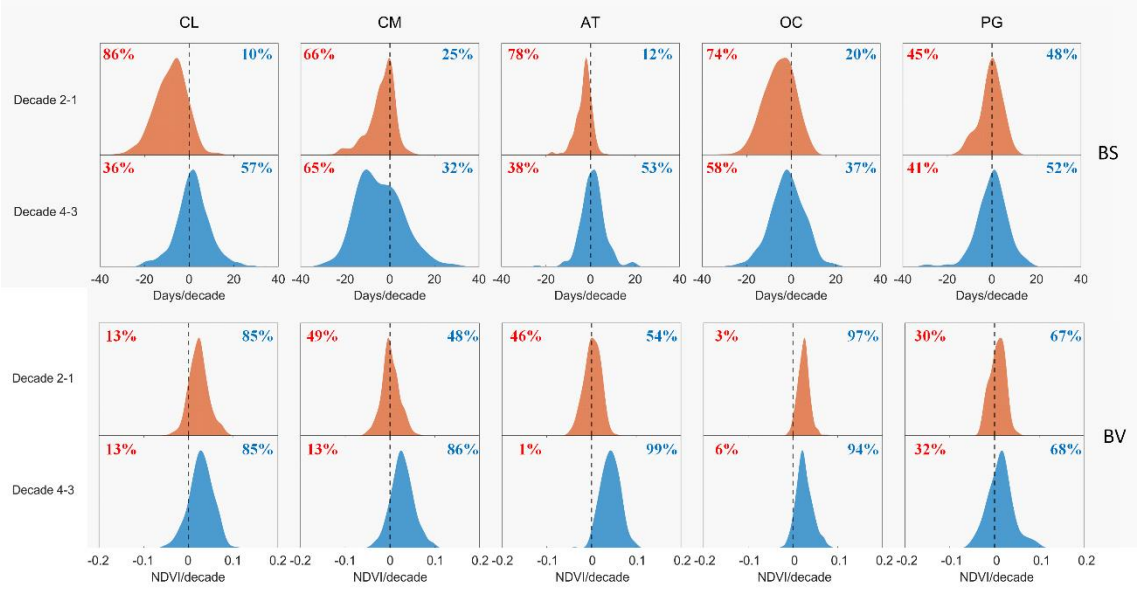

Figure 3.8. Histograms of the distribution of the differences in the booting stage (BS) and the NDVI value in the BS (BV) between the second (1993–2002) and first (1982–1992) decade (Decade 2–1, brown) and between the fourth (2013–2022) and third (2003–2012) decade (Decade 4–3, blue), represented at the pixel scale in Castilla y León (CL), Castilla-La Mancha (CM), Alentejo (AT), Occitanie (OC) and Puglia (PG). Values equal to 0 are excluded from the percentages (advance, red; delay, blue).

3.3.2. Temporal Patterns of Phenological Trends

The trends of the phenological parameters during the first and second periods are shown in Table 3.1, and the values of the slopes of these trends are shown in Table 3.2. Significant changes in the SOS, EOS, LOS and BS were observed in the two study periods, with an inverse pattern between them. During the first period, the SOS, EOS and BS dates tended to advance in all regions, with 76%, 65% and 75%, respectively, of the pixels showing negative trends (Table 3.1). The average pixels across all regions with significant trends toward advancing dates for the SOS, EOS, and BS represented nearly 55% of the total pixels. The SOS presented an average advance of 7.5 days, with the AT and PG regions experiencing the greatest advancements, exceeding 10 days (Table 3.2). The EOS presented an average advance of 3.1 days, while the BS advanced by 7 days, with the OC and CL regions showing the greatest advancements in both cases. In most regions, the LOS exhibited increases, although the distribution was more heterogeneous, with the CL and OC regions showing decreases due to greater advancements of the EOS than of the SOS. The average increase in the LOS across all regions was 4.3 days, with

an average increase in regions with a higher percentage of positive pixels of 9 days and a mean decrease in CL and OC of 2.2 days. When contrasting regions with LOS increases and decreases, the increases in the number of days were observed to be four times greater than the decreases.

Table 3.1. Trends of the cereal phenological parameters, SOS, EOS, LOS, BS and BV, at the pixel scale in CL, CM, AT, OC and PG and the averages of these parameters for the two study periods. The data indicate the percentages of pixels with positive trends (P), negative trends (N), statistically significant trends $p < 0.05$ (S), significant positive trends (SP) and significant negative trends (SN). The highest percentages (above 50) for each parameter have been colored in red (negative trends) and blue (positive trends).

Regions	1st period (%)					2nd period (%)				
	P	N	S	SP	SN	P	N	S	SP	SN
					SOS					
CL	38	62	62	22	40	68	32	64	45	19
CM	26	73	67	13	54	66	33	65	44	21
AT	18	81	75	7	68	89	11	77	73	4
OC	21	79	70	13	57	75	25	81	64	17
PG	14	86	75	7	68	55	38	60	40	20
Average	23	76	69	12	57	71	28	69	53	16
					EOS					
CL	15	85	70	8	62	39	61	59	21	38
CM	45	54	54	25	30	53	46	62	34	28
AT	48	51	59	27	32	73	27	67	51	16
OC	32	68	80	22	58	58	41	63	40	22
PG	35	65	70	25	45	75	17	72	59	13
Average	35	65	66	21	45	60	38	65	41	23
					LOS					
CL	38	61	61	20	41	30	70	68	18	50
CM	66	34	55	41	14	39	60	62	23	39
AT	78	22	68	59	10	21	78	66	8	58
OC	44	55	64	27	37	32	68	62	15	47
PG	82	18	71	60	11	40	52	56	26	29
Average	62	38	64	41	23	32	66	63	18	45
					BS					
CL	7	93	80	4	77	67	33	73	51	22
CM	21	78	65	10	56	38	61	82	29	54
AT	27	73	63	8	55	84	15	73	67	6
OC	16	84	74	7	67	49	51	71	34	37
PG	49	49	56	22	34	57	35	61	39	22
Average	24	75	68	10	58	59	39	72	44	28
					BV					
CL	70	30	62	49	13	79	21	73	62	11
CM	58	42	62	41	21	84	16	83	73	11
AT	58	42	48	28	20	90	10	84	80	4
OC	98	2	96	94	1	92	8	93	87	6
PG	68	32	74	50	24	66	27	74	52	22
Average	70	30	68	52	16	82	17	81	71	11

In contrast, during the second period, there was a predominant trend toward delays in the SOS, EOS, and BS dates across all regions, with 70%, 60%, and 59%, respectively, of the pixels showing positive trends (Table 3.1). On average, nearly 43% of the pixels across all regions exhibited significant trends toward delayed SOS, EOS, and BS dates. The SOS presented an average delay of 7.5 days, with AT and OC being the regions with the greatest advances, averaging 10.6 days (Table 3.2). The EOS presented an average advance of 1.7 days, and the BS presented an average advance of 1.6 days, with AT experiencing the most prolonged delay. The BS trend was more heterogeneous across all regions, as it advanced in CM and OC, while in the remaining regions, it was delayed, which was similar to what occurred in CL with the EOS, which was the only region with a higher percentage of positives. However, compared to the first period, the rate of advancement slowed, with the average advancement of the BS decreasing from 8.8 days to 2.8 days in CM and OC and from 6.6 days to 2 days in the EOS for CL. Considering all territories as a whole, the LOS presented a decreasing trend in 66% of the pixels, 68% of which were significant, with an average decrease of 6 days. BV increased in both periods, with a 47% difference in the increase between the second and first periods (Table 3.2). Overall, clear inverse trends in the phenological parameters were observed between the two periods, with a tendency toward delayed SOS, EOS, and BS, along with a reduction in the LOS in the latter years.

Table 3.2. Slopes of the MK trends of the phenological parameters of SOS, EOS, LOS, BS and BV cereals in CL, CM, AT, OC and PG and the average of these parameters for the two study periods. Δ% indicates the percentage increase in the NDVI from the first period (1P) to the second period (2P).

Periods	Regions	SOS	EOS	LOS	BS	BV	
		Days/period				NDVI/period	Δ% 2P-1P
1	CL	-3,2	-6,6	-3,3	-13,0	0,009	
	CM	-6,1	0,0	5,6	-6,9	0,005	
	AT	-10,6	-1,1	9,5	-3,7	0,004	
	OC	-5,9	-7,3	-1,1	-10,6	0,021	
	PG	-11,4	-0,6	10,5	-1,0	0,005	
	Average	-7,5	-3,1	4,3	-7,0	0,009	
2	CL	6,5	-2,0	-8,7	4,7	0,015	40
	CM	4,2	1,4	-3,3	-5,0	0,018	69
	AT	11,8	3,3	-8,7	6,6	0,020	81
	OC	9,4	2,9	-6,5	-0,6	0,020	-8
	PG	5,5	2,8	-2,6	2,4	0,012	54
	Average	7,5	1,7	-6,0	1,6	0,017	47

3.3.3. Relationships between the Phenological Parameters of Vegetation

The interrelationships among the main phenological parameters of cereals, namely, the SOS, EOS and LOS, were analyzed (Table 3.3). The results showed that there were no clear relationships between the SOS and EOS in either period since no marked patterns were detected in any region. The percentage of positive correlations is slightly greater than that of negative correlations, with an average percentage of significant positive correlations in all regions of approximately 55% in both the first and second periods. The mean R value in all regions was irrelevant, with values of 0.03 and 0.09 in the first and second periods, respectively.

However, when the relationships of the SOS and EOS with the LOS were analyzed, very marked patterns were observed in both periods. During the first period, there was an inverse relationship between the SOS and LOS, with an average of 93% of pixels having a negative correlation in all regions, 89% of which were significant, with an average R value of −0.71. The AT and PG regions had inverse correlations for 100% of their pixels, with 100% and 95% of the correlations being significant and with average pixel R values of −0.96 and −0.87, respectively. This indicates that the SOS advances caused an increase in the LOS, as shown in the previous section.

In the second period, relationships between the SOS and LOS were observed to be in the same direction as those in the first period but were more pronounced (Table 3.3). Across all regions, there were pixel percentages with inverse correlations between 92% and 99%, of which an average of 94% were significant. The average R value for the study region was −0.80. OC increased the number of pixels with a negative correlation by 16%, increased the number of pixels with an inverse and significant correlation by 26%, and increased the R value from −0.41 to −0.70. Although the relationship between the SOS and LOS remained consistent in both periods, it was slightly more pronounced in the second period. Thus, the dynamics of the SOS inversely influenced the LOS, with a stronger relationship observed in later years.

Table 3.3. Correlation coefficients between the phenological parameters, SOS, EOS and LOS, at the pixel scale in CL, CM, CM, AT, OC, and PG and the averages of these parameters for the two study periods. The data indicate the average R value in pixels (R), the percentage of pixels with a positive correlation (P), a negative correlation (N), a statistical significance of $p < 0.05$ (S), a positive significant correlation (SP) and a significant negative correlation (SN). The highest percentages (above 50) for each parameter have been colored in red (negative trends) and blue (positive trends).

Regions	1st period						2nd period					
	P	N	S	SP	SN	R	P	N	S	SP	SN	R
	SOS - EOS											
CL	57	41	52	32	20	0,09	55	45	50	28	23	0,05
CM	47	52	52	26	27	-0,02	55	44	56	33	23	0,08
AT	41	57	52	20	32	-0,09	68	32	53	43	10	0,24
OC	62	37	61	41	21	0,16	57	43	56	34	23	0,09
PG	46	52	52	24	28	-0,01	51	49	59	33	25	0,02
Average	51	48	54	28	26	0,03	57	43	55	34	21	0,09
	SOS - LOS											
CL	5	95	81	0	81	-0,67	2	98	92	0	91	-0,82
CM	7	92	82	3	79	-0,65	8	92	86	4	82	-0,70
AT	0	100	95	0	95	-0,87	2	98	96	0	95	-0,84
OC	22	77	65	7	57	-0,41	6	93	84	1	83	-0,70
PG	0	100	100	0	100	-0,96	1	99	99	0	99	-0,94
Average	7	93	85	2	83	-0,71	4	96	91	1	90	-0,80
	EOS - LOS											
CL	88	12	74	72	2	0,56	79	21	60	54	6	0,40
CM	90	9	78	77	1	0,64	83	17	67	62	5	0,49
AT	83	17	68	62	6	0,46	68	32	54	38	16	0,19
OC	93	7	86	84	2	0,71	83	17	67	62	5	0,50
PG	66	34	61	42	19	0,22	61	39	62	45	17	0,20
Average	84	16	73	67	6	0,52	75	25	62	52	10	0,36

The relationships between the EOS and LOS (Table 3.3) were direct in both study periods, in contrast to the relationships between the SOS and LOS. In the first and second study periods, the average percentages of pixels showing direct correlations were 84% and 75%, respectively, of which 80% and 69%, respectively, were statistically significant. Across all regions, there were slight decreases in the percentages of positively correlated pixels from the first to the second period. The average R values were 0.52 and 0.36 in the first and second periods, respectively. Although this relationship remained consistent in both periods, it was slightly less pronounced in the second period. Consequently, the EOS has become less decisive in affecting the LOS in recent years. Therefore, while the SOS is becoming more determinant of the LOS, the EOS has the opposite influence. This

suggests that the SOS varied more significantly than the EOS, as observed in the trend analysis.

3.3.4. Influence of Hydroclimatic Variables on Phenological Parameters

The analysis of the potential controls of the hydroclimatic variables on the dynamics of phenological parameters under Mediterranean conditions is shown in Table 3.4. During the first period, a distinctive pattern of statistically significant inverse correlations was observed, involving the relationships of the SOS and EOS with the Tmax, Tmin and VPD variables of the previous summer and spring, respectively. Among these, the highest R values correspond to the relationships of the SOS and EOS with Tmin and Tmax, respectively, with R values of −0.71 in both cases. During the second period, a similar pattern was also observed for both phenological parameters, with significant direct correlations of the autumn and summer Tmax values with the SOS and EOS dates, with R values of 0.53 and 0.45, respectively. Furthermore, during the spring of the first period, the EOS also showed a significant direct correlation with SM, with R values of 0.50. Similarly, during the summer of the first period, an inverse correlation between the EOS and Tmin was observed, with an R value of −0.61.

Table 3.4. Correlation coefficients between the SOS, EOS and hydroclimatic variables during the current phenological season and the previous season for the five study regions as a whole, considering the first (1P) and second (2P) periods. $p < 0.05$ indicates statistical significance (*).

Variables	SOS				EOS			
	Autumn		Last summer		Summer		Spring	
	1P	2P	1P	2P	1P	2P	1P	2P
P	-0,10	-0,17	0,04	0,11	-0,16	0,08	0,09	0,06
Tmax	0,27	0,53 *	-0,52 *	0,30	-0,37	0,45 *	-0,71 *	0,26
Tmin	0,08	0,03	-0,71 *	-0,14	-0,61 *	0,04	-0,58 *	-0,04
VPD	0,36	0,40	-0,45 *	0,28	-0,26	0,41	-0,54 *	0,19
SM	-0,17	-0,36	0,40	0,07	0,29	-0,04	0,50 *	-0,15

Specifically, the energy variables and SM could have played a significant role in the observed variations in the SOS and EOS during the first study period. However, in

recent decades, Tmax has emerged as the variable that exerts predominant control over the dynamics of these key phenological parameters.

3.4. Discussion

The results revealed a clearly delineated pattern of reversal or slowdown of the phenological parameters from the beginning of the 21st century. During the first period, the SOS, EOS, and BS dates improved by averages of 7.5 days, 3.1 days, and 7 days, respectively, while the LOS increased by 4.3 days. These results are consistent with those of many previous investigations, such as Stöckli and Vidale (2004), which revealed a general shift toward earlier and longer growing periods in Europe, which were approximately 5.4 days/decade and 9.6 days/decade, respectively, during the period from 1982 to 2001. Piao et al. (2006) reported that in China from 1982 to 1999, the SOS advanced at a rate of 7.9 days/decade, and the LOS increased by 10.16 days/decade. Furthermore, there is extensive evidence that spring events such as BS occurred increasingly earlier in the studies prior to the 2000s. For instance, Menzel et al. (2006) reported an advance of 2.5 days/decade in spring phenology in Europe from 1971–2000. A study carried out by Peñuelas et al. (2002) revealed that in the Mediterranean region, plants altered their cycles, with advances in phenological phases of approximately 6 days during the period from 1952 to 2000.

However, during the first decades of the 21st century, changes in the trends of phenological parameters were evident. In the present study, average delays of 7.5 days in the SOS, 1.7 days in the EOS and 1.6 days in the BS were recorded, while the LOS decreased by 6 days. Similar results were obtained by Touhami et al. (2022), who detected an average delay in the SOS of 7.8 days and a decrease in the LOS of 12.8 days from 2000 to 2017 in the Mediterranean region of northeastern Tunisia. Additionally, several studies have reported trends toward delayed EOS in recent decades (Fan et al., 2022; Liu et al., 2023). Thus, Zhu et al. (2024) reported a delayed EOS of 1.6 days/decade in China. Zhang et al. (2020) studied the phenology in the Northern Hemisphere and observed EOS delays of 6.3 days/decade.

The present study found strong evidence that the BV tended to increase in both periods, with average increases in the first period of 0.009 NDVI and 0.017 NDVI in the

second period. The observed increase in the second period was significantly greater than that in the first period, being 47% greater. This finding is consistent with that obtained in the study of Gao et al. (2022), who also identified a trend toward greening during the 1982–2020 growing season, with an average increase of 0.048 NDVI per decade. This trend showed two distinct periods, one of gradual growth before 2006 and another of drastic increase in the NDVI after 2006. De Jong et al. (2013) reported a continuous increase in plant activity in Europe. Several studies have shown that the increasing rate of CO2 fertilization caused by increasing temperatures and CO2 levels are the main drivers of the observed greening (Kumar et al., 2022; Mishra and Mainali, 2017; Piao et al., 2015). The Intergovernmental Panel on Climate Change (IPCC) 2023 report (IPCC, 2023) highlights that the greenhouse gas (GHG) emissions during 2010–2019 were higher than those in any previous decade. In 2019, GHG emissions were 12% higher than those in 2010 and 54% higher than those in 1990, which explains the notable increase observed in the second study period.

According to previous studies (Julien and Sobrino, 2009; Wu et al., 2012, 2016), an advanced SOS was associated with a longer LOS in the first study period, and this association was slightly stronger in the second period, when a delayed SOS was associated with a shorter LOS. Alternatively, it was observed that an earlier EOS was associated with a shorter LOS in the first period, but this relationship was also weaker in the second period, with a more delayed EOS associated with a longer LOS. The relationships between the SOS and LOS were slightly stronger than those between the EOS and LOS, suggesting that the SOS had a greater impact on the LOS than did the EOS; moreover, this impact was slightly more pronounced in the second period than in the first period. Additionally, a negligible relationship was found in the first period, although it was slightly more prominent in the second period between the SOS and EOS, with a positive relationship of 57% of pixels, of which 60% were significant. This finding suggests that in the second period, later SOS in autumn are usually accompanied by later EOS in summer, regardless of the summer conditions.

Changes in vegetation phenology are considered to be a consequence of adaptive responses to climatic factors (Hmimina et al., 2013). Particularly in rainfed agriculture, environmental conditions determine the correct development of crops. A greater influence of the energetic variables and SM was observed during the first period in the previous season on the SOS and EOS. The discrepancy between the first and second

periods coincides with the changes observed in the trends of the phenological parameters. Stronger and more significant associations were found between the first periods of the SOS and EOS in the previous summer and spring, respectively, and Tmax, Tmin, VPD and SM. More specifically, in the first period, the variables Tmax, Tmin and VPD of the previous summer were the variables that most influenced the SOS with an inverse relationship. The same pattern was observed for the EOS, except for SM aggregation, which had a direct relationship. Thus, increases in Tmax, Tmin and VPD would lead to advances in the SOS and EOS, while a decrease in SM would also advance the EOS. Several studies obtained similar results (Yuan et al., 2019a, 2024), and others have confirmed these results since at the end of the 20th century there were increases in VPD (Yuan et al., 2019b) and a warming of the Earth's surface with significant increases in temperature (Braganza et al., 2004). Furthermore, in the study by Almendra-Martín et al. (2022a), a general decreasing trend in SM in Europe was observed. However, in the second period, the pattern that was observed in the first period changed, and only the direct relationships of Tmax in autumn and summer with the SOS and EOS, respectively, were significant. Thus, an increase in Tmax would cause delays in the SOS and EOS. In agreement with these results, Del Río et al. (2012) observed an increase in Tmax at a greater rate than in Tmin.

As previously observed, there is a disparity in the phenological patterns as well as in the relationships among these patterns and climatic factors between the first and second periods of this study, with the inflection point that occurred around the beginning of the 21st century. A reversal of the SOS, EOS, LOS and BV was observed after 2002. From the late 20th century until approximately 2012, the global surface temperature did not increase as rapidly as predicted by global climate models (Fyfe et al., 2013; Medhaug et al., 2017). This slowdown in warming is known as the global warming hiatus. However, since approximately 2012, particularly more intense warming has been observed (Huang et al., 2021; Zahradníček et al., 2021). In the Mediterranean region under study, a reversal of the dynamics of the phenological parameters as well as a decrease in the influence of climatic variables and SM on the phenology of cereals between the first and second periods of study was obtained. This phenomenon can be attributed to the global warming hiatus, which resulted in a pause in warming around the early 2000s, as observed in most of the world (Kosaka and Xie, 2013). Consequently, further studies in other regions are suggested to evaluate the generalizability of these

findings and to better understand the impact of the global warming hiatus on crop plant phenological trends.

3.5. Conclusions

The results obtained in this study reveal a clear distinction between the last decades of the 20th century and the first decades of the 21st century. The trends in SOS, EOS, LOS and BS experienced significant changes between these periods. In the first period, advances in SOS, EOS and BS were observed, as well as an increase in LOS; in the second period, these trends reversed, showing delays in SOS, EOS and BS and a decrease in LOS. However, BV continued to show a steady increase in both study periods. Additionally, the SOS was more decisive than the EOS in determining the lengthening of the LOS. A greater influence of the energy climatic variables and SM was observed in the season prior to the SOS and EOS. In addition, a decrease in the influence of the energetic and SM variables on the SOS and EOS was detected throughout the study period. In the first period, the energetic variables with an inverse relationship and SM with a direct relationship during the previous season had a more significant impact on the progression of the SOS and EOS. However, in the second period, only Tmax during the SOS and EOS emergence seasons showed a direct relationship with their delays.

These findings, which are consistent with the timing of the global warming hiatus, reflect changes in the trends of phenological parameters around the beginning of the 21st century. Furthermore, they highlight the suitability of using the NDVI obtained through remote sensing to analyze the dynamics of cereal phenological parameters over time. These results extend the understanding of the changes in cereal phenology in regions under a Mediterranean climate and provide a valuable reference for understanding ecosystem responses to climate change.

Continuous monitoring of phenological parameters using remote sensing is essential for detecting long-term changes in vegetation and for better understanding the ecosystem responses to climate change. These detected phenological changes are crucial because they could impact food security, especially in regions susceptible to SM scarcity due to climate change. However, it is recommended to explore the phenology of vegetation and crops other than cereals, as well as in other areas under different

environmental conditions, to determine whether this trend is generalizable. This study demonstrated the importance of understanding the phenological trends and their relationships with climate change to develop adaptation strategies and strengthen the resilience of agricultural systems to changing environmental conditions. These findings may be useful for agricultural management practices, such as sowing planning, seed and crop selection and management, as well as for developing strategies and strengthening the resilience of agricultural systems to changing environmental conditions. Furthermore, these results provide a solid basis for future research in this field, thus contributing to the advancement of knowledge and management of agricultural systems in a constantly evolving context of climate change.

CAPÍTULO 4

IMPACT OF FLASH DROUGHTS ON CEREAL CROPS UNDER MEDITERRANEAN CONDITIONS

Benito-Verdugo, P., González-Zamora, Á., & Martínez-Fernández, J. (2025). Impact of flash droughts on cereal crops under Mediterranean conditions. *Spanish Journal of Agricultural Research* (in press).

Resumen

Objetivo del estudio: Identificar y caracterizar las sequías repentinas (FD) en zonas con cereales de secano bajo condiciones mediterráneas, analizando sus efectos sobre la Productividad Primaria Bruta (GPP), el rendimiento y la fenología de los cereales entre 2000 y 2023.

Área de estudio: Principales regiones mediterráneas cerealistas de España, Portugal, Francia e Italia.

Materiales y métodos: Las FD se identificaron utilizando la humedad del suelo obtenida de la base de datos de reanálisis ERA5-Land y se caracterizaron según su frecuencia, duración y severidad. La respuesta de la GPP a las FD se analizó utilizando dos índices de tiempo de respuesta. Para evaluar el impacto de las FD sobre el rendimiento de trigo y cebada, se calculó el porcentaje de reducción del rendimiento durante los años con FD, mientras que el efecto de las FD sobre el estado y la fenología de los cereales se evaluó utilizando el Índice de Vegetación de Diferencia Normalizada (NDVI). Los datos de GPP y NDVI se obtuvieron de MODIS.

Resultados principales: Las FD afectaron significativamente a los cereales bajo condiciones mediterráneas, con una mayor frecuencia e intensidad durante los meses críticos de su desarrollo. Los cereales respondieron rápidamente a las FD, mostrando un estrés máximo durante los meses críticos. Las FD provocaron una reducción de hasta un 33% en los rendimientos de trigo y cebada, empeoraron el estado de los cereales en comparación con los años sin FD y adelantaron levemente las fases fenológicas.

Aspectos destacados de la investigación: Estos resultados alertan sobre los efectos de las FD en los cultivos de cereales bajo condiciones mediterráneas y en regiones con limitación hídricas en general, destacando las repercusiones que ya están afectando a estos cultivos. Este análisis ayuda a identificar patrones de respuesta que determinan la resiliencia de los cultivos a las FD, facilitando el desarrollo de estrategias para enfrentar futuras adversidades bajo escenarios de cambio climático

Palabras clave: Humedad del suelo; Cereales de secano; Trigo; Cebada; Clima mediterráneo.

Abstract

Aim of study: To identify and characterize flash droughts (FD) in areas with rainfed cereal crops under Mediterranean conditions, analyzing their effects on cereal gross primary productivity (GPP), yield, and phenology from 2000–2023.

Area of study: The main Mediterranean cereal-producing regions of Spain, Portugal, France, and Italy.

Material and methods: FD were identified using soil moisture from the ERA5-Land reanalysis database and characterized in terms of frequency, duration, and severity. GPP sensitivity to FD was analyzed using two response time indices. To evaluate the impact of FD on wheat and barley yield, the percent yield reduction during FD years was calculated, while the effect of FD on cereal health and phenology was assessed using the normalized difference vegetation index (NDVI). GPP and NDVI data were obtained from the Moderate Resolution Imaging Spectroradiometer (MODIS).

Main results: FD had a significant impact on cereal under Mediterranean conditions, with higher frequency and intensity during months critical for cereal development. Cereals responded rapidly to FD, experiencing peak stress during critical months. FD reduced wheat and barley yields by up to 33%, led to poorer cereal health compared with years without FD events, and caused a slight advancement in the phenological phases.

Research highlights: These results warn about the effects of FD on cereal crops under Mediterranean conditions and in water-limited regions in general, highlighting the potential consequences that are already affecting these crops. This knowledge helps identify response patterns that determine crop resilience to FD, facilitating the development of strategies to cope with future adversities under climate change scenarios.

Additional keywords: Soil moisture; Rainfed cereals; Wheat; Barley; Mediterranean climate.

4.1. Introduction

Drought is one of the most damaging natural hazards, and its frequency and intensity are expected to increase under the context of climate change, particularly in water-limited regions (Martínez-Fernández et al., 2015; Tramblay et al., 2020). In recent years, increasing attention has been given to flash droughts (FD), which are characterized by their rapid onset, intensification, and short duration (Lovino et al., 2024). The abrupt onset of FD makes them difficult to predict and significantly reduces the time available to mitigate their impact, which exacerbates the adverse effects on agriculture and society (Christian et al., 2024).

FD are caused by multiple factors, such as high temperature and evaporative stress, precipitation shortages and soil moisture deficits (Hu et al., 2024). Consequently, indicators have been developed to identify FD based on various hydrometeorological factors. Among these, soil moisture (SM) is recognized as an effective indicator of FD (Osman et al., 2024) and has been widely used for FD identification (Hu et al., 2024; O and Park, 2023). Osman et al. (2024) analyzed the main climatic variables used to define FD and concluded that root-zone SM is the most reliable indicator of these events. This variable is particularly relevant in regions such as Europe, where SM has been observed to generally decrease, with a significant projected reduction in the southern part of the continent (Almendra-Martín et al., 2022a; Ruosteenoja et al., 2018). Although SM is widely used as the main agricultural drought indicator, it is important to note that it exhibits metric-dependent responses to changes in temperature (Burke, 2011). Rising temperatures under climate change conditions can significantly affect SM levels by intensifying surface evaporation and plant transpiration (Berg and Sheffield, 2018). This process increases vapor pressure deficit and atmospheric evaporative demand, which raises evapotranspiration even under dry conditions, potentially further depleting SM and intensifying drought stress in crops (Seneviratne et al., 2010).

FD interfere with the physiological dynamics of vegetation, especially photosynthesis (Zhang et al., 2024b). Vegetation indicators obtained through remote sensing have been frequently employed for the dynamic monitoring of vegetation and its reactions to FD, such as the normalized difference vegetation index (NDVI), the leaf area index (LAI), solar-induced chlorophyll fluorescence (SIF) and gross primary productivity

(GPP), among others (Adhikari et al., 2024). However, although these tools provide information on general vegetation responses, studies that explicitly analyze the impact of the phenological cycle during FD are lacking. Most research has documented the overall behavior of vegetation in the face of these events (Barbosa, 2023; Zhang et al., 2024b), but how FD affect phenological phases is still unknown. This issue becomes even more relevant considering that, in recent years, changes in the phenology of crops such as cereals have been observed in regions susceptible to SM deficits (Benito-Verdugo et al., 2024).

Under global climate change scenario, the frequency and intensity of FD are projected to increase worldwide, posing a significant threat to ecosystems, particularly croplands (Lovino et al., 2024). A substantial increase in FD has been observed in the Mediterranean region (O and Park, 2023), with rainfed croplands being the most affected (Li et al., 2024). This situation is of particular concern for the Mediterranean region, as it is characterized by water-limited conditions, where rainfed cereal cultivation predominates, with wheat and barley being the most widely grown crops (Savin et al., 2022). In fact, Benito-Verdugo et al. (2023) reported that cereals grown in water-limited areas are particularly vulnerable to agricultural droughts, with drought-induced cereal yield reductions exceeding 30%. Despite clear evidence of the threat that FD pose to essential crops such as cereals, studies of FD in agricultural contexts remain very scarce, with most research focusing on FD in areas with natural vegetation (Barbosa, 2023; O and Park, 2023). Moreover, the few studies of FD in agricultural regions are limited to very specific geographic areas or to isolated events (Hunt et al., 2021; Jin et al., 2019b; Otkin et al., 2021) or focus broadly on croplands without considering impacts on specific crops (O and Park, 2024). Consequently, Shah et al. (2022) reported that analysis of the integral impact of FD on crop growth and productivity losses is crucial, emphasizing the need for research that addresses the impacts of FD on agriculture and facilitates the development of effective adaptation strategies.

This study aimed to identify and characterize FD in areas with rainfed cereal crops under Mediterranean conditions using SM data from the ERA5-Land reanalysis database to assess the impact of FD on the GPP, yield, and phenology of cereals. The analysis focused on the main cereal-producing regions of Spain, Portugal, France, and Italy from 2000–2023. This research aims to improve the understanding of FD and their impacts on cereals in water-limited regions, where managing and forecasting yields under climate

change is particularly important. Furthermore, this study provides insights into the ecological impacts of FD, helping to develop more effective monitoring and early warning systems. This work can inform management decisions in future scenarios for these key crops in water-stressed regions and help mitigate the adverse effects of FD on agriculture.

4.2. Materials and Methods

4.2.1. Study area

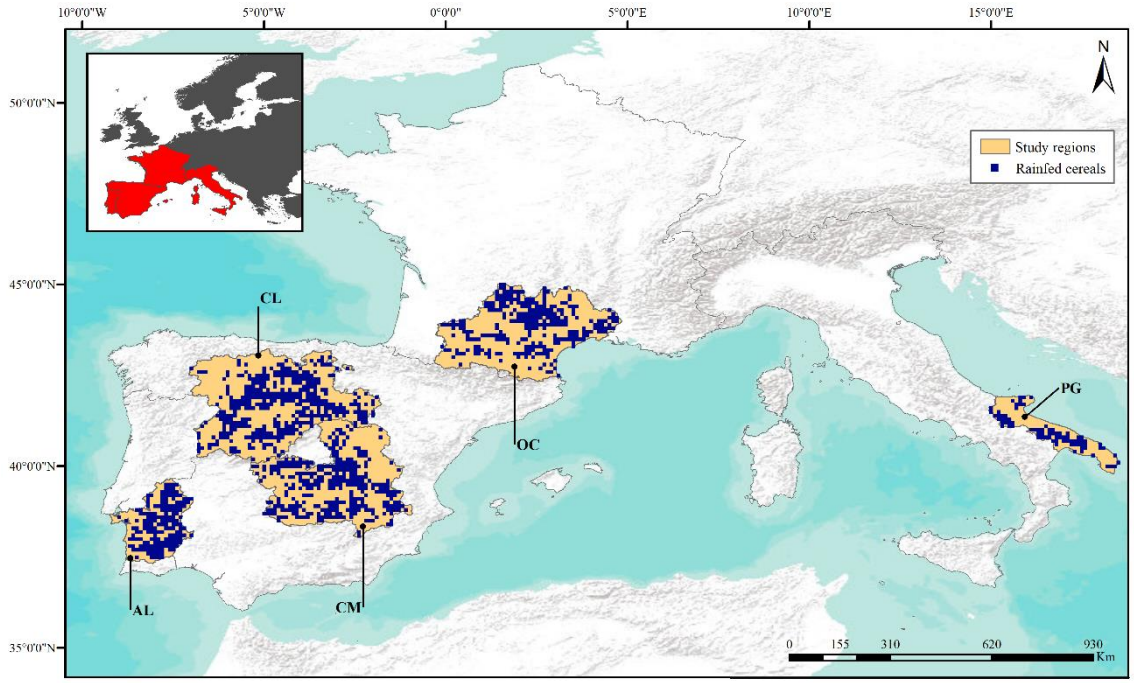

Figure 4.1. Location map of the areas with rainfed cereal crops in the study regions: Castilla y León (CL) and Castilla-La Mancha (CM) in Spain; Alentejo (AL) in Portugal; Occitanie (OC) in France; and Puglia (PG) in Italy.

The Mediterranean region is characterized by water-limited conditions, with mild and humid winters followed by dry and hot summers. Annual rainfall in the Mediterranean region is reduced and highly variable (Careddu et al., 2024). The predominant crops in the region are rainfed cereals, with wheat and barley being the most widely grown (Savin et al., 2022). The main cereal-growing regions under Mediterranean

climate in Spain (e.g., Castilla y León and Castilla-La Mancha [CL and CM, respectively]), Portugal (e.g., Alentejo [AT]), France (e.g., Occitanie [OC]), and Italy (e.g., Puglia [PG]), as highlighted in previous works (Benito-Verdugo et al., 2024; Careddu et al., 2024; Gameiro et al., 2024; Moojen et al., 2024), were selected as the study areas (Figure 4.1).

4.2.2. Irrigation and cereal cover mask

To analyze areas with rainfed cereal crops in the selected regions (Figure 4.1), two datasets were utilized to create a mask that filtered out all the areas other than the target areas. The Digital Global Map of Irrigation Areas of the Food and Agriculture Organization (FAO) was used to exclude irrigated areas. This map represents global areas equipped with irrigation, with a spatial resolution of 5 arc min (Siebert et al., 2013). In addition, to exclude areas with land cover types other than cereal crops, the Climate Change Initiative (CCI) Land Cover (LC) map from the European Space Agency (ESA) was used. This dataset has been widely used in drought studies (Akinyemi, 2021; Barbosa, 2024; Crocetti et al., 2020; Stoyanova et al., 2023). It categorizes the Earth's surface into 37 original LC classes based on the United Nations Land Cover Classification System (UN-LCCS), with a spatial resolution of 300 m (Di Gregorio, 2005). The irrigation and the LC maps were resampled into SM grids using a majority filter. Pixels with land cover types different from those of rainfed and mosaic cropland and those with more than 10% irrigation were excluded from this study. The applied mask then filtered all datasets, leaving only pixels representing rainfed cereal crops, assuming that cereals were the predominant crop in each region.

4.2.3. Soil moisture data

The SM data for FD identification were obtained from the ERA5-Land reanalysis database. This database is provided by the European Centre for Medium-Range Weather Forecasts (ECMWF), framed within the Copernicus Climate Change Service (C3S) of the European Commission (Muñoz-Sabater et al., 2021). This reanalysis database has been widely validated and used (O and Park, 2023; Shah et al., 2022). It provides SM data from 1981 to the present, with an hourly temporal resolution and a regular 10 × 10 km

resolution grid. The dataset also includes a four-layer representation of SM (0–7, 7–28, 28–100 and 100–289 cm). According to the average rooting depth of cereals, SM satisfies vegetation demands up to a soil depth of 100 cm (Wang et al., 2023a; Zhang et al., 2024c). Therefore, the SM data from the first three layers were selected. To estimate the daily root-zone soil moisture (0–100 cm), the SM values from these layers at different depths were averaged at 12 am and 12 pm.

4.2.4. Cereal crop data

Yield data for wheat and barley crops were obtained on an annual scale for each region of the study area from 2001–2023. Regional yield data for the Spanish regions CL and CM, the Portuguese region AL, the French region OC, and the Italian region PG were obtained from the Statistical Yearbook of the Ministry of Agriculture (MAPA, 2025a), the agricultural statistics publications of the National Institute of Statistics of Portugal (INE, 2025), the annual agricultural statistics of the Ministry of Agriculture and Food Security of France (AGRESTE, 2025), and the National Institute of Statistics of Italy (Istat, 2025), respectively.

The gross primary productivity (GPP) and normalized difference vegetation index (NDVI) were also used, as they are two important indicators for characterizing vegetation conditions (Adhikari et al., 2024). The GPP refers to the amount of carbon dioxide captured from the atmosphere by terrestrial plants through photosynthesis, a crucial process in the terrestrial carbon cycle (Zhang and Yuan, 2020). The NDVI is a common indicator used to monitor vegetation status and has been widely used in the study of vegetation changes (Adhikari et al., 2024; Magney et al., 2016). Therefore, both variables were obtained from the Moderate Resolution Imaging Spectroradiometer (MODIS). GPP data were obtained from the MOD17A2HGF and MYD17A2HGF version 6.1 products from the Terra and Aqua satellites, respectively. These products have a temporal resolution of 8 days and a spatial resolution of 500 m (Running and Zhao, 2021a, 2021b) and have been satisfactorily used recently to analyze vegetation responses to drought (Kashyap and Kuttippurath, 2024; Wang et al., 2023b; Zou et al., 2024). NDVI data were obtained from MOD13A1 (Terra) and MYD13A1 (Aqua) version 6.1 products with a temporal resolution of 16 days and a spatial resolution of 500 m (Didan, 2021a, 2021b). GPP and NDVI data were resampled into SM grids using a majority filter.

4.2.5. Flash drought identification and characterization

The analysis considered only the months corresponding to the phenological cycle of wheat and barley. The agricultural year was defined as the period from the month of sowing to the month of harvest. In all the selected regions, sowing occurs in October and harvesting occurs in July of the following year (Dare-Idowu et al., 2021; García-León et al., 2020; MAPA, 2025b; Morais et al., 2018). Therefore, the agricultural year was considered to be from October 1 to July 31 of the following year.

FD are defined based on rapid changes in SM, mainly following the approach of O and Park (2023) and Shah et al. (2022), who recently studied flash droughts in Europe. The SM data for each agricultural year during the study period are aggregated into 5-day averages (pentads) and then converted to percentiles via the nonparametric Gringorten plot position approach (Gringorten, 1963). This methodology has been widely used in previous studies (Christian et al., 2019b; Mukherjee and Mishra, 2022; Qing et al., 2022). The percentiles are determined at each pixel in each region for the same pentad over the entire study period. FD initiate when the SM decreases from at least the 40th percentile to less than the 20th percentile within the subsequent two pentads (Figure 4.2).

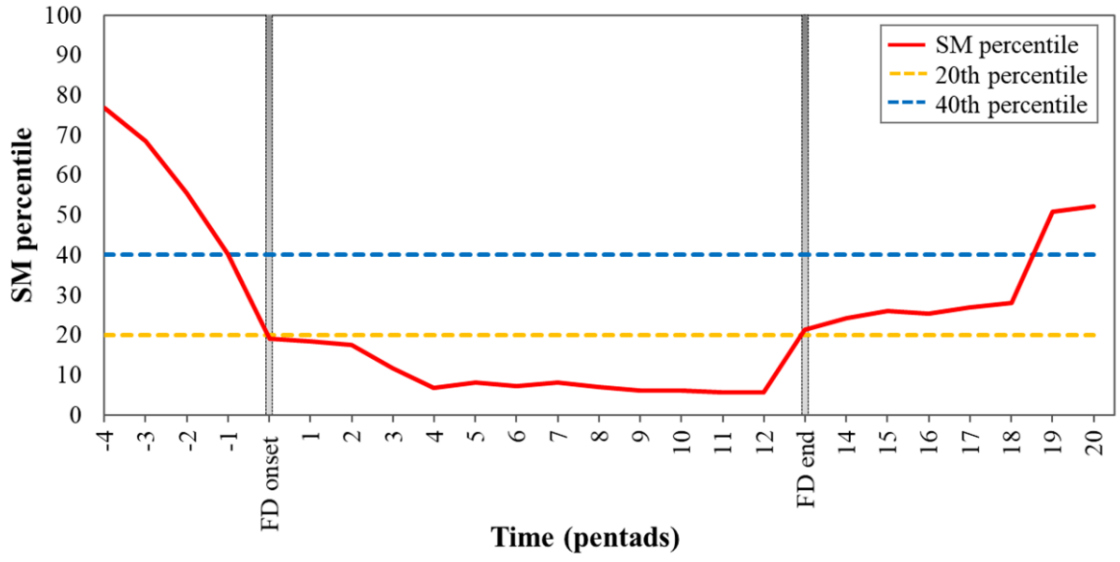

Figure 4.2. Schematic diagram of the evolution of a flash drought (FD) event, showing changes in soil moisture (SM).

SM percentiles in that interval must continuously decrease at an average rate of at least 0.1 per pentad to be considered a rapid SM reduction intensification, thus qualifying

as an FD (Wang et al., 2023a). Finally, FD end when SM increases above the 20th percentile and is maintained for at least two pentads (Figure 4.2). In addition, FD must have durations of 6–18 pentads (30-90 days) to distinguish them from long-duration traditional droughts (O and Park, 2023).

To characterize the FD identified, the total mean frequency, mean duration, and monthly frequency for the study period were calculated for each region. To calculate FD frequency, only the onset pentad of each FD was considered. In addition, FD severity (FDS) was determined using the FD intensity index (FDI) developed by Zhang et al. (2021b), which was applied to the pentads of each FD across all pixels and regions and was calculated as follows:

$$FDI = (1 - RI)x\,(1 - SM) \tag{4.1}$$

$$FDS = \sum_{i=1}^{n} FDI \tag{4.2}$$

where RI is the rapidity of FD between two consecutive pentads and varies from the range -1 to 1 (i.e., from -100 to 100%). A negative value of RI indicates a decrease in SM. FDS is the sum of FDI values along each FD.

4.2.6. Analyzing the sensitivity of plant indicators and yield to flash droughts

GPP constitutes the main carbon sink in global terrestrial ecosystems, and its reduction during periods of water stress is attributed mainly to stomatal closure, as well as nonstomatal limitations such as a decreased carboxylation rate and lower active leaf area (Zhang and Yuan, 2020). In particular, negative GPP anomalies during FD are interpreted as the onset of the ecological response (Zhang and Yuan, 2020). To evaluate the ecological impact, the GPP time series was adjusted to the SM data format and resolution. For this, daily GPP data were obtained using the linear interpolation method (O and Park, 2023) and subsequently aggregated into pentads. Finally, the normalized anomalies of GPP were calculated as follows:

$$SGPPA = \frac{GPP_t - \mu_{GPP}}{\sigma_{GPP}} \quad (4.3)$$

where GPP represents the GPP value for pentad t, μ_{GPP} is the average of the GPP values across all pentads in the time series and σ_{GPP} is the standard deviation of the GPP values across all pentads in the time series.

In this analysis, two response time indices were used to examine the relationship between FD and ecological drought (Zhang and Yuan, 2020). On the one hand, the response time of the vegetation to the FD was calculated for each FD event in all pixels of each region. This index is defined as the time elapsed until the first occurrence of the standardized negative GPP anomaly, which allows for the evaluation of how quickly vegetation responds to the onset of a FD. On the other hand, the time at which the GPP reached its minimum value in each FD of all pixels in each region was calculated to analyze the period during which the vegetation experienced the greatest impact of the FD. From these data, the minimum GPP value recorded for each FD was assigned to the corresponding pentad, and these values were then averaged by both month and region according to the timing of occurrence to obtain the monthly average minimum GPP. This allowed for the evaluation of cereal behavior throughout the phenological cycle.

To analyze the impact of FD on cereal crop yields, the Pearson correlation coefficient (R) between annual wheat and barley yields and the monthly average frequency and the monthly average FDS were calculated in each region. Additionally, to quantify the impact of FD on crop yields, the percentage reduction in wheat and barley yields during years with FD in each region was calculated. FD years are those in which any FD is present in the total sum of FD across all pixels for each year in each region. A normal yield year is defined as a year without an FD, with the average yield from normal years used as a reference. In years classified as FD affected, the annual rate of yield reduction is calculated as follows (Benito-Verdugo et al., 2023):

$$Yield_{std} = \frac{Yield_{n1} + Yield_{n2} + \cdots + Yield_{nx}}{x} \quad (4.4)$$

$$YR_d = \frac{Yield_{std} - Yield_{yd}}{Yield_{std}} \text{ x } 100\% \quad (4.5)$$

where $Yield_{std}$ represents the average yield in years without an FD for the selected region, x represents the number of years without FD in the study period, $Yield_{nx}$ (x = 1, 2, …, 23) represents the yield of year x, YR_d is the yield reduction rate of the selected region in year d (d = 1, 2, …, 23), and $Yield_{yd}$ (d = 1, 2, …, 23) represents the yield in year d identified with an FD.

Finally, the NDVI was used to study the influence of FD on the phenology of cereal crops because it is a widely used indicator and a representative index for studying the phenological stages of crops (Benito-Verdugo et al., 2024). Wheat and barley were grouped, as recommended by Zheng et al. (2015), who suggest grouping them given their erectophile canopy structure and very similar phenological development. The cubic spline interpolation method was employed to obtain the daily NDVI time series, as it is one of the most common methods used for time interpolation (Wolberg and Alfy, 1999). In addition, the NDVI time series was smoothed using a 30-d moving average to reduce noise. Following the methodology of Magney et al. (2016), the onset dates of the key growth stages of cereals, such as tillering, stem extension, heading, and ripening, were calculated, corresponding to stages 10, 31, 50, and 70, respectively, according to the Zadoks scale (Zadoks et al., 1974). The onset date of each phenological stage was determined using piecewise linear regression (Magney et al., 2016) for each agricultural year and pixel. The mean annual dates of each phenological stage were calculated for all pixels in each region, allowing for the determination of the average date of each phenological stage in each agricultural year and region. Finally, the mean dates for years with and without FD were calculated and compared.

4.3. Results and discussion

4.3.1. Flash drought patterns and characteristics in areas with cereal crops

The results of the analysis of the total mean frequency and mean duration of FD events in the studied regions are shown in Figure 4.3. The predominant frequency of 7–9 FD events was observed in most regions, affecting approximately 50% of the pixels. However, in OC and PG, a higher predominant frequency of 10–12 FD events was

observed, with these regions also experiencing approximately 50% of the affected pixels. These results are notable compared with those reported by O and Park (2023), who reported that 4 FD events occurred in Europe from 2000–2019. This result is also supported by the findings of Shah et al. (2022), who reported an increase in the frequency of FD events in the Mediterranean region, especially in recent years. In terms of duration, FD events lasting 10–12 pentads (50–60 days) were the most frequent across all regions, affecting an average of 85% of the pixels in each region. These results are consistent with those of previous studies, which reported an average FD duration of approximately 11 pentads (55 days) (Wang et al., 2023a; Zhang et al., 2024c).

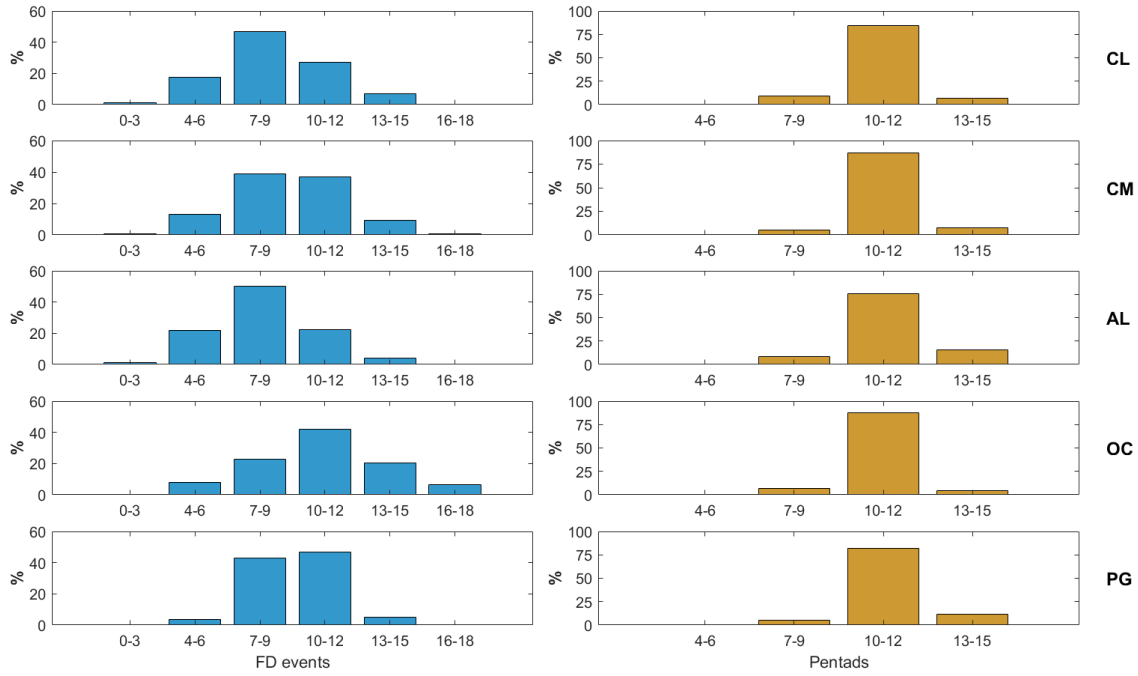

Figure 4.3. The mean frequency of flash drought (FD) events (left, in blue) and the mean duration of FD events (right, in yellow), expressed as the percentage of pixels affected in each region during the agricultural years from 2001–2023.

The analysis of the monthly distribution of FD frequency in the phenological cycle of cereal crops is shown in Figure 4.4a. The results revealed a generally higher incidence of FD in the late spring months. In particular, the highest frequency of FD occurred in April in CL in May in CM, AL and PG; and in June in OC. During these months, CL and CM experienced almost 1.6 FD events, AL and OC experienced approximately 1.5 FD events, and PG experienced more than 1.7 FD events.

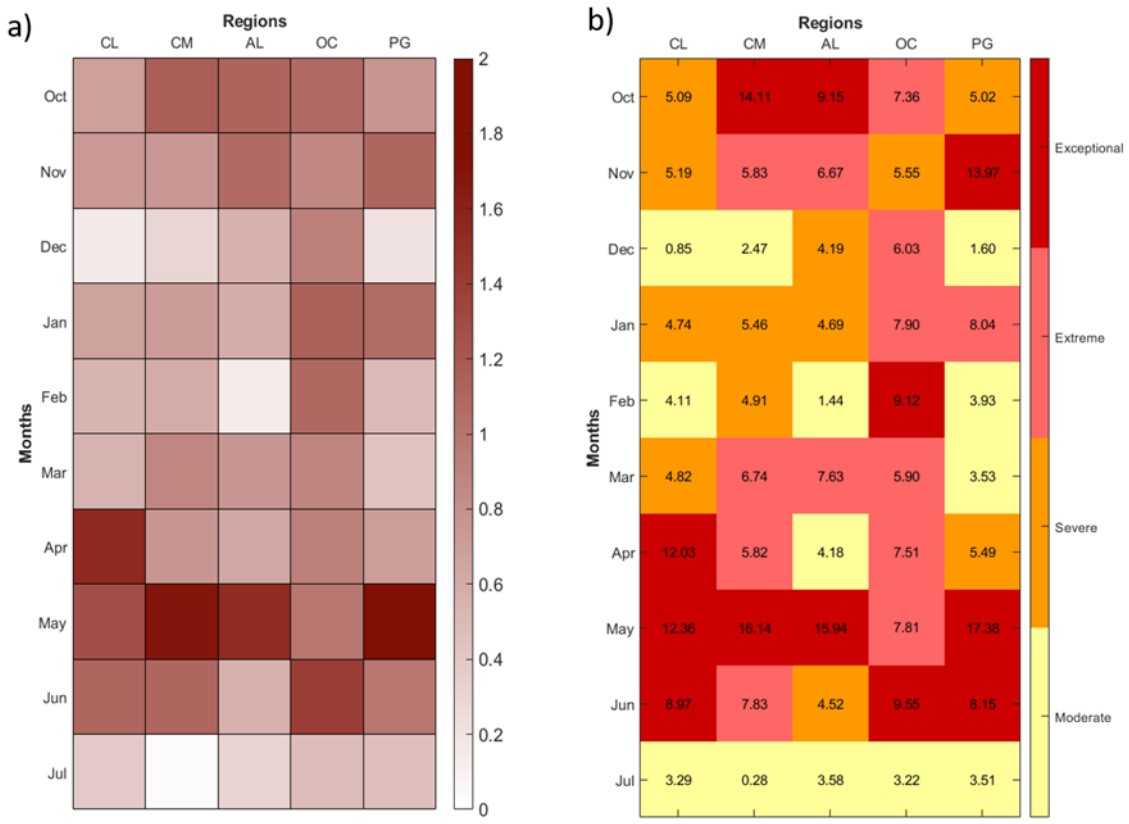

Figure 4.4. a) Average monthly frequency of flash drought (FD) events in each study region. b) Categorical representation of the average monthly flash drought severity (FDS) in each study region, with cells colored according to severity.

These results are consistent with those of Lovino et al. (2024), who observed that agricultural FD occurred most frequently during critical crop growth periods, with the highest frequency in Europe during spring and with effects extending into June. In addition, the monthly distribution of FDS was analyzed (Figure 4.4b), revealing a pattern almost identical to that of frequency, with approximately 70% of the most severe events, classified as exceptional FD, concentrated in the critical months for cereal development. These events were concentrated mainly in May, which was the month of highest severity in all regions, except in OC, where the highest severity occurred in June. This deviation observed in OC may be related to the impacts of climate change, whose consequences are not spatially uniform and can vary in magnitude from one region to another (Bento et al., 2021). These results align with those of the study by Christian et al. (2019a), which revealed that FDS tends to increase during the growing season, as crops exhibit greater sensitivity to SM conditions during their reproductive stages (Ho et al., 2023). The

months with the highest frequency and severity coincided with the critical period for cereal crop development, particularly with respect to SM demand (Benito-Verdugo et al., 2023; Gaona et al., 2022). During this period, crops are in their most important phases (reproductive and grain-filling phases), and deficits in SM can impair enzymatic activity, reduce nutrient absorption, and increase pollen sterility, which result in hindered grain setting and other negative impacts on yield (Farooq et al., 2012).

4.3.2. Impact of flash droughts on GPP

Analysis of the timing of the response of cereal GPP to FD events (Figure 4.5) revealed a clear pattern across all FD events in the study regions, and negative GPP anomalies occurred predominantly during the first pentad. These findings indicate that cereals under Mediterranean conditions responded quickly to FD, resulting in signs of stress from the onset. Thus, more than 80% of FD in CL, OC, and PG and approximately 75% in CM and AL (Figure 4.5) exhibited evident responses within the first 5 days of an FD.

These results are consistent with those of previous studies examining the response of semiarid ecosystems to water availability, which can be explained by the relationship between SM availability and GPP. A deficit in SM induces stomatal closure in most vegetation, which limits the ability of plants to photosynthesize and consequently reduces GPP (Qiu et al., 2023). The strong response observed in the present analysis may be attributed to the fact that, in water-limited areas where SM is a critical limiting factor, its variation dominates the GPP dynamics compared to other variables. Dang et al. (2022) noted that, in arid and semiarid regions, variations in SM are a key factor in modulating GPP. In addition, Stocker et al. (2018) reported that SM can reduce GPP by more than 40% in these areas.

These findings revealed faster responses of cereals to FD events compared to those previously reported. Thus, Zhang and Yuan (2020) reported negative GPP anomalies in rainfed crops in 40% of cases within the first 8 days. Additionally, Zhang et al. (2024b) observed in southern China that FD events generated widespread GPP responses within the first three pentads in agricultural areas.

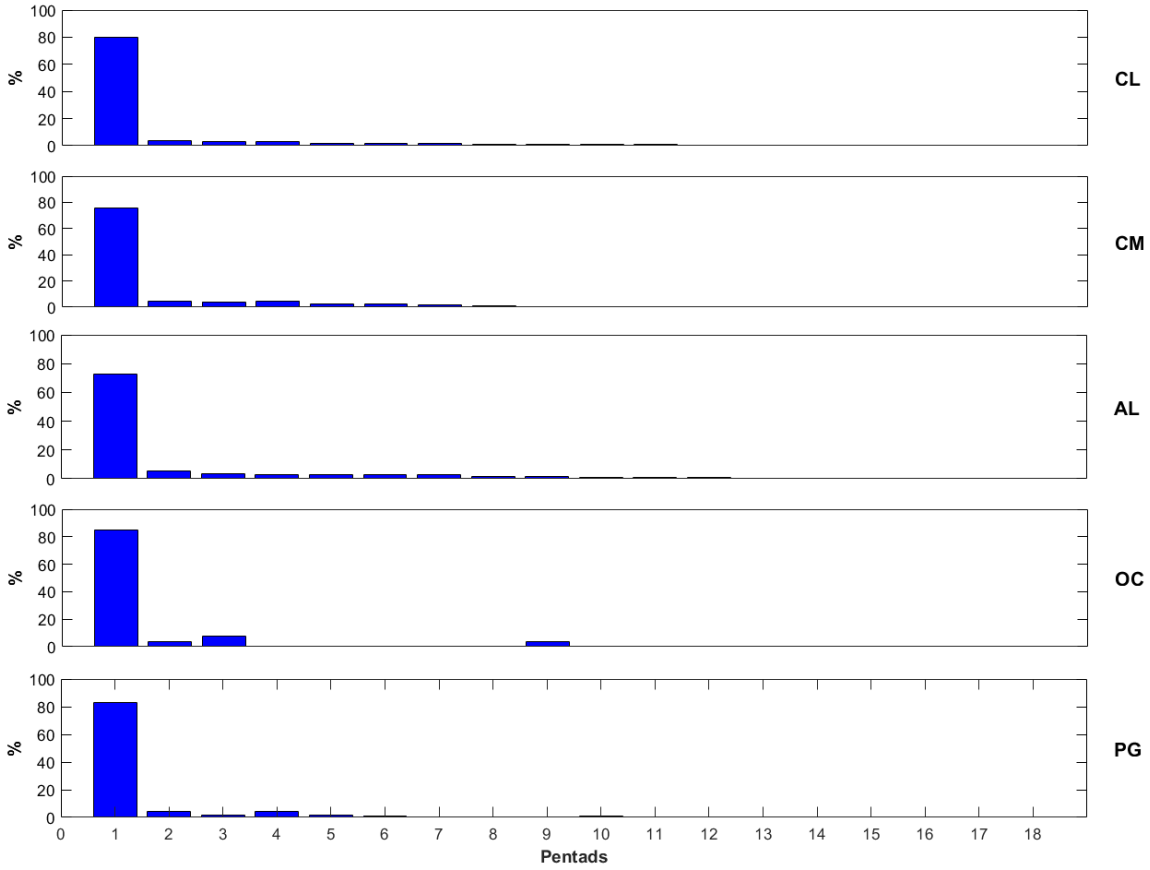

Figure 4.5. Percentage of the response time (in pentads) for the first occurrence of a negative GPP anomaly during flash drought (FD) events over the cereal phenological cycle and the study period in all pixels of the study regions.

The analysis of the monthly average minimum GPP during FD events is shown in Figure 4.6. The results revealed that the lowest minimum GPP value occurred in May for CM, AL, and PG, with values of -0.79, -0.61, and -1.07 g C, respectively. In CL, the lowest minimum GPP value occurred in April, with a value of -0.55 g C, whereas in OC, the lowest value was observed in June, with a value of -0.71 g C. Compared with the other regions, PG presented the lowest monthly GPP value. All regions showed a strong negative impact of FD on cereals during the months critical for cereal development, which is consistent with the results obtained in the previous section. This suggests that these months were the most critical for cereals in terms of FD, which directly impacted on their productivity. Drought directly affects the photosynthetic capacity of crops, leading to reductions in leaf area, stomatal closure, decreased nutrient uptake, deterioration of carboxylation enzyme activities, ATP synthesis, and destruction of the photosynthetic apparatus, which are key factors that reduce carbon fixation (Farooq et al., 2012).

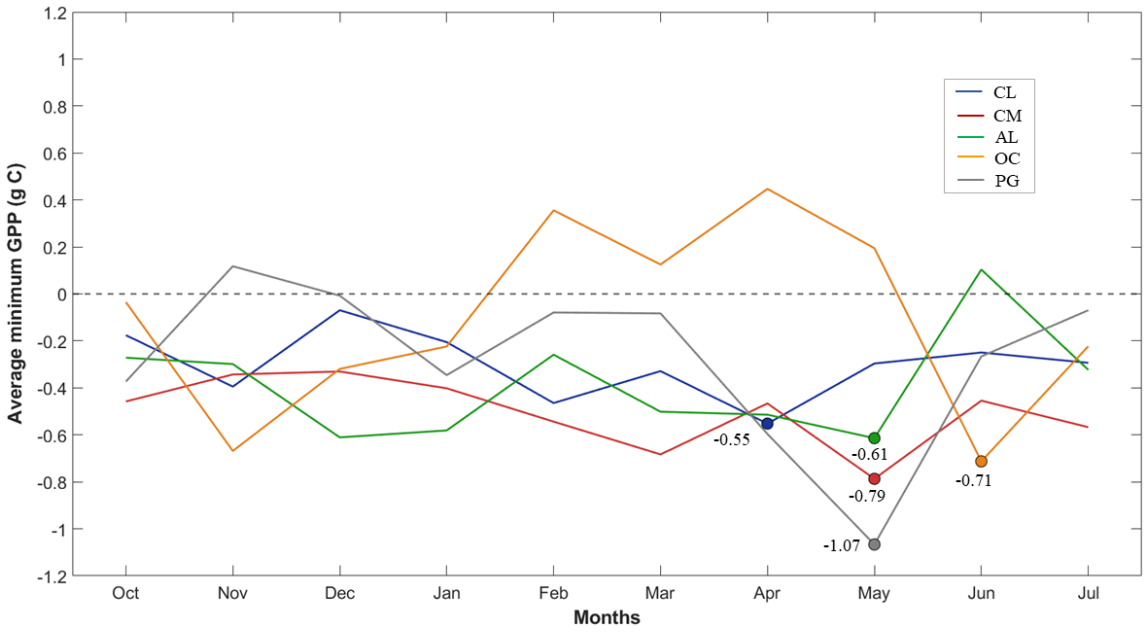

Figure 4.6. Monthly average of the minimum GPP during flash drought (FD) events in the phenological cycle of cereals for all pixels in each region throughout the study period. The shaded circles represent the lowest minimum GPP value for each region, and their numerical value is also indicated.

4.3.3. Impact of flash droughts on crop yield

The R values calculated between the wheat and barley yields and the monthly average FD frequency (Figure 4.7a), as well as the monthly average FDS (Figure 4.7b), are presented in Figure 4.7. In general, the results showed a pattern consistent with previous findings, where negative and significant R values were identified mainly in the months critical for cereal growth. With respect to the relationships between the monthly FD frequency and wheat and barley yields (Figure 4.7a), significant negative R values for both crops were observed in CL and CM predominantly from April to June and March to July, respectively. In CL, May and June had the lowest significant R values for wheat and barley, respectively, both at -0.66. In CM, April had the lowest significant negative R values for wheat and barley, at -0.83 and -0.76, respectively. Similarly, in AL, April was the only month with statistically significant values for wheat and barley, at -0.47 and -0.45, respectively. These results are consistent with those reported by Noguera et al. (2020), who documented a higher number of FD during spring and summer in Spain. In fact, previous studies (Benito-Verdugo et al., 2023; Farooq et al., 2012) have shown that grain yields are strongly affected by water stress during critical periods. In contrast, OC had a significantly positive R value in November for both wheat and barley. In PG, no

significant values were observed in any month, but negative R values were recorded, especially in May, a critical month for this region, when the lowest values were predominantly observed. FD frequency is projected to increase worldwide, with the greatest increases expected in Europe, including a notable increase in the Iberian Peninsula (Christian et al., 2023). Therefore, the results obtained are concerning for key cereals in Mediterranean areas, as an increase in FD frequency could even more significantly reduce the yields of essential crops such as wheat and barley.

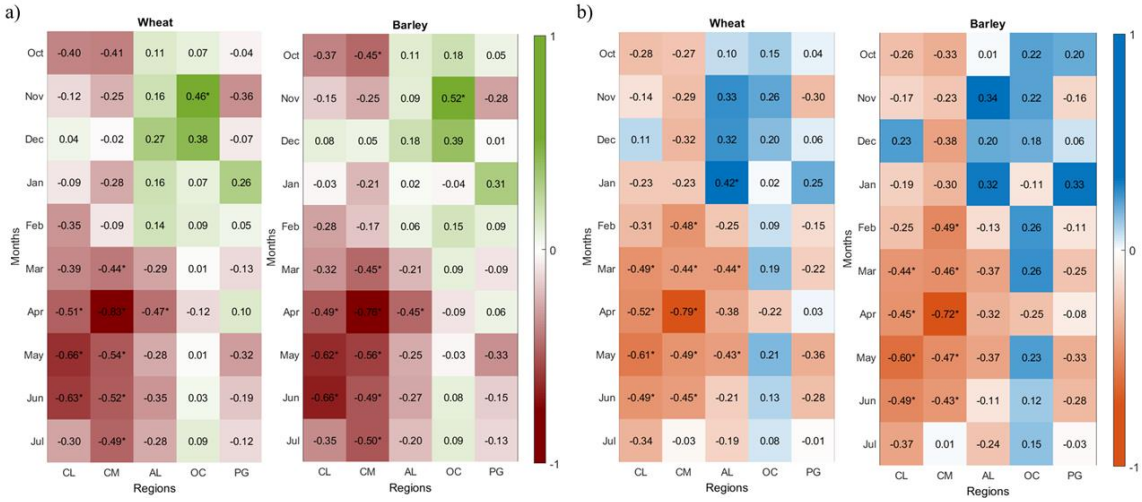

Figure 4.7. a) Correlation coefficient (R) between monthly average flash drought (FD) frequency and annual wheat yield (left) and barley yield (right) in the study regions during the agricultural years from 2001–2023. b) R between monthly average flash drought severity (FDS) and annual wheat yield (left) and barley yield (right) in the study regions during the agricultural years from 2001–2023. (*) Months with statistical significance at $p < 0.05$.

The relationship between FDS and wheat and barley yields (Figure 4.7b) followed a pattern similar to that observed between FD frequency and yields. Negative and significant R values for both crops were identified in CL and CM mainly from March to June and February to June, respectively. In CL, May presented the lowest and most significant R values, at -0.61 for wheat and -0.60 for barley. In CM, April had R values of -0.79 for wheat and -0.72 for barley. In AL, negative and significant R values were observed for wheat in March and May, whereas no significant values were recorded for barley. In OC and PG, no significant relationships were identified in any of the analyzed months, although PG presented the lowest negative R values in May, the critical month. Drought stress during the reproductive and grain-filling phases is the most devastating to

crop yield (Benito-Verdugo et al., 2023). Shah et al. (2022) reported an increase in FDS, especially in the Mediterranean region. Additionally, FDS is projected to increase globally, with prominent hotspots in water-limited regions such as the Mediterranean (Christian et al., 2023). Therefore, under climate change, increases in both FD frequency and severity will have an even greater impact on cereal yields in the Mediterranean region due to its high vulnerability.

To quantify the impact of FD on the yield of the two main cereals of the Mediterranean region, the yield reduction of wheat and barley in the studied regions was analyzed (Table 4.1). The greatest reduction occurred in CM, with a 33% decrease in wheat and barley yields. These results are in accordance with previous results, in which CM presented the lowest R values between the frequency and severity of FD and cereal yields (Figure 4.7). CL presented yield reductions of 16% for wheat and 20% for barley, which is in line with previous results. Although AL, OC, and PG did not show significant relationships or showed relationships that were not as strong as those in CL and CM between the frequency and severity of FD and cereal yields (Figure 4.7), they also experienced yield reductions in both crops, albeit to a lesser extent. In AL, the average reduction in wheat and barley yields was 5%, whereas in PG, it was 8%. OC was the region with the lowest reduction, in line with previous results (Figure 4.7), as practically no negative R values were observed. There is notable variability in yield reduction across regions, which can be attributed to the fact that the impacts of climate change and its consequences are not uniformly distributed across space, with their magnitude varying significantly from one region to another (Bento et al., 2021; Trenberth, 2011).

Table 4.1. Average percentage of yield reduction in flash drought (FD) years for wheat and barley in the study regions.

Cereals crops	Castilla y León (CL)	Castilla-La Mancha (CM)	Alentejo (AL)	Occitanie (OC)	Puglia (PG)
Wheat	16	33	3	1	9
Barley	20	33	7	1	7

These results are consistent with those of previous studies indicating that FD negatively affect crop yields (Christian et al., 2024; Hunt et al., 2021). Previous studies that exclusively analyzed individual FD events, particularly the most severe events, reported significant reductions in agricultural yields. In this context, during the 2010 FD in Russia, Hunt et al. (2021) reported a decrease of over 70% in wheat yields. Similarly,

Otkin et al. (2021) documented that the 2012 FD across the US caused a decrease of approximately 25% in corn and soybean yields. However, the present study considered all FD events over 23 years, regardless of their severity, and therefore revealed more moderate, although highly significant, mean reductions. In fact, in some cases, such as in CL, the mean yield reduction was greater than that observed in the more severe FD reported by Otkin et al. (2021).

4.3.4. Effects of flash droughts on cereal phenology

Figure 4.8 shows the difference in the NDVI between years with FD and years without FD. Predominantly, years with FD presented lower NDVI values than did years without FD. The most pronounced differences are observed during April, May and June. Specifically, in CL and CM, the largest difference in the NDVI between years with and without FD occurred in May, with an average value below -10%. In AL and PG, the greatest difference was observed in April, with an average value close to -10%, whereas in OC, the month with the greatest difference was June, with a value of less than -5%. These months correspond, as shown in the previous results, to the critical periods for cereal crops. The regions with the greatest differences in NDVI (CL and CM) were also those that experienced the greatest reduction in crop yield, whereas the region that experienced the least reduction in yield (OC) was the one that presented the smallest differences in NDVI. These findings underscore the role of the NDVI as a useful indicator for assessing the impact of FD events on vegetation health and its direct relationship with crop yield. The NDVI, as a reliable indicator of vegetation conditions, plays an important role in monitoring stress and vegetative dynamics in the context of sudden changes in SM in the context of FD (Adhikari et al., 2024). Moreover, in semiarid areas, the NDVI is closely correlated with SM deficits (Barbosa, 2023). Therefore, the results obtained revealed the negative impact of FD on NDVI and, consequently, on cereal health, leading to vegetation damage. These findings are consistent with several previous studies that identified significant reductions in NDVI under FD (Adhikari et al., 2024; Jin et al., 2019b).

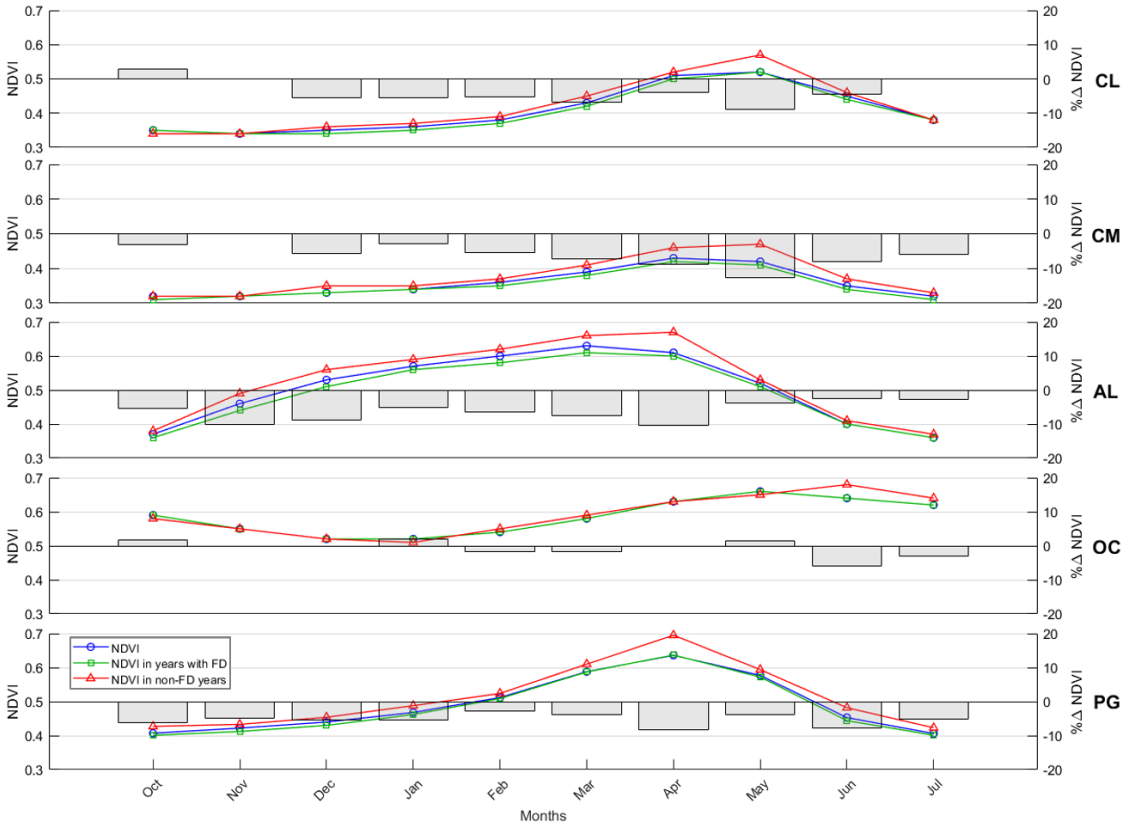

Figure 4.8. The left y-axis shows three series: the average monthly NDVI during the study period (blue line), the average monthly NDVI in years with flash drought (FD) events (green line), and the average monthly NDVI in years without FD events (red line). The right y-axis shows the percentage difference between the NDVI values in years with and without FD, expressed through light gray bars.

Regarding the impact of FD on cereal phenology, Table 4.2 shows the differences (in days, d) in the dates of the main developmental stages of cereals between years with FD and years without FD during the study period, for each region and for the average of these. In general, FD caused a slight advancement of all developmental stages in all regions. The tillering stage showed the smallest advancement, with an average of 1.5 d, particularly in OC and PG, where the advancement was 2 d, whereas in the other regions, it was only 1 d. The stem extension stage, which was the phase with the greatest advance, presented an average advance of 3.6 d, with PG standing out with an advancement of 7 d. On the other hand, the heading stage showed an average advance of 2.8 d, with AL standing out with a change of 5 d and PG standing out with a change of 4 d. Finally, the ripening stage was the second most advanced stage, with an average advance of 3 d. In this stage, AL, OC and PG stood out, each with an average of 4 d. These results indicate that FD slightly altered the phenological stages of cereals by advancing their occurrence.

Notably, the most significant changes occurred in those phenological stages that take place during the critical periods of cereal development, specifically in the spring and summer months. This finding aligns with the results shown in the previous sections, which revealed that both the frequency and intensity of FD, as well as their most significant impacts on cereal variables, were predominantly concentrated in these critical months. In addition, the advancement of phenological stages could represent a viable strategy to mitigate the impacts of climate change on yields (Bento et al., 2021), as it has been shown that exposure for 1 d to temperatures above 32 °C results in a 2.9% decrease in yield (Gammans et al., 2017), which may help explain the regional variability in yield reduction results presented in the previous section (Table 4.1). Although few studies have specifically analyzed the impact of FD on crop phenological stages, the results obtained in the present study are in line with those of Jin et al. (2019b), who observed an advancement in phenological stages during the 2012 FD in the US.

Table 4.2. Differences between the dates of the main growth stages of the cereals in years with and without FD for each region and the average for all regions for the study period, expressed in days.

Regions	Tillering	Stem Extension	Heading	Ripening
Castilla y León (CL)	-1	-2	-1	-2
Castilla-La Mancha (CM)	-1	-2	-2	-1
Alentejo (AL)	-1	-4	-5	-4
Occitanie (OC)	-2	-3	-2	-4
Puglia (PG)	-2	-7	-4	-4
Average	-1.4	-3.6	-2.8	-3

Drought affects crop phenology by shortening its growth cycle, as SM deficits induce a signal that triggers an early change in plant development, which accelerates the crop life cycle as a mechanism to complete its development before unfavorable conditions further restrict its growth (Farooq et al., 2012). In fact, several studies have shown that spring phenological phases in the Mediterranean tend to advance under drought conditions (Bernal et al., 2011; Spano et al., 2024). In addition, wheat and barley crops respond to drought by accelerating flowering and physiological maturity, resulting in yield reductions (McMaster and Wilhelm, 2003), as evidenced in the previous section.

4.4. Conclusions

This study expands the knowledge of the effects of FD on cereal crops under Mediterranean conditions and in water-limited regions in general and provide warnings about the potential consequences that are already affecting these crops. Given the projections of increased frequency and intensity of FD in water-limited regions, these effects are anticipated to worsen over time. Additionally, yield reductions, crop health affection and slight acceleration of phenological cycles caused by FD underscore the urgency of adopting more efficient agricultural management approaches that ensure agricultural sustainability. Event forecasting becomes crucial, as disaster mitigation and loss prevention depend on the ability to anticipate these phenomena. In this context, understanding how FD impact vegetation is crucial not only for the early detection of damage but also for identifying response patterns that can determine crop resistance to FD. This knowledge could be essential for developing more adaptive and efficient agricultural management strategies and improving the resilience of crop systems to future adversities.

The impact of FD on a greater variety of crops and regions under different environmental conditions should be investigated to assess the extent of these effects. These results not only provide a solid basis for future research in this field, addressing a significant gap in the current literature, but also offer useful information to improve agricultural management and planning in the context of ongoing climate change. The integration of this knowledge into adaptive approaches will allow progress toward a more sustainable and efficient agricultural model, helping to mitigate the adverse effects of FD and ensuring food security.

CAPÍTULO 5

CONCLUSIONES Y LÍNEAS FUTURAS DE INVESTIGACIÓN

5.1 Conclusiones

Esta tesis ha abordado el análisis de los efectos de la sequía agrícola en los principales cultivos de cereales bajo condiciones mediterráneas, mediante la integración de un indicador clave como la SM. A través de tres estudios interrelacionados, se han empleado distintos enfoques metodológicos con el objetivo de profundizar en el impacto de la sequía agrícola sobre el trigo y la cebada, analizar sus variaciones fenológicas y evaluar los efectos de las sequías repentinas en un contexto de cambio climático.

En primer lugar, considerando las limitaciones existentes en la utilización de la SM como indicador principal para el análisis de la sequía agrícola, y dada la importancia de evaluar sus impactos en regiones vulnerables y propensas a este fenómeno, esta tesis evaluó el impacto de la sequía agrícola sobre el rendimiento del trigo y la cebada en las principales regiones cerealistas de España y Alemania. Los resultados destacan la importancia de la SM para el rendimiento de los cereales, especialmente durante las etapas de reproducción y maduración del cultivo. En este contexto, la relación entre la sequía agrícola y la productividad vegetal presentó comportamientos similares en entornos limitados por agua, y patrones opuestos en regiones donde la disponibilidad energética representa el principal condicionante, lo que evidencia la influencia directa de la SM sobre el desarrollo de estos indicadores de vegetación. En aquellas regiones donde el agua no se consideraba tradicionalmente el principal factor limitante, se detectó un aumento en la incidencia de sequías agrícolas durante la última década del período analizado, lo que constituye una señal de alerta ante posibles cambios en las condiciones climáticas. Las pérdidas de rendimiento debidas a las sequías agrícolas superaron el 30% en las zonas bajo condiciones mediterráneas, aunque también se registraron reducciones de rendimiento, más moderadas, en regiones donde el agua no se ha considerado hasta ahora el principal factor limitante. Esto sugiere un posible cambio en las condiciones limitantes, que podría aumentar la vulnerabilidad de regiones hasta ahora no consideradas especialmente expuestas. En conjunto, los hallazgos aportan evidencia sólida del creciente impacto de la sequía agrícola sobre la producción cerealista y subrayan la necesidad urgente de desarrollar estrategias de adaptación y mitigación frente a un escenario climático cada vez más incierto. Además, advierten sobre un futuro potencialmente adverso para la producción agrícola, ya que regiones donde la SM no había constituido un factor limitante podrían experimentar pérdidas significativas,

replicando patrones ya observados en las regiones españolas. En este sentido, los resultados resultan clave para orientar medidas adaptativas que contribuyan a reducir la exposición de los cereales a los impactos negativos de la sequía agrícola.

En segundo lugar, dada la importancia del estudio de las variaciones fenológicas de la vegetación, y considerando la escasa atención prestada a los cultivos agrícolas en este ámbito, así como la limitada incorporación de la SM en dichos análisis, esta tesis analizó las tendencias fenológicas de los cereales en regiones bajo condiciones mediterráneas. Los resultados revelaron un cambio evidente entre las últimas décadas del siglo XX y las primeras del XXI. Durante el primer periodo, se adelantaron SOS y EOS y aumentó LOS, mientras que en el segundo periodo se registraron retrasos en SOS y EOS, y una reducción de LOS, y la biomasa de los cultivos continuó aumentando en ambos periodos. Además, se constató que el SOS tiene una mayor influencia que el EOS en LOS, y que tanto las variables energéticas como la SM durante la estación previa a SOS y EOS ejercen un papel fundamental, especialmente en el primer periodo analizado. Estos resultados son consistentes con lo encontrado en relación con la pausa del calentamiento global, reflejando un cambio en la tendencia de los parámetros fenológicos a comienzos del siglo XXI. En este contexto, los hallazgos obtenidos son relevantes para la planificación agronómica, ya que ofrecen una referencia para comprender las respuestas de los cultivos al cambio climático y orientan el desarrollo de estrategias que aumenten la resiliencia de los cultivos en un contexto de cambio climático en constante evolución.

Por último, en relación con el creciente interés en los últimos años por las FD y la escasa investigación sobre su impacto en cultivos agrícolas, esta tesis identificó y caracterizó la incidencia de las FD en las principales regiones cerealistas de secano bajo condiciones mediterráneas en Europa. Los resultados revelaron una clara incidencia de las FD en estas regiones, con mayor frecuencia e intensidad durante los meses críticos de abril, mayo y junio. Los cereales respondieron rápidamente al estrés provocado por las FD, las cuales causaron reducciones en el rendimiento de trigo y cebada de hasta un 33%, con diferencias significativas entre regiones, así como un deterioro en el estado de los cultivos. Estos impactos reflejan la creciente vulnerabilidad de los sistemas agrícolas frente a las FD, cuyas consecuencias podrían agravarse en el futuro, afectando de manera crítica la sostenibilidad de los sistemas productivos. Además, estos resultados ayudan a identificar patrones de respuesta frente a las FD que pueden ser clave para seleccionar

variedades más resistentes y desarrollar enfoques de manejo adaptativos, orientados a fortalecer la resiliencia de los sistemas agrícolas frente al cambio climático y garantizar la seguridad alimentaria.

5.2 Líneas futuras de investigación

En esta tesis se han alcanzado de manera satisfactoria los objetivos planteados. No obstante, durante su desarrollo se han puesto de manifiesto diferentes incertidumbres que requieren mayor profundización, lo que permite la formulación de nuevas líneas de investigación para ser abordadas en futuros trabajos.

El análisis del impacto de la sequía agrícola sobre los cereales evidenció la importancia crítica de este fenómeno y, por lo tanto, del contenido de SM en la producción cerealista, especialmente durante las fases más sensibles del ciclo fenológico. Los resultados indicaron que las regiones con limitaciones hídricas experimentaron fuertes descensos del rendimiento del trigo y la cebada, mientras que en zonas tradicionalmente menos vulnerables también se registraron pérdidas, aunque de forma más moderada. En este sentido, una posible vía de investigación sería ampliar el análisis a otras zonas agrícolas con diferentes condiciones climáticas, para validar si estos resultados siguen el mismo patrón. Asimismo, de cara a las importantes reducciones de rendimiento observadas, resulta prioritario evaluar la eficacia de distintas prácticas de manejo agrícola, con el fin de diseñar estrategias de adaptación que mitiguen o reduzcan el impacto de la sequía agrícola sobre los sistemas productivos.

El cambio en las tendencias fenológicas de los cereales bajo condiciones mediterráneas entre finales del siglo XX y principios del XXI abre una línea de investigación orientada a continuar con la monitorización fenológica. Esto permitirá verificar si la inflexión detectada persiste o si se reanudan los patrones fenológicos previos en el contexto del cambio climático, tanto en las regiones estudiadas como en otras zonas con condiciones ambientales diferentes. Asimismo, resultaría relevante aplicar esta metodología en otros cultivos, con el fin de evaluar si los cambios fenológicos responden a dinámicas específicas del cultivo o si reflejan dinámicas generales comunes a diferentes especies cultivadas.

Por último, los resultados obtenidos evidencian de manera clara la incidencia y los efectos de las FD en los cultivos de trigo y cebada bajo condiciones mediterráneas. Considerando la creciente frecuencia e intensidad proyectada de estos eventos, una línea futura de investigación sería ampliar la monitorización de las FD a otras regiones agrícolas y a otros cultivos estratégicos, con el fin de evaluar la generalidad de los efectos

observados y diseñar posibles estrategias de manejo más adaptativas y eficientes, fortaleciendo así la resiliencia de los sistemas agrícolas frente al cambio climático. Además, sería fundamental desarrollar sistemas de predicción y alerta temprana que permitan anticipar estos eventos y minimizar sus impactos, facilitando la toma de decisiones agronómicas en tiempo real.

REFERENCIAS

Abeledo, L. G., Savin, R., & Slafer, G. A. (2008). Wheat productivity in the Mediterranean Ebro Valley: Analyzing the gap between attainable and potential yield with a simulation model. *European Journal of Agronomy*, *28*(4), 541-550. https://doi.org/10.1016/j.eja.2007.12.001

Abi Saab, M. T., Houssemeddine Sellami, M., Giorio, P., Basile, A., Bonfante, A., Rouphael, Y., Fahed, S., Jomaa, I., Stephan, C., Kabalan, R., Massaad, R., Todorovic, M., & Albrizio, R. (2019). Assessing the Potential of Cereal Production Systems to Adapt to Contrasting Weather Conditions in the Mediterranean Region. *Agronomy*, *9*(7), 393. https://doi.org/10.3390/agronomy9070393

Achite, M., Ceribasi, G., Ceyhunlu, A. I., Wałęga, A., & Caloiero, T. (2021). The Innovative Polygon Trend Analysis (IPTA) as a Simple Qualitative Method to Detect Changes in Environment—Example Detecting Trends of the Total Monthly Precipitation in Semiarid Area. *Sustainability*, *13*(22), 12674. https://doi.org/10.3390/su132212674

Adhikari, S., Zhou, W., Dou, Z., Sakib, N., Ma, R., Chaudhari, B., & Liu, B. (2024). Analysis of Flash Drought and Its Impact on Forest Normalized Difference Vegetation Index (NDVI) in Northeast China from 2000 to 2020. *Atmosphere*, *15*(7), 818. https://doi.org/10.3390/atmos15070818

AGRESTE (Ministère de l'Agriculture et de la Sécurité alimentaire). (2025). *Statistique agricole annuelle*. https://draaf.occitanie.agriculture.gouv.fr/cop-surfaces-rendements-et-productions-de-2010-a-2023-par-departement-d-a8145.html

Ahmad, W., Bibi, N., Sanwal, M., Ahmed, R., Jamil, M., Kalsoom, R., Arif, M., & Fahad, S. (2024). Cereal Crops in the Era of Climate Change: An Overview. In S. Fahad, S. Saud, T. Nawaz, L. Gu, M. Ahmad, & R. Zhou (Eds.), Environment, Climate, Plant and Vegetation Growth (pp. 609-630). Springer Nature Switzerland. https://doi.org/10.1007/978-3-031-69417-2_21

Akinyemi, F. O. (2021). Vegetation Trends, Drought Severity and Land Use-Land Cover Change during the Growing Season in Semi-Arid Contexts. *Remote Sensing*, *13*(5), 836. https://doi.org/10.3390/rs13050836

Albergel, C., Dorigo, W., Reichle, R. H., Balsamo, G., Derosnay, P., Muñoz-sabater, J., Isaksen, L., Dejeu, R., & Wagner, W. (2013). Skill and global trend analysis of soil moisture from reanalyses and microwave remote sensing. *Journal of Hydrometeorology*, *14*(4), 1259-1277. Scopus. https://doi.org/10.1175/JHM-D-12-0161.1

Albrizio, R., Todorovic, M., Matic, T., & Stellacci, A. M. (2010). Comparing the interactive effects of water and nitrogen on durum wheat and barley grown in a Mediterranean environment. *Field Crops Research*, *115*(2), 179-190. https://doi.org/10.1016/j.fcr.2009.11.003

Alkhalidi, A., Assaf, M. N., Alkaylani, H., Halaweh, G., & Salcedo, F. P. (2023). Integrated innovative technique to assess and priorities risks associated with drought: Impacts, measures/strategies, and actions, global study. *International Journal of Disaster Risk Reduction*, *94*, 103800. https://doi.org/10.1016/j.ijdrr.2023.103800

Allen, R. G., Pereira, L. S., Raes, D., & Smith, M. (1998). *Crop evapotranspiration: Guidelines for computing crop water requirements* (FAO Irrigation and Drainage Paper No. 56). Food and Agriculture Organization of the United Nations (FAO).

Almazroui, M., & Şen, Z. (2020). Trend Analyses Methodologies in Hydro-meteorological Records. *Earth Systems and Environment*, *4*(4), 713-738. https://doi.org/10.1007/s41748-020-00190-6

Almendra-Martín, L., (2022). *Uso de métodos avanzados para la monitorización y el análisis de los cambios de la humedad del suelo en Europa* [Tesis doctoral, Universidad de Salamanca].

Almendra-Martín, L., Martínez-Fernández, J., González-Zamora, Á., Benito-Verdugo, P., & Herrero-Jiménez, C. M. (2021a). Agricultural Drought Trends on the Iberian Peninsula: An Analysis Using Modeled and Reanalysis Soil Moisture Products. *Atmosphere*, *12*(2), 236. https://doi.org/10.3390/atmos12020236

Almendra-Martín, L., Martínez-Fernández, J., Piles, M., & González-Zamora, Á. (2021b). Comparison of gap-filling techniques applied to the CCI soil moisture database in Southern Europe. *Remote Sensing of Environment*, *258*, 112377. https://doi.org/10.1016/j.rse.2021.112377

Almendra-Martín, L., Martínez-Fernández, J., Piles, M., González-Zamora, Á., Benito-Verdugo, P., & Gaona, J. (2022a). Analysis of soil moisture trends in Europe using rank-based and empirical decomposition approaches. *Global and Planetary Change*, *215*, 103868. https://doi.org/10.1016/j.gloplacha.2022.103868

Almendra-Martín, L., Martínez-Fernández, J., Piles, M., González-Zamora, Á., Benito-Verdugo, P., & Gaona, J. (2022b). Influence of atmospheric patterns on soil moisture dynamics in Europe. *Science of The Total Environment*, *846*, 157537. https://doi.org/10.1016/j.scitotenv.2022.157537

Alrteimei, H. A., Ash'aari, Z. H., & Muharram, F. M. (2022). Last decade assessment of the impacts of regional climate change on crop yield variations in the Mediterranean region. *Agriculture*, *12*(11), 1787. https://doi.org/10.3390/agriculture12111787

Al-Yaari, A., Wigneron, J.-P., Dorigo, W., Colliander, A., Pellarin, T., Hahn, S., Mialon, A., Richaume, P., Fernandez-Moran, R., Fan, L., Kerr, Y. H., & De Lannoy, G. (2019). Assessment and inter-comparison of recently developed/reprocessed microwave satellite soil moisture products using ISMN ground-based measurements. *Remote Sensing of Environment*, *224*, 289-303. https://doi.org/10.1016/j.rse.2019.02.008

An, R., Zhang, L., Wang, Z., Quaye-Ballard, J. A., You, J., Shen, X., Gao, W., Huang, L., Zhao, Y., & Ke, Z. (2016). Validation of the ESA CCI soil moisture product in China. *Advances in the Validation and Application of Remotely Sensed Soil Moisture - Part 2*, *48*, 28-36. https://doi.org/10.1016/j.jag.2015.09.009

Anav, A., Friedlingstein, P., Beer, C., Ciais, P., Harper, A., Jones, C., Murray-Tortarolo, G., Papale, D., Parazoo, N. C., Peylin, P., Piao, S., Sitch, S., Viovy, N., Wiltshire, A., & Zhao, M. (2015). Spatiotemporal patterns of terrestrial gross primary production: A review. *Reviews of Geophysics*, *53*(3), 785-818. https://doi.org/10.1002/2015RG000483

Anderson, M. C., Zolin, C. A., Sentelhas, P. C., Hain, C. R., Semmens, K., Tugrul Yilmaz, M., Gao, F., Otkin, J. A., & Tetrault, R. (2016). The Evaporative Stress Index as an indicator of agricultural drought in Brazil: An assessment based on crop yield impacts. *Remote Sensing of Environment*, *174*, 82-99. https://doi.org/10.1016/j.rse.2015.11.034

Andreadis, K. M., Clark, E. A., Wood, A. W., Hamlet, A. F., & Lettenmaier, D. P. (2005). Twentieth-Century Drought in the Conterminous United States. *Journal of Hydrometeorology*, *6*(6), 985-1001. https://doi.org/10.1175/JHM450.1

Araus, J. L., Bort, J., Steduto, P., Villegas, D., & Royo, C. (2003). Breeding cereals for Mediterranean conditions: Ecophysiological clues for biotechnology application. *Annals of Applied Biology*, *142*(2), 129-141. https://doi.org/10.1111/j.1744-7348.2003.tb00238.x

Arora, V. K. (2002). The use of the aridity index to assess climate change effect on annual runoff. *Journal of Hydrology*, *265*(1), 164-177. https://doi.org/10.1016/S0022-1694(02)00101-4

Aurelle, D., Thomas, S., Albert, C., Bally, M., Bondeau, A., Boudouresque, C.-F., Cahill, A. E., Carlotti, F., Chenuil, A., Cramer, W., Davi, H., De Jode, A., Ereskovsky, A., Farnet, A.-M., Fernandez, C., Gauquelin, T., Mirleau, P., Monnet, A.-C., Prévosto, B., Rossi, V., Sartoretto, S., Van Wambeke, F., & Fady, B. (2022). Biodiversity, climate change, and adaptation in the Mediterranean. *Ecosphere*, *13*(4), e3915. https://doi.org/10.1002/ecs2.3915

Balsamo, G., Albergel, C., Beljaars, A., Boussetta, S., Brun, E., Cloke, H., Dee, D., Dutra, E., Muñoz-Sabater, J., Pappenberger, F., de Rosnay, P., Stockdale, T., & Vitart, F. (2015). ERA-Interim/Land: A global land surface reanalysis data set.

Hydrology and Earth System Sciences, *19*(1), 389-407. https://doi.org/10.5194/hess-19-389-2015

Bandhauer, M., Isotta, F., Lakatos, M., Lussana, C., Båserud, L., Izsák, B., Szentes, O., Tveito, O. E., & Frei, C. (2022). Evaluation of daily precipitation analyses in E-OBS (v19.0e) and ERA5 by comparison to regional high-resolution datasets in European regions. *International Journal of Climatology*, *42*(2), 727-747. https://doi.org/10.1002/joc.7269

Bandoc, G., Piticar, A., Patriche, C., Roșca, B., & Dragomir, E. (2022). Climate Warming-Induced Changes in Plant Phenology in the Most Important Agricultural Region of Romania. *Sustainability*, *14*(5), 2776. https://doi.org/10.3390/su14052776

Barbosa, H. A. (2023). Flash Drought and Its Characteristics in Northeastern South America during 2004–2022 Using Satellite-Based Products. *Atmosphere*, *14*(11), 1629. https://doi.org/10.3390/atmos14111629

Barbosa, H. A. (2024). Understanding the rapid increase in drought stress and its connections with climate desertification since the early 1990s over the Brazilian semi-arid region. *Journal of Arid Environments*, *222*, 105142. https://doi.org/10.1016/j.jaridenv.2024.105142

Basara, J. B., Christian, J. I., Wakefield, R. A., Otkin, J. A., Hunt, E. H., & Brown, D. P. (2019). The evolution, propagation, and spread of flash drought in the Central United States during 2012. *Environmental Research Letters*, *14*(8), 084025. https://doi.org/10.1088/1748-9326/ab2cc0

Bayazit, M., & Önöz, B. (2007). To prewhiten or not to prewhiten in trend analysis? *Hydrological Sciences Journal*, *52*(4), 611-624. https://doi.org/10.1623/hysj.52.4.611

Beck, H. E., Zimmermann, N. E., McVicar, T. R., Vergopolan, N., Berg, A., & Wood, E. F. (2018). Present and future Köppen-Geiger climate classification maps at 1-km resolution. *Scientific data*, *5*(1), 1-12. https://doi.org/10.1038/sdata.2018.214

Bednar-Friedl, B., Biesbroek, R., Schmidt, D. N., Alexander, P., Børsheim, K. Y., Carnicer, J., Georgopoulou, E., Haasnoot, M., Cozannet, G. L., Lionello, P., Lipka, O., Möllmann, C., Muccione, V., Mustonen, T., Piepenburg, D., & Whitmarsh, L. (2022). Europe. In H. O. Pörtner, D. C. Roberts, M. Tignor, E. S. Poloczanska, K. Mintenbeck, A. Alegría, M. Craig, S. Langsdorf, S. Löschke, V. Möller, A. Okem, & B. Rama (Eds.), *Climate Change 2022: Impacts, Adaptation and Vulnerability. Contribution of Working Group II to the Sixth Assessment Report of the Intergovernmental Panel on Climate Change* (pp. 1817-1927). Cambridge University Press. https://doi.org/10.1017/9781009325844.015.1817

Beer, C., Reichstein, M., Tomelleri, E., Ciais, P., Jung, M., Carvalhais, N., Rödenbeck, C., Arain, M. A., Baldocchi, D., Bonan, G. B., & others. (2010). Terrestrial gross

carbon dioxide uptake: Global distribution and covariation with climate. *Science*, *329*(5993), 834-838.

Beldring, S., Gottschalk, L., Seibert, J., & Tallaksen, L. M. (1999). Distribution of soil moisture and groundwater levels at patch and catchment scales. *Agricultural and Forest Meteorology*, *98-99*, 305-324. https://doi.org/10.1016/S0168-1923(99)00103-3

Benedetti, R., & Rossini, P. (1993). On the use of NDVI profiles as a tool for agricultural statistics: The case study of wheat yield estimate and forecast in Emilia Romagna. *Remote Sensing of Environment*, *45*(3), 311-326. https://doi.org/10.1016/0034-4257(93)90113-C

Benito-Verdugo, P., Martínez-Fernández, J., González-Zamora, Á., Almendra-Martín, L., Gaona, J., & Herrero-Jiménez, C. M. (2023). Impact of agricultural drought on barley and wheat yield: A comparative case study of Spain and Germany. *Agriculture*, *13*(11), 2111. https://doi.org/10.3390/agriculture13112111

Benito-Verdugo, P., González-Zamora, Á., & Martínez-Fernández, J. (2024). Recent Cereal Phenological Variations under Mediterranean Conditions. *Remote Sensing*, *16*(11), 1879. https://doi.org/10.3390/rs16111879

Bento, V. A., Ribeiro, A. F. S., Russo, A., Gouveia, C. M., Cardoso, R. M., & Soares, P. M. M. (2021). The impact of climate change in wheat and barley yields in the Iberian Peninsula. *Scientific Reports*, *11*(1), 15484. https://doi.org/10.1038/s41598-021-95014-6

Berg, A., & Sheffield, J. (2018). Climate Change and Drought: The Soil Moisture Perspective. *Current Climate Change Reports*, *4*(2), 180-191. https://doi.org/10.1007/s40641-018-0095-0

Bernal, M., Estiarte, M., & Peñuelas, J. (2011). Drought advances spring growth phenology of the Mediterranean shrub Erica multiflora. *Plant Biology*, *13*(2), 252-257. https://doi.org/10.1111/j.1438-8677.2010.00358.x

Bianchi, M., Boyle, M., & Hollingsworth, D. (1999). A comparison of methods for trend estimation. *Applied Economics Letters*, *6*(2), 103-109. https://doi.org/10.1080/135048599353726

Bjarke, N., Livneh, B., & Barsugli, J. (2024). Storylines for Global Hydrologic Drought Within CMIP6. *Earth's Future*, *12*(6), e2023EF004117. https://doi.org/10.1029/2023EF004117

Blondel, J. (2010). *The Mediterranean region: Biological diversity in space and time*. Oxford University Press, USA.

Borrelli, P., Robinson, D. A., Panagos, P., Lugato, E., Yang, J. E., Alewell, C., Wuepper, D., Montanarella, L., & Ballabio, C. (2020). Land use and climate change impacts on global soil erosion by water (2015-2070). *Proceedings of the National*

Academy of Sciences, *117*(36), 21994-22001. https://doi.org/10.1073/pnas.2001403117

Bracho-Mujica, G., Hayman, P. T., & Ostendorf, B. (2019). Modelling long-term risk profiles of wheat grain yield with limited climate data. *Agricultural Systems*, *173*, 393-402. https://doi.org/10.1016/j.agsy.2019.03.010

Braganza, K., Karoly, D. J., & Arblaster, J. M. (2004). Diurnal temperature range as an index of global climate change during the twentieth century. *Geophysical Research Letters*, *31*(13). https://doi.org/10.1029/2004GL019998

Brisson, N., Gate, P., Gouache, D., Charmet, G., Oury, F.-X., & Huard, F. (2010). Why are wheat yields stagnating in Europe? A comprehensive data analysis for France. *Field Crops Research*, *119*(1), 201-212. https://doi.org/10.1016/j.fcr.2010.07.012

Brocca, L., Camici, S., Melone, F., Moramarco, T., Martínez-Fernández, J., Didon-Lescot, J.-F., & Morbidelli, R. (2014). Improving the representation of soil moisture by using a semi-analytical infiltration model. *Hydrological Processes*, *28*(4), 2103-2115. https://doi.org/10.1002/hyp.9766

Brocca, L., Ciabatta, L., Massari, C., Camici, S., & Tarpanelli, A. (2017). Soil Moisture for Hydrological Applications: Open Questions and New Opportunities. *Water*, *9*(2), 140. https://doi.org/10.3390/w9020140

Bruscantini, C. A., Grings, F., Barber, M., Perna, P., & Karszenbaum, H. (2014). A Bayesian approach for a SAC-D/aquarius soil moisture product. *2014 13th Specialist Meeting on Microwave Radiometry and Remote Sensing of the Environment (MicroRad)*, 1-4. https://doi.org/10.1109/MicroRad.2014.6878896

Burek, P., Roo, A., & Knijff, J. (2013). *LISFLOOD - Distributed Water Balance and Flood Simulation Model—Revised User Manual*. https://doi.org/10.2788/24719

Burke, E. J. (2011). Understanding the Sensitivity of Different Drought Metrics to the Drivers of Drought under Increased Atmospheric CO2. *Journal of Hydrometeorology*, *12*(6), 1378-1394. https://doi.org/10.1175/2011JHM1386.1

Burn, D. H., & Elnur, M. A. H. (2002). Detection of hydrologic trends and variability. *Journal of hydrology*, *255*(1-4), 107-122. https://doi.org/10.1016/S0022-1694(01)00514-5

Cammalleri, C., Vogt, J., Salamon, P., & others. (2017). Near-real time hydrological drought monitoring in the European Drought Observatory. In *EWRA European Water* (pp. 189-193).

Candiago, S., Remondino, F., De Giglio, M., Dubbini, M., & Gattelli, M. (2015). Evaluating Multispectral Images and Vegetation Indices for Precision Farming Applications from UAV Images. *Remote Sensing*, *7*(4), 4026-4047. https://doi.org/10.3390/rs70404026

Cao, M., Chen, M., Liu, J., & Liu, Y. (2022). Assessing the performance of satellite soil moisture on agricultural drought monitoring in the North China Plain. *Agricultural Water Management*, *263*, 107450. https://doi.org/10.1016/j.agwat.2021.107450

Capa-Morocho, M., Ines, A. V. M., Baethgen, W. E., Rodríguez-Fonseca, B., Han, E., & Ruiz-Ramos, M. (2016). Crop yield outlooks in the Iberian Peninsula: Connecting seasonal climate forecasts with crop simulation models. *Agricultural Systems*, *149*, 75-87. https://doi.org/10.1016/j.agsy.2016.08.008

Careddu, M. L., Giunta, F., & Motzo, R. (2024). Lessons from the Varietal Evolution of Durum Wheat in Italy. *Agronomy*, *14*(1), 87. https://doi.org/10.3390/agronomy14010087

Carvalho, D., Pereira, S. C., Silva, R., & Rocha, A. (2022). Aridity and desertification in the Mediterranean under EURO-CORDEX future climate change scenarios. *Climatic Change*, *174*(3), 28. https://doi.org/10.1007/s10584-022-03454-4

Chagas, V. B., Chaffe, P. L., & Blöschl, G. (2022). Climate and land management accelerate the Brazilian water cycle. *Nature Communications*, *13*(1), 5136. https://doi.org/10.1038/s41467-022-32580-x

Champagne, C., Davidson, A., Cherneski, P., L'Heureux, J., & Hadwen, T. (2015). Monitoring Agricultural Risk in Canada Using L-Band Passive Microwave Soil Moisture from SMOS. *Journal of Hydrometeorology*, *16*(1), 5-18. https://doi.org/10.1175/JHM-D-14-0039.1

Chan, S. K., Bindlish, R., O'Neill, P., Jackson, T., Njoku, E., Dunbar, S., Chaubell, J., Piepmeier, J., Yueh, S., Entekhabi, D., Colliander, A., Chen, F., Cosh, M. H., Caldwell, T., Walker, J., Berg, A., McNairn, H., Thibeault, M., Martínez-Fernández, J., Uldall, F., Seyfried, M., Bosch, D., Starks, P., Holifield Collins, C., Prueger, J., Van der Velde, R., Asanuma, J., Palecki, M., Small, E. E., Zresa, M., Calvet, J., Crow, W. T., & Kerr, Y. (2018). Development and assessment of the SMAP enhanced passive soil moisture product. *Remote Sensing of Environment*, *204*, 931-941. https://doi.org/10.1016/j.rse.2017.08.025

Chowdhury, M., Anand, R., Dhar, T., Kurmi, R., Sahni, R. K., & Kushwah, A. (2024). Digital Insights into Plant Health: Exploring Vegetation Indices Through Computer Vision. In S. S. Chouhan, U. P. Singh, & S. Jain (Eds.), *Applications of Computer Vision and Drone Technology in Agriculture 4.0* (pp. 7-30). Springer Nature Singapore. https://doi.org/10.1007/978-981-99-8684-2_2

Christian, J. I., Basara, J. B., Otkin, J. A., & Hunt, E. D. (2019a). Regional characteristics of flash droughts across the United States. *Environmental Research Communications*, *1*(12), 125004. https://doi.org/10.1088/2515-7620/ab50ca

Christian, J. I., Basara, J. B., Otkin, J. A., Hunt, E. D., Wakefield, R. A., Flanagan, P. X., & Xiao, X. (2019b). A Methodology for Flash Drought Identification: Application

of Flash Drought Frequency across the United States. *Journal of Hydrometeorology*, *20*(5), 833-846. https://doi.org/10.1175/JHM-D-18-0198.1

Christian, J. I., Basara, J. B., Hunt, E. D., Otkin, J. A., & Xiao, X. (2020). Flash drought development and cascading impacts associated with the 2010 Russian heatwave. *Environmental Research Letters*, *15*(9), 094078. https://doi.org/10.1088/1748-9326/ab9faf

Christian, J. I., Basara, J. B., Hunt, E. D., Otkin, J. A., Furtado, J. C., Mishra, V., Xiao, X., & Randall, R. M. (2021). Global distribution, trends, and drivers of flash drought occurrence. *Nature Communications*, *12*(1), 6330. https://doi.org/10.1038/s41467-021-26692-z

Christian, J. I., Martin, E. R., Basara, J. B., Furtado, J. C., Otkin, J. A., Lowman, L. E. L., Hunt, E. D., Mishra, V., & Xiao, X. (2023). Global projections of flash drought show increased risk in a warming climate. *Communications Earth & Environment*, *4*(1), 165. https://doi.org/10.1038/s43247-023-00826-1

Christian, J. I., Hobbins, M., Hoell, A., Otkin, J. A., Ford, T. W., Cravens, A. E., Powlen, K. A., Wang, H., & Mishra, V. (2024). Flash drought: A state of the science review. *WIREs Water*, *11*(3), e1714. https://doi.org/10.1002/wat2.1714

Compo, G. P., Whitaker, J. S., Sardeshmukh, P. D., Matsui, N., Allan, R. J., Yin, X., Gleason, B. E., Vose, R. S., Rutledge, G., Bessemoulin, P., Brönnimann, S., Brunet, M., Crouthamel, R. I., Grant, A. N., Groisman, P. Y., Jones, P. D., Kruk, M. C., Kruger, A. C., Marshall, G. J., Maugeri, M., Mok, H. Y., Nordli, O., Ross, T. F., Trigo, R. M., Wang, X. L., Woodruff, S. D., & Worley, S. J. (2011). The Twentieth Century Reanalysis Project. *Quarterly Journal of the Royal Meteorological Society*, *137*(654), 1-28. https://doi.org/10.1002/qj.776

Cong, N., Wang, T., Nan, H., Ma, Y., Wang, X., Myneni, R. B., & Piao, S. (2013). Changes in satellite-derived spring vegetation green-up date and its linkage to climate in China from 1982 to 2010: A multimethod analysis. *Global change biology*, *19*(3), 881-891. https://doi.org/10.1111/gcb.12077

Cook, B. I., Mankin, J. S., & Anchukaitis, K. J. (2018). Climate Change and Drought: From Past to Future. *Current Climate Change Reports*, *4*(2), 164-179. https://doi.org/10.1007/s40641-018-0093-2

Cos, J., Doblas-Reyes, F., Jury, M., Marcos, R., Bretonnière, P.-A., & Samsó, M. (2022). The Mediterranean climate change hotspot in the CMIP5 and CMIP6 projections. *Earth System Dynamics*, *13*(1), 321-340. https://doi.org/10.5194/esd-13-321-2022

Cossani, C. M., Savin, R., & Slafer, G. A. (2007). Contrasting performance of barley and wheat in a wide range of conditions in Mediterranean Catalonia (Spain). *Annals of Applied Biology*, *151*(2), 167-173. https://doi.org/10.1111/j.1744-7348.2007.00177.x

Cossani, C. M., Slafer, G. A., & Savin, R. (2009). Yield and biomass in wheat and barley under a range of conditions in a Mediterranean site. *Field Crops Research*, *112*(2), 205-213. https://doi.org/10.1016/j.fcr.2009.03.003

Cossani, C. M., Slafer, G. A., & Savin, R. (2012). Nitrogen and water use efficiencies of wheat and barley under a Mediterranean environment in Catalonia. *Field Crops Research*, *128*, 109-118. https://doi.org/10.1016/j.fcr.2012.01.001

Coulibaly, P., & Baldwin, C. K. (2005). Nonstationary hydrological time series forecasting using nonlinear dynamic methods. *Journal of Hydrology*, *307*(1), 164-174. https://doi.org/10.1016/j.jhydrol.2004.10.008

Crausbay, S. D., Ramirez, A. R., Carter, S. L., Cross, M. S., Hall, K. R., Bathke, D. J., Betancourt, J. L., Colt, S., Cravens, A. E., Dalton, M. S., Dunham, J. B., Hay, L. E., Hayes, M. J., McEvoy, J., McNutt, C. A., Moritz, M. A., Nislow, K. H., Raheem, N., & Sanford, T. (2017). Defining Ecological Drought for the Twenty-First Century. *Bulletin of the American Meteorological Society*, *98*(12), 2543-2550. https://doi.org/10.1175/BAMS-D-16-0292.1

Crocetti, L., Forkel, M., Fischer, M., Jurečka, F., Grlj, A., Salentinig, A., Trnka, M., Anderson, M., Ng, W.-T., Kokalj, Ž., Bucur, A., & Dorigo, W. (2020). Earth Observation for agricultural drought monitoring in the Pannonian Basin (southeastern Europe): Current state and future directions. *Regional Environmental Change*, *20*(4), 123. https://doi.org/10.1007/s10113-020-01710-w

Dai, A. (2013). Increasing drought under global warming in observations and models. *Nature Climate Change*, *3*(1), 52-58. https://doi.org/10.1038/nclimate1633

Damberg, L., & AghaKouchak, A. (2014). Global trends and patterns of drought from space. *Theoretical and Applied Climatology*, *117*(3), 441-448. https://doi.org/10.1007/s00704-013-1019-5

Dang, C., Shao, Z., Huang, X., Qian, J., Cheng, G., Ding, Q., & Fan, Y. (2022). Assessment of the importance of increasing temperature and decreasing soil moisture on global ecosystem productivity using solar-induced chlorophyll fluorescence. *Global Change Biology*, *28*(6), 2066-2080. https://doi.org/10.1111/gcb.16043

Dao, P. U., Heuzard, A. G., Le, T. X. H., Zhao, J., Yin, R., Shang, C., & Fan, C. (2024). The impacts of climate change on groundwater quality: A review. *Science of The Total Environment*, *912*, 169241. https://doi.org/10.1016/j.scitotenv.2023.169241

Dare-Idowu, O., Brut, A., Cuxart, J., Tallec, T., Rivalland, V., Zawilski, B., Ceschia, E., & Jarlan, L. (2021). Surface energy balance and flux partitioning of annual crops in southwestern France. *Agricultural and Forest Meteorology*, *308-309*, 108529. https://doi.org/10.1016/j.agrformet.2021.108529

Das, K., & Paul, P. K. (2015). Present status of soil moisture estimation by microwave remote sensing. *Cogent Geoscience*, *1*(1), 1084669. https://doi.org/10.1080/23312041.2015.1084669

Davamani, V., John, J. E., Poornachandhra, C., Gopalakrishnan, B., Arulmani, S., Parameswari, E., Santhosh, A., Srinivasulu, A., Lal, A., & Naidu, R. (2024). A Critical Review of Climate Change Impacts on Groundwater Resources: A Focus on the Current Status, Future Possibilities, and Role of Simulation Models. *Atmosphere*, *15*(1), 122. https://doi.org/10.3390/atmos15010122

De Jong, R., Verbesselt, J., Zeileis, A., & Schaepman, M. E. (2013). Shifts in Global Vegetation Activity Trends. *Remote Sensing*, *5*(3), 1117-1133. https://doi.org/10.3390/rs5031117

De Roo, A. P. J. (1999). LISFLOOD: a rainfall-runoff model for large river basins to assess the influence of land use changes on flood risk. *Ribamod: river basin modelling, management and flood mitigation. Concerted action, European Commission, EUR, 18287*, 349-357.

De Roo, A. P. J., Wesseling, C. G., & Van Deursen, W. P. A. (2000). Physically based river basin modelling within a GIS: the LISFLOOD model. *Hydrological Processes*, *14*(11-12), 1981-1992. https://doi.org/10.1002/1099-1085(20000815/30)14:11/12<1981::AID-HYP49>3.0.CO;2-F

Defourny, P., Kirches, G., Brockmann, C., Boettcher, M., Peters, M., Bontemps, S., Lamarche, C., Schlerf, M., & Santoro, M. (2012). *Land Cover CCI: Product User Guide Version 2.0*. European Space Agency. https://maps.elie.ucl.ac.be/CCI/viewer/download/ESACCI-LC-Ph2-PUGv2_2.0.pdf

Del Río, S., Cano-Ortiz, A., Herrero, L., & Penas, A. (2012). Recent trends in mean maximum and minimum air temperatures over Spain (1961–2006). *Theoretical and Applied Climatology*, *109*(3), 605-626. https://doi.org/10.1007/s00704-012-0593-2

Deng, C., Zhang, L., Xu, T., Yang, S., Guo, J., Si, L., Kang, R., & Kaufmann, H. J. (2024). An Integrated Drought Index (Vapor Pressure Deficit–Soil Moisture–Sun-Induced Chlorophyll Fluorescence Dryness Index, VMFDI) Based on Multisource Data and Its Applications in Agricultural Drought Management. *Remote Sensing*, *16*(24), 4666. https://doi.org/10.3390/rs16244666

Denissen, J. M. C., Teuling, A. J., Pitman, A. J., Koirala, S., Migliavacca, M., Li, W., Reichstein, M., Winkler, A. J., Zhan, C., & Orth, R. (2022). Widespread shift from ecosystem energy to water limitation with climate change. *Nature Climate Change*, *12*(7), 677-684. https://doi.org/10.1038/s41558-022-01403-8

DESTATIS (Statistisches Bundesamt). (2023). *Erträge Ausgewählter Landwirtschaftlicher Feldfrüchte—Jahressumme—Regionale Ebenen.*

https://www.regionalstatistik.de/genesis//online?operation=table&code=41241-01-03-4-B&bypass=true&levelindex=1&levelid=1695656650535#abreadcrumb

Detto, M., Montaldo, N., Albertson, J. D., Mancini, M., & Katul, G. (2006). Soil moisture and vegetation controls on evapotranspiration in a heterogeneous Mediterranean ecosystem on Sardinia, Italy. *Water Resources Research, 42*(8). https://doi.org/10.1029/2005WR004693

Di Gregorio, A. (2005). *Land cover classification system: Classification concepts and user manual: LCCS* (Vol. 2). Food & Agriculture Organization of the United Nations.

Didan, K. (2021a). *MODIS/Terra vegetation indices 16-day L3 global 500m SIN grid V061* [Data set]. NASA EOSDIS Land Processes Distributed Active Archive Center. https://doi.org/10.5067/MODIS/MOD13A1.061

Didan, K. (2021b). *MODIS/Aqua vegetation indices 16-day L3 global 500m SIN grid V061* [Data set]. NASA EOSDIS Land Processes Distributed Active Archive Center. https://doi.org/10.5067/MODIS/MYD13A1.061

Dirmeyer, P. A., & Tan, L. (2001). *A multi-decadal global land-surface data set of state variables and fluxes* (Vol. 102). Center for Ocean-Land-Atmosphere Studies.

Dobriyal, P., Qureshi, A., Badola, R., & Hussain, S. A. (2012). A review of the methods available for estimating soil moisture and its implications for water resource management. *Journal of Hydrology, 458-459*, 110-117. https://doi.org/10.1016/j.jhydrol.2012.06.021

Dorigo, W., Wagner, W., Hohensinn, R., Hahn, S., Paulik, C., Xaver, A., Gruber, A., Drusch, M., Mecklenburg, S., van Oevelen, P., & others. (2011). The International Soil Moisture Network: A data hosting facility for global in situ soil moisture measurements. *Hydrology and Earth system sciences, 15*(5), 1675-1698. https://doi.org/10.5194/hess-15-1675-2011, 2011

Dorigo, W. A., Gruber, A., De Jeu, R. A. M., Wagner, W., Stacke, T., Loew, A., Albergel, C., Brocca, L., Chung, D., Parinussa, R. M., & Kidd, R. (2015). Evaluation of the ESA CCI soil moisture product using ground-based observations. *Remote Sensing of Environment, 162*, 380-395. https://doi.org/10.1016/j.rse.2014.07.023

DRAAF (Direction Régionale de l'Alimentation, de l'Agriculture et de la Forêt). (2024). *Statistique Agricole Annuelle 2022 et Nouvelles Séries 2010–2022*. DRAAF Occitanie. https://draaf.occitanie.agriculture.gouv.fr/statistique-agricole-annuelle-2022-et-nouvelles-series-2010-2022-a7672.html

Dracup, J. A., Lee, K. S., & Paulson Jr., E. G. (1980). On the definition of droughts. *Water Resources Research, 16*(2), 297-302. https://doi.org/10.1029/WR016i002p00297

Drastig, K., Prochnow, A., Baumecker, M., Berg, W., & Brunsch, R. (2011). Agricultural Water Management in Brandenburg. *DIE ERDE – Journal of the Geographical*

Society of Berlin, 142(1-2), 119-140. https://www.die-erde.org/index.php/die-erde/article/view/45

Drastig, K., Prochnow, A., Libra, J., Koch, H., & Rolinski, S. (2016). Irrigation water demand of selected agricultural crops in Germany between 1902 and 2010. *Science of The Total Environment, 569-570*, 1299-1314. https://doi.org/10.1016/j.scitotenv.2016.06.206

Dube, K., Nhamo, G., & Chikodzi, D. (2022). Climate change-induced droughts and tourism: Impacts and responses of Western Cape province, South Africa. *Journal of Outdoor Recreation and Tourism, 39*, 100319. https://doi.org/10.1016/j.jort.2020.100319

Duchemin, B., Goubier, J., & Courrier, G. (1999). Monitoring Phenological Key Stages and Cycle Duration of Temperate Deciduous Forest Ecosystems with NOAA/AVHRR Data. *Remote Sensing of Environment, 67*(1), 68-82. https://doi.org/10.1016/S0034-4257(98)00067-4

Dudney, J., Latimer, A. M., van Mantgem, P., Zald, H., Willing, C. E., Nesmith, J. C. B., Cribbs, J., & Milano, E. (2023). The energy–water limitation threshold explains divergent drought responses in tree growth, needle length, and stable isotope ratios. *Global Change Biology*, *29*(15), 4368-4382. https://doi.org/10.1111/gcb.16740

DWD (DeutscheWetterdienst). (2023). *Phänologische Jahresstatistik*. https://www.dwd.de/DE/leistungen/phaeno_sta/phaenosta.html#buehneTop

EC (European Commission). (2023). *EU Agricultural Outlook for Markets, Income and Environment, 2022–2032*. https://agriculture.ec.europa.eu/system/files/2023-04/agricultural-outlook-2022-report_en_0.pdf

EEA (European Environment Agency). (2023a). *Climate Change Adaptation in the Agriculture Sector in Europe.* https://www.eea.europa.eu/publications/cc-adaptation-agriculture

EEA (European Environment Agency). (2023b). *Climate Change, Impacts and Vulnerability in Europe 2016.* https://www.eea.europa.eu/publications/climate-change-impacts-and-vulnerability-2016

Eitzinger, J., Štastná, M., Žalud, Z., & Dubrovský, M. (2003). A simulation study of the effect of soil water balance and water stress on winter wheat production under different climate change scenarios. *Agricultural Water Management, 61*(3), 195-217. https://doi.org/10.1016/S0378-3774(03)00024-6

Engman, E. T. (1990). Progress in Microwave Remote Sensing of Soil Moisture. *Canadian Journal of Remote Sensing*, *16*(3), 6-14. https://doi.org/10.1080/07038992.1990.11487620

Erfurt, M., Glaser, R., & Blauhut, V. (2019). Changing impacts and societal responses to drought in southwestern Germany since 1800. *Regional Environmental Change*, *19*(8), 2311-2323. https://doi.org/10.1007/s10113-019-01522-7

Erfurt, M., Skiadaresis, G., Tijdeman, E., Blauhut, V., Bauhus, J., Glaser, R., Schwarz, J., Tegel, W., & Stahl, K. (2020). A multidisciplinary drought catalogue for southwestern Germany dating back to 1801. *Natural Hazards and Earth System Sciences*, *20*(11), 2979-2995. https://doi.org/10.5194/nhess-20-2979-2020

Ersi, C., Bayaer, T., Bao, Y., Bao, Y., Yong, M., Lai, Q., Zhang, X., & Zhang, Y. (2023). Comparison of Phenological Parameters Extracted from SIF, NDVI and NIRv Data on the Mongolian Plateau. *Remote Sensing*, *15*(1), 187. https://doi.org/10.3390/rs15010187

Escorihuela, M. J., & Quintana-Seguí, P. (2016). Comparison of remote sensing and simulated soil moisture datasets in Mediterranean landscapes. *Special Issue: ESA's Soil Moisture and Ocean Salinity Mission - Achievements and Applications*, *180*, 99-114. https://doi.org/10.1016/j.rse.2016.02.046

Essa, Y. H., Hirschi, M., Thiery, W., El-Kenawy, A. M., & Yang, C. (2023). Drought characteristics in Mediterranean under future climate change. *npj Climate and Atmospheric Science*, *6*(1), 133. https://doi.org/10.1038/s41612-023-00458-4

Estefania-Salazar, E., & Iglesias, E. (2025). Assessing vegetation phenology dynamics in West African rangelands: Implications for livestock sustainability and transhumance. *Ecological Informatics*, *88*, 103138. https://doi.org/10.1016/j.ecoinf.2025.103138

Eswar, R., Das, N. N., Poulsen, C., Behrangi, A., Swigart, J., Svoboda, M., Entekhabi, D., Yueh, S., Doorn, B., & Entin, J. (2018). SMAP Soil Moisture Change as an Indicator of Drought Conditions. *Remote Sensing*, *10*(5), 788. https://doi.org/10.3390/rs10050788

EUROSTAT (Statistical Office of the European Communities). (2023a). *Crop Production in EU Standard Humidity*. https://ec.europa.eu/eurostat/databrowser/view/apro_cpsh1/default/table?lang=en

EUROSTAT (Statistical Office of the European Communities). (2023b). *Crop Production in EU Standard Humidity by NUTS 2 Regions.* https://ec.europa.eu/eurostat/databrowser/view/apro_cpshr/default/table?lang=en

Ewert, F., Rounsevell, M. D. A., Reginster, I., Metzger, M. J., & Leemans, R. (2005). Future scenarios of European agricultural land use: I. Estimating changes in crop productivity. *Agriculture, Ecosystems & Environment*, *107*(2), 101-116. https://doi.org/10.1016/j.agee.2004.12.003

Eyshi Rezaei, E., Siebert, S., & Ewert, F. (2015). Impact of data resolution on heat and drought stress simulated for winter wheat in Germany. *European Journal of Agronomy, 65*, 69-82. https://doi.org/10.1016/j.eja.2015.02.003

Falloon, P., Jones, C. D., Ades, M., & Paul, K. (2011). Direct soil moisture controls of future global soil carbon changes: An important source of uncertainty. *Global Biogeochemical Cycles, 25*(3). https://doi.org/10.1029/2010GB003938

Famiglietti, J. S., & Wood, E. F. (1994). Multiscale modeling of spatially variable water and energy balance processes. *Water Resources Research, 30*(11), 3061-3078. https://doi.org/10.1029/94WR01498

Fan, J., Min, J., Yang, Q., Na, J., & Wang, X. (2022). Spatial-Temporal Relationship Analysis of Vegetation Phenology and Meteorological Parameters in an Agro-Pasture Ecotone in China. *Remote Sensing, 14*(21), 5417. https://doi.org/10.3390/rs14215417

Fang, H., Baret, F., Plummer, S., & Schaepman-Strub, G. (2019). An Overview of Global Leaf Area Index (LAI): Methods, Products, Validation, and Applications. *Reviews of Geophysics, 57*(3), 739-799. https://doi.org/10.1029/2018RG000608

Fang, H., Sha, M., Xie, Y., Lin, W., Qiu, D., Tu, J., Tan, X., Li, X., & Sha, Z. (2023). Shifted Global Vegetation Phenology in Response to Climate Changes and Its Feedback on Vegetation Carbon Uptake. *Remote Sensing, 15*(9), 2288. https://doi.org/10.3390/rs15092288

FAO (Food and Agriculture Organization). (2024a). *Land statistics 2001–2022 – Global, regional and country trends*. https://doi.org/10.4060/cd1484en

FAO (Food and Agriculture Organization). (2024b). *Agricultural production statistics 2010–2023*. https://www.fao.org/statistics/highlights-archive/highlights-detail/agricultural-production-statistics-2010-2023/en

Farooq, M., Wahid, A., Kobayashi, N., Fujita, D., & Basra, S. M. A. (2009). Plant Drought Stress: Effects, Mechanisms and Management. In E. Lichtfouse, M. Navarrete, P. Debaeke, S. Véronique, & C. Alberola (Eds.), *Sustainable Agriculture* (pp. 153-188). Springer Netherlands. https://doi.org/10.1007/978-90-481-2666-8_12

Farooq, M., Hussain, M., Wahid, A., & Siddique, K. H. M. (2012). Drought Stress in Plants: An Overview. In R. Aroca (Ed.), *Plant Responses to Drought Stress: From Morphological to Molecular Features* (pp. 1-33). Springer Berlin Heidelberg. https://doi.org/10.1007/978-3-642-32653-0_1

Feekes, W. (1941). *Verslagen van de Technische Tarwe Commissie XVII De Tarwe en haar milieu* (pp. 523-588). Groningen: Gebroeders Hoitsema.

Feng, P., Wang, B., Liu, D. L., & Yu, Q. (2019). Machine learning-based integration of remotely-sensed drought factors can improve the estimation of agricultural

drought in South-Eastern Australia. *Agricultural Systems*, *173*, 303-316. https://doi.org/10.1016/j.agsy.2019.03.015

Feng, Y., Cao, H., Song, H., Huang, K., Zhang, Y., Zhang, Y., Li, S., Li, Y., Lu, J., & Guan, X. (2024). The formation mechanism, analysis strategies and regulation measures of cereal aroma: A review. *Trends in Food Science & Technology*, *147*, 104452. https://doi.org/10.1016/j.tifs.2024.104452

Ferreira, C. S. S., Seifollahi-Aghmiuni, S., Destouni, G., Ghajarnia, N., & Kalantari, Z. (2022). Soil degradation in the European Mediterranean region: Processes, status and consequences. *Science of The Total Environment*, *805*, 150106. https://doi.org/10.1016/j.scitotenv.2021.150106

Fioravanti, G., Toreti, A., Cammalleri, C., Muñoz, C. A., Bavera, D., De Jager, A., Hrast Essenfelder, A., Di Ciollo, C., Masante, D., Magni, D., Navarro, J. A., Mazzesch, M., & Maetens, W. (2025). A dataset for monitoring agricultural drought in Europe. *Scientific Data*, *12*(1), 308. https://doi.org/10.1038/s41597-024-04199-8

Flexas, J., Diaz-Espejo, A., Gago, J., Gallé, A., Galmés, J., Gulías, J., & Medrano, H. (2014). Photosynthetic limitations in Mediterranean plants: A review. *Response to abiotic stresses of plants of Mediterranean-type ecosystems*, *103*, 12-23. https://doi.org/10.1016/j.envexpbot.2013.09.002

Forzieri, G., Feyen, L., Rojas, R., Flörke, M., Wimmer, F., & Bianchi, A. (2014). Ensemble projections of future streamflow droughts in Europe. *Hydrology and Earth System Sciences*, *18*(1), 85-108. https://doi.org/10.5194/hess-18-85-2014

Fu, Y. H., Piao, S., Op de Beeck, M., Cong, N., Zhao, H., Zhang, Y., Menzel, A., & Janssens, I. A. (2014). Recent spring phenology shifts in western C entral E urope based on multiscale observations. *Global ecology and biogeography*, *23*(11), 1255-1263. https://doi.org/10.1111/geb.12210

Fu, Y., He, H. S., Zhao, J., Larsen, D. R., Zhang, H., Sunde, M. G., & Duan, S. (2018). Climate and Spring Phenology Effects on Autumn Phenology in the Greater Khingan Mountains, Northeastern China. *Remote Sensing*, *10*(3), 449. https://doi.org/10.3390/rs10030449

Fu, Z., Ciais, P., Prentice, I. C., Gentine, P., Makowski, D., Bastos, A., Luo, X., Green, J. K., Stoy, P. C., Yang, H., & Hajima, T. (2022). Atmospheric dryness reduces photosynthesis along a large range of soil water deficits. *Nature Communications*, *13*(1), 989. https://doi.org/10.1038/s41467-022-28652-7

Fuentes, I., Lopatin, J., Galleguillos, M., & McPhee, J. (2025). Vegetation browning as an indicator of drought impact and ecosystem resilience. *Science of Remote Sensing*, *11*, 100219. https://doi.org/10.1016/j.srs.2025.100219

Fyfe, J. C., Gillett, N. P., & Zwiers, F. W. (2013). Overestimated global warming over the past 20 years. *Nature Climate Change*, *3*(9), 767-769. https://doi.org/10.1038/nclimate1972

Galmés, J., Medrano, H., & Flexas, J. (2007). Photosynthetic limitations in response to water stress and recovery in Mediterranean plants with different growth forms. *New Phytologist*, *175*(1), 81-93. https://doi.org/10.1111/j.1469-8137.2007.02087.x

Gameiro, J., Marques, A. T., Venâncio, L., Valerio, F., Pacheco, C., Guedes, A., Pereira, J., Ribeiro, L., Moreira, F., Beja, P., Arroyo, B., & Silva, J. P. (2024). Evidence of a twofold ecological trap driven by agricultural change causing a priority farmland bird population crash. *Conservation Science and Practice*, *6*(10), e13168. https://doi.org/10.1111/csp2.13168

Gammans, M., Mérel, P., & Ortiz-Bobea, A. (2017). Negative impacts of climate change on cereal yields: Statistical evidence from France. *Environmental Research Letters*, *12*(5), 054007. https://doi.org/10.1088/1748-9326/aa6b0c

Gao, W., Zheng, C., Liu, X., Lu, Y., Chen, Y., Wei, Y., & Ma, Y. (2022). NDVI-based vegetation dynamics and their responses to climate change and human activities from 1982 to 2020: A case study in the Mu Us Sandy Land, China. *Ecological Indicators*, *137*, 108745. https://doi.org/10.1016/j.ecolind.2022.108745

Gaona, J., Benito-Verdugo, P., Martínez-Fernández, J., González-Zamora, Á., Almendra-Martín, L., & Herrero-Jiménez, C. M. (2022). Soil Moisture Outweighs Climatic Factors in Critical Periods for Rainfed Cereal Yields: An Analysis in Spain. *Agriculture*, *12*(4), 533. https://doi.org/10.3390/agriculture12040533

Gaona, J., Benito-Verdugo, P., Martínez-Fernández, J., González-Zamora, Á., Almendra-Martín, L., & Herrero-Jiménez, C. M. (2023). Predictive value of soil moisture and concurrent variables in the multivariate modelling of cereal yields in water-limited environments. *Agricultural Water Management*, *282*, 108280. https://doi.org/10.1016/j.agwat.2023.108280

Garcia y Garcia, A., Guerra, L. C., & Hoogenboom, G. (2008). Impact of generated solar radiation on simulated crop growth and yield. *Ecological Modelling*, *210*(3), 312-326. https://doi.org/10.1016/j.ecolmodel.2007.08.003

García-Herrera, R., Hernández, E., Barriopedro, D., Paredes, D., Trigo, R. M., Trigo, I. F., & Mendes, M. A. (2007). The Outstanding 2004/05 Drought in the Iberian Peninsula: Associated Atmospheric Circulation. *Journal of Hydrometeorology*, *8*(3), 483-498. https://doi.org/10.1175/JHM578.1

García-Herrera, R., Garrido-Perez, J. M., Barriopedro, D., Ordóñez, C., Vicente-Serrano, S. M., Nieto, R., Gimeno, L., Sorí, R., & Yiou, P. (2019). The European 2016/17 drought. *Journal of Climate*, *32*(11), 3169-3187. https://doi.org/10.1175/JCLI-D-18-0331.1

García-León, D., López-Lozano, R., Toreti, A., & Zampieri, M. (2020). Local-Scale Cereal Yield Forecasting in Italy: Lessons from Different Statistical Models and Spatial Aggregations. *Agronomy*, *10*(6), 809. https://doi.org/10.3390/agronomy10060809

GCOS (Global Climate Observing System). (2022). *The 2022 GCOS ECVs requirements*. https://meetings.wmo.int/INFCOM-2/InformationDocuments/INFCOM-2-INF06-1(11-2)-2022-GCOS-ECVS-REQUIREMENTS_en.pdf

Gerard, F. F., George, C. T., Hayman, G., Chavana-Bryant, C., & Weedon, G. P. (2020). Leaf phenology amplitude derived from MODIS NDVI and EVI: Maps of leaf phenology synchrony for Meso-and South America. *Geoscience Data Journal*, *7*(1), 13-26. https://doi.org/10.1002/gdj3.87

Giorgi, F. (2006). Climate change hot-spots. *Geophysical research letters*, *33*(8). https://doi.org/10.1029/2006GL025734

Giorgi, F., & Lionello, P. (2008). Climate change projections for the Mediterranean region. *Mediterranean climate: trends, variability and change*, 63(2), 90-104. https://doi.org/10.1016/j.gloplacha.2007.09.005

Golian, S., Mazdiyasni, O., & AghaKouchak, A. (2015). Trends in meteorological and agricultural droughts in Iran. *Theoretical and Applied Climatology*, *119*(3), 679-688. https://doi.org/10.1007/s00704-014-1139-6

Gong, Z., Ge, W., Guo, J., & Liu, J. (2024). Satellite remote sensing of vegetation phenology: Progress, challenges, and opportunities. *ISPRS Journal of Photogrammetry and Remote Sensing*, *217*, 149-164. https://doi.org/10.1016/j.isprsjprs.2024.08.011

González-Zamora, Á., (2017). *Análisis y validación de nuevos productos SMOS de interés en agricultura e hidrología* [Tesis doctoral, Universidad de Salamanca].

González-Zamora, Á., Sánchez, N., Pablos, M., & Martínez-Fernández, J. (2019). CCI soil moisture assessment with SMOS soil moisture and in situ data under different environmental conditions and spatial scales in Spain. *Remote Sensing of Environment*, *225*, 469-482. https://doi.org/10.1016/j.rse.2018.02.010

González-Zamora, Á., Almendra-Martín, L., de Luis, M., & Martínez-Fernández, J. (2021). Influence of Soil Moisture vs. Climatic Factors in Pinus Halepensis Growth Variability in Spain: A Study with Remote Sensing and Modeled Data. *Remote Sensing*, *13*(4), 757. https://doi.org/10.3390/rs13040757

González-Zamora, Á., García-Barreda, S., Martínez-Fernández, J., Almendra-Martín, L., Gaona, J., & Benito-Verdugo, P. (2022). Soil Moisture and Black Truffle Production Variability in the Iberian Peninsula. *Forests*, *13*(6), 819. https://doi.org/10.3390/f13060819

González-Zamora, Á., Almendra-Martín, L., de Luis, M., Gaona, J., & Martínez-Fernández, J. (2023). How Are Pine Species Responding to Soil Drought and Climate Change in the Iberian Peninsula? *Forests*, *14*(8), 1530. https://doi.org/10.3390/f14081530

Gordo, O., & Sanz, J. J. (2010). Impact of climate change on plant phenology in Mediterranean ecosystems. *Global Change Biology*, *16*(3), 1082-1106. https://doi.org/10.1111/j.1365-2486.2009.02084.x

Gouveia, C., & Trigo, R. M. (2008). Influence of Climate Variability on Wheat Production in Portugal. In A. Soares, M. J. Pereira, & R. Dimitrakopoulos (Eds.), *geoENV VI – Geostatistics for Environmental Applications: Proceedings of the Sixth European Conference on Geostatistics for Environmental Applications* (pp. 335-345). Springer Netherlands. https://doi.org/10.1007/978-1-4020-6448-7_28

Grillakis, M. G. (2019). Increase in severe and extreme soil moisture droughts for Europe under climate change. *Science of The Total Environment*, *660*, 1245-1255. https://doi.org/10.1016/j.scitotenv.2019.01.001

Gringorten, I. I. (1963). A plotting rule for extreme probability paper. *Journal of Geophysical Research (1896-1977)*, *68*(3), 813-814. https://doi.org/10.1029/JZ068i003p00813

Gu, L., Chen, J., Yin, J., Sullivan, S. C., Wang, H.-M., Guo, S., Zhang, L., & Kim, J.-S. (2020). Projected increases in magnitude and socioeconomic exposure of global droughts in 1.5 and 2 °C warmer climates. *Hydrology and Earth System Sciences*, *24*(1), 451-472. https://doi.org/10.5194/hess-24-451-2020

Guo, J., & Hu, Y. (2022). Spatiotemporal Variations in Satellite-Derived Vegetation Phenological Parameters in Northeast China. *Remote Sensing*, *14*(3), 705. https://doi.org/10.3390/rs14030705

Hamed, K. H., & Ramachandra Rao, A. (1998). A modified Mann-Kendall trend test for autocorrelated data. *Journal of Hydrology*, *204*(1), 182-196. https://doi.org/10.1016/S0022-1694(97)00125-X

Hamed, K. H. (2008). Trend detection in hydrologic data: The Mann–Kendall trend test under the scaling hypothesis. *Journal of Hydrology*, *349*(3), 350-363. https://doi.org/10.1016/j.jhydrol.2007.11.009

Hänsel, S., Ustrnul, Z., Łupikasza, E., & Skalak, P. (2019). Assessing seasonal drought variations and trends over Central Europe. *Advances in Water Resources*, *127*, 53-75. https://doi.org/10.1016/j.advwatres.2019.03.005

Hao, Z., & Singh, V. P. (2015). Drought characterization from a multivariate perspective: A review. *Journal of Hydrology*, *527*, 668-678. https://doi.org/10.1016/j.jhydrol.2015.05.031

He, B., Wu, J., Lü, A., Cui, X., Zhou, L., Liu, M., & Zhao, L. (2013). Quantitative assessment and spatial characteristic analysis of agricultural drought risk in China. *Natural Hazards*, *66*(2), 155-166. https://doi.org/10.1007/s11069-012-0398-8

Hernandez-Barrera, S., Rodriguez-Puebla, C., & Challinor, A. J. (2017). Effects of diurnal temperature range and drought on wheat yield in Spain. *Theoretical and Applied Climatology*, *129*(1), 503-519. https://doi.org/10.1007/s00704-016-1779-9

Hirsch, R. M., Alexander, R. B., & Smith, R. A. (1991). Selection of methods for the detection and estimation of trends in water quality. *Water Resources Research*, *27*(5), 803-813. https://doi.org/10.1029/91WR00259

Hlavinka, P., Trnka, M., Semerádová, D., Dubrovský, M., Žalud, Z., & Možný, M. (2009). Effect of drought on yield variability of key crops in Czech Republic. *Agricultural and Forest Meteorology*, *149*(3), 431-442. https://doi.org/10.1016/j.agrformet.2008.09.004

Hmimina, G., Dufrêne, E., Pontailler, J.-Y., Delpierre, N., Aubinet, M., Caquet, B., de Grandcourt, A., Burban, B., Flechard, C., Granier, A., Gross, P., Heinesch, B., Longdoz, B., Moureaux, C., Ourcival, J.-M., Rambal, S., Saint André, L., & Soudani, K. (2013). Evaluation of the potential of MODIS satellite data to predict vegetation phenology in different biomes: An investigation using ground-based NDVI measurements. *Remote Sensing of Environment*, *132*, 145-158. https://doi.org/10.1016/j.rse.2013.01.010

Ho, S., Buras, A., & Tuo, Y. (2023). Comparing Agriculture-Related Characteristics of Flash and Normal Drought Reveals Heterogeneous Crop Response. *Water Resources Research*, *59*(11), e2023WR034994. https://doi.org/10.1029/2023WR034994

Hobbins, M. T., Wood, A., McEvoy, D. J., Huntington, J. L., Morton, C., Anderson, M., & Hain, C. (2016). The Evaporative Demand Drought Index. Part I: Linking Drought Evolution to Variations in Evaporative Demand. *Journal of Hydrometeorology*, *17*(6), 1745-1761. https://doi.org/10.1175/JHM-D-15-0121.1

Hossain, A., da Silva, J. A. T., Lozovskaya, M. V., & Zvolinsky, V. P. (2012). High temperature combined with drought affect rainfed spring wheat and barley in South-Eastern Russia: I. Phenology and growth. *Saudi journal of biological sciences*, *19*(4), 473-487. https://doi.org/10.1016/j.sjbs.2012.07.005

Hu, Z., Piao, S., Knapp, A. K., Wang, X., Peng, S., Yuan, W., Running, S., Mao, J., Shi, X., Ciais, P., Huntzinger, D. N., Yang, J., & Yu, G. (2022). Decoupling of greenness and gross primary productivity as aridity decreases. *Remote Sensing of Environment*, *279*, 113120. https://doi.org/10.1016/j.rse.2022.113120

Hu, C., She, D., Wang, G., Zhang, L., Jing, Z., Hong, S., Song, Z., & Xia, J. (2024). Soil moisture and precipitation dominate the response and recovery times of

ecosystems from different types of flash drought in the Yangtze River Basin. *Agricultural and Forest Meteorology*, *358*, 110236. https://doi.org/10.1016/j.agrformet.2024.110236

Hua, Y.-W., Meng, D., Hu, F.-F., Zhao, Y., Zhang, C.-C., & Li, X.-J. (2025). Changes of remote sensing vegetation phenology in Beijing-Tianjin-Hebei region under the background of urbanization. *Ying Yong Sheng Tai Xue Bao = The Journal of Applied Ecology*, *36*(3), 693-702. https://doi.org/10.13287/j.1001-9332.202503.022

Huang, Y., Gerber, S., Huang, T., & Lichstein, J. W. (2016). Evaluating the drought response of CMIP5 models using global gross primary productivity, leaf area, precipitation, and soil moisture data. *Global Biogeochemical Cycles*, *30*(12), 1827-1846. https://doi.org/10.1002/2016GB005480

Huang, X., Liu, J., Zhu, W., Atzberger, C., & Liu, Q. (2019). The Optimal Threshold and Vegetation Index Time Series for Retrieving Crop Phenology Based on a Modified Dynamic Threshold Method. *Remote Sensing*, *11*(23). https://doi.org/10.3390/rs11232725

Huang, X., Ma, L., Liu, T., Sun, B., Chen, Y., Qiao, Z., & Liang, L. (2021). Response relationship between the abrupt temperature change-climate warming hiatus and changes in influencing factors in China. *International Journal of Climatology*, *41*(11), 5178-5200. https://doi.org/10.1002/joc.7123

Huete, A., Didan, K., Miura, T., Rodriguez, E. P., Gao, X., & Ferreira, L. G. (2002). Overview of the radiometric and biophysical performance of the MODIS vegetation indices. *The Moderate Resolution Imaging Spectroradiometer (MODIS): a new generation of Land Surface Monitoring*, *83*(1), 195-213. https://doi.org/10.1016/S0034-4257(02)00096-2

Hunt, E. D., Hubbard, K. G., Wilhite, D. A., Arkebauer, T., & Dutcher, A. L. (2009). The development and evaluation of a soil moisture index. *Int. J. Climatol.*, *29*, 747-759. https://doi.org/10.1002/joc.1749

Hunt, E., Femia, F., Werrell, C., Christian, J. I., Otkin, J. A., Basara, J., Anderson, M., White, T., Hain, C., Randall, R., & McGaughey, K. (2021). Agricultural and food security impacts from the 2010 Russia flash drought. *Weather and Climate Extremes*, *34*, 100383. https://doi.org/10.1016/j.wace.2021.100383

Iglesias, A., Cancelliere, A., Wilhite, D. A., Garrote, L., & Cubillo, F. (2009). *Coping with drought risk in agriculture and water supply systems: Drought management and policy development in the Mediterranean* (Vol. 26). Springer.

Iglesias, A., Quiroga, S., Moneo, M., & Garrote, L. (2012). From climate change impacts to the development of adaptation strategies: Challenges for agriculture in Europe. *Climatic Change*, *112*, 143-168.

Iglesias, A., & Garrote, L. (2015). Adaptation strategies for agricultural water management under climate change in Europe. *Agricultural Water Management*, *155*, 113-124. https://doi.org/10.1016/j.agwat.2015.03.014

INE (Instituto Nacional de Estatística de Portugal). (2025). *Estatísticas agrícolas*. https://www.ine.pt/xportal/xmain?xpid=INE&xpgid=ine_publicacoes&PUBLICACOESpagenumber=1&PUBLICACOEStema=55505

Ionita, M., Tallaksen, L. M., Kingston, D. G., Stagge, J. H., Laaha, G., Van Lanen, H. A. J., Scholz, P., Chelcea, S. M., & Haslinger, K. (2017). The European 2015 drought from a climatological perspective. *Hydrology and Earth System Sciences*, *21*(3), 1397-1419. https://doi.org/10.5194/hess-21-1397-2017

IPCC (Intergovernmental Panel on Climate Change). (2023). Contribution of Working Groups I, II and III to the Sixth Assessment Report of the Intergovernmental Panel on Climate Change. In Core Writing Team, H. Lee, & J. Romero (Eds.), *Climate change 2023: Synthesis report* (pp. 35–115). https://doi.org/10.59327/IPCC/AR6-9789291691647

Istat (Istituto Nazionale di Statistica). (2025). *Statistica agricola*. http://dati.istat.it/Index.aspx?QueryId=37850

Jaagus, J., Aasa, A., Aniskevich, S., Boincean, B., Bojariu, R., Briede, A., Danilovich, I., Castro, F. D., Dumitrescu, A., Labuda, M., Labudová, L., Lõhmus, K., Melnik, V., Mõisja, K., Pongracz, R., Potopová, V., Řezníčková, L., Rimkus, E., Semenova, I., Stonevičius, E., Štěpánek, P., Trnka, M., Vicente-Serrano, S. M., Wibig, J., & Zahradníček, P. (2022). Long-term changes in drought indices in eastern and central Europe. *International Journal of Climatology*, *42*(1), 225-249. https://doi.org/10.1002/joc.7241

Jacobsen, S.-E., Jensen, C. R., & Liu, F. (2012). Improving crop production in the arid Mediterranean climate. *Field Crops Research*, *128*, 34-47. https://doi.org/10.1016/j.fcr.2011.12.001

Jamali, M., & Eslamian, S. (2023). Chapter 14—Parametric and nonparametric methods for analyzing the trend of extreme events. In S. Eslamian & F. Eslamian (Eds.), *Handbook of Hydroinformatics* (pp. 223-237). Elsevier. https://doi.org/10.1016/B978-0-12-821961-4.00010-5

Janáček, J. (1994). Wilhite, D.A.: Drought assessment, management and planning: Theory and case studies. *Biologia Plantarum*, *36*, 628. https://doi.org/10.1007/BF02921195

Jeong, S.-J., Ho, C.-H., Gim, H.-J., & Brown, M. E. (2011). Phenology shifts at start vs. End of growing season in temperate vegetation over the Northern Hemisphere for the period 1982–2008. *Global change biology*, *17*(7), 2385-2399. https://doi.org/10.1111/j.1365-2486.2011.02397.x

Jiao, F., Liu, H., Xu, X., Gong, H., & Lin, Z. (2020). Trend Evolution of Vegetation Phenology in China during the Period of 1981–2016. *Remote Sensing*, *12*(3), 572. https://doi.org/10.3390/rs12030572

Jiménez-de-Santiago, D. E., Lidón, A., & Bosch-Serra, À. D. (2019). Soil Water Dynamics in a Rainfed Mediterranean Agricultural System. *Water*, *11*(4), 799. https://doi.org/10.3390/w11040799

Jin, H., & Eklundh, L. (2014). A physically based vegetation index for improved monitoring of plant phenology. *Remote Sensing of Environment*, *152*, 512-525. https://doi.org/10.1016/j.rse.2014.07.010

Jin, H., Jönsson, A. M., Olsson, C., Lindström, J., Jönsson, P., & Eklundh, L. (2019a). New satellite-based estimates show significant trends in spring phenology and complex sensitivities to temperature and precipitation at northern European latitudes. *International Journal of Biometeorology*, *63*(6), 763-775. https://doi.org/10.1007/s00484-019-01690-5

Jin, C., Luo, X., Xiao, X., Dong, J., Li, X., Yang, J., & Zhao, D. (2019b). The 2012 Flash Drought Threatened US Midwest Agroecosystems. *Chinese Geographical Science*, *29*(5), 768-783. https://doi.org/10.1007/s11769-019-1066-7

Jonsson, P., & Eklundh, L. (2002). Seasonality extraction by function fitting to time-series of satellite sensor data. *IEEE transactions on Geoscience and Remote Sensing*, *40*(8), 1824-1832.

Joseph, E. R., Jakir, H., Thangavel, B., Nor, A., Lim, T. L., & Mariathangam, P. R. (2024). Tool-Emitted Sound Signal Decomposition Using Wavelet and Empirical Mode Decomposition Techniques—A Comparison. *Symmetry*, *16*(9), 1223. https://doi.org/10.3390/sym16091223

Julien, Y., & Sobrino, J. (2009). Global land surface phenology trends from GIMMS database. *International Journal of Remote Sensing*, *30*(13), 3495-3513. https://doi.org/10.1080/01431160802562255

Jung, M., Reichstein, M., Ciais, P., Seneviratne, S. I., Sheffield, J., Goulden, M. L., Bonan, G., Cescatti, A., Chen, J., de Jeu, R., Dolman, A. J., Eugster, W., Gerten, D., Gianelle, D., Gobron, N., Heinke, J., Kimball, J., Law, B. E., Montagnani, L., Mu, Q., Mueller, B., Oleson, K., Papale, D., Richardson, A. D., Roupsard, O., Running, S., Tomelleri, E., Viovy, N., Weber, U., Williams, C., Wood, E., Zaehle, S., & Zhang, K. (2010). Recent decline in the global land evapotranspiration trend due to limited moisture supply. *Nature*, *467*(7318), 951-954. https://doi.org/10.1038/nature09396

Karkauskaite, P., Tagesson, T., & Fensholt, R. (2017). Evaluation of the Plant Phenology Index (PPI), NDVI and EVI for Start-of-Season Trend Analysis of the Northern Hemisphere Boreal Zone. *Remote Sensing*, *9*(5), 485. https://doi.org/10.3390/rs9050485

Karnieli, A., Ohana-Levi, N., Silver, M., Paz-Kagan, T., Panov, N., Varghese, D., Chrysoulakis, N., & Provenzale, A. (2019). Spatial and Seasonal Patterns in Vegetation Growth-Limiting Factors over Europe. *Remote Sensing*, *11*(20), 2406. https://doi.org/10.3390/rs11202406

Kashyap, R., & Kuttippurath, J. (2024). Warming-induced soil moisture stress threatens food security in India. *Environmental Science and Pollution Research*, *31*(49), 59202-59218. https://doi.org/10.1007/s11356-024-35107-7

Kendall, M. G. (1948). *Rank correlation methods.* Griffin.

Kern, A., Marjanović, H., & Barcza, Z. (2020). Spring vegetation green-up dynamics in Central Europe based on 20-year long MODIS NDVI data. *Agricultural and Forest Meteorology*, *287*, 107969. https://doi.org/10.1016/j.agrformet.2020.107969

Kerr, Y. H., Al-Yaari, A., Rodriguez-Fernandez, N., Parrens, M., Molero, B., Leroux, D., Bircher, S., Mahmoodi, A., Mialon, A., Richaume, P., Delwart, S., Al Bitar, A., Pellarin, T., Bindlish, R., Jackson, T. J., Rüdiger, C., Waldteufel, P., Mecklenburg, S., & Wigneron, J.-P. (2016). Overview of SMOS performance in terms of global soil moisture monitoring after six years in operation. *Special Issue: ESA's Soil Moisture and Ocean Salinity Mission - Achievements and Applications*, *180*, 40-63. https://doi.org/10.1016/j.rse.2016.02.042

Khoury, S., & Coomes, D. A. (2020). Resilience of Spanish forests to recent droughts and climate change. *Global Change Biology*, *26*(12), 7079-7098. https://doi.org/10.1111/gcb.15268

Kibret, K. S., Marohn, C., & Cadisch, G. (2020). Use of MODIS EVI to map crop phenology, identify cropping systems, detect land use change and drought risk in Ethiopia – an application of Google Earth Engine. *European Journal of Remote Sensing*, *53*(1), 176-191. https://doi.org/10.1080/22797254.2020.1786466

Kim, T. K. (2015). T test as a parametric statistic. *kja*, *68*(6), 540-546. https://doi.org/10.4097/kjae.2015.68.6.540

Kloos, S., Yuan, Y., Castelli, M., & Menzel, A. (2021). Agricultural Drought Detection with MODIS Based Vegetation Health Indices in Southeast Germany. *Remote Sensing*, *13*(19), 3907. https://doi.org/10.3390/rs13193907

Koenker, R. (2005). *Quantile regression* (Vol. 38). Cambridge university press.

Kosaka, Y., & Xie, S.-P. (2013). Recent global-warming hiatus tied to equatorial Pacific surface cooling. *Nature*, *501*(7467), 403-407. https://doi.org/10.1038/nature12534

Krishnamurthy, R. P. K., Fisher, J. B., Choularton, R. J., & Kareiva, P. M. (2022). Anticipating drought-related food security changes. *Nature Sustainability*, *5*(11), 956-964. https://doi.org/10.1038/s41893-022-00962-0

Krueger, E. S., Ochsner, T. E., & Quiring, S. M. (2019). Development and Evaluation of Soil Moisture-Based Indices for Agricultural Drought Monitoring. *Agronomy Journal*, *111*(3), 1392-1406. https://doi.org/10.2134/agronj2018.09.0558

Kumar, R., Nath, A. J., Nath, A., Sahu, N., & Pandey, R. (2022). Landsat-based multi-decadal spatio-temporal assessment of the vegetation greening and browning trend in the Eastern Indian Himalayan Region. *Remote Sensing Applications: Society and Environment*, *25*, 100695. https://doi.org/10.1016/j.rsase.2022.100695

Kundzewicz, Z. W. (2008). Climate change impacts on the hydrological cycle. *Ecohydrology & Hydrobiology*, *8*(2), 195-203. https://doi.org/10.2478/v10104-009-0015-y

Laaha, G., Gauster, T., Tallaksen, L. M., Vidal, J.-P., Stahl, K., Prudhomme, C., Heudorfer, B., Vlnas, R., Ionita, M., Van Lanen, H. A., & others. (2017). The European 2015 drought from a hydrological perspective. *Hydrology and Earth System Sciences*, *21*(6), 3001-3024. https://doi.org/10.5194/hess-21-3001-2017

Labędzki, L., & Bąk, B. (2014). Meteorological and agricultural drought indices used in drought monitoring in Poland: A review. *Meteorology Hydrology and Water Management. Research and Operational Applications*, *2*(2), 3-13.

Laguardia, G., & Niemeyer, S. (2008). On the comparison between the LISFLOOD modelled and the ERS/SCAT derived soil moisture estimates. *Hydrology and Earth System Sciences*, *12*(6), 1339-1351. https://doi.org/10.5194/hess-12-1339-2008

Lakhankar, T., Ghedira, H., Temimi, M., Sengupta, M., Khanbilvardi, R., & Blake, R. (2009). Non-parametric Methods for Soil Moisture Retrieval from Satellite Remote Sensing Data. *Remote Sensing*, *1*(1), 3-21. https://doi.org/10.3390/rs1010003

Laymon, C. A., Crosson, W. L., Jackson, T. J., Manu, A., & Tsegaye, T. D. (2001). Ground-based passive microwave remote sensing observations of soil moisture at S-band and L-band with insight into measurement accuracy. *IEEE Transactions on Geoscience and Remote Sensing*, *39*(9), 1844-1858. https://doi.org/10.1109/36.951075

Lawless, J. F. (2011). *Statistical models and methods for lifetime data*. John Wiley & Sons.

Lazoglou, G., Papadopoulos-Zachos, A., Georgiades, P., Zittis, G., Velikou, K., Manios, E. M., & Anagnostopoulou, C. (2024). Identification of climate change hotspots in the Mediterranean. *Scientific Reports*, *14*(1), 29817. https://doi.org/10.1038/s41598-024-80139-1

Lekshmi, S.U., Singh, D. N., & Shojaei Baghini, M. (2014). A critical review of soil moisture measurement. *Measurement*, *54*, 92-105. https://doi.org/10.1016/j.measurement.2014.04.007

Li, R., Tsunekawa, A., & Tsubo, M. (2017). Assessment of agricultural drought in rainfed cereal production areas of northern China. *Theoretical and Applied Climatology*, *127*(3), 597-609. https://doi.org/10.1007/s00704-015-1657-x

Li, X., & Qu, Y. (2018). Evaluation of Vegetation Responses to Climatic Factors and Global Vegetation Trends using GLASS LAI from 1982 to 2010. *Canadian Journal of Remote Sensing*, *44*(4), 357-372. https://doi.org/10.1080/07038992.2018.1526064

Li, M., Wu, P., & Ma, Z. (2020). A comprehensive evaluation of soil moisture and soil temperature from third-generation atmospheric and land reanalysis data sets. *International Journal of Climatology*, *40*(13), 5744-5766. https://doi.org/10.1002/joc.6549

Li, X., Guo, W., Li, S., Zhang, J., & Ni, X. (2021). The different impacts of the daytime and nighttime land surface temperatures on the alpine grassland phenology. *Ecosphere*, *12*(6), e03578. https://doi.org/10.1002/ecs2.3578

Li, Q., Cao, Y., Miao, S., & Huang, X. (2022). Spatiotemporal Characteristics of Drought and Wet Events and Their Impacts on Agriculture in the Yellow River Basin. *Land*, *11*(4), 556. https://doi.org/10.3390/land11040556

Li, P., Jia, L., Lu, J., Jiang, M., Zheng, C., & Menenti, M. (2024). Investigating the Response of Vegetation to Flash Droughts by Using Cross-Spectral Analysis and an Evapotranspiration-Based Drought Index. *Remote Sensing*, *16*(9), 1564. https://doi.org/10.3390/rs16091564

Li, Y., Zhuang, Q., Zhao, H., Zhang, W., Cai, P., Zhang, Y., & Lv, J. (2025). Evaluation of the resistance and resilience of terrestrial ecosystems to drought in southwest China. *Journal of Hydrology*, *646*, 132318. https://doi.org/10.1016/j.jhydrol.2024.132318

Liao, C., Wang, J., Shan, B., Shang, J., Dong, T., & He, Y. (2023). Near real-time detection and forecasting of within-field phenology of winter wheat and corn using Sentinel-2 time-series data. *ISPRS Journal of Photogrammetry and Remote Sensing*, *196*, 105-119. https://doi.org/10.1016/j.isprsjprs.2022.12.025

Lionello, P., Malanotte-Rizzoli, P., Boscolo, R., Alpert, P., Artale, V., Li, L., Luterbacher, J., May, W., Trigo, R., Tsimplis, M., Ulbrich, U., & Xoplaki, E. (2006). The Mediterranean climate: An overview of the main characteristics and issues. In P. Lionello, P. Malanotte-Rizzoli, & R. Boscolo (Eds.), *Developments in Earth and Environmental Sciences* (Vol. 4, pp. 1-26). Elsevier. https://doi.org/10.1016/S1571-9197(06)80003-0

Lionello, P., & Scarascia, L. (2018). The relation between climate change in the Mediterranean region and global warming. *Regional Environmental Change*, *18*(5), 1481-1493. https://doi.org/10.1007/s10113-018-1290-1

Lisonbee, J., Woloszyn, M., & Skumanich, M. (2022). Making sense of flash drought: definitions, indicators, and where we go from here. *Journal of Applied and Service Climatology, 2021*(1), 1–19. https://doi.org/10.46275/JOASC.2021.02.001

Liu, X., Zhu, X., Pan, Y., Li, S., Liu, Y., & Ma, Y. (2016). Agricultural drought monitoring: Progress, challenges, and prospects. *Journal of Geographical Sciences*, *26*(6), 750-767. https://doi.org/10.1007/s11442-016-1297-9

Liu, Y., Zhu, Y., Ren, L., Otkin, J., Hunt, E. D., Yang, X., Yuan, F., & Jiang, S. (2020a). Two Different Methods for Flash Drought Identification: Comparison of Their Strengths and Limitations. *Journal of Hydrometeorology*, *21*(4), 691-704. https://doi.org/10.1175/JHM-D-19-0088.1

Liu, Y., Zhu, Y., Zhang, L., Ren, L., Yuan, F., Yang, X., & Jiang, S. (2020b). Flash droughts characterization over China: From a perspective of the rapid intensification rate. *Science of The Total Environment*, *704*, 135373. https://doi.org/10.1016/j.scitotenv.2019.135373

Liu, Y., Shen, X., Zhang, J., Wang, Y., Wu, L., Ma, R., Lu, X., & Jiang, M. (2023). Variation in Vegetation Phenology and Its Response to Climate Change in Marshes of Inner Mongolian. *Plants*, *12*(11), 2072. https://doi.org/10.3390/plants12112072

Llorens, P., & Domingo, F. (2007). Rainfall partitioning by vegetation under Mediterranean conditions. A review of studies in Europe. *Journal of Hydrology*, *335*(1), 37-54. https://doi.org/10.1016/j.jhydrol.2006.10.032

López-Bermúdez, F. (1993). Reflexiones sobre la degradación de los suelos y su gestión sostenible en la cuenca mediterránea. *Paralelo, 37*, *16*, 211-217.

López-Bermúdez, F., Romero-Díaz, A., Martínez-Fernandez, J., & Martínez-Fernandez, J. (1998). Vegetation and soil erosion under a semi-arid Mediterranean climate: A case study from Murcia (Spain). *Geomorphology*, *24*(1), 51-58. https://doi.org/10.1016/S0169-555X(97)00100-1

López-Castañeda, C., & Richards, R. A. (1994). Variation in temperate cereals in rainfed environments I. Grain yield, biomass and agronomic characteristics. *Field Crops Research*, *37*(1), 51-62. https://doi.org/10.1016/0378-4290(94)90081-7

Lorenzo, M. N., Alvarez, I., & Taboada, J. J. (2022). Drought evolution in the NW Iberian Peninsula over a 60 year period (1960–2020). *Journal of Hydrology*, *610*, 127923. https://doi.org/10.1016/j.jhydrol.2022.127923

Lovino, M. A., Pierrestegui, M. J., Müller, O. V., Müller, G. V., & Berbery, E. H. (2024). The prevalent life cycle of agricultural flash droughts. *npj Climate and Atmospheric Science*, *7*(1), 73. https://doi.org/10.1038/s41612-024-00618-0

Lu, J., Carbone, G. J., & Grego, J. M. (2019). Uncertainty and hotspots in 21st century projections of agricultural drought from CMIP5 models. *Scientific reports*, *9*(1), 4922. https://doi.org/10.1038/s41598-019-41196-z

Lüttge, U., & Scarano, F. R. (2004). Ecophysiology. *Brazilian Journal of Botany*, *27*, 1-10. https://doi.org/10.1590/S0100-84042004000100001

Magney, T. S., Eitel, J. U. H., Huggins, D. R., & Vierling, L. A. (2016). Proximal NDVI derived phenology improves in-season predictions of wheat quantity and quality. *Agricultural and Forest Meteorology*, *217*, 46-60. https://doi.org/10.1016/j.agrformet.2015.11.009

Malhi, G. S., Kaur, M., & Kaushik, P. (2021). Impact of Climate Change on Agriculture and Its Mitigation Strategies: A Review. *Sustainability*, *13*(3), 1318. https://doi.org/10.3390/su13031318

Manfron, G., Delmotte, S., Busetto, L., Hossard, L., Ranghetti, L., Brivio, P. A., & Boschetti, M. (2017). Estimating inter-annual variability in winter wheat sowing dates from satellite time series in Camargue, France. *International journal of applied earth observation and geoinformation*, *57*, 190-201. https://doi.org/10.1016/j.jag.2017.01.001

Mann, H. B. (1945). Nonparametric tests against trend. *Econometrica, 13*(3), 245–259. https://doi.org/10.2307/1907187

MAPA (Ministerio de Agricultura Pesca y Alimentación). (2025a). Anuario de Estadística. https://www.mapa.gob.es/es/estadistica/temas/publicaciones/anuario-de-estadistica/default.aspx

MAPA (Ministerio de Agricultura Pesca y Alimentación). (2025b). Calendario de Siembra, Recolección y Comercialización. https://www.mapa.gob.es/es/estadistica/temas/estadisticas-agrarias/agricultura/calendarios-siembras-recoleccion/

Markonis, Y., Kumar, R., Hanel, M., Rakovec, O., Máca, P., & AghaKouchak, A. (2021). The rise of compound warm-season droughts in Europe. *Science Advances*, *7*(6), eabb9668. https://doi.org/10.1126/sciadv.abb9668

Marshall, M., Tu, K., & Brown, J. (2018). Optimizing a remote sensing production efficiency model for macro-scale GPP and yield estimation in agroecosystems. *Remote Sensing of Environment*, *217*, 258-271. https://doi.org/10.1016/j.rse.2018.08.001

Martínez-Fernández, J., & Ceballos, A. (2003). Temporal Stability of Soil Moisture in a Large-Field Experiment in Spain. *Soil Science Society of America Journal*, *67*(6), 1647-1656. https://doi.org/10.2136/sssaj2003.1647

Martínez-Fernández, J., González-Zamora, A., Sánchez, N., & Gumuzzio, A. (2015). A soil water based index as a suitable agricultural drought indicator. *Journal of Hydrology*, *522*, 265-273. https://doi.org/10.1016/j.jhydrol.2014.12.051

Martínez-Fernández, J., González-Zamora, A., Sánchez, N., Gumuzzio, A., & Herrero-Jiménez, C. M. (2016). Satellite soil moisture for agricultural drought monitoring: Assessment of the SMOS derived Soil Water Deficit Index. *Remote Sensing of Environment*, *177*, 277-286. https://doi.org/10.1016/j.rse.2016.02.064

Martínez-Fernández, J., Almendra-Martín, L., de Luis, M., González-Zamora, A., & Herrero-Jiménez, C. (2019). Tracking tree growth through satellite soil moisture monitoring: A case study of Pinus halepensis in Spain. *Remote Sensing of Environment*, *235*, 111422. https://doi.org/10.1016/j.rse.2019.111422

Martínez-Fernández, J., González-Zamora, A., & Almendra-Martín, L. (2021). Soil moisture memory and soil properties: An analysis with the stored precipitation fraction. *Journal of Hydrology*, *593*, 125622. https://doi.org/10.1016/j.jhydrol.2020.125622

Martínez-Fernández, J., Molina-Navarro, E., González-Zamora, Á., Sánchez-Gómez, A., & Almendra-Martín, L. (2023). SWAT soil moisture assessment under Mediterranean conditions: An intercomparison analysis in the Henares basin (Spain). *Journal of Hydrology: Regional Studies*, *48*, 101460. https://doi.org/10.1016/j.ejrh.2023.101460

McEvoy, D. J., Huntington, J. L., Hobbins, M. T., Wood, A., Morton, C., Anderson, M., & Hain, C. (2016). The Evaporative Demand Drought Index. Part II: CONUS-Wide Assessment against Common Drought Indicators. *Journal of Hydrometeorology*, *17*(6), 1763-1779. https://doi.org/10.1175/JHM-D-15-0122.1

McKee, T. B., Doesken, N. J., Kleist, J., & others. (1993). The relationship of drought frequency and duration to time scales. *Proceedings of the 8th Conference on Applied Climatology*, *17*(22), 179-183.

McMaster, G. S., & Wilhelm, W. W. (2003). Phenological responses of wheat and barley to water and temperature: Improving simulation models. *The Journal of Agricultural Science*, *141*(2), 129-147. https://doi.org/10.1017/S0021859603003460

McNally, A., Shukla, S., Arsenault, K. R., Wang, S., Peters-Lidard, C. D., & Verdin, J. P. (2016). Evaluating ESA CCI soil moisture in East Africa. *Advances in the Validation and Application of Remotely Sensed Soil Moisture - Part 2*, *48*, 96-109. https://doi.org/10.1016/j.jag.2016.01.001

Measho, S., Li, F., Chen, G., & Hirwa, H. (2023). Characterizing Cropland Patterns Across North-East Africa Using Time Series Vegetation Indices. *Journal of Geophysical Research: Biogeosciences*, *128*(3), e2022JG007075. https://doi.org/10.1029/2022JG007075

Medhaug, I., Stolpe, M. B., Fischer, E. M., & Knutti, R. (2017). Reconciling controversies about the 'global warming hiatus'. *Nature*, *545*(7652), 41-47. https://doi.org/10.1038/nature22315

Mefleh, M. (2021). Cereals of the Mediterranean Region: Their Origin, Breeding History and Grain Quality Traits. In F. Boukid (Ed.), *Cereal-Based Foodstuffs: The Backbone of Mediterranean Cuisine* (pp. 1-18). Springer International Publishing. https://doi.org/10.1007/978-3-030-69228-5_1

Meng, L., Zhou, Y., Gu, L., Richardson, A. D., Peñuelas, J., Fu, Y., Wang, Y., Asrar, G. R., De Boeck, H. J., Mao, J., & others. (2021). Photoperiod decelerates the advance of spring phenology of six deciduous tree species under climate warming. *Global Change Biology*, *27*(12), 2914-2927. https://doi.org/10.1111/gcb.15575

Menzel, A., Sparks, T. H., Estrella, N., Koch, E., Aasa, A., Ahas, R., Alm-Kübler, K., Bissolli, P., Braslavská, O., Briede, A., Chmielewski, F. M., Crepinsek, Z., Curnel, Y., Dahl, Å., Defila, C., Donnelly, A., Filella, Y., Jatczak, K., Måge, F., Mestre, A., Nordli, Ø., Peñuelas, J., Pirinen, P., Remišová, V., Scheifinger, H., Striz, M., Susnik, A., van Vliet, A. J. H., Wielgolaski, F.-E., Zach, S., & Zust, A. (2006). European phenological response to climate change matches the warming pattern. *Global Change Biology*, *12*(10), 1969-1976. https://doi.org/10.1111/j.1365-2486.2006.01193.x

Menzel, A., Yuan, Y., Matiu, M., Sparks, T., Scheifinger, H., Gehrig, R., & Estrella, N. (2020). Climate change fingerprints in recent European plant phenology. *Global Change Biology*, *26*(4), 2599-2612. https://doi.org/10.1111/gcb.15000

Meroni, M., Verstraete, M. M., Rembold, F., Urbano, F., & Kayitakire, F. (2014). A phenology-based method to derive biomass production anomalies for food security monitoring in the Horn of Africa. *International Journal of Remote Sensing*, *35*(7), 2472-2492. https://doi.org/10.1080/01431161.2014.883090

Meyer, N., Bergez, J.-E., Constantin, J., Belleville, P., & Justes, E. (2020). Cover crops reduce drainage but not always soil water content due to interactions between rainfall distribution and management. *Agricultural Water Management*, *231*, 105998. https://doi.org/10.1016/j.agwat.2019.105998

Mishra, A. K., & Singh, V. P. (2010). A review of drought concepts. *Journal of Hydrology*, *391*(1), 202-216. https://doi.org/10.1016/j.jhydrol.2010.07.012

Mishra, A., Vu, T., Veettil, A. V., & Entekhabi, D. (2017). Drought monitoring with soil moisture active passive (SMAP) measurements. *Journal of Hydrology*, *552*, 620-632. https://doi.org/10.1016/j.jhydrol.2017.07.033

Mishra, N. B., & Mainali, K. P. (2017). Greening and browning of the Himalaya: Spatial patterns and the role of climatic change and human drivers. *Science of The Total Environment*, *587-588*, 326-339. https://doi.org/10.1016/j.scitotenv.2017.02.156

Mladenova, I. E., Jackson, T. J., Njoku, E., Bindlish, R., Chan, S., Cosh, M. H., Holmes, T. R. H., de Jeu, R. A. M., Jones, L., Kimball, J., Paloscia, S., & Santi, E. (2014). Remote monitoring of soil moisture using passive microwave-based techniques—Theoretical basis and overview of selected algorithms for AMSR-E. *Remote Sensing of Environment*, *144*, 197-213. https://doi.org/10.1016/j.rse.2014.01.013

Mohammed, S., Alsafadi, K., Enaruvbe, G. O., Bashir, B., Elbeltagi, A., Széles, A., Alsalman, A., & Harsanyi, E. (2022). Assessing the impacts of agricultural drought (SPI/SPEI) on maize and wheat yields across Hungary. *Scientific Reports*, *12*(1), 8838. https://doi.org/10.1038/s41598-022-12799-w

Mohanty, B. P., Cosh, M. H., Lakshmi, V., & Montzka, C. (2017). Soil Moisture Remote Sensing: State-of-the-Science. *Vadose Zone Journal*, *16*(1), vzj2016.10.0105. https://doi.org/10.2136/vzj2016.10.0105

Moojen, F. G., Ryschawy, J., Wulfhorst, J. D., Archer, D. W., de Faccio Carvalho, P. C., & Hendrickson, J. R. (2024). Case study analysis of innovative producers toward sustainable integrated crop-livestock systems: Trajectory, achievements, and thought process. *Agronomy for Sustainable Development*, *44*(3), 26. https://doi.org/10.1007/s13593-024-00953-9

Morais, T. G., Silva, C., Jebari, A., Álvaro-Fuentes, J., Domingos, T., & Teixeira, R. F. (2018). A proposal for using process-based soil models for land use Life cycle impact assessment: Application to Alentejo, Portugal. *Journal of cleaner production*, *192*, 864-876. https://doi.org/10.1016/j.jclepro.2018.05.061

Moreno, M., Bertolín, C., Ortiz, P., & Ortiz, R. (2022). Satellite product to map drought and extreme precipitation trend in Andalusia, Spain: A novel method to assess heritage landscapes at risk. *International Journal of Applied Earth Observation and Geoinformation*, *110*, 102810. https://doi.org/10.1016/j.jag.2022.102810

Moriondo, M., Bindi, M., Brilli, L., Costafreda-Aumedes, S., Dibari, C., Leolini, L., Padovan, G., Trombi, G., Karali, A., Varotsos, K. V., Lemesios, G., Giannakopoulos, C., Papadaskalopoulou, C., & Merante, P. (2021). Assessing climate change impacts on crops by adopting a set of crop performance indicators. *Euro-Mediterranean Journal for Environmental Integration*, *6*(2), 45. https://doi.org/10.1007/s41207-021-00246-7

Mukherjee, S., & Mishra, A. K. (2022). Global Flash Drought Analysis: Uncertainties From Indicators and Datasets. *Earth's Future*, *10*(6), e2022EF002660. https://doi.org/10.1029/2022EF002660

Mullapudi, A., Vibhute, A. D., Mali, S., & Patil, C. H. (2023). A review of agricultural drought assessment with remote sensing data: Methods, issues, challenges and

opportunities. *Applied Geomatics*, *15*(1), 1-13. https://doi.org/10.1007/s12518-022-00484-6

Muñoz-Sabater, J., Dutra, E., Agustí-Panareda, A., Albergel, C., Arduini, G., Balsamo, G., Boussetta, S., Choulga, M., Harrigan, S., Hersbach, H., Martens, B., Miralles, D. G., Piles, M., Rodríguez-Fernández, N. J., Zsoter, E., Buontempo, C., & Thépaut, J.-N. (2021). ERA5-Land: A state-of-the-art global reanalysis dataset for land applications. *Earth System Science Data*, *13*(9), 4349-4383. https://doi.org/10.5194/essd-13-4349-2021

Myneni, R., Knyazikhin, Y., & Park, T. (2023). *MOD15A2H MODIS/Terra Leaf Area Index/FPAR 8-Day L4 Global 500 m SIN Grid V006* [Data Set]. NASA EOSDIS Land Processes DAAC. https://lpdaac.usgs.gov/products/mcd15a2hv061/

Narasimhan, B., & Srinivasan, R. (2005). Development and evaluation of Soil Moisture Deficit Index (SMDI) and Evapotranspiration Deficit Index (ETDI) for agricultural drought monitoring. *Agricultural and Forest Meteorology*, *133*(1), 69-88. https://doi.org/10.1016/j.agrformet.2005.07.012

Nath, R., Nath, D., Li, Q., Chen, W., & Cui, X. (2017). Impact of drought on agriculture in the Indo-Gangetic Plain, India. *Advances in Atmospheric Sciences*, *34*(3), 335-346. https://doi.org/10.1007/s00376-016-6102-2

Naumann, G., Cammalleri, C., Mentaschi, L., & Feyen, L. (2021). Increased economic drought impacts in Europe with anthropogenic warming. *Nature Climate Change*, *11*(6), 485-491. https://doi.org/10.1038/s41558-021-01044-3

Nazari, A., Jamshidi, M., Roozbahani, A., & Golparvar, B. (2025). Groundwater level forecasting using empirical mode decomposition and wavelet-based long short-term memory (LSTM) neural networks. *Groundwater for Sustainable Development*, *28*, 101397. https://doi.org/10.1016/j.gsd.2024.101397

Ndayiragije, J. M., & Li, F. (2022). Effectiveness of Drought Indices in the Assessment of Different Types of Droughts, Managing and Mitigating Their Effects. *Climate*, *10*(9), 125. https://doi.org/10.3390/cli10090125

Nemani, R. R., Keeling, C. D., Hashimoto, H., Jolly, W. M., Piper, S. C., Tucker, C. J., Myneni, R. B., & Running, S. W. (2003). Climate-Driven Increases in Global Terrestrial Net Primary Production from 1982 to 1999. *Science*, *300*(5625), 1560-1563. https://doi.org/10.1126/science.1082750

Nicolai-Shaw, N., Zscheischler, J., Hirschi, M., Gudmundsson, L., & Seneviratne, S. I. (2017). A drought event composite analysis using satellite remote-sensing based soil moisture. *Earth Observation of Essential Climate Variables*, *203*, 216-225. https://doi.org/10.1016/j.rse.2017.06.014

Njoku, E. G., & Entekhabi, D. (1996). Passive microwave remote sensing of soil moisture. *Soil Moisture Theories and Observations*, *184*(1), 101-129. https://doi.org/10.1016/0022-1694(95)02970-2

Noguera, I., Domínguez-Castro, F., & Vicente-Serrano, S. M. (2020). Characteristics and trends of flash droughts in Spain, 1961–2018. *Annals of the New York Academy of Sciences*, *1472*(1), 155-172. https://doi.org/10.1111/nyas.14365

Noguera, I., Domínguez-Castro, F., Vicente-Serrano, S. M., & Reig, F. (2023). Near-real time flash drought monitoring system and dataset for Spain. *Data in Brief*, *47*, 108908. https://doi.org/10.1016/j.dib.2023.108908

Norgard, J., & Best, G. L. (2017). The electromagnetic spectrum. In *National Association of Broadcasters Engineering Handbook* (pp. 3-10). Routledge.

O, S., & Park, S. K. (2023). Flash drought drives rapid vegetation stress in arid regions in Europe. *Environmental Research Letters*, *18*(1), 014028. https://doi.org/10.1088/1748-9326/acae3a

O, S., & Park, S. K. (2024). Global ecosystem responses to flash droughts are modulated by background climate and vegetation conditions. *Communications Earth & Environment*, *5*(1), 88. https://doi.org/10.1038/s43247-024-01247-4

Obladen, N., Dechering, P., Skiadaresis, G., Tegel, W., Keßler, J., Höllerl, S., Kaps, S., Hertel, M., Dulamsuren, C., Seifert, T., Hirsch, M., & Seim, A. (2021). Tree mortality of European beech and Norway spruce induced by 2018-2019 hot droughts in central Germany. *Agricultural and Forest Meteorology*, *307*, 108482. https://doi.org/10.1016/j.agrformet.2021.108482

Oikonomou, P. D., Karavitis, C. A., Tsesmelis, D. E., Kolokytha, E., & Maia, R. (2020). Drought Characteristics Assessment in Europe over the Past 50 Years. *Water Resources Management*, *34*(15), 4757-4772. https://doi.org/10.1007/s11269-020-02688-0

Oki, T., & Kanae, S. (2006). Global Hydrological Cycles and World Water Resources. *Science*, *313*(5790), 1068-1072. https://doi.org/10.1126/science.1128845

Olesen, J. E., Carter, T. R., Diaz-Ambrona, C., Fronzek, S., Heidmann, T., Hickler, T., Holt, T., Minguez, M. I., Morales, P., Palutikof, J. P., & others. (2007). Uncertainties in projected impacts of climate change on European agriculture and terrestrial ecosystems based on scenarios from regional climate models. *Climatic Change*, *81*, 123-143. https://doi.org/10.1007/s10584-006-9216-1

Orimoloye, I. R. (2022). Agricultural Drought and Its Potential Impacts: Enabling Decision-Support for Food Security in Vulnerable Regions. *Frontiers in Sustainable Food Systems*, *6*(2022), 838824. https://doi.org/10.3389/fsufs.2022.838824

Orth, R., & Destouni, G. (2018). Drought reduces blue-water fluxes more strongly than green-water fluxes in Europe. *Nature communications*, *9*(1), 3602. https://doi.org/10.1038/s41467-018-06013-7

Osman, M., Zaitchik, B., Otkin, J., & Anderson, M. (2024). A global flash drought inventory based on soil moisture volatility. *Scientific Data*, *11*(1), 965. https://doi.org/10.1038/s41597-024-03809-9

Otkin, J. A., Anderson, M. C., Hain, C., & Svoboda, M. (2014). Examining the Relationship between Drought Development and Rapid Changes in the Evaporative Stress Index. *Journal of Hydrometeorology*, *15*(3), 938-956. https://doi.org/10.1175/JHM-D-13-0110.1

Otkin, J. A., Anderson, M. C., Hain, C., Svoboda, M., Johnson, D., Mueller, R., Tadesse, T., Wardlow, B., & Brown, J. (2016). Assessing the evolution of soil moisture and vegetation conditions during the 2012 United States flash drought. *Agricultural and Forest Meteorology*, *218-219*, 230-242. https://doi.org/10.1016/j.agrformet.2015.12.065

Otkin, J. A., Svoboda, M., Hunt, E. D., Ford, T. W., Anderson, M. C., Hain, C., Basara, J. B., Otkin, J. A., Svoboda, M., Hunt, E. D., Ford, T. W., Anderson, M. C., Hain, C., & Basara, J. B. (2018a). Flash Droughts: A Review and Assessment of the Challenges Imposed by Rapid-Onset Droughts in the United States. *Bulletin of the American Meteorological Society*, *99*(5), 911-919. https://doi.org/10.1175/BAMS-D-17-0149.1

Otkin, J. A., Haigh, T., Mucia, A., Anderson, M. C., & Hain, C. (2018b). Comparison of Agricultural Stakeholder Survey Results and Drought Monitoring Datasets during the 2016 U.S. Northern Plains Flash Drought. *Weather, Climate, and Society*, *10*(4), 867-883. https://doi.org/10.1175/WCAS-D-18-0051.1

Otkin, J. A., Zhong, Y., Hunt, E. D., Christian, J. I., Basara, J. B., Nguyen, H., Wheeler, M. C., Ford, T. W., Hoell, A., Svoboda, M., & Anderson, M. C. (2021). Development of a Flash Drought Intensity Index. *Atmosphere*, *12*(6), 741. https://doi.org/10.3390/atmos12060741

Otkin, J. A., Woloszyn, M., Wang, H., Svoboda, M., Skumanich, M., Pulwarty, R., Lisonbee, J., Hoell, A., Hobbins, M., Haigh, T., & Cravens, A. E. (2022). Getting ahead of Flash Drought: From Early Warning to Early Action. *Bulletin of the American Meteorological Society*, *103*(10), E2188-E2202. https://doi.org/10.1175/BAMS-D-21-0288.1

Oweis, T., Zhang, H., & Pala, M. (2000). Water Use Efficiency of Rainfed and Irrigated Bread Wheat in a Mediterranean Environment. *Agronomy Journal*, *92*(2), 231-238. https://doi.org/10.2134/agronj2000.922231x

Palmer, W. C. (1965). *Meteorological drought* (Research Paper 45). U.S. Department of Commerce, Weather Bureau.

Palmer, W. C. (1968). Keeping Track of Crop Moisture Conditions, Nationwide: The New Crop Moisture Index. *Weatherwise*, *21*(4), 156-161. https://doi.org/10.1080/00431672.1968.9932814

Pan, Z., Huang, J., Zhou, Q., Wang, L., Cheng, Y., Zhang, H., Blackburn, G. A., Yan, J., & Liu, J. (2015). Mapping crop phenology using NDVI time-series derived from HJ-1 A/B data. *International Journal of Applied Earth Observation and Geoinformation*, *34*, 188-197. https://doi.org/10.1016/j.jag.2014.08.011

Pan, Y., Zhu, Y., Lü, H., Yagci, A. L., Fu, X., Liu, E., Xu, H., Ding, Z., & Liu, R. (2023). Accuracy of agricultural drought indices and analysis of agricultural drought characteristics in China between 2000 and 2019. *Agricultural Water Management*, *283*, 108305. https://doi.org/10.1016/j.agwat.2023.108305

Panek, E., & Gozdowski, D. (2020). Analysis of relationship between cereal yield and NDVI for selected regions of Central Europe based on MODIS satellite data. *Remote Sensing Applications: Society and Environment*, *17*, 100286. https://doi.org/10.1016/j.rsase.2019.100286

Panu, U. S., & Sharma, T. C. (2002). Challenges in drought research: Some perspectives and future directions. *Hydrological Sciences Journal*, *47*(sup1), S19-S30. https://doi.org/10.1080/02626660209493019

Páscoa, P., Gouveia, C. M., Russo, A., & Trigo, R. M. (2017). The role of drought on wheat yield interannual variability in the Iberian Peninsula from 1929 to 2012. *International Journal of Biometeorology*, *61*(3), 439-451. https://doi.org/10.1007/s00484-016-1224-x

Páscoa, P., Russo, A., Gouveia, C. M., Soares, P. M. M., Cardoso, R. M., Careto, J. A. M., & Ribeiro, A. F. S. (2021). A high-resolution view of the recent drought trends over the Iberian Peninsula. *Weather and Climate Extremes*, *32*, 100320. https://doi.org/10.1016/j.wace.2021.100320

Passarella, V. S., Savin, R., & Slafer, G. A. (2002). Grain weight and malting quality in barley as affected by brief periods of increased spike temperature under field conditions. *Australian Journal of Agricultural Research*, *53*(11), 1219-1227. https://doi.org/10.1071/AR02096

Passarella, V. S., Savin, R., & Slafer, G. A. (2005). Breeding effects on sensitivity of barley grain weight and quality to events of high temperature during grain filling. *Euphytica*, *141*(1), 41-48. https://doi.org/10.1007/s10681-005-5068-4

Peña-Gallardo, M., Vicente-Serrano, S. M., Domínguez-Castro, F., & Beguería, S. (2019). The impact of drought on the productivity of two rainfed crops in Spain. *Natural Hazards and Earth System Sciences*, *19*(6), 1215-1234. https://doi.org/10.5194/nhess-19-1215-2019

Peñuelas, J., Filella, I., & Comas, P. (2002). Changed plant and animal life cycles from 1952 to 2000 in the Mediterranean region. *Global Change Biology*, *8*(6), 531-544. https://doi.org/10.1046/j.1365-2486.2002.00489.x

Peters, A. J., Walter-Shea, E. A., Ji, L., Vina, A., Hayes, M., & Svoboda, M. D. (2002). Drought monitoring with NDVI-based standardized vegetation index. *Photogrammetric engineering and remote sensing*, *68*(1), 71-75.

Piao, S., Fang, J., Zhou, L., Ciais, P., & Zhu, B. (2006). Variations in satellite-derived phenology in China's temperate vegetation. *Global change biology*, *12*(4), 672-685. https://doi.org/10.1111/j.1365-2486.2006.01123.x

Piao, S., Yin, G., Tan, J., Cheng, L., Huang, M., Li, Y., Liu, R., Mao, J., Myneni, R. B., Peng, S., Poulter, B., Shi, X., Xiao, Z., Zeng, N., Zeng, Z., & Wang, Y. (2015). Detection and attribution of vegetation greening trend in China over the last 30 years. *Global Change Biology*, *21*(4), 1601-1609. https://doi.org/10.1111/gcb.12795

Piao, S., Liu, Q., Chen, A., Janssens, I. A., Fu, Y., Dai, J., Liu, L., Lian, X., Shen, M., & Zhu, X. (2019). Plant phenology and global climate change: Current progresses and challenges. *Global Change Biology*, *25*(6), 1922-1940. https://doi.org/10.1111/gcb.14619

Pinzon, J.E., Pak, E.W., Tucker, C.J., Bhatt, U.S., Frost, G.V., & Macander M.J. (2023). *Global Vegetation Greenness (NDVI) from AVHRR GIMMS-3G+, 1981–2022* [Data set]. ORNL DAAC. https://doi.org/10.3334/ORNLDAAC/2187

Poggi, G. M., Aloisi, I., Corneti, S., Esposito, E., Naldi, M., Fiori, J., Piana, S., & Ventura, F. (2022). Climate change effects on bread wheat phenology and grain quality: A case study in the north of Italy. *Frontiers in Plant Science*, *13*, *936991*. https://doi.org/10.3389/fpls.2022.936991

Potopová, V., Boroneanţ, C., Boincean, B., & Soukup, J. (2016). Impact of agricultural drought on main crop yields in the Republic of Moldova. *International Journal of Climatology*, *36*(4), 2063-2082. https://doi.org/10.1002/joc.4481

Poutanen, K. S., Kårlund, A. O., Gómez-Gallego, C., Johansson, D. P., Scheers, N. M., Marklinder, I. M., Eriksen, A. K., Silventoinen, P. C., Nordlund, E., Sozer, N., Hanhineva, K. J., Kolehmainen, M., & Landberg, R. (2022). Grains – a major source of sustainable protein for health. *Nutrition Reviews*, *80*(6), 1648-1663. https://doi.org/10.1093/nutrit/nuab084

Pulighe, G., Lupia, F., Chen, H., & Yin, H. (2021). Modeling Climate Change Impacts on Water Balance of a Mediterranean Watershed Using SWAT+. *Hydrology*, *8*(4), 157. https://doi.org/10.3390/hydrology8040157

Purcell, L. C., Sinclair, T. R., & McNew, R. W. (2003). Drought Avoidance Assessment for Summer Annual Crops Using Long-Term Weather Data. *Agronomy Journal*, *95*(6), 1566-1576. https://doi.org/10.2134/agronj2003.1566

Qin, Q., Xu, D., Hou, L., Shen, B., & Xin, X. (2021). Comparing vegetation indices from Sentinel-2 and Landsat 8 under different vegetation gradients based on a controlled grazing experiment. *Ecological Indicators*, *133*, 108363. https://doi.org/10.1016/j.ecolind.2021.108363

Qing, Y., Wang, S., Ancell, B. C., & Yang, Z.-L. (2022). Accelerating flash droughts induced by the joint influence of soil moisture depletion and atmospheric aridity. *Nature Communications*, *13*(1), 1139. https://doi.org/10.1038/s41467-022-28752-4

Qiu, R., Han, G., Li, S., Tian, F., Ma, X., & Gong, W. (2023). Soil moisture dominates the variation of gross primary productivity during hot drought in drylands. *Science of The Total Environment*, *899*, 165686. https://doi.org/10.1016/j.scitotenv.2023.165686

Quiring, S. M., & Papakryiakou, T. N. (2003). An evaluation of agricultural drought indices for the Canadian prairies. *Agricultural and Forest Meteorology*, *118*(1), 49-62. https://doi.org/10.1016/S0168-1923(03)00072-8

Rahman, M. M., & Zhang, W. (2019). Review on estimation methods of the Earth's surface energy balance components from ground and satellite measurements. *Journal of Earth System Science*, *128*(4), 84. https://doi.org/10.1007/s12040-019-1098-5

Rao, C. S., & Gopinath, K. A. (2016). Resilient rainfed technologies for drought mitigation and sustainable food security. *MAUSAM*, *67*(1), 169-182. https://doi.org/10.54302/mausam.v67i1.1174

Rehana, S., & Monish, N. T. (2020). Characterization of Regional Drought Over Water and Energy Limited Zones of India Using Potential and Actual Evapotranspiration. *Earth and Space Science*, *7*(10), e2020EA001264. https://doi.org/10.1029/2020EA001264

Reichle, R. H., Koster, R. D., De Lannoy, G. J. M., Forman, B. A., Liu, Q., Mahanama, S. P. P., & Touré, A. (2011). Assessment and Enhancement of MERRA Land Surface Hydrology Estimates. *Journal of Climate*, *24*(24), 6322-6338. https://doi.org/10.1175/JCLI-D-10-05033.1

Reidsma, P., Ewert, F., Boogaard, H., & Diepen, K. van. (2009). Regional crop modelling in Europe: The impact of climatic conditions and farm characteristics on maize yields. *Agricultural Systems*, *100*(1), 51-60. https://doi.org/10.1016/j.agsy.2008.12.009

Ren, S., & An, S. (2021). Temporal Pattern Analysis of Cropland Phenology in Shandong Province of China Based on Two Long-Sequence Remote Sensing Data. *Remote Sensing*, *13*(20). https://doi.org/10.3390/rs13204071

Rey, D., Holman, I. P., & Knox, J. W. (2017). Developing drought resilience in irrigated agriculture in the face of increasing water scarcity. *Regional Environmental Change*, *17*(5), 1527-1540. https://doi.org/10.1007/s10113-017-1116-6

Rezzouk, F. Z., Gracia-Romero, A., Kefauver, S. C., Nieto-Taladriz, M. T., Serret, M. D., & Araus, J. L. (2022). Durum wheat ideotypes in Mediterranean environments differing in water and temperature conditions. *Agricultural Water Management*, *259*, 107257. https://doi.org/10.1016/j.agwat.2021.107257

Rocha, A. V., & Shaver, G. R. (2009). Advantages of a two band EVI calculated from solar and photosynthetically active radiation fluxes. *Agricultural and Forest Meteorology*, *149*(9), 1560-1563. https://doi.org/10.1016/j.agrformet.2009.03.016

Rosero, E., Yang, Z.-L., Gulden, L. E., Niu, G.-Y., & Gochis, D. J. (2009). Evaluating Enhanced Hydrological Representations in Noah LSM over Transition Zones: Implications for Model Development. *Journal of Hydrometeorology*, *10*(3), 600-622. https://doi.org/10.1175/2009JHM1029.1

Rossato, L., Alvalá, R. C. dos S., Marengo, J. A., Zeri, M., Cunha, A. P. M. do A., Pires, L. B. M., & Barbosa, H. A. (2017). Impact of Soil Moisture on Crop Yields over Brazilian Semiarid. *Frontiers in Environmental Science*, *5*. https://doi.org/10.3389/fenvs.2017.00073

Rouse Jr, J. W., Haas, R. H., Deering, D., Schell, J., & Harlan, J. C. (1974). *Monitoring the vernal advancement and retrogradation (green wave effect) of natural vegetation* (NASA/GSFC Type III Final Report). Goddard Space Flight Center.

Running, S., Mu, Q., & Zhao, M. (2015a). *MOD17A2H MODIS/Terra Gross Primary Productivity 8-Day L4 Global 500m SIN Grid V006* [Data Set]. NASA EOSDIS Land Processes DAAC. https://lpdaac.usgs.gov/products/mod17a2hv061/

Running, S., Mu, Q., & Zhao, M. (2015b). *MYD17A2H MODIS/Aqua Gross Primary Productivity 8-Day L4 Global 500m SIN Grid V006* [Data Set]. NASA EOSDIS Land Processes DAAC. https://lpdaac.usgs.gov/products/myd17a2hv061/

Running, S., & Zhao, M. (2021a). *MODIS/Terra gross primary productivity gap-filled 8-day L4 global 500m SIN grid V061* [Data set]. NASA EOSDIS Land Processes Distributed Active Archive Center. https://doi.org/10.5067/MODIS/MOD17A2HGF.061

Running, S., & Zhao, M. (2021b). *MODIS/Aqua gross primary productivity gap-filled 8-day L4 global 500m SIN grid V061* [Data set]. NASA EOSDIS Land Processes

Distributed Active Archive Center. https://doi.org/10.5067/MODIS/MYD17A2HGF.061

Ruosteenoja, K., Markkanen, T., Venäläinen, A., Räisänen, P., & Peltola, H. (2018). Seasonal soil moisture and drought occurrence in Europe in CMIP5 projections for the 21st century. *Climate Dynamics*, *50*(3), 1177-1192. https://doi.org/10.1007/s00382-017-3671-4

Sadok, W., Schoppach, R., Ghanem, M. E., Zucca, C., & Sinclair, T. R. (2019). Wheat drought-tolerance to enhance food security in Tunisia, birthplace of the Arab Spring. *European Journal of Agronomy*, *107*, 1-9. https://doi.org/10.1016/j.eja.2019.03.009

Sakamoto, T., Yokozawa, M., Toritani, H., Shibayama, M., Ishitsuka, N., & Ohno, H. (2005). A crop phenology detection method using time-series MODIS data. *Remote Sensing of Environment*, *96*(3), 366-374. https://doi.org/10.1016/j.rse.2005.03.008

Salazar, M. R., Hook, J. E., Garcia y Garcia, A., Paz, J. O., Chaves, B., & Hoogenboom, G. (2012). Estimating irrigation water use for maize in the Southeastern USA: A modeling approach. *Agricultural Water Management*, *107*, 104-111. https://doi.org/10.1016/j.agwat.2012.01.015

Sánchez, N., González-Zamora, Á., Piles, M., & Martínez-Fernández, J. (2016). A New Soil Moisture Agricultural Drought Index (SMADI) Integrating MODIS and SMOS Products: A Case of Study over the Iberian Peninsula. *Remote Sensing*, *8*(4), 287. https://doi.org/10.3390/rs8040287

Sarmiento, E. F. E., Heidari, F., Lin, Q., & Xoplaki, E. (2023). Evaluation of the performance of the 1-arc min hydrological model LISFLOOD in German catchments. *EGU General Assembly 2023*, Vienna, Austria, 24–28 April 2023. https://doi.org/10.5194/egusphere-egu23-15296

Savin, R., Slafer, G. A., Cossani, C. M., Abeledo, L. G., & Sadras, V. O. (2015). Chapter 7—Cereal yield in Mediterranean-type environments: Challenging the paradigms on terminal drought, the adaptability of barley vs wheat and the role of nitrogen fertilization. In V. O. Sadras & D. F. Calderini (Eds.), *Crop Physiology* (2nd ed., pp. 141–158). Academic Press. https://doi.org/10.1016/B978-0-12-417104-6.00007-8

Savin, R., Cossani, C. M., Dahan, R., Ayad, J. Y., Albrizio, R., Todorovic, M., Karrou, M., & Slafer, G. A. (2022). Intensifying cereal management in dryland Mediterranean agriculture: Rainfed wheat and barley responses to nitrogen fertilisation. *European Journal of Agronomy*, *137*, 126518. https://doi.org/10.1016/j.eja.2022.126518

Scaini, A., Sánchez, N., Vicente-Serrano, S. M., & Martínez-Fernández, J. (2015). SMOS-derived soil moisture anomalies and drought indices: A comparative

analysis using in situ measurements. *Hydrological Processes*, *29*(3), 373-383. https://doi.org/10.1002/hyp.10150

Schils, R., Olesen, J. E., Kersebaum, K.-C., Rijk, B., Oberforster, M., Kalyada, V., Khitrykau, M., Gobin, A., Kirchev, H., Manolova, V., Manolov, I., Trnka, M., Hlavinka, P., Palosuo, T., Peltonen-Sainio, P., Jauhiainen, L., Lorgeou, J., Marrou, H., Danalatos, N., Archontoulis, S., Fodor, N., Spink, J., Roggero, P. P., Bassu, S., Pulina, A., Seehusen, T., Uhlen, A. K., Żyłowska, K., Nieróbca, A., Kozyra, J., Silva, J. V., Maçãs, B., Coutinho, J., Ion, V., Takáč, J., Mínguez, M. I., Eckersten, H., Levy, L., Herrera, J. M., Hiltbrunner, J., Kryvobok, O., Kryvoshein, O., Sylvester-Bradley, R., Kindred, D., Topp, C. F. E., Boogaard, H., de Groot, H., Lesschen, J. P., van Bussel, L., Wolf, J., Zijlstra, M., van Loon, M. P., van Ittersum, M. K. (2018). Cereal yield gaps across Europe. *European Journal of Agronomy*, *101*, 109-120. https://doi.org/10.1016/j.eja.2018.09.003

Schumacher, D. L., Keune, J., & Miralles, D. G. (2020). Atmospheric heat and moisture transport to energy- and water-limited ecosystems. *Annals of the New York Academy of Sciences*, *1472*(1), 123-138. https://doi.org/10.1111/nyas.14357

Schumacher, D. L., Zachariah, M., Otto, F., Barnes, C., Philip, S., Kew, S., Vahlberg, M., Singh, R., Heinrich, D., Arrighi, J., van Aalst, M., Hauser, M., Hirschi, M., Bessenbacher, V., Gudmundsson, L., Beaudoing, H. K., Rodell, M., Li, S., Yang, W., Vecchi, G. A., Harrington, L. J., Lehner, F., Balsamo, G., & Seneviratne, S. I. (2023). Detecting the human fingerprint in the summer 2022 West-Central European soil drought. *EGUsphere*. https://doi.org/10.5194/egusphere-2023-717

Schwartz, M. D. (Ed.). (2003). *Phenology: An integrative environmental science* (Vol. 132). Kluwer Academic Publishers. https://doi.org/10.1007/978-94-007-0632-3

Seker, M., & Gumus, V. (2022). Projection of temperature and precipitation in the Mediterranean region through multi-model ensemble from CMIP6. *Atmospheric Research*, *280*, 106440. https://doi.org/10.1016/j.atmosres.2022.106440

Seneviratne, S. I., Corti, T., Davin, E. L., Hirschi, M., Jaeger, E. B., Lehner, I., Orlowsky, B., & Teuling, A. J. (2010). Investigating soil moisture–climate interactions in a changing climate: A review. *Earth-Science Reviews*, *99*(3), 125-161. https://doi.org/10.1016/j.earscirev.2010.02.004

Sepulcre-Canto, G., Horion, S., Singleton, A., Carrao, H., & Vogt, J. (2012). Development of a Combined Drought Indicator to detect agricultural drought in Europe. *Natural Hazards and Earth System Sciences*, *12*(11), 3519-3531. https://doi.org/10.5194/nhess-12-3519-2012

Shah, J., Hari, V., Rakovec, O., Markonis, Y., Samaniego, L., Mishra, V., Hanel, M., Hinz, C., & Kumar, R. (2022). Increasing footprint of climate warming on flash droughts occurrence in Europe. *Environmental Research Letters*, *17*(6), 064017. https://doi.org/10.1088/1748-9326/ac6888

Sheffield, J., Goteti, G., Wen, F., & Wood, E. F. (2004). A simulated soil moisture based drought analysis for the United States. *Journal of Geophysical Research: Atmospheres*, *109*(D24). https://doi.org/10.1029/2004JD005182

Sheffield, J., Andreadis, K. M., Wood, E. F., & Lettenmaier, D. P. (2009). Global and Continental Drought in the Second Half of the Twentieth Century: Severity–Area–Duration Analysis and Temporal Variability of Large-Scale Events. *Journal of Climate*, *22*(8), 1962-1981. https://doi.org/10.1175/2008JCLI2722.1

Sherratt, A. (1980). Water, soil and seasonality in early cereal cultivation. *World Archaeology*, *11*(3), 313-330. https://doi.org/10.1080/00438243.1980.9979770

Shukla, S., McNally, A., Husak, G., & Funk, C. (2014). A seasonal agricultural drought forecast system for food-insecure regions of East Africa. *Hydrology and Earth System Sciences*, *18*(10), 3907-3921. https://doi.org/10.5194/hess-18-3907-2014

Siebert, S., Henrich, V., Frenken, K., & Burke, J. (2013). *Update of the digital global map of irrigation areas to version 5*. Rheinische Friedrich-Wilhelms-Universität, Bonn, Germany and Food and Agriculture Organization of the United Nations, Rome, Italy.

Sisheber, B., Marshall, M., Mengistu, D., & Nelson, A. (2023). Detecting the long-term spatiotemporal crop phenology changes in a highly fragmented agricultural landscape. *Agricultural and Forest Meteorology*, *340*, 109601. https://doi.org/10.1016/j.agrformet.2023.109601

Slafer, G. A., & Savin, R. (2023). Comparative performance of barley and wheat across a wide range of yielding conditions. Does barley outyield wheat consistently in low-yielding conditions? *European Journal of Agronomy*, *143*, 126689. https://doi.org/10.1016/j.eja.2022.126689

Son, N. T., Chen, C. F., Chen, C. R., Minh, V. Q., & Trung, N. H. (2014). A comparative analysis of multitemporal MODIS EVI and NDVI data for large-scale rice yield estimation. *Agricultural and Forest Meteorology*, *197*, 52-64. https://doi.org/10.1016/j.agrformet.2014.06.007

Spano, D., Snyder, R. L., & Cesaraccio, C. (2024). Mediterranean Phenology. In M. D. Schwartz (Ed.), *Phenology: An Integrative Environmental Science* (pp. 171-201). Springer Nature Switzerland. https://doi.org/10.1007/978-3-031-75027-4_9

Spiertz, J., & Ewert, F. (2009). Crop production and resource use to meet the growing demand for food, feed and fuel: Opportunities and constraints. *NJAS: Wageningen Journal of Life Sciences*, *56*(4), 281-300. https://doi.org/10.1016/S1573-5214(09)80001-8

Spinoni, J., Vogt, J. V., Naumann, G., Barbosa, P., & Dosio, A. (2018). Will drought events become more frequent and severe in Europe? *International Journal of Climatology*, *38*(4), 1718-1736. https://doi.org/10.1002/joc.5291

Sridhar, V., Hubbard, K. G., You, J., & Hunt, E. D. (2008). Development of the Soil Moisture Index to Quantify Agricultural Drought and Its "User Friendliness" in Severity-Area-Duration Assessment. *Journal of Hydrometeorology*, *9*(4), 660-676. https://doi.org/10.1175/2007JHM892.1

Stoate, C., Borralho, R., & Araújo, M. (2000). Factors affecting corn bunting Miliaria calandra abundance in a Portuguese agricultural landscape. *Agriculture, Ecosystems & Environment*, *77*(3), 219-226. https://doi.org/10.1016/S0167-8809(99)00101-2

Stocker, B. D., Zscheischler, J., Keenan, T. F., Prentice, I. C., Peñuelas, J., & Seneviratne, S. I. (2018). Quantifying soil moisture impacts on light use efficiency across biomes. *New Phytologist*, *218*(4), 1430-1449. https://doi.org/10.1111/nph.15123

Stöckli, R., & Vidale, P. L. (2004). European plant phenology and climate as seen in a 20-year AVHRR land-surface parameter dataset. *International Journal of Remote Sensing*, *25*(17), 3303-3330. https://doi.org/10.1080/01431160310001618149

Stoyanova, J. S., Georgiev, C. G., & Neytchev, P. N. (2023). Drought Monitoring in Terms of Evapotranspiration Based on Satellite Data from Meteosat in Areas of Strong Land–Atmosphere Coupling. *Land*, *12*(1), 240. https://doi.org/10.3390/land12010240

Sun, Z., Wang, X., Zhang, X., Tani, H., Guo, E., Yin, S., & Zhang, T. (2019). Evaluating and comparing remote sensing terrestrial GPP models for their response to climate variability and CO2 trends. *Science of The Total Environment*, *668*, 696-713. https://doi.org/10.1016/j.scitotenv.2019.03.025

Sung, J. H., Baek, D., Ryu, Y., Seo, S. B., & Seong, K.-W. (2021). Effects of Hydro-Meteorological Factors on Streamflow Withdrawal for Irrigation in Yeongsan River Basin. *Sustainability*, *13*(9), 4969. https://doi.org/10.3390/su13094969

Svoboda, M., LeComte, D., Hayes, M., Heim, R., Gleason, K., Angel, J., Rippey, B., Tinker, R., Palecki, M., Stooksbury, D., Miskus, D., & Stephens, S. (2002). The drought monitor. *Bulletin of the American Meteorological Society*, *83*(8), 1181-1190. https://doi.org/10.1175/1520-0477-83.8.1181

Talebi, H., Samadianfard, S., & Valizadeh Kamran, K. (2023). Estimation of daily reference evapotranspiration implementing satellite image data and strategy of ensemble optimization algorithm of stochastic gradient descent with multilayer perceptron. *Environment, Development and Sustainability*, *27*, 3707-3729. https://doi.org/10.1007/s10668-023-04037-8

Tan, C., Yang, J., & Li, M. (2015). Temporal-spatial variation of drought indicated by SPI and SPEI in Ningxia Hui Autonomous Region, China. *Atmosphere*, *6*(10), 1399-1421. https://doi.org/10.3390/atmos6101399

Thielen, J., Bartholmes, J., Ramos, M.-H., & de Roo, A. (2009). The European Flood Alert System – Part 1: Concept and development. *Hydrology and Earth System Sciences*, *13*(2), 125-140. https://doi.org/10.5194/hess-13-125-2009

Thomas, W. (2014). The value of decimal cereal growth stages. *Annals of Applied Biology, 165*(3), 303–304. https://doi.org/10.1111/aab.12149

Tian, L., & Quiring, S. M. (2019). Spatial and temporal patterns of drought in Oklahoma (1901–2014). *International Journal of Climatology*, *39*(7), 3365-3378. https://doi.org/10.1002/joc.6026

Tian, R., Li, J., Zheng, J., Liu, L., Liu, Y., Han, W., & Wang, X. (2024a). The spatial-temporal patterns of spring phenology in the temperate grasslands of China and their response mechanisms to climatic factors. *Journal of Spatial Science*, 1-19. https://doi.org/10.1080/14498596.2024.2333753

Tian, F., Zhu, Z., Cao, S., Zhao, W., Li, M., & Wu, J. (2024b). Satellite-observed increasing coupling between vegetation productivity and greenness in the semiarid Loess Plateau of China is not captured by process-based models. *Science of The Total Environment*, *906*, 167664. https://doi.org/10.1016/j.scitotenv.2023.167664

Toledo, R. (2023). *Representación de la clave fenológica de Cereales de invierno*. https://doi.org/10.13140/RG.2.2.33226.54722

Tottman, D. R. (1987). The decimal code for the growth stages of cereals, with illustrations. *Annals of Applied Biology*, *110*(2), 441-454. https://doi.org/10.1111/j.1744-7348.1987.tb03275.x

Touhami, I., Moutahir, H., Assoul, D., Bergaoui, K., Aouinti, H., Bellot, J., & Andreu, J. M. (2022). Multi-year monitoring land surface phenology in relation to climatic variables using MODIS-NDVI time-series in Mediterranean forest, Northeast Tunisia. *Acta Oecologica*, *114*, 103804. https://doi.org/10.1016/j.actao.2021.103804

Tramblay, Y., Koutroulis, A., Samaniego, L., Vicente-Serrano, S. M., Volaire, F., Boone, A., Le Page, M., Llasat, M. C., Albergel, C., Burak, S., Cailleret, M., Cindrić Kalin, K., Davi, H., Dupuy, J.-L., Greve, P., Grillakis, M., Hanich, L., Jarlan, L., Martin-StPaul, N., Martínez-Vilalta, J., Mouillot, F., Pulido-Velazquez, D., Quintana-Seguí, P., Renard, D., Turco, M., Türkeş, M., Trigo, R., Vidal, J.-P., Vilagrosa, A., Zribi, M., & Polcher, J. (2020). Challenges for drought assessment in the Mediterranean region under future climate scenarios. *Earth-Science Reviews, 210*, 103348. https://doi.org/10.1016/j.earscirev.2020.103348

Trenberth KE. (2011). Changes in precipitation with climate change. *Climate Research*, *47*(1-2), 123-138. https://www.int-res.com/abstracts/cr/v47/n1-2/p123-138

Tufail, T., Ain, H. B. U., Hussain, M., Farooq, M. A., Nayik, G. A., & Ansari, M. J. (2023). Cereals: An overview. In G. A. Nayik, T. Tufail, F. M. Anjum, & M. J. Ansari (Eds.), *Cereal grains: Composition, nutritional attributes, and potential applications* (pp. 1–13). CRC Press. https://doi.org/10.1201/9781003252023

Tyagi, S., Zhang, X., Saraswat, D., Sahany, S., Mishra, S. K., & Niyogi, D. (2022). Flash Drought: Review of Concept, Prediction and the Potential for Machine Learning, Deep Learning Methods. *Earth's Future*, *10*(11), e2022EF002723. https://doi.org/10.1029/2022EF002723

UnNisa, Z., Govind, A., Marchetti, M., & Lasserre, B. (2022). A review of crop water productivity in the Mediterranean basin under a changing climate: Wheat and barley as test cases. *Irrigation and Drainage*, *71*(S1), 51-70. https://doi.org/10.1002/ird.2710

Valliere, J. M., Ruscalleda Alvarez, J., Cross, A. T., Lewandrowski, W., Riviera, F., Stevens, J. C., Tomlinson, S., Tudor, E. P., Wong, W. S., Yong, J. W. H., & Veneklaas, E. J. (2022). Restoration ecophysiology: An ecophysiological approach to improve restoration strategies and outcomes in severely disturbed landscapes. *Restoration Ecology*, *30*(S1), e13571. https://doi.org/10.1111/rec.13571

Valmassoi, A., Keller, J. D., Kleist, D. T., English, S., Ahrens, B., Ďurán, I. B., Bauernschubert, E., Bosilovich, M. G., Fujiwara, M., Hersbach, H., Lei, L., Löhnert, U., Mamnun, N., Martin, C. R., Moore, A., Niermann, D., Ruiz, J. J., & Scheck, L. (2023). Current Challenges and Future Directions in Data Assimilation and Reanalysis. *Bulletin of the American Meteorological Society*, *104*(4), E756-E767. https://doi.org/10.1175/BAMS-D-21-0331.1

Van Der Knijff, J. M., Younis, J., & De Roo, A. P. J. (2010). LISFLOOD: a GIS-based distributed model for river basin scale water balance and flood simulation. *International Journal of Geographical Information Science*, *24*(2), 189-212. https://doi.org/10.1080/13658810802549154

Van Lanen, H. A. J., Vogt, J. V., Andreu, J., Carrão, H., De Stefano, L., Dutra, E., Forzieri, G., Iglesias, A., Lavaysse, C., Naumann, G., Pulwarty, R., Spinoni, J., Stahl, K., Stefanski, R., Stilianakis, N., Svoboda, M., & Tallaksen, L. M. (2017). Climatological risk: Droughts. In K. Poljanšek, M. Marín Ferrer, T. De Groeve, & I. Clark (Eds.), *Science for disaster risk management 2017: Knowing better and losing less* (pp. 271–293). Publications Office of the European Union. https://doi.org/10.2788/688605

Van Loon, A. F. (2015). Hydrological drought explained. *WIREs Water*, *2*(4), 359-392. https://doi.org/10.1002/wat2.1085

Ventrella, D., Stellacci, A. M., Castrignano, A., Charfeddine, M., & Castellini, M. (2016). Effects of crop residue management on winter durum wheat productivity in a long

term experiment in Southern Italy. *European journal of agronomy, 77*, 188-198. https://doi.org/10.1016/j.eja.2016.02.010

Vicente-Serrano, S. M., Gouveia, C., Camarero, J. J., Beguería, S., Trigo, R., López-Moreno, J. I., Azorín-Molina, C., Pasho, E., Lorenzo-Lacruz, J., Revuelto, J., Morán-Tejeda, E., & Sanchez-Lorenzo, A. (2013). Response of vegetation to drought time-scales across global land biomes. *Proceedings of the National Academy of Sciences, 110*(1), 52-57. https://doi.org/10.1073/pnas.1207068110

Vicente-Serrano, S. M., McVicar, T. R., Miralles, D. G., Yang, Y., & Tomas-Burguera, M. (2020). Unraveling the influence of atmospheric evaporative demand on drought and its response to climate change. *WIREs Climate Change*, *11*(2), e632. https://doi.org/10.1002/wcc.632

Viljanen, N., Honkavaara, E., Näsi, R., Hakala, T., Niemeläinen, O., & Kaivosoja, J. (2018). A Novel Machine Learning Method for Estimating Biomass of Grass Swards Using a Photogrammetric Canopy Height Model, Images and Vegetation Indices Captured by a Drone. *Agriculture*, *8*(5), 70. https://doi.org/10.3390/agriculture8050070

Vogel, E., Donat, M. G., Alexander, L. V., Meinshausen, M., Ray, D. K., Karoly, D., Meinshausen, N., & Frieler, K. (2019). The effects of climate extremes on global agricultural yields. *Environmental Research Letters*, *14*(5), 054010. https://doi.org/10.1088/1748-9326/ab154b

Von Storch, H. (1999). Misuses of statistical analysis in climate research. In H. Von Storch & A. Navarra (Eds.), *Analysis of Climate Variability: Applications of Statistical Techniques* (pp. 11–26). Springer-Verlag. https://doi.org/10.1007/978-3-662-03167-4_2

Walther, G.-R., Post, E., Convey, P., Menzel, A., Parmesan, C., Beebee, T. J., Fromentin, J.-M., Hoegh-Guldberg, O., & Bairlein, F. (2002). Ecological responses to recent climate change. *Nature, 416*(6879), 389-395. https://doi.org/10.1038/416389a

Wang, F., Chen, B., Lin, X., & Zhang, H. (2020). Solar-induced chlorophyll fluorescence as an indicator for determining the end date of the vegetation growing season. *Ecological Indicators*, *109*, 105755. https://doi.org/10.1016/j.ecolind.2019.105755

Wang, W., Pijl, A., & Tarolli, P. (2022). Future climate-zone shifts are threatening steep-slope agriculture. *Nature Food, 3*(3), 193-196. https://doi.org/10.1038/s43016-021-00454-y

Wang, M., Menzel, L., Jiang, S., Ren, L., Xu, C.-Y., & Cui, H. (2023a). Evaluation of flash drought under the impact of heat wave events in southwestern Germany. *Science of The Total Environment*, *904*, 166815. https://doi.org/10.1016/j.scitotenv.2023.166815

Wang, H., Zhu, Q., Wang, Y., & Zhang, H. (2023b). Spatio-temporal characteristics and driving factors of flash drought recovery: From the perspective of soil moisture and GPP changes. *Weather and Climate Extremes*, *42*, 100605. https://doi.org/10.1016/j.wace.2023.100605

Wang, L., Wei, W., Wang, L., Chen, S., Duan, W., Zhang, Q., Tong, B., Han, Z., Li, Z., & Chen, L. (2025a). Trigger thresholds and propagation mechanism of meteorological drought to agricultural drought in an inland river basin. *Agricultural Water Management*, *311*, 109378. https://doi.org/10.1016/j.agwat.2025.109378

Wang, Y., Sun, P., Yao, R., & Ge, C. (2025b). Rising temperature increases the response time of LAI and GPP to meteorological drought in China. *Atmospheric Research*, *319*, 107989. https://doi.org/10.1016/j.atmosres.2025.107989

Watson, G. S. (1967). Linear Least Squares Regression. *The Annals of Mathematical Statistics*, *38*(6), 1679-1699. http://www.jstor.org/stable/2238648

Wei, X., Huang, S., Li, J., Huang, Q., Leng, G., Liu, D., Guo, W., Zheng, X., & Bai, Q. (2024). The negative-positive feedback transition thresholds of meteorological drought in response to agricultural drought and their dynamics. *Science of The Total Environment*, *906*, 167817. https://doi.org/10.1016/j.scitotenv.2023.167817

White, M. A., Thornton, P. E., & Running, S. W. (1997). A continental phenology model for monitoring vegetation responses to interannual climatic variability. *Global biogeochemical cycles*, *11*(2), 217-234. https://doi.org/10.1029/97GB00330

White, K., Pontius, J., & Schaberg, P. (2014). Remote sensing of spring phenology in northeastern forests: A comparison of methods, field metrics and sources of uncertainty. *Remote Sensing of Environment*, *148*, 97-107. https://doi.org/10.1016/j.rse.2014.03.017

Wigneron, J.-P., Jackson, T. J., O'Neill, P., De Lannoy, G., de Rosnay, P., Walker, J. P., Ferrazzoli, P., Mironov, V., Bircher, S., Grant, J. P., Kurum, M., Schwank, M., Munoz-Sabater, J., Das, N., Royer, A., Al-Yaari, A., Al Bitar, A., Fernandez-Moran, R., Lawrence, H., Mialon, A., Parrens, M., Richaume, P., Delwart, S., & Kerr, Y. (2017). Modelling the passive microwave signature from land surfaces: A review of recent results and application to the L-band SMOS & SMAP soil moisture retrieval algorithms. *Remote Sensing of Environment*, *192*, 238-262. https://doi.org/10.1016/j.rse.2017.01.024

Wolberg & Alfy. (1999). Monotonic cubic spline interpolation. *1999 Proceedings Computer Graphics International*, 188-195. https://doi.org/10.1109/CGI.1999.777953

Wu, C., Chen, J., Gonsamo, A., Price, D., Black, T., & Kurz, W. (2012). Interannual variability of carbon sequestration is determined by the lag between ends of net uptake and photosynthesis: Evidence from long records of two contrasting forest

stands. *Agricultural and Forest Meteorology, 164*, 29-38. https://doi.org/10.1016/j.agrformet.2012.05.002

Wu, C., Hou, X., Peng, D., Gonsamo, A., & Xu, S. (2016). Land surface phenology of China's temperate ecosystems over 1999–2013: Spatial–temporal patterns, interaction effects, covariation with climate and implications for productivity. *Agricultural and Forest Meteorology*, *216*, 177-187. https://doi.org/10.1016/j.agrformet.2015.10.015

Xu, X., Zhou, G., Du, H., Mao, F., Xu, L., Li, X., & Liu, L. (2020). Combined MODIS land surface temperature and greenness data for modeling vegetation phenology, physiology, and gross primary production in terrestrial ecosystems. *Science of The Total Environment*, *726*, 137948. https://doi.org/10.1016/j.scitotenv.2020.137948

Xue, J., & Su, B. (2017). Significant Remote Sensing Vegetation Indices: A Review of Developments and Applications. *Journal of Sensors*, *2017*(1), 1353691. https://doi.org/10.1155/2017/1353691

Xue, C., Ghirardelli, A., Chen, J., & Tarolli, P. (2024). Investigating agricultural drought in Northern Italy through explainable Machine Learning: Insights from the 2022 drought. *Computers and Electronics in Agriculture*, *227*, 109572. https://doi.org/10.1016/j.compag.2024.109572

Yang, C., Fraga, H., van Ieperen, W., & Santos, J. A. (2020). Assessing the impacts of recent-past climatic constraints on potential wheat yield and adaptation options under Mediterranean climate in southern Portugal. *Agricultural systems*, *182*, 102844. https://doi.org/10.1016/j.agsy.2020.102844

Yang, F., Liu, C., Chen, Q., Lai, J., & Liu, T. (2024). Earlier Spring-Summer Phenology and Higher Photosynthetic Peak Altered the Seasonal Patterns of Vegetation Productivity in Alpine Ecosystems. *Remote Sensing*, *16*(9), 1580. https://doi.org/10.3390/rs16091580

Yao, N., Li, Y., Liu, Q., Zhang, S., Chen, X., Ji, Y., Liu, F., Pulatov, A., & Feng, P. (2022). Response of wheat and maize growth-yields to meteorological and agricultural droughts based on standardized precipitation evapotranspiration indexes and soil moisture deficit indexes. *Agricultural Water Management*, *266*, 107566. https://doi.org/10.1016/j.agwat.2022.107566

Yin, J., Guo, S., Yang, Y., Chen, J., Gu, L., Wang, J., He, S., Wu, B., & Xiong, J. (2022). Projection of droughts and their socioeconomic exposures based on terrestrial water storage anomaly over China. *Science China Earth Sciences*, *65*(9), 1772-1787. https://doi.org/10.1007/s11430-021-9927-x

Yoder, R. E., Odhiambo, L. O., & Wright, W. C. (2005). Effects of vapor-pressure deficit and net-irradiance calculation methods on accuracy of standardized Penman-Monteith equation in a humid climate. *Journal of irrigation and drainage*

engineering, *131*(3), 228-237. https://doi.org/10.1061/(ASCE)0733-9437(2005)131:3(228)

You, X., Meng, J., Zhang, M., & Dong, T. (2013). Remote Sensing Based Detection of Crop Phenology for Agricultural Zones in China Using a New Threshold Method. *Remote Sensing*, *5*(7), 3190-3211. https://doi.org/10.3390/rs5073190

Yuan, M., Wang, L., Lin, A., Liu, Z., & Qu, S. (2019a). Variations in land surface phenology and their response to climate change in Yangtze River basin during 1982–2015. *Theoretical and Applied Climatology*, *137*(3), 1659-1674. https://doi.org/10.1007/s00704-018-2699-7

Yuan, W., Zheng, Y., Piao, S., Ciais, P., Lombardozzi, D., Wang, Y., Ryu, Y., Chen, G., Dong, W., Hu, Z., Jain, A. K., Jiang, C., Kato, E., Li, S., Lienert, S., Liu, S., Nabel, J. E. M. S., Qin, Z., Quine, T., Sitch, S., Smith, W. K., Wang, F., Wu, C., Xiao, Z., & Yang, S. (2019b). Increased atmospheric vapor pressure deficit reduces global vegetation growth. *Science Advances*, *5*(8), eaax1396. https://doi.org/10.1126/sciadv.aax1396

Yuan, Z., Bao, G., Dorjsuren, A., Oyont, A., Chen, J., Li, F., Dong, G., Guo, E., Shao, C., & Du, L. (2024). Climatic Constraints of Spring Phenology and Its Variability on the Mongolian Plateau From 1982 to 2021. *Journal of Geophysical Research: Biogeosciences*, *129*(2), e2023JG007689. https://doi.org/10.1029/2023JG007689

Yue, S., & Pilon, P. (2004). A comparison of the power of the t test, Mann-Kendall and bootstrap tests for trend detection / Une comparaison de la puissance des tests *t* de Student, de Mann-Kendall et du bootstrap pour la détection de tendance. *Hydrological Sciences Journal*, *49*(1), 21-37. https://doi.org/10.1623/hysj.49.1.21.53996

Zadoks, J. C., Chang, T. T., & Konzak, C. F. (1974). A decimal code for the growth stages of cereals. *Weed Research*, *14*(6), 415-421. https://doi.org/10.1111/j.1365-3180.1974.tb01084.x

Zahradníček, P., Brázdil, R., Štěpánek, P., & Trnka, M. (2021). Reflections of global warming in trends of temperature characteristics in the Czech Republic, 1961–2019. *International Journal of Climatology*, *41*(2), 1211-1229. https://doi.org/10.1002/joc.6791

Zargar, A., Sadiq, R., Naser, B., & Khan, F. I. (2011). A review of drought indices. *Environmental Reviews*, *19*, 333-349. https://doi.org/10.1139/a11-013

Zhan, W., Luo, F., Luo, H., Li, J., Wu, Y., Yin, Z., Wu, Y., & Wu, P. (2024). Time-Series-Based Spatiotemporal Fusion Network for Improving Crop Type Mapping. *Remote Sensing*, *16*(2), 235. https://doi.org/10.3390/rs16020235

Zhang, X., Friedl, M. A., Schaaf, C. B., Strahler, A. H., Hodges, J. C., Gao, F., Reed, B. C., & Huete, A. (2003). Monitoring vegetation phenology using MODIS. *Remote*

sensing of environment, *84*(3), 471-475. https://doi.org/10.1016/S0034-4257(02)00135-9

Zhang, A., & Jia, G. (2013). Monitoring meteorological drought in semiarid regions using multi-sensor microwave remote sensing data. *Remote Sensing of Environment*, *134*, 12-23. https://doi.org/10.1016/j.rse.2013.02.023

Zhang, L., Liu, Y., Ren, L., Jiang, S., Yang, X., Yuan, F., Wang, M., & Wei, L. (2019). Drought Monitoring and Evaluation by ESA CCI Soil Moisture Products Over the Yellow River Basin. *IEEE Journal of Selected Topics in Applied Earth Observations and Remote Sensing*, *12*(9), 3376-3386. https://doi.org/10.1109/JSTARS.2019.2934732

Zhang, M., & Yuan, X. (2020). Rapid reduction in ecosystem productivity caused by flash droughts based on decade-long FLUXNET observations. *Hydrology and Earth System Sciences*, *24*(11), 5579-5593. https://doi.org/10.5194/hess-24-5579-2020

Zhang, J., Zhao, J., Wang, Y., Zhang, H., Zhang, Z., & Guo, X. (2020). Comparison of land surface phenology in the Northern Hemisphere based on AVHRR GIMMS3g and MODIS datasets. *ISPRS Journal of Photogrammetry and Remote Sensing*, *169*, 1-16. https://doi.org/10.1016/j.isprsjprs.2020.08.020

Zhang, Y., Hao, Z., Feng, S., Zhang, X., Xu, Y., & Hao, F. (2021a). Agricultural drought prediction in China based on drought propagation and large-scale drivers. *Agricultural Water Management*, *255*, 107028. https://doi.org/10.1016/j.agwat.2021.107028

Zhang, Y., You, Q., Mao, G., Chen, C., Li, X., & Yu, J. (2021b). Flash Drought Characteristics by Different Severities in Humid Subtropical Basins: A Case Study in the Gan River Basin, China. *Journal of Climate*, *34*(18), 7337-7357. https://doi.org/10.1175/JCLI-D-20-0596.1

Zhang, R., Zhou, Y., Hu, T., Sun, W., Zhang, S., Wu, J., & Wang, H. (2023). Detecting the Spatiotemporal Variation of Vegetation Phenology in Northeastern China Based on MODIS NDVI and Solar-Induced Chlorophyll Fluorescence Dataset. *Sustainability*, *15*(7), 6012. https://doi.org/10.3390/su15076012

Zhang, R., Shangguan, W., Liu, J., Dong, W., & Wu, D. (2024a). Assessing meteorological and agricultural drought characteristics and drought propagation in Guangdong, China. *Journal of Hydrology: Regional Studies*, *51*, 101611. https://doi.org/10.1016/j.ejrh.2023.101611

Zhang, Y., Liu, F., Liu, T., Chen, C., & Lu, Z. (2024b). Characteristics of Vegetation Photosynthesis under Flash Droughts in the Major Agricultural Areas of Southern China. *Atmosphere*, *15*(8), 886. https://doi.org/10.3390/atmos15080886

Zhang, S., Li, M., Ma, Z., Jian, D., Lv, M., yang, Q., Duan, Y., & Amin, D. (2024c). The intensification of flash droughts across China from 1981 to 2021. *Climate Dynamics*, *62*(2), 1233-1247. https://doi.org/10.1007/s00382-023-06980-8

Zhang, Y., Wu, X., Wang, X., Dai, M., & Peng, Y. (2025). Crop root system architecture in drought response. *Journal of Genetics and Genomics*, *52*(1), 4-13. https://doi.org/10.1016/j.jgg.2024.05.001

Zhao, J., Zhang, H., Zhang, Z., Guo, X., Li, X., & Chen, C. (2015). Spatial and Temporal Changes in Vegetation Phenology at Middle and High Latitudes of the Northern Hemisphere over the Past Three Decades. *Remote Sensing*, *7*(8), 10973-10995. https://doi.org/10.3390/rs70810973

Zhao, Y., Peng, X., Frauenfeld, O. W., Cui, X., Bi, J., Ma, X., Wei, G., Mu, C., Sun, H., & Sui, J. (2024). Evaluation of Land Surface Phenology in Northern Hemisphere Permafrost Regions. *Journal of Geophysical Research: Biogeosciences*, *129*(5), e2023JG007951. https://doi.org/10.1029/2023JG007951

Zheng, B., Myint, S. W., Thenkabail, P. S., & Aggarwal, R. M. (2015). A support vector machine to identify irrigated crop types using time-series Landsat NDVI data. *International Journal of Applied Earth Observation and Geoinformation*, *34*, 103-112. https://doi.org/10.1016/j.jag.2014.07.002

Zhou, L., Zhou, W., Chen, J., Xu, X., Wang, Y., Zhuang, J., & Chi, Y. (2022). Land surface phenology detections from multi-source remote sensing indices capturing canopy photosynthesis phenology across major land cover types in the Northern Hemisphere. *Ecological Indicators*, *135*, 108579. https://doi.org/10.1016/j.ecolind.2022.108579

Zhu, W., Tian, H., Xu, X., Pan, Y., Chen, G., & Lin, W. (2012). Extension of the growing season due to delayed autumn over mid and high latitudes in North America during 1982–2006. *Global Ecology and Biogeography*, *21*(2), 260-271. https://doi.org/10.1111/j.1466-8238.2011.00675.x

Zhu, E., Fang, D., Chen, L., Qu, Y., & Liu, T. (2024). The Impact of Urbanization on Spatial–Temporal Variation in Vegetation Phenology: A Case Study of the Yangtze River Delta, China. *Remote Sensing*, *16*(5), 914. https://doi.org/10.3390/rs16050914

Zou, K., Cheng, L., Wu, M., Wang, S., Qin, S., Liu, P., & Zhang, L. (2024). Contrasting variations of ecosystem gross primary productivity during flash droughts caused by competing water demand and supply. *Environmental Research Letters*, *19*(2), 024031. https://doi.org/10.1088/1748-9326/ad2164

Zreda, M., Desilets, D., Ferré, T. P. A., & Scott, R. L. (2008). Measuring soil moisture content non-invasively at intermediate spatial scale using cosmic-ray neutrons. *Geophysical Research Letters*, *35*(21), L21402. https://doi.org/10.1029/2008GL035655

Zscheischler, J., Michalak, A. M., Schwalm, C., Mahecha, M. D., Huntzinger, D. N., Reichstein, M., Berthier, G., Ciais, P., Cook, R. B., El-Masri, B., Huang, M., Ito, A., Jain, A., King, A., Lei, H., Lu, C., Mao, J., Peng, S., Poulter, B., Ricciuto, D., Shi, X., Tao, B., Tian, H., Viovy, N., Wang, W., Wei, Y., Yang, J., & Zeng, N. (2014). Impact of large-scale climate extremes on biospheric carbon fluxes: An intercomparison based on MsTMIP data. *Global Biogeochemical Cycles*, *28*(6), 585-600. https://doi.org/10.1002/2014GB004826